CHALMERS

Compression perpendicular to the grain and reinforcement of a pre-stressed timber deck

Theoretical studies, Laboratory tests and FE-analyses

Master's Thesis in the International Master's programme Structural Engineering

SILVIO FORMOLO

ROLAND GRANSTRÖM

Department of Civil and Environmental Engineering
Division of Structural Engineering
Steel and Timber Structures
CHALMERS UNIVERSITY OF TECHNOLOGY
Göteborg, Sweden 2007

Master's Thesis 2007:25

MASTER'S THESIS 2007:25

Compression perpendicular to the grain and reinforcement of a pre-stressed timber deck

Theoretical studies, Laboratory tests and FE-analyses

Master's Thesis in the International Master's programme Structural Engineering

SILVIO FORMOLO

ROLAND GRANSTRÖM

Department of Civil and Environmental Engineering
Division of Structural Engineering
Steel and Timber Structures
CHALMERS UNIVERSITY OF TECHNOLOGY
Göteborg, Sweden 2007

Compression perpendicular to the grain and reinforcement of a pre-stressed timber deck
Theoretical studies, Laboratory tests and FE-analyses
Master's Thesis in the International Master's programme Structural Engineering
SILVIO FORMOLO
ROLAND GRANSTRÖM

Master's Thesis 2007:25
Department of Civil and Environmental Engineering
Division of Structural Engineering
Steel and Timber *Structures*
Chalmers University of Technology
SE-412 96 Göteborg
Sweden
Telephone: + 46 (0)31-772 1000

Cover:
Figure Buckling of full-threaded screws

Chalmers Reproservice / Department of Civil and Environmental Engineering
Göteborg, Sweden 2007

Compression perpendicular to the grain and reinforcement of a pre-stressed timber deck
Theoretical studies, Laboratory tests and FE-analyses
Master's Thesis in the International Master's programme Structural Engineering
SILVIO FORMOLO
ROLAND GRANSTRÖM
Department of Civil and Environmental Engineering
Division of Structural Engineering
Steel and Timber *Structures*
Chalmers University of Technology

ABSTRACT

The evolution of timber bridge decks has led to the development of stress-laminated timber bridge decks. This type of bridge is pre-fabricated in the factory and to be assembled at site. The use of transversal pre-stressing increases the performance of the deck in terms of both a structural performance and durability. The pre-stressing force introduces a concentrated compressive stress perpendicular to the grain and the magnitude depends on the load and choice of anchor configuration.

This thesis regards the improvement of the anchor region by increasing the glue-laminated timber's ability to withstand compression perpendicular to the grain caused by the pre-stressing force. The use of full-threaded screws as reinforcement is investigated. The failure in compression perpendicular to the grain is ductile. However, the consequence of failure, among others, is a great reduction of the pre-stressing force, thus reducing the overall performance of the deck. The choice of anchor configuration is therefore of great importance.

Since the pre-stressing force is concentrated on the glue-laminated timber deck, a behaviour that depends on the unloaded length presents itself. A secondary study is conducted around the effect of the unloaded length and compared to the different approaches proposed by current building codes.

This thesis is divided into several parts. The first part treats the technical evolution of timber bridge decks from a historical perspective and the principles regarding pre-stressing are introduced. The different aspects of compression perpendicular to the grain and the reinforcement with full-threaded screws are described in detail together with recommendations by different building codes. The second part regards the design of a new anchor configuration, laboratory tests, both in ultimate load carrying capacity and long-term behaviour in order to evaluate the effect of the reinforcement. Furthermore, FE-analyses are performed in Abaqus® both regarding the anchor configuration and the effect of the unloaded length in order to increase the knowledge about the behaviour of glue-laminated timber in compression perpendicular to the grain. Test showed that the use of screws as reinforcement increases the capacity in compression perpendicular to the grain with 50 to 85 % depending on the diameter of the screw thus reducing the loss of pre-stressing force over time. However, it is of importance to consider the plate thickness when designing the anchor since plate bending proved to be very disadvantageous considering the performance of the anchor.

Keywords: Stress-laminated timber bridge deck, anchor, pre-stressing, compression perpendicular to the grain, reinforcement with self-tapping screws, unloaded length effect

Tryck vinkelrätt fiberriktningen och förstärkning av förspända brodäck i trä
Teoretiska studier, Laboratorieförsök och FE-analyser
Examensarbete inom Konstruktionsteknik
SILVIO FORMOLO
ROLAND GRANSTRÖM
Institutionen för bygg- och miljöteknik
Avdelningen för Stål- och Träbyggnad
Forskargruppsnamn
Chalmers tekniska högskola

SAMMANFATTNING

Evolutionen av brodäck i trä har lett till utvecklingen av spännigs - laminerade brodäck. Den här typen av broar är prefabricerade i en fabrik och monterade vid byggplatsen. Användning av transversell förspänning ökar prestanda hos däcket både strukturmässigt och i termer av långsiktig hållbarhet. Förspänningen skapar en koncentrerad trycklast vinkelrätt fiberriktningen och storleken är beroende på förspänningskraften och ankarets utformning.

Den här uppsatsen sätter fokus på förbättringen av tryckkapaciteten vinkelrätt fiberriktningen i ankarområdet orsakat av förspänningskraften. Däröver är nyttjandet av skruvar som förstärkningsåtgärd, skruvarmering, undersökt. Tryck vinkelrätt fiberriktningen genererar ett segt brott, dock så är en konsekvens av brottet, bland andra, anmärkningsvärd reduktion av förspänningskraften samt en generell reduktion av prestanda hos brodäcket. Utformningen av ankaret är därav av stor vikt för att bibehålla prestanda hos däcket.

Då förspänningskraften är koncentrerad ger den upphov till en effekt som är beroende av den obelastade längden. En sekundär studie av detta fenomen är genomförd och jämförs med de riktlinjer som ges i olika aktuella byggnormer.

Uppsatsen är uppdelad i flera delar. Den första delen behandlar den tekniska utvecklingen av brodäck i trä ur ett historiskt perspektiv samt introduktion av principerna angående förspänning. Olika aspekter gällande tryck vinkelrätt fiberriktningen och förstärkning med helgängade skruvar avhandlas i detalj tillsammans med rekommendationer givna av olika europeiska byggnormer. Den andra delen beaktar utformningen av ett nytt ankar, laboratorieförsök med avseende på brottkapacitet och prestation under längre tid undersöks med motivet att evaluera effekten av förstärkningen. Utöver detta genomförs FE - analyser i Abaqus® med avseende att utvärdera och öka kunskapen om tryck vinkelrätt fiberriktningen i ankarområdet samt skapa en övergriplig förståelse för effekten av den icke belastade längden. De genomförda testen visade på en ökning av tryckkapaciteten vinkelrätt fiberriktningen med 50 till 85 % då förstärkning med skruvar av två olika diametrar tillämpats. En reduktion av förlust i förspänningskraft över tid kunde uppmätas då provkropparna var förstärkta. Det är dock av vikt att poängtera att plattans tjocklek inte kan förbises då det har visat sig att en för tunn platta leder böjning av plattan vilket i sin tur leder till oönskade konsekvenser då ankarets prestanda beaktas.

Nyckelord: Spännings - laminerade brodäck, förspänning, tryck vinkelrätt fiberriktningen, skruvarmering, effekt av den obelastade längden

Compressione perpendicolare alle fibre e rinforzo di un'impalcato da ponte in legno pre-tensionato
Studi teorici, prove di laboratorio e analisi agli elementi finiti
Master's Thesis in the International Master's programme Structural Engineering

SILVIO FORMOLO
ROLAND GRANSTRÖM
Department of Civil and Environmental Engineering
Division of Structural Engineering
Steel and Timber *Structures*
Chalmers University of Technology

ABSTRACT

L'evoluzione degli impalcati da ponte in legno ha portato allo sviluppo dell'impalcato da ponte in legno lamellare pre-tensionato. Questo tipo di ponte viene prefabbricato in fabbrica e assemblato in sito. L'impiego del sistema di pre-tensionamento trasversale incrementa le prestazioni dell'impalcato sia in termini strutturali che di durabilità. La forza di pre-tensione introdotta nel legno induce una concentrazione di compressioni ortogonali alle fibre la cui intensità dipendono dal carico applicato e dalla configurazione scelta per l'ancoraggio.

Questa tesi tratta il perfezionamento della regione di ancoraggio incrementando la capacità del legno lamellare a resistere alla compressione ortogonale alle fibre quando soggetto alla forza di pre-tensionamento. Come rinforzo viene considerato l'uso di viti a completo filetto. Anche se la modalità di rottura per compressione perpendicolare alle fibre é duttile, una tra le conseguenza della rottura é la perdita della forza di pre-tensionamento e quindi una riduzione delle complessive prestazioni dell'impalcato da ponte. La scelta della configurazione dell'ancoraggio risulta dunque di grande importanza.

Essendo la forza di pre-tensionamento applicata in modo concentrato all'impalcato da ponte, il comportamento dipendente dal confinamento viene a presentarsi. Uno studio secondario viene cosi condotto sull'effetto di confinamento e comparato con i diversi approcci proposti dalle diverse normative di calcolo in vigore.

La tesi é divisa in più parti. La prima parte tratta dell´evoluzione tecnica degli impalcati da ponte in legno da un punto di vista storico, successivamente viene introdotto il principio alla base del pre-tensionamento. Vengono descritti in dettaglio i diversi aspetti della compressione ortogonale alle fibre e del rinforzo attraverso viti a tutto filetto, considerando le prescizioni delle diverse normative di calcolo. La seconda parte riguarda il progetto della nuova configurazione di rinforzo del sistema di ancoraggio e delle relative prove di laboratorio effettuate per valutarne l´efficacia in termini di capacita portante ultima e di comportamento a lungo termine. Ulteriormente, si sono sviluppati dei modelli agli elementi finiti tramite il programma Abaqus® sia riguardanti le diverse configurazioni dell'ancoraggio sia riguardanti l'effetto di confinamento in modo da incrementare la conoscenza del comportamento del legno lamellare in compressione ortogonale alle fibre. Le prove effettuate mostrano che il rinforzo tramite viti a tutto filetto incrementa la capacità alla compressione ortogonale alle fibre dal 50 all'85% a seconda del diametro delle viti e nel contempo si riducono le perdite nel tempo della forza di pre-tensione. Tuttavia, é risultato importante considerare in fase di progetto lo spessore della piastra in quanto lo snervamento di questa produce una considerevole riduzione della prestazione dell'ancoraggio.

Paralole chiave: Impalcato da ponte in legno lamellare pre-tensionato, ancoraggio, pre-tensionamento, compressione perpendicolare alle fibre, rinforzo con viti autofilettanti, effetto di confinamento

Contents

Preface

This master thesis was carried out from September 2006 to February 2007 at the Division of Structural Engineering, Department of Civil and Environmental Engineering at Chalmers University of Technology in Göteborg, Sweden.

First of all, we would like to thank our examiner Professor Robert Kliger, for his continuous support during this thesis and all the literature borrowed from him, and Professor Maurizio Piazza at Università degli studi di Trento, for his collaboration.

We would like to thank our supervisor Dr. Eng. Roberto Crocetti, engineer at MOELVEN Töreboda AB, Sweden, for proposing the subject of the thesis assisting us throughout the work. We would like to thank him for the possibility to visit the factory and have the opportunity to collaborate with him.

We would also like to thank our supervisor Assistant Professor Mohammad Al-Emrani for his dedication and all the help.

Lars Wahlström deserves a big thank you for all the helpful and experienced assistance in the laboratory. From the practical point of view we learned a lot from him during the hours spent in the laboratory.

We would also like to thank our opponent Jobin Jacob and Olga Lucia Garzon Barragan for their interest and comments on the thesis.

This thesis gave us the possibility to improve our knowledge in the field of timber structures and obtaining practical experience during the end of our educational phase.

Finally, our gratitude goes to our relatives and the persons close to us for their support and understanding.

Göteborg February 2007

Silvio Formolo

Roland Granström

Notations

Roman upper case letters

A Contact area

A_{ef} Effective contact area

C Stiffness

E modulus of elasticity

E_L E-modulus longitudinal

E_R E-modulus radial

E_T E-modulus tangential

F Applied load

$F_{c,90,k}$ Characteristic capacity in compression perpendicular to the grain

$F_{c,90,d}$ Design capacity in compression perpendicular to the grain

G_{LR} Shear modulus longitudinal-radial

G_{LT} Shear modulus longitudinal-tangential

G_{RT} Shear modulus radial-tangential

J Modulus of inertia

K Rotational spring stiffness

M_S Applied moment

M_y Yield moment

M_t Transverse bending moment

N Pre-stressing force

N_i Initial pre-stressing force

N_{ki} Critical buckling load

N_{pl} Plastic axial force

P Critical buckling load

R_{90} Resistance in compression perpendicular to the grain

R Resistance of screw

R_{ax} Withdrawal resistance of screw

R_c Buckling resistance of screw

UL Unloaded length

V_t Transverse shear

Roman lower case letters

a Distance

b Width

c_h Horizontal spring stiffness

c_v Vertical spring stiffness

d Diameter

$f_{c,90,k}$ Characteristic compressive strength perpendicular to the grain

$f_{c,90,d}$ Design compressive strength perpendicular to the grain

f_1 Withdrawal capacity

f_y Yield strength

f_{ax} Withdrawal parameter

h Height

l Contact length

l_{sup} Length of support

l_{ef} Effective contact length

l_s Length of the screw

n Number of screws

n_{ef} Effective number of screws

k Coefficient

$k_{c,90}$ Amplification factor

k_{mod} Modification factor

t Thickness

w Deformation

Greek letters

α	Angle
β	Coefficient
ε	Strain
ϕ	Diameter
γ	Safety coefficient
λ	Slenderness ratio
μ	Friction coefficient
ν	Poisson coefficient
ρ_k	Characteristic density
σ	Stress
τ	Shear
ξ	Coefficient
Γ	Coefficient

1 Introduction

1.1 Background

Compression perpendicular to the grain is a common phenomenon that occurs in contact areas between two or more structural elements. The capacity in compression perpendicular to the grain is influenced by two parts. The first part treats the crushing of the fibres that occurs in the case of full loaded area, f_{c90k}, and the second part considers the effect of the unloaded length. The second effect is treated differently in different building codes and the phenomenon is therefore more complex to understand. In short, the unloaded length effect suggests that if only a segment of the total length is loaded the capacity in compression perpendicular to the grain can be increased. This is taken into account in the building codes as either a coefficient k_{c90} or as an effective length, l_{ef}.

The failure in compression perpendicular to the grain is ductile and therefore does not lead to immediate failure of the structure. However, failure in compression perpendicular to the grain leads to decreased performance of the structure. In stress-laminated timber bridge deck compression perpendicular to the grain is inevitable and since the pre-stressing force is of high magnitude the performance of the stress-laminated deck is highly dependent on the decks ability to withstand compression perpendicular to the grain. The design of the anchor that preserves the pre-stressing force and applies pressure on the timber deck is of crucial importance since it governs the zone in the timber which is to be compressed. In other words, the performance of the deck is not only related to the timber itself but also related to the design of the anchor and the anchor zone.

Compression perpendicular to the grain in stress-laminated decks and the ductile failure of the compressed timber results in loss of pre-stressing force due to creep, relaxation of the pre-stressing bar and shrinkage and swelling of the timber due to climatic changes. In order to reduce this loss and increase the capacity of the timber, applying reinforcement could give a solution to the problem by increasing and maintaining the performance of the structure. The use of self-tapping screws as reinforcement in compression perpendicular to the grain is a simple and cost effective method of reinforcement. An analytical model has been developed in the University of Karlsruhe and is designed to be compatible with the German code (DIN 1052:2004). This model treats both the capacity of the timber in compression perpendicular to the grain as well as the failure modes of the screws. The question has arisen whether the model of Karlsruhe is applicable with other building codes and whether the different approaches to the treatment of the unloaded length effect has any significant importance when designing a stress-laminated timber bridge deck and the ever so crucial anchors.

1.2 Aim

The subject of this thesis is to analyze the anchor zone of a stress-laminated bridge deck and improve the capacity in compression perpendicular to the grain by use of a new configuration. This is done by substituting the hardwood plate used today with a steel plate and by applying reinforcement in terms of self-tapping screws. In order to verify that the substitution is effective, laboratory tests and FE-models were conducted. The performance of the screws is of interest and the results obtained by tests and FE-analyses are to be compared to the analytical solutions proposed by the University of Karlsruhe. Furthermore, a secondary aim of this thesis is to consider the analytical approach to the unloaded length effect composed by different codes by performing a FE-model. A third aim of this thesis is to investigate the loss of pre-stressing force due to long term effects by performing laboratory tests in a controlled climate over a period of time.

1.3 Outlines

The work has been divided into several parts in order to satisfy the different aims.

The first part, Chapter 2 to Chapter 4, treats the literature study regarding different types of timber bridge decks and their evolution in a historical point of view up to the stress-laminated timber bridge deck where the pre-stressing system is introduced. Some different examples of decks are presented in order to represent the versatility of different decks. Furthermore, compression perpendicular to the grain is explained in general and more in detail when considering the effect of the unloaded length. The analytical model of reinforcement with screws is presented and comparison with previous test and reinforcement with full-threaded screws are also described and different approaches in different building codes are introduced.

In the second part, Chapter 5, the laboratory tests are described and in the end the results are presented. In this chapter, the design of the specimen and the anchor is introduced and both short term and long term test configurations are explained together with comments of the results obtained.

In the third part, Chapter 6, the FE-modelling is described and the results are displayed and commented. The FE-model are divided in two part, the first that regard the test configuration described in the previous chapter and the second that regard the study of unloaded length effect by adopting the configuration used in the test performed by Reichegger, [11].

In the final part, Chapter 7, the conclusions and further research regarding this subject is presented. Furthermore, Chapter 7 puts light on problem areas that need to be refined and further investigated and topics that was not possible to treat in this thesis.

2 General introduction to timber bridge decks

This chapter deals with the development and evolution of timber bridge decks. The report was written concerning this topic in the University of Arkansas, USA, [16].

The principal purpose of a bridge deck is to distribute the load from the traffic to the supporting elements of the bridge. If the deck is designed as a structural diaphragm, it can be used as a key load-bearing element by itself. It can also brace other main components, and transfer horizontal wind or brake loads through to other parts of the structure, and ultimately to the foundations.

Depending of the location, a secondary function of the deck may be to protect the main structure from moisture and mechanical damage from the traffic. An effective and durable protection of substantial parts of timber structure may be achieved with closed, high decks.

Timber bridge decks include plank decks, nail-laminated decks, glue-laminated decks and stress-laminated decks. The choice of what type of deck that is suitable depends on the traffic density, expected life of the bridge and economics.

2.1 Different types and historical evolution

2.1.1 Transverse plank decks

The bridge is composed by stringers with a series of transverse plank deck members, see Figure 2.1. The deck planks have to carry a moment effect of the wheel load when it is located between the stringers and applied directly to the planks. This requires more stringers since the span of the planks must be kept small.

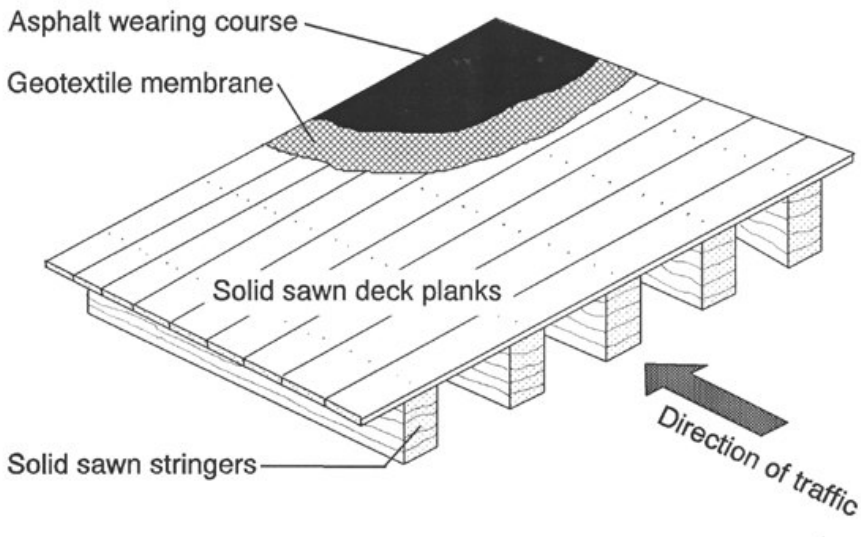

Figure 2.1 Example of a transverse plank deck, [16]

2.1.2 Nail-laminated transverse decks

In the effort to spread the stringers further apart and reduce the need of stringers, the first form of lamination was invented, see Figure 2.2. The deck pieces were turned on edge and nailed to one another. At first the planks were nailed in sequence in the field, later the deck was done in modular widths in the factory. This type of deck does not provide any additional longitudinal strength to the longitudinal stringers since it only distributes the wheel load and adds dead load.

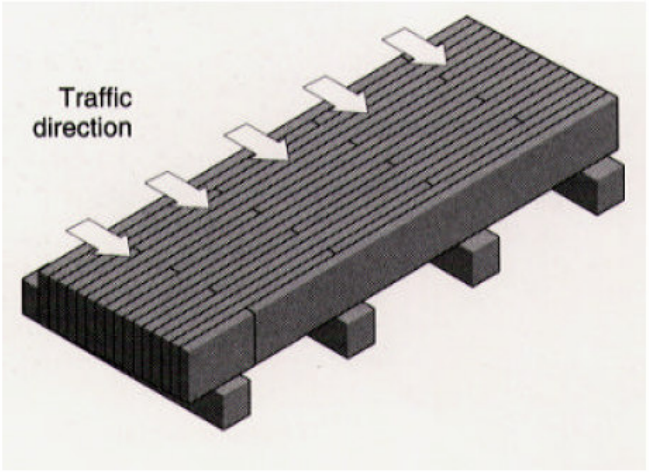

Figure 2.2 Example of a nail-laminated transverse deck, [16]

2.1.3 Dowel-laminated transverse decks

A procedure was developed so that deck section could be composed in a factory by prefabricated transverse panels with uniform width and connectors as dowel spread out in a triangular pattern. An overlapping was also introduced in the connection interface by means of "half deep" planks added to the modular transverse panels, see Figure 2.3.

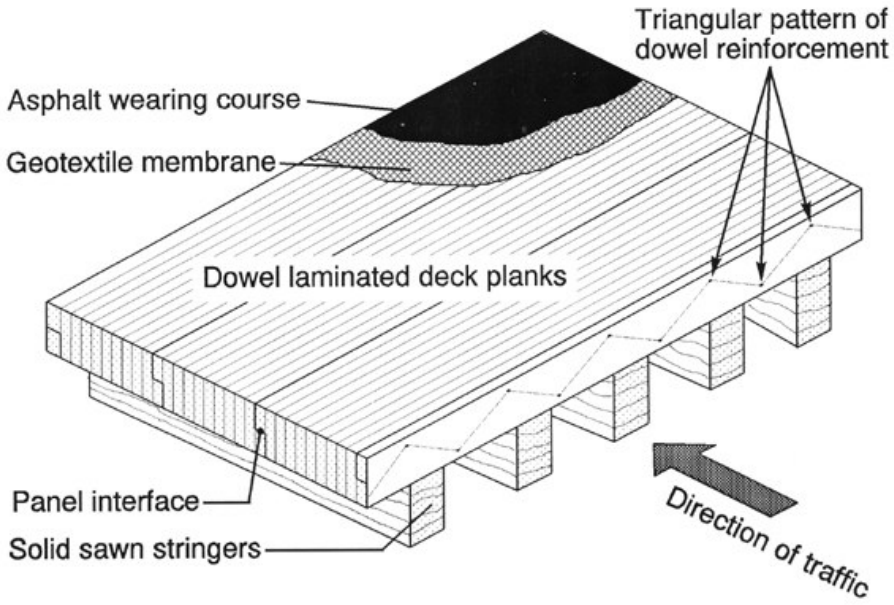

Figure 2.3 Example of a dowel-laminated transverse deck, [16]

2.1.4 Glue-laminated transverse decks

The use of flexural stronger decks and the need of longer spans led to the development of the glue laminated timber bridge deck. The glue-laminated timber was used in both the stringers and the deck panels, see Figure 2.4. The transversal decks were again made in modular widths and the stringers in standard widths. The number of laminations was selected to give a depth needed to reach the flexural strength and stiffness required for a given amount of stringers and deck span. With that method, the material could be used in the most efficient way as possible.

Because the stringers could become quite deep and yet remain rather narrow, as one tries to expand the span and decrease the number of stingers, there is a need of introducing lateral supports between the stringers for resisting to the effect of lateral torsion buckling.

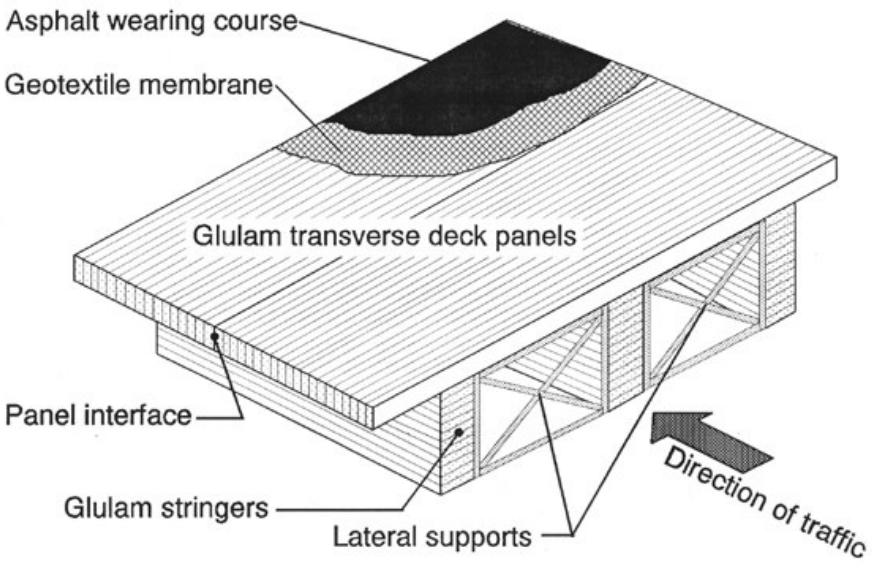

Figure 2.4 Example of a glue-laminated transverse deck, [16]

Another issue introduced when using glue-laminated transverse deck panels side by side was the problem of shear transfer between the two panels. As a wheel load moves forward to the edge of a panel, that panel is vertically displaced on one side of the panel interface and the panel ahead of it is not. Therefore, it was necessary to find a way to lock the deflection of the two adjacent panels, for example by using dowel-type connectors, see Figure 2.5.

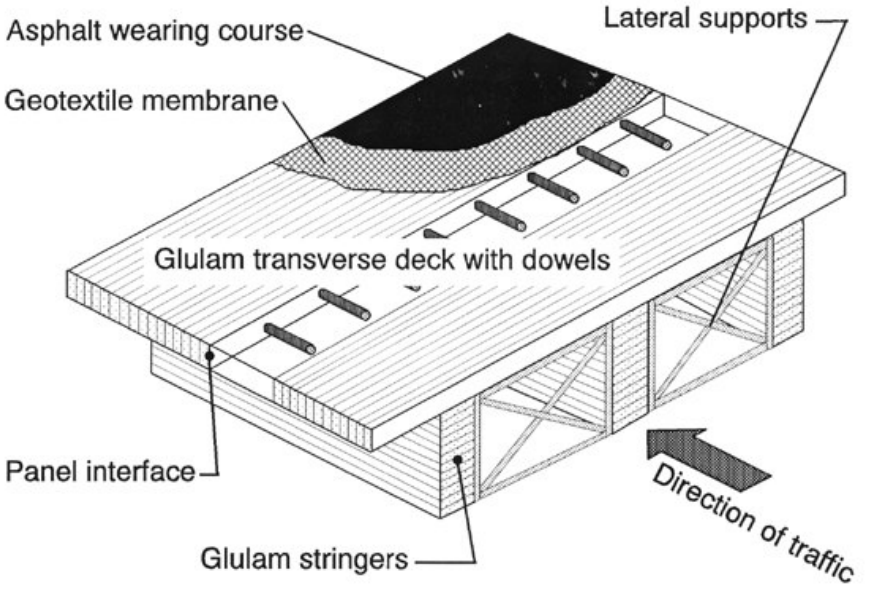

Figure 2.5 Example of a glue-laminated transverse deck with dowels, [16]

2.1.5 Longitudinal nail-laminated decks

Improvements of the procedures of lamination and the influence of many reinforced concrete bridges led to the use of longitudinal decks. In that way the decks worked better under the lateral actions, in fact, the transverse stiffness was higher. In longitudinal laminated decks, the timber laminations are oriented parallel to the direction of the traffic. Further development led to the use of longitudinal dowel-laminated decks; see Figure 2.6 and Figure 2.7.

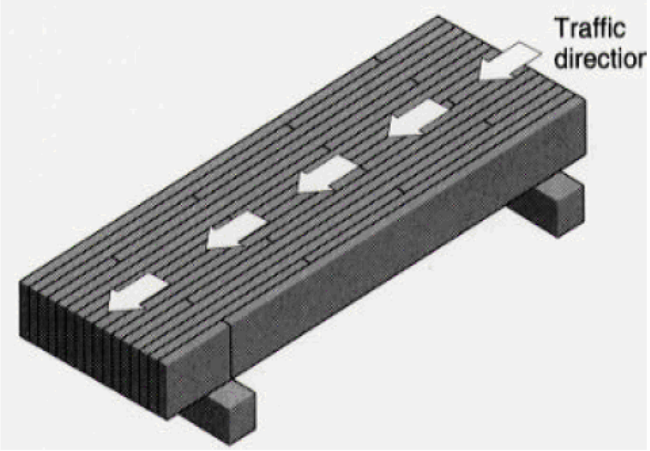

Figure 2.6 Example of a longitudinal nail-laminated deck, [16]

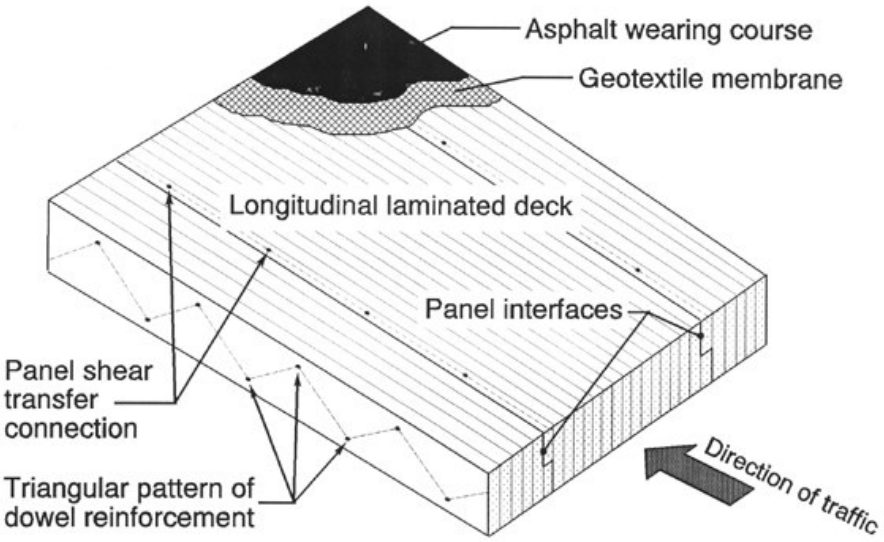

Figure 2.7 Example of a longitudinal dowel-laminated deck [16]

2.1.6 Stress-laminated decks

The next technological improvement was the development of stress laminated decks; see Figures 2.8, 2.9 and 2.10.

It was initially introduced in Canada as a method of strengthening existing longitudinal decks then the same principle was applied also to new bridges. Pre-drilled holes spacing along the span at a regular interval were made at mid-depth of the decks. Then high strength rods were inserted and then pre-stressed using distributed or individual anchors. The pre-stressing introduced lateral pressure between the timber sections so that friction forced them to act as a large block of timber. This was done in order to add the transverse orthotropic strength of the total bridge and, therefore, the longitudinal resistance as well. However, in this method there are some losses of flexural efficiency in the deck. The presence of butt joints, due the limited length of the laminate, does not allow the bending capacity to be developed fully when considering the cross-section of the deck.

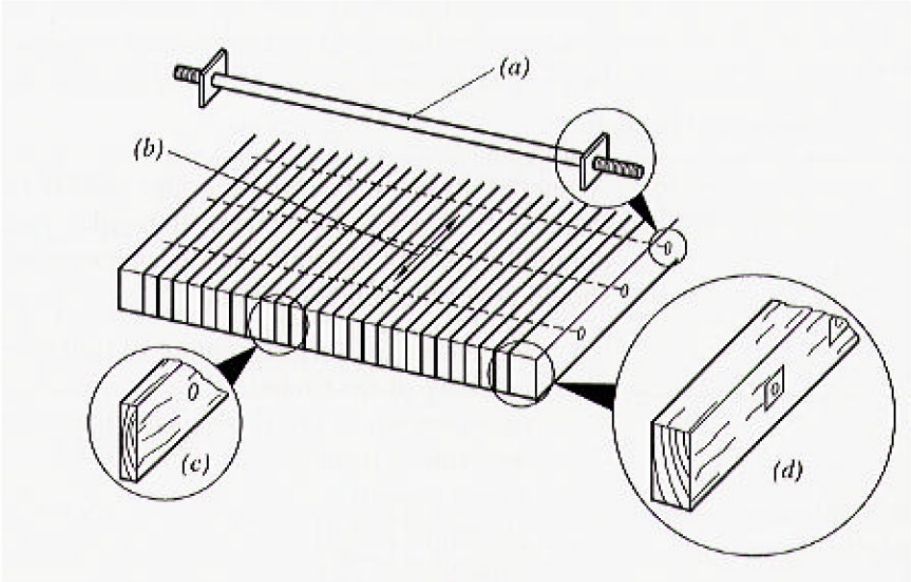

Figure 2.8 Example of stress-lamination, [16]

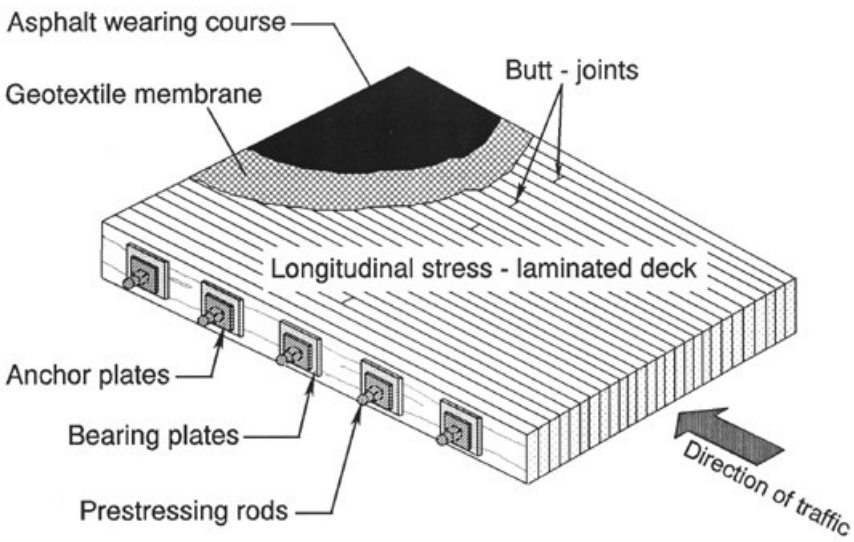

Figure 2.9 Example of a stress-laminated timber deck, [16]

The deck is typically delivered to the building site in panels of full span length, and then assembled side by side. This reduces the building time at the construction site and can be considered as a great advantage.

The deck consists of glue-laminated timber sections placed side by side spanning from one abutment to the other before stress laminated together through pre-drilled holes. The increased depth of the glue-laminated beams may require use of two or more levels of pre-stressing rods.

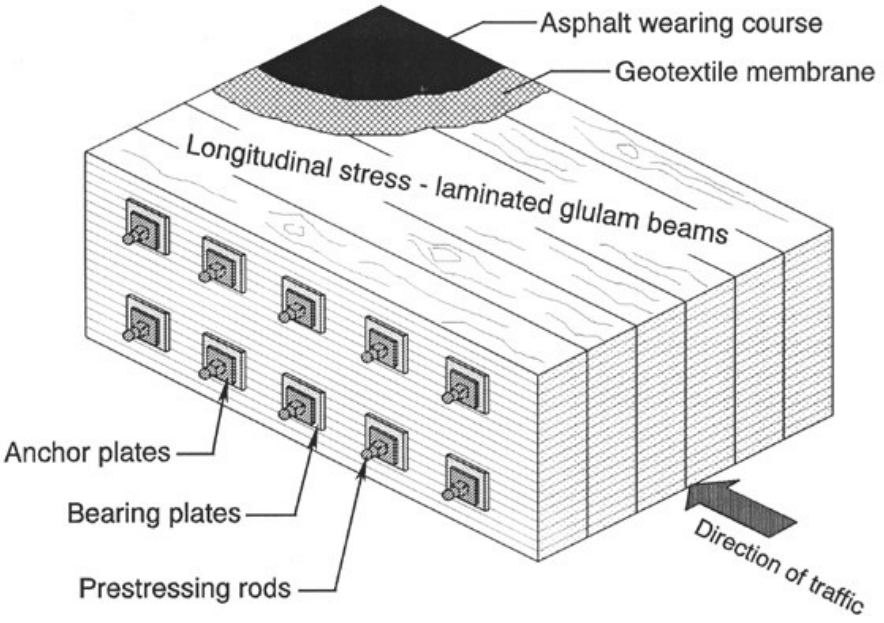

Figure 2.10 Example of a stress-laminated glue-laminated timber deck, [16]

Continued development of the technology regarding timber bridges generated more economical types of configuration and achieving longer span lengths for significant increase in load. As an example, Figure 2.11 illustrates two sections of assembled stress-laminated box girder bridges. The first type was built in Washington County in Northwest Arkansas. The section consists of primarily "I" sections spanning the full length between the abutments. The webs are full depth glue laminated sections to which flanges have been added on both sides by means of dowel lamination. The bridge edges are closed by "C" shaped sections at both side. These sections have dowel-laminated flanges on only one side. When all the sections are in place the pre-stressing rods are applied through pre-drilled holes in the flanges and through the upper webs of the "I" sections. The bar is then anchored at both ends, and tensioned to a suitable value. This tension force will have to be re-established later due to the presence creep in the timber and relaxation of the steel which both reduces the pre-stressing force.

The second type of box section seen in Figure 2.11 is a set of side by side "box" sections. These are easier to construct, and the effect of creep in the timber is also reduced compared to the first section seen in Figure 2.11.

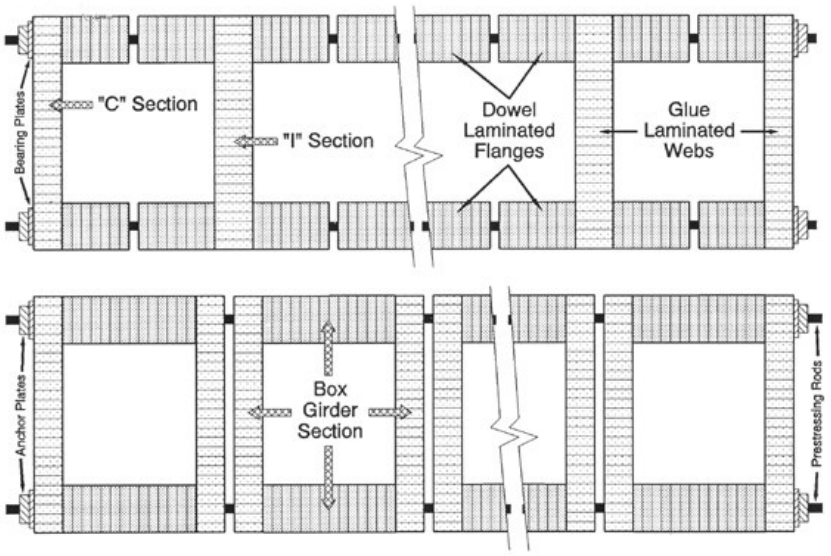

Figure 2.11 Examples of two different types of "box" sections, [16]

Furthermore, recent developments in Fibre Reinforced Plastics (FRP) have enabled a "T" type of section that can be used together with stress-laminated timber, see Figure 2.12. The flanges are pre-stressed together with the glue-laminated timber webs creating the "T" section. The FRP is used at the lower parts of the webs to increase the longitudinal tensile capacity of the section.

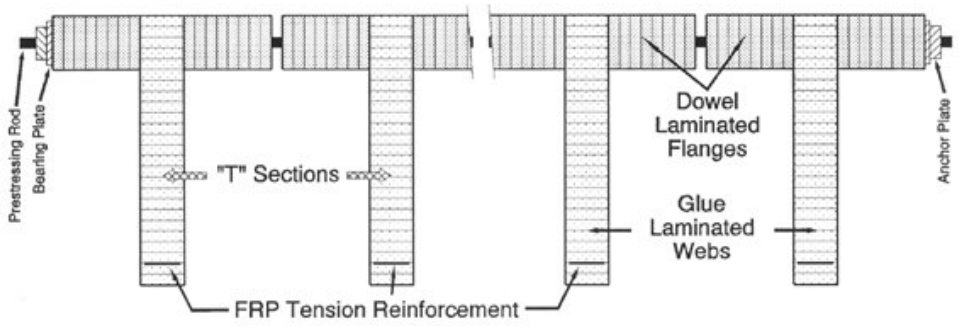

Figure 2.12 Example of stress-laminated timber section with FRP-reinforcement, [16]

2.2 Pre-stressing phase of stress-laminated bridge

The pre-stressing phase is the most important phase of the construction of a stress-laminated bridge because it holds the bridge together and develops the necessary friction for load transfer between the laminations. Thus, it is important that the bars are properly tensioned and a uniform compressive pre-stress are maintained. The most common way to do that is by use of singular hydraulic jacks. The equipment needed and the procedure and sequence adopted are described in the sequent paragraphs. This topic was discussed in a book written by Ritter, [14].

2.2.1 Tension equipment

Stress-laminated bridge decks are stressed together with a hydraulic jack that applies tension to the pre-stressing bar by pulling the bar away from the anchor plate. After bar tension is applied, the nut is properly tightened so the tension in the bar remains locked when the hydraulic jack pressure is released. The typical equipment for bar tensioning consists of a hydraulic hollow-core jack, compressor, hose and gauge, steel tensioning chair and backnut, see Figure 2.13. Some recommendation should be considered regarding the equipment:

a) *b)* *c)*

Figure 2.13 Tension equipment: a) hydraulic hollow-core jack, b) tensioning chair and c) backnut

- The capacity of the jack must be sufficient to provide the design tension force
- The scale of the hydraulic gauge attached to the pump may be calibrated in units of jack force. If the gauge is calibrated for hydraulic pressure, a table that convert pressure to the jack in unit of jack force must be provided.
- The steel tensioning chair is usually fabricated locally. An example is shown in Figure 2.11. It is important that the legs of the chair are direct applied over the anchor plate and the contact is large enough to spread the pre-stressing force.
- To tension the bar properly, there must be sufficient bar length beyond the nut to place the tension equipment. Instead of in the other side the bar must be extended beyond the nut for about 25 mm.

2.2.2 Bar tensioning procedure

To tension the bars in the stress-laminated bridge decks, normally one deck edge is chosen and on this edge the bars are consequently extended. The equipment is heavy and proper steps must be taken to ensure workers safety. If the bridge is close to the ground, the equipment can be lifted onto the bars from beneath the bridge. For higher bridges, ladders or scaffolding should be used and worker safety lines provided when necessary. The following steps outline the recommended procedures for bar tensioning.

Figure 2.14 Assembly of tension equipment

1. Place the chair and jack on the bar after assembly the anchor configuration on both deck edges.

2. Place the backnut on the bar. Provide a small gap of approximately 5 mm between the backnut and the jack to prevent binding when the hydraulic pressure is released.

3. Apply hydraulic pressure to the jack until the gauge indicates the required reading. It is common to apply 5-10 % greater force to compensate the loss when the nut is tightened.

4. Tighten the nut against the bridge anchor plate using an open –end wrench.

5. Release the pump hydraulic pressure slowly and remove the tensioning equipment.

During all bar tensioning procedures, it is important that personnel do not stay in line with or beneath the bar or place hands or other body parts on or near the tensioning equipment. In case of breaking, high bar force is suddenly released and the bar can exit at great force and speed and cause serious injury or death.

2.2.3 Tensioning sequence

For a stress-laminated bridge to function properly, all bars must be tensioned properly to the design force in order to reach a uniform transverse compression of the deck. To minimize bar tension loss due to the relaxation of the steel, creep and shrinkage in the timber, bar tensioning should be completed in different times during the construction process. When using a single hydraulic jack, tensioning the sequent bar brings a decrease of pre-stressing force in the adjacent bar. To compensate this effect, bars must be sequentially tensioned several times to equalize the force. This is generally done by tensioning the first bar in one end and sequentially tensioned each successive bar along the bridge length. The process is repeated several times

until all bars are fully tensioned to the design level. The sequence adopted is not unique and can depend on the specific case and site condition. Adequate care must be taken to prevent a distortion of the deck edge. For example a sequence used in United States for stress-laminated bridges can be suggested, [12]:

1. Starting at one end of the bridge, sequentially tensioning each bar to approximately 25% of the design level.

2. Following the same procedure, one week after the first tensioning, tension each bar to approximately 50% of the design level.

3. Starting at one hand again, sequentially tension each bar to design level.

4. Return to the first bar and repeat step 3.

5. Check the force in several bars using the procedures. If the force is 10% or more below the design level, re-tension the bar.

6. All these steps are repeated several times during the construction process after the initial pre-stressing in order to reduce the loss of pre-stressing force. In Figure 2.15 it is possible to compare this effect for different sequences normally used in practice.

It is recommended in the end to check the bar force in order to ensure that the bridge performs properly over the design life.

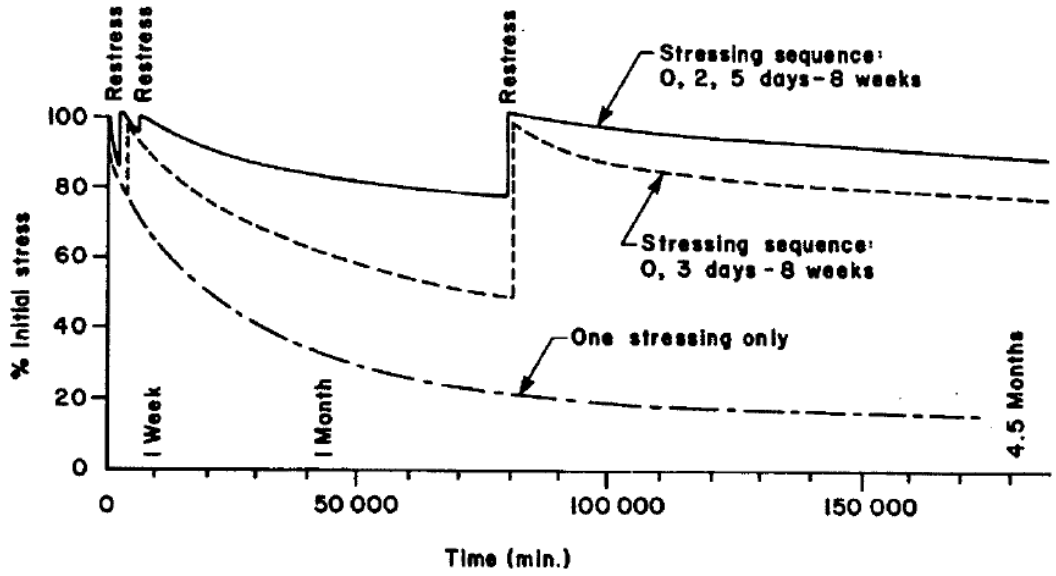

Figure 2.15 Loss of pre-stressing force over time and pre-stressing effects, [14]

2.3 Pre-stressing force

2.3.1 Principle function of pre-stressing in the stress laminated decks

As previously discussed, adding transverse compressive stress in stress-laminated decks makes the different pieces act as a large plate that is held together by compressive forces applied through the pre-stressing elements. In the book by Ritter, [14], this phenomenon is discussed further. When subjected to vehicle load, the deck behaves as an orthotropic plate with different properties in the longitudinal and transverse directions. When a wheal load is applied at a point on the deck, the entire deck deflects, resulting in displacement in both longitudinal and transverse directions. Due to this behaviour, bending moment is also developed in longitudinal and transverse directions. The magnitude of these moments depends on five variables: load magnitude, deck span, deck width, longitudinal deck stiffness, and transverse deck stiffness. The transverse moment, which also produces bending stress and deflection, decides the amount of compressive pre-stress that must be applied between the laminations. When a truck wheel load is placed over the deck, two primary actions occur that weakens the plate behaviour of the deck, see Figure 2.16. The first action (on the left) result from transverse shear, which creates a tendency for vertical slip between the laminations. The second action (on the right) results in transverse bending, which produces a tendency for opening up the laminations on the underside of the deck.

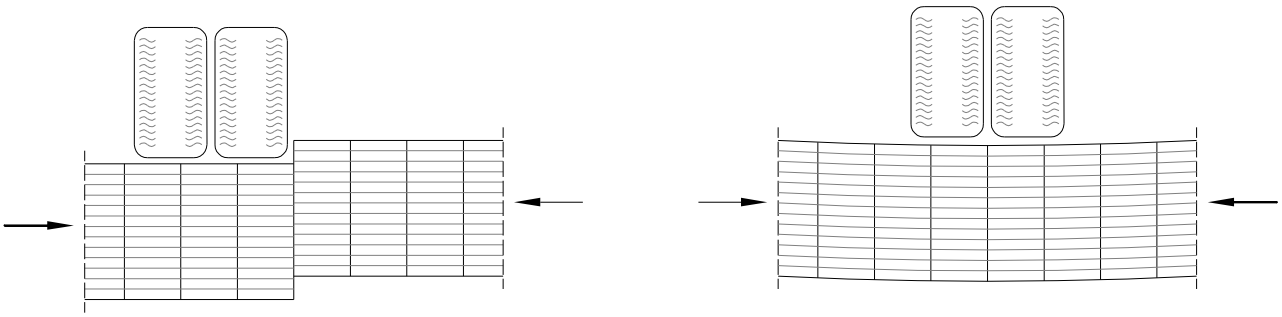

Figure 2.16 Action of the wheel load on stress-laminated glulam deck, [14]

In both cases the actions do not occur if a sufficient compressive pre-stress is applied between the laminations, see Figure 2.17. In the case of transverse bending the compressive pre-stress compensates the tensile stress on the underside of the deck. Regarding shear, the compressive pre-stress prevents the slip by friction between the glue-laminated beams. For this reason an adequate level of compressive pre-stress must be maintained during the lifespan of the bridge.

Figure 2.17 Transverse stress fields in the stress-laminated glulam deck, [14]

2.3.2 Calculation method of the required pre-stress level

The level of compressive pre-stress between the laminations must be sufficient to offset flexural tension stress caused by transverse moment and slip caused by transverse shear. For stress-laminated deck design, the level of uniform pre-stress must be determined for two conditions; in service and at installation. The pre-stress level in service represents the minimum compressive pre-stress required for adequate deck performance, assuming all time-related stress loss has occurred. The pre-stress level at installation is the amount of pre-stress that must be introduced into the deck at time of stressing.

The minimum level of uniform compressive pre-stress in service, N, is the largest value obtained from the following equations, see equation (2.1), but not less than 0.28 MPa:

$$N = \max\left\{\frac{6M_t}{t^2}\,;\frac{1.5\cdot V_t}{t\cdot\mu}\right\} \tag{2.1}$$

Where:

N is the minimum uniform compressive pre-stress in service [MPa]

Mt is the transverse bending moment due the applied wheel load [kN]

Vt is the transverse shear due the applied wheel load [kN]

μ is the coefficient of friction

Over the bridge life, timer-related creep losses appear. If it is assumed that the level of compressive pre-stress is reduced to 40 % of the initial level at installation (60% stress loss), The level of uniform pre-stress at the time of installation, N_i must be greaten than 2.5 times the minimum required pre-stress level in service, as calculated by

$$N_i - 0.6\cdot N_i \geq N \rightarrow N_i \geq 2.5\,N$$

Where:

Ni is the level of uniform compressive pre-stress required at the time of installation, [kN]

3 Compression perpendicular to the grain

3.1 General introduction

The timber is a material with high anisotropic behaviour and with different mechanisms of failure for different inclination of the applied load with respect to the direction of the grain. This aspect is crucial during the design process and is mainly due to the elongated shape of the wood cells and the oriented structure of the cell walls. The cells of the timber can be schematised as a simplified model with a series of tubes connected together with elastic glue that represent the lignin. This simplified model has limitations due the fact that the structural timber and glue-laminated timber has knots and other characteristics governed by the natural growth of the trees. This means that on the structural point of view these characteristics are considered as defects. Also other more complex models were developed but considering the aim of this thesis, it is not of main importance. However, it is important to notice that when compression perpendicular to the grain are introduced the fracture is reached in a layer where the weakest cells are placed and buckling failure of the cells are achieved due the radial compression stress. In the sequent pictures this radial compression failure behaviour of the cells is shown on a micro-structural level, see Figure 3.1.

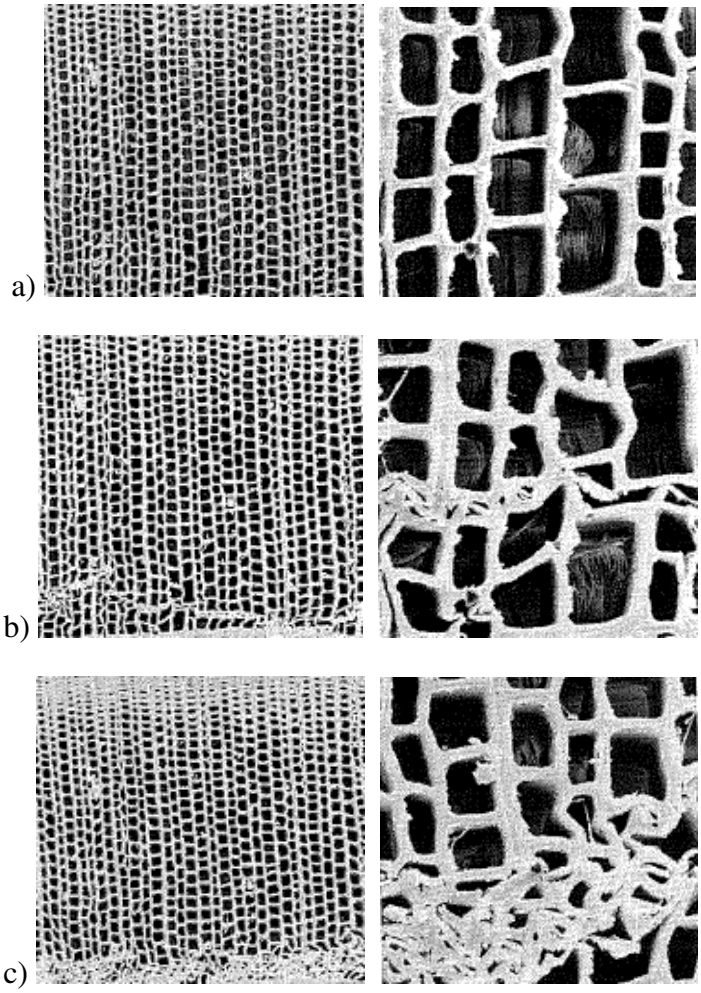

Figure 3.1, Micro-structural deformations for radial compression load. a) Un-deformed b) single layer failure c) Multi layer failure, [10]

High compression perpendicular to the grain occurs when a concentrated force of compression is introduced in the timber. These situations are common in many locations in the timber

structure. In Figure 3.2 some typical situations are displayed where particular care must be considered during the design procedure:

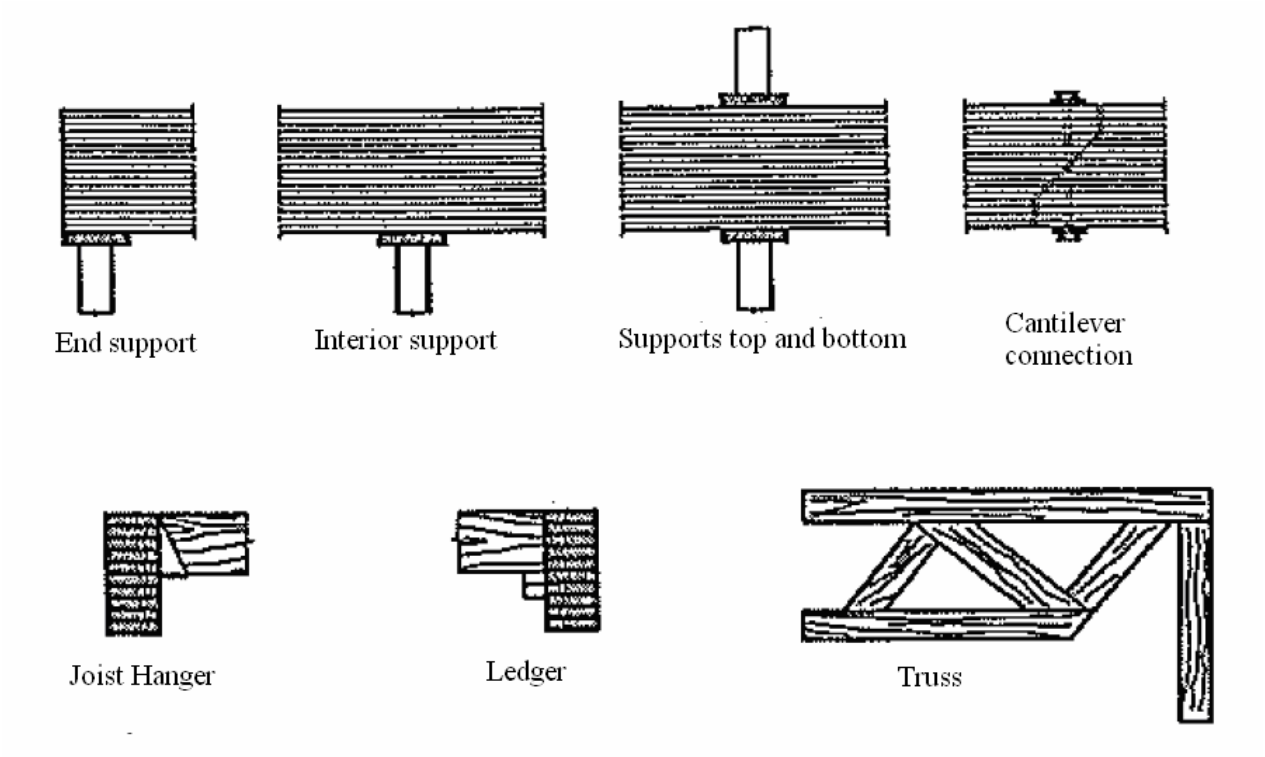

Figure 3.2 Examples where the compression perpendicular to the grain are introduced in the timber member, [4]

In most situations where a concentrated compressive load is applied an intermediate element is introduced, e.g. by using a steel plate. By using a steel plate a uniform pressure is achieved which is favourable since it generates uniform deformations in the timber subjected to the load. In some cases like in the truss connections the loads are introduced with timber to timber contact without an intermediate element. The compression perpendicular to the grain does not develop a brittle failure mechanism, considering the ultimate limit state; however high unfavourable levels of deformation could bring the behaviour of the structural system out of the serviceability limit state. Furthermore, compression perpendicular to the grain can also be found in anchor systems, seen in Chapter 2, where high concentrated loads due to the pre-stressing force are distributed into the elements by a relatively small surface.

The mode of failure for compression perpendicular to the grain can easily be shown by considering the support zone of a timber beam loaded by a steel plate, see Figure 3.3. The compression on the surface of the applied load induces an accumulation of the fibres close to the support. This effect can be modelled as an elastic bed of evenly distributed springs, whose strain represents the penetration of the steel plate in the timber. The progressive deformation consists of a progressive collapse of the cellular planes, with a subsequent increase of the density in the material close to the load, c.f Figure 3.1. In this case, the cells collapse close to each other and generally in the same horizontal plane as the first rupture. Even if all the cells in the horizontal plane are collapsed, the material is still able to display a load bearing capacity, as the load increases due to the applied load the second plane collapses and so on.

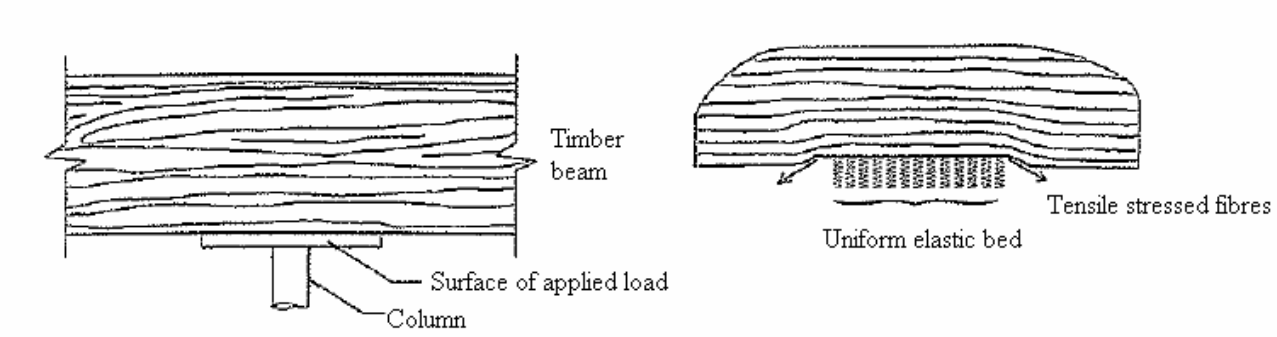

Figure 3.3 Beam on column support (left), Deformations modelled as an uniform elastic bed (right), [4]

The capacity of the element is based on the strength perpendicular to the grain, $f_{c,90,k}$, as a function of the timber class. This value is obtained by an axial compression test. It is of interest to notice that, to be separated from the stress field regarding tension, imperfections in the timber does not have influence the compression strength perpendicular to the grain negatively, and sometimes the knot could limit the local deformation.The two main parameters that influence the load-bearing capacity in compression perpendicular to the grain regarding a specific timber class are:

- Crushing of the fibres perpendicular to their axes
- The effect of the unloaded length

3.2 Definition of the load carrying capacity according to UNI EN 408

It is possible to estimate the strength in compression perpendicular to the grain $F_{c,90,max}$ of the tests performed with reference to the standard UNI EN 408 (substitutes the old version, UNI EN 1193). The following iterative procedure is considered:

Estimating the value of the load $F_{c,90,max}$ by using the results of the test, then plotting the curve of load/deformation in the form illustrated in Figure 3.4. Then by calculating 0,1 $F_{c,90,max}$ and 0,4 $F_{c,90,max}$ and determining where these two values intersect the load/deformation curve. By using these two points a straight line 1 as illustrated in Figure 3.4 can be drawn. Parallel to straight line 1, another straight line, 2, with the deformation at the origin F = 0 equal to 0,01 h_0 as illustrated in the figure can be drawn. $F_{c,90,max}$ corresponds to the value of F that corresponds to the intersection point of line 2 and the curve of the test results. If the value of $F_{c,90,max}$ as determined is within 5% of the estimated $F_{c,90,max\ ,est}$, this value can be used to calculate the strength in compression; otherwise, the procedure is repeated until the value of $F_{c,90,max}$ is inside the tolerance.

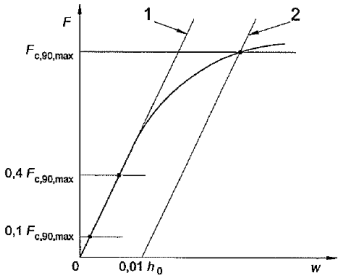

Figure 3.4 Calculation procedure of the ultimate load carrying capacity

3.3 The effect of the unloaded length

Compression perpendicular to the grain is described in STEP 1 [1] both for regular timber and generally for structural timber as glue-laminated timber. Four different cases can be identified for a timber specimen subjected to compression. The four different cases are separated by the length the load is applied on, see Figure 3.5. These tests were made by Suenson in 1938.

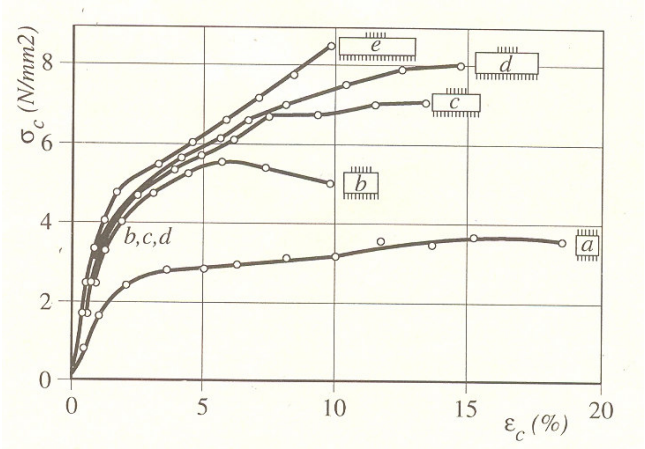

Figure 3.5 Applied stress perpendicular to the grain vs. vertical compressive strain from tests on timber, the loaded surface is 15 x 15 cm^2 (Suenson 1938). [1]

Case a) represents a situation where the whole specimen is loaded. The consequences are that the fibres are crushed when the "yielding-load" is reached. When this maximum load has been reached the deformations increases greatly with small change in load.

Case b) represents a situation where just a portion of the element is subjected to the compressive load; in this case the stiffness of the specimen is higher than for case a) thus the change in stiffness will occur at a higher stress level. The change in stiffness is less distinct compared to case a), this is shown by a smooth bend in the stiffness diagram, see Figure 3.5.

Cases c), d) and e) represent the influence of increased proportions of unloaded length compared to loaded length. The more of the specimen that is unloaded the greater the volume that can take the load hence higher stresses can be reached before failure. The reason for this is that the concentrated load will be carried over by the fibres to the neighbouring unloaded parts. However, the deformations will be considerable this is explained as local crushing due to patch loading.

Also another series of tests were performed for understand the effect of unload length. These tests were performed in Trento, Italy by Reichegger [11]. Different geometries of the specimens are taken into account, see Table 3.1.

Table 3.1 Test configuration investigated by Reichegger, [11]

n°	Dimension [mm]	Glulam	Plate	Dimension [mm]
2	80x120x200	GL24 or BS11	steel	120x120
2	120x120x200	GL24 or BS11	steel	120x80
2	200x120x200	GL24 or BS11	steel	120x80
2	300x120x200	GL24 or BS11	steel	120x80
2	400x120x200	GL24 or BS11	steel	120x80

The tests were performed as follows. A compression force was applied on a steel plate in a symmetric configuration and instruments measuring the magnitude of the force and the displacement of the timber were placed on both sides. Consequently, the deformation of the specimen was calculated as the average value of the pair of displacements divided by the height of the specimens, as seen in equation (3.1).

$$\varepsilon = \frac{\sum_{1}^{2} \Delta l_i}{2 \cdot h} \tag{3.1}$$

Where:

Δl_i is the measured displacement according to the instrument i, where i = 1 or 2

h is the height of the specimen

The stress in compression perpendicular to the grain was calculated as seen in equation (3.2).

$$\sigma = \frac{F}{A} \tag{3.2}$$

Where:

F is the applied load

A is the area of the applied load

In this way it was possible to rule out the difference in height and compare the results in terms of epsilon rather than displacements. All the test results made by Reichegger, [11], share these properties.

For the evaluation of the characteristic strength both the European standard UN1193 and American standard ASTM D143 were used. Furthermore, a comparison with the characteristic capacity in according to different codes was made. The following codes were taking into account when evaluating the test results:

- DIN 1052-1996
- UNI ENV 1995-1
- DIN 1052-2000
- DIN 1052-2002
- NiCoLe (The version of the Italian code prior to CNR-DT 206:2006)
- prEN 1995-1-1:2003

The results of the tests performed regarding the unloaded length can be viewed in Figures 3.6 to 3.10.

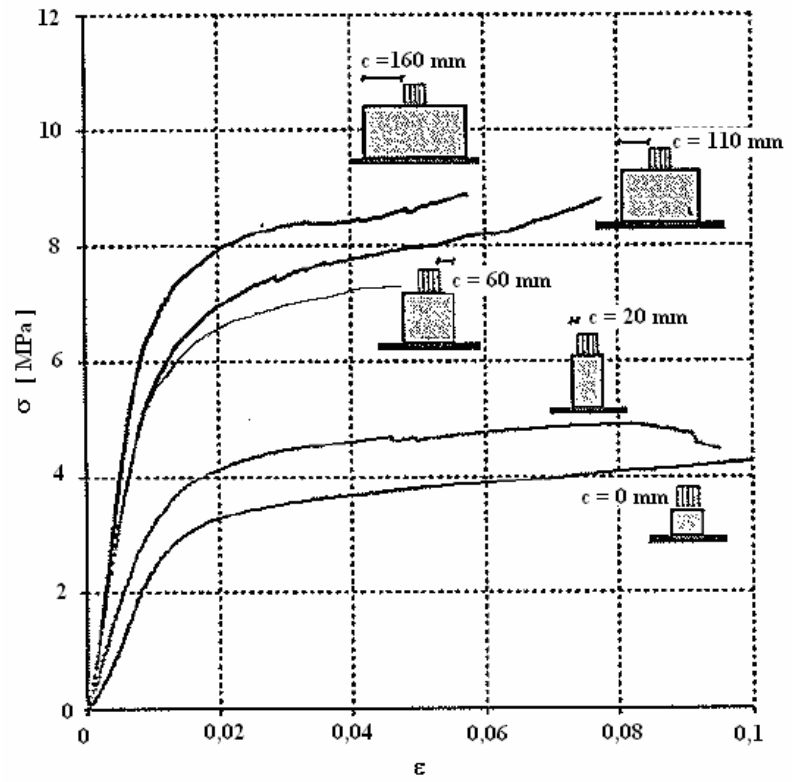

Figure 3.6 σ–ε curves of mean values from tests results of the different tests configuration, [11]

It can be seen in Figure 3.6 that the capacity increase as the unloaded length increases. Furthermore, the elastic stiffness increases with increase of unloaded length. The test results prove the theory by Suenson, [1]. This behaviour is due the fact that with an increase of the unloaded length, the fibres close to the support are anchored and for this reason there is a limitation to the transverse deformation of the specimen close to the applied load. Also, in the plastic behaviour it is possible to notice that with the increasing of the unloaded length the curves has a higher inclination which shows signs of continuous plastic deformations until the whole specimens reach full plasticity.

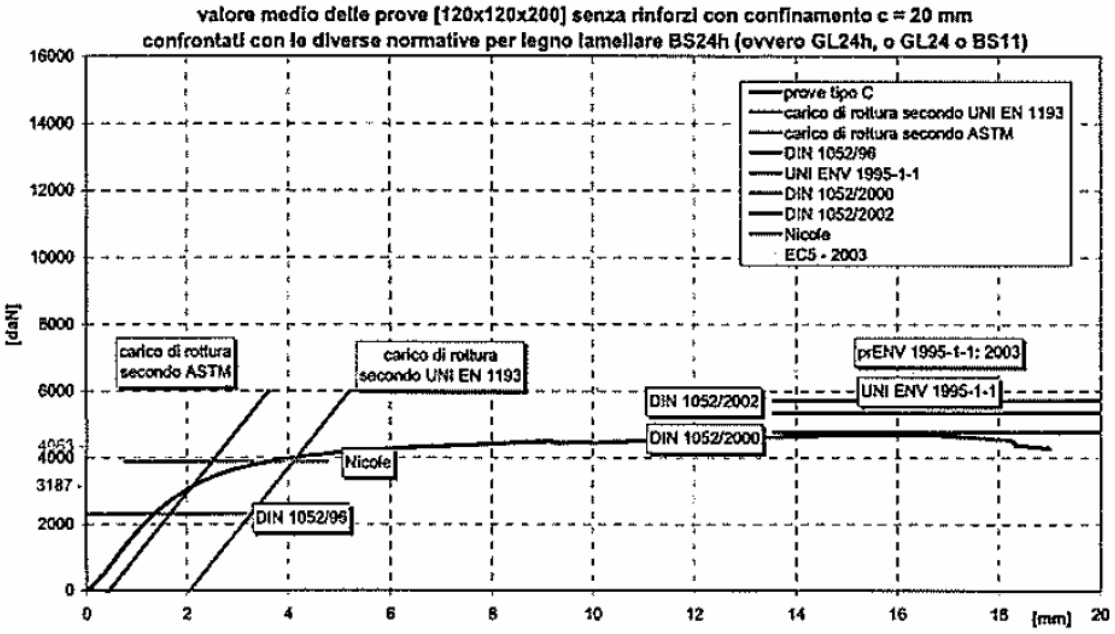

Figure 3.7 F–d relationship of mean value of test results on [120x120x200] specimens and a comparison with the characteristic strength in accordance to EN 1193 and different codes, [11].

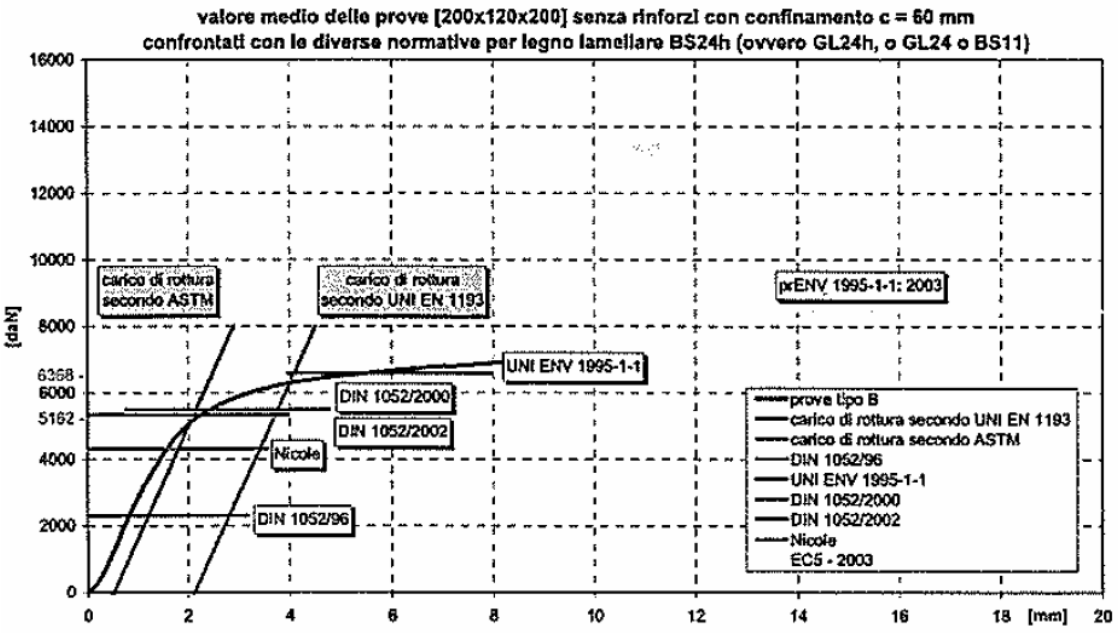

Figure 3.8 F–d relationship of mean value of test results on [200x120x200] specimens and comparison with the characteristic strength in accordonce to EN 1193 and different codes, [11].

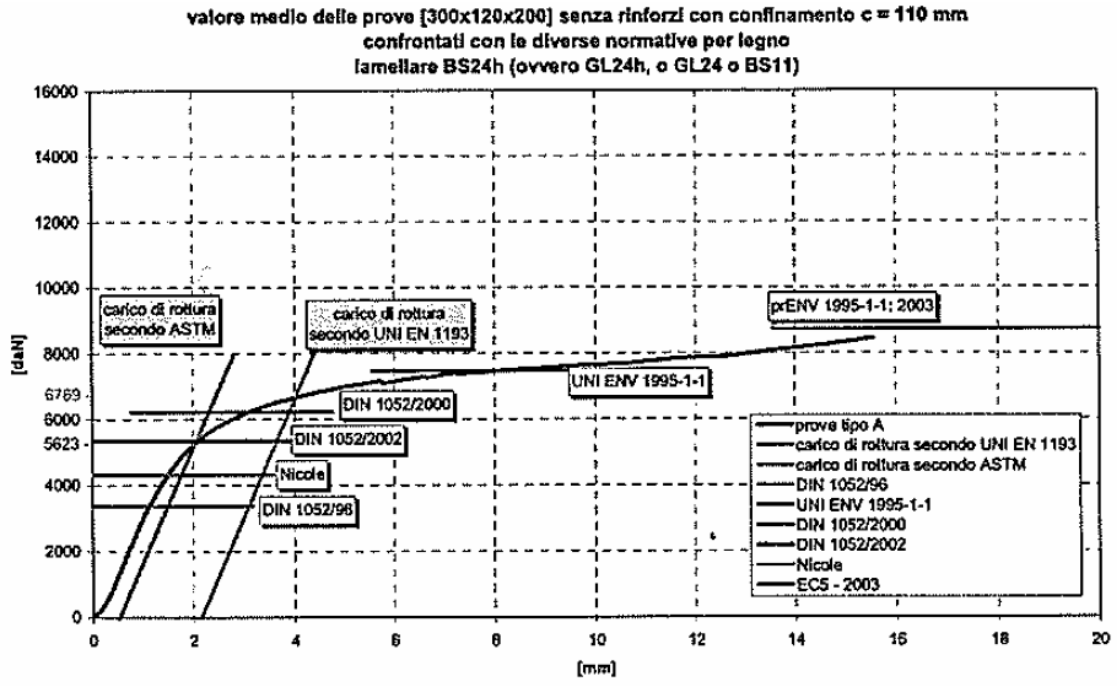

Figure 3.9 F–d relationship of mean values of tests results on [300x120x200] specimens and comparison with the characteristic strength in accordance to EN 1193 and different codes, [11].

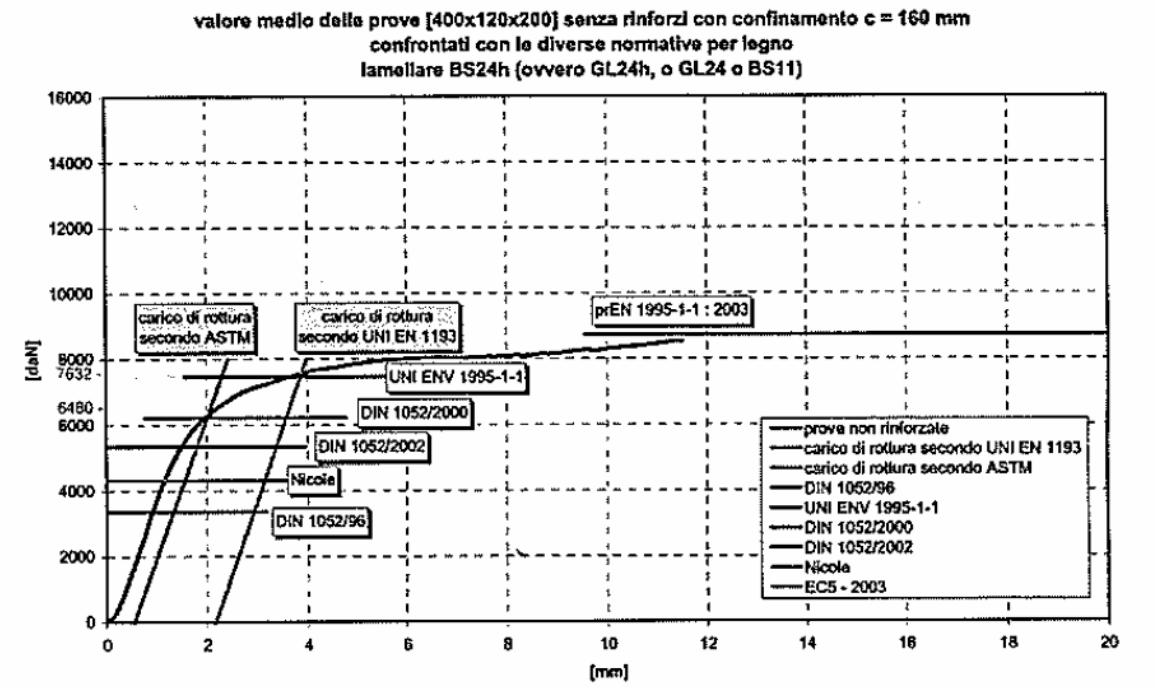

Figure 3.10 F–d relationship of mean value of test results on [400x120x200] specimens and comparison with the characteristic strength in accordance to EN 1193 and different codes, [11].

It can be noticed in Figures 3.7 to 3.10 that the different codes treats the capacities differently. This is due to differences in assumed safety parameters and currently the general trend is to decrease the suggested values of capacity, see chapter 3.3 for further recommendations by the codes regarding the unloaded length.

The conclusions that can be drawn when comparing the results presented by Suenson, [1] in 1938 and the tests performed by Reichegger, [11] in 2004 is that Reichegger´s values corresponds well with those of Suenson's. Hence, the relatively old tests and theory is still valid when treating the effect of the unloaded length.

3.4 Recommendations in the codes

Concerning structural timber such as glue-laminated timber, referred to as glulam, the behaviour is similar as for plain timber. Considering the relationship in Figure 3.11 the compression capacity increases as the distribution length of the load decreases, provided that there is enough unloaded length a from the load to the end of the loaded member. However, different codes treat the unloaded length differently and in this chapter it is described how the unloaded length effect is treated and the comparisons between the values. All codes have in common a possibility of increasing the load-bearing capacity if a significant unloaded length is present.

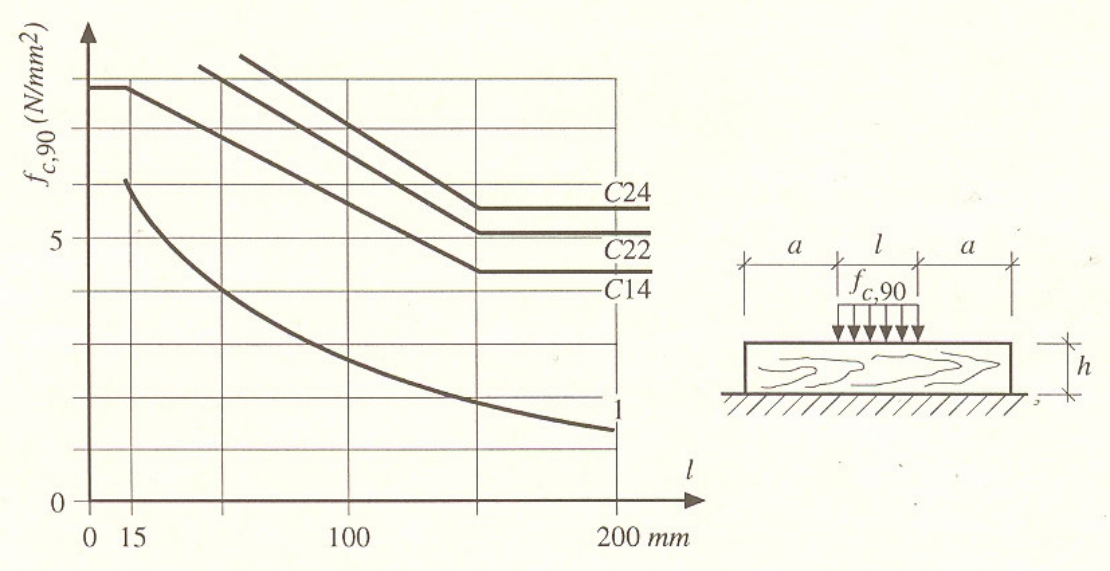

Figure 3.11, Compressive "yield" stresses for patch loading with length l on a member supported along its whole length compared with strength values for different strength classes according to EC5. [1]

The unloaded length effect in the different codes is given the notation $k_{c,90}$.

3.4.1 Eurocode 5 (prEN 1995-1-1:2004)

The Eurocode 5 treats the unloaded length as follows, [7]:

1) The following expressions shall be satisfied:

$$\sigma_{c,90,d} \leq k_{c,90} f_{c,90,d} \tag{3.3}$$

Where:

$\sigma_{c,90,d}$ is the design compressive stress in the contact area perpendicular to the grain

$f_{c,90,d}$ is the design compressive strength perpendicular to the grain

$k_{c,90}$ is a factor taking into account the load configuration (unloaded length), possibility of splitting and degree of compressive deformation.

2) The value of $k_{c,90}$ should be taken as 1,0, unless the number of arrangements in the following paragraphs apply. In these cases the higher value of $k_{c,90}$ specified may be taken, up to a limiting value of $k_{c,90} = 4,0$.

NOTE: When a higher value of $k_{c,90}$ is used, and contact extends over the full member width b, the resulting compressive deformation at the ultimate limit state will be approximately 10% of the member depth.

3) For a beam member resting on supports, see Figure 3.12, the factor $k_{c,90}$ should be calculated from the following expressions:

- When the distance from the edge of support to the end of a beam $a \leq h/3$:

$$k_{c,90} = \left(2,38 - \frac{l}{250}\right)\left(1 + \frac{h}{12l}\right) \tag{3.4}$$

- At internal supports:

$$k_{c,90} = \left(2,38 - \frac{l}{250}\right)\left(1 + \frac{h}{6l}\right) \tag{3.5}$$

Where:

l is the contact length in mm

h is member depth in mm

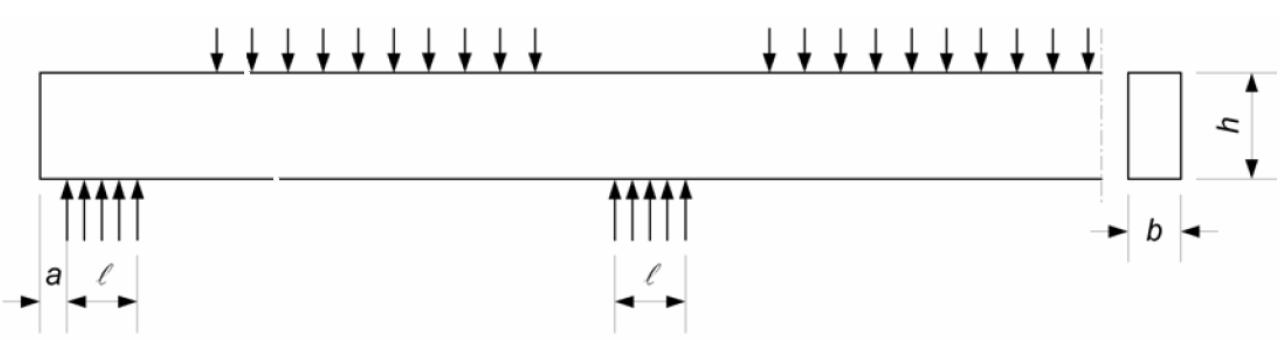

Figure 3.12 Beam on support, [7]

4) For a member with a depth $h \leq 2,5b$ where a concentrated force with contact over the full width b of the member is applied to one face directly over a continuous or discrete support on the opposite face, see Figure 3.13, the factor $k_{c,90}$ is given by:

$$k_{c,90} = \left(2,38 - \frac{l}{250}\right)\left(\frac{l_{ef}}{l}\right)^{0,5} \tag{3.6}$$

Where:

l_{ef} is the effective length of distribution, in mm, see Figure 3.13

l is the contact length in mm, see Figure 3.13

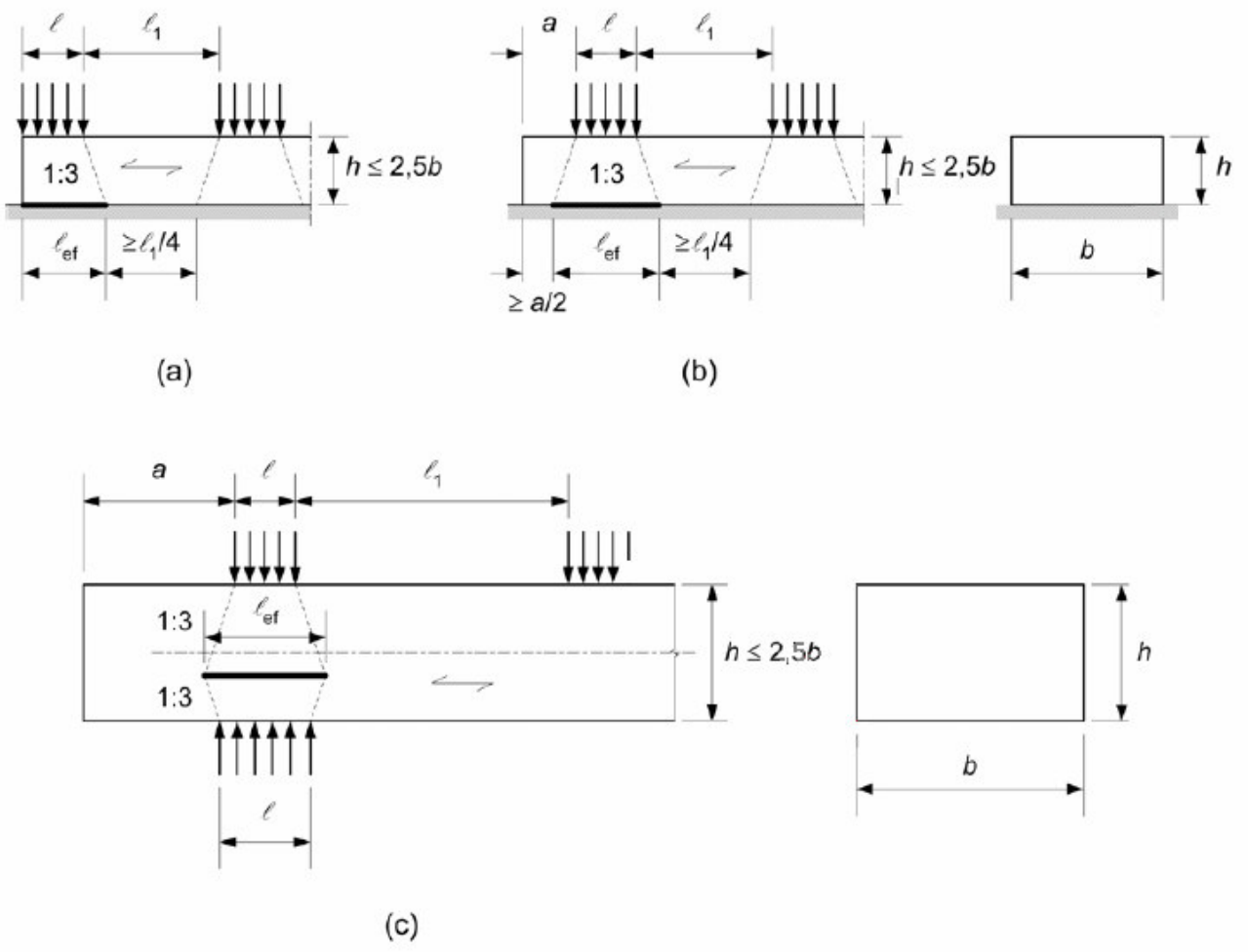

Figure 3.13 Determination of effective lengths for a member with h/b ≤ 2,5, (a) and (b) continuous support, (c) discrete supports, [7]

5) The effective length of distribution l_{ef} should be determined from a stress dispersal line with a vertical inclination of 1:3 over the depth h, but curtailed by a distance of a/2 from any end, or a distance of $l_1/4$ from any adjacent compressed area, see Figure 3.13(a) and (b).

For the particular positions of forces below, the effective length is given by:

- For loads adjacent to the end of the member, see Figure 3.13(a)

$$l_{ef} = l + \frac{h}{3} \tag{3.7}$$

- When the distance from the edge of a concentrated load to the end of the member a, ≥ 2/3 h, see Figure 3.13(b)

$$l_{ef} = l + \frac{2h}{3} \tag{3.8}$$

Where h is the depth of the member or 40 mm, whichever the largest.

For members on discrete supports, provided that a ≥ h and l_1 ≥ h, see Figure 3.13(c), the effective length should be calculated as:

$$l_{ef} = 0{,}5\left(l + l_s + \frac{2h}{3}\right) \tag{3.9}$$

Where h is the depth of member or 40 mm, whichever the largest.

6) For a member with a depth h>2,5b loaded with a concentrated compressive force on two opposite sides as shown in Figure 3.14(b), or with a concentrated compressive force on one side and a continuous support on the other, see Figure 3.14(a), the factor $k_{c,90}$ should be calculated according to expression (3.10), provided that the following conditions are fulfilled:

- the applied compressive force occurs over the full member width b
- the contact length l is less than the greater of h or 100mm

$$k_{c,90} = \frac{l_{ef}}{l} \tag{3.10}$$

Where:

l is the contact length according to Figure 3.14

l_{ef} is the effective length of distribution according to Figure 3.14

The effective length of distribution should not extend by more than l beyond either edge of the contact length.

7) For members whose depth varies linearly over the support (e.g. bottom chords of trusses at the heel joint), the depth h should be taken as the member depth at the centreline of the support, and the effective length l_{ef} should be taken as equal to the contact length l.

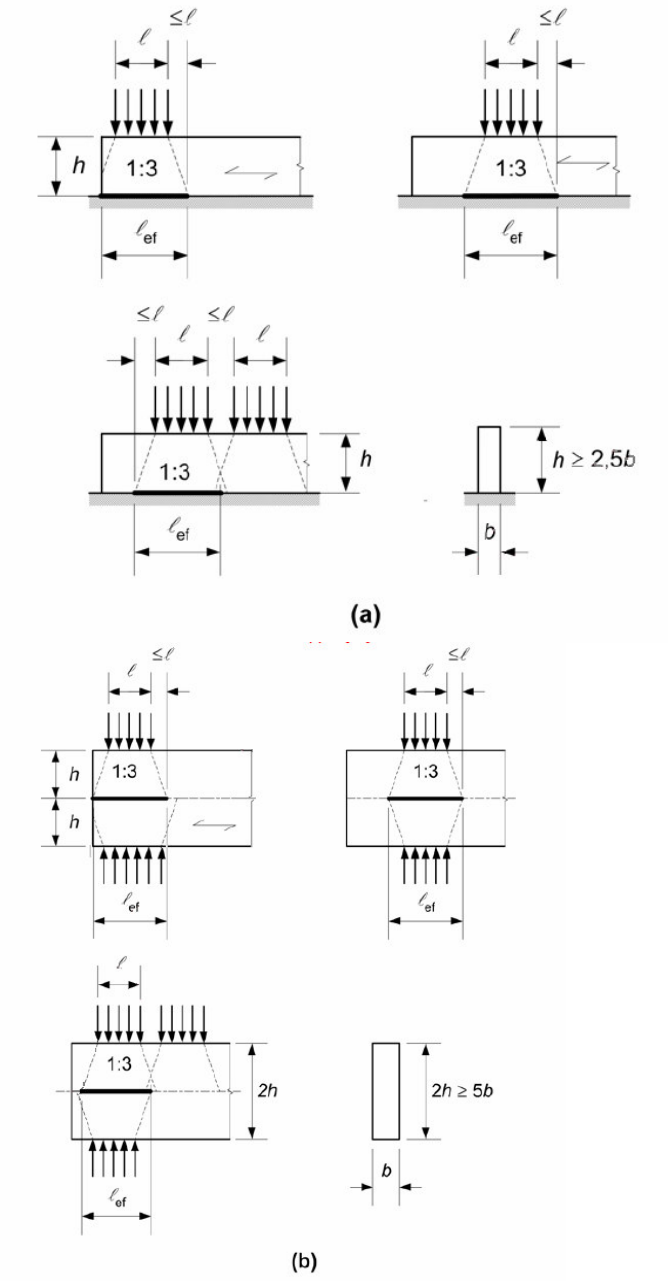

Figure 3.14 Determination of effective lengths for a member with h/b > 2,5 on (a) a continuous support, (b) discrete supports, [7]

A simplified interpretation of the behaviour of $k_{c,90}$ as treated above thus an evaluation of the maximum capacity, $F_{c,90}$, reached according to Eurocode 5 is considered in Appendix H.

3.4.2 German code (DIN 1052:2004)

The German code treats the unloaded length as follows, [5]:

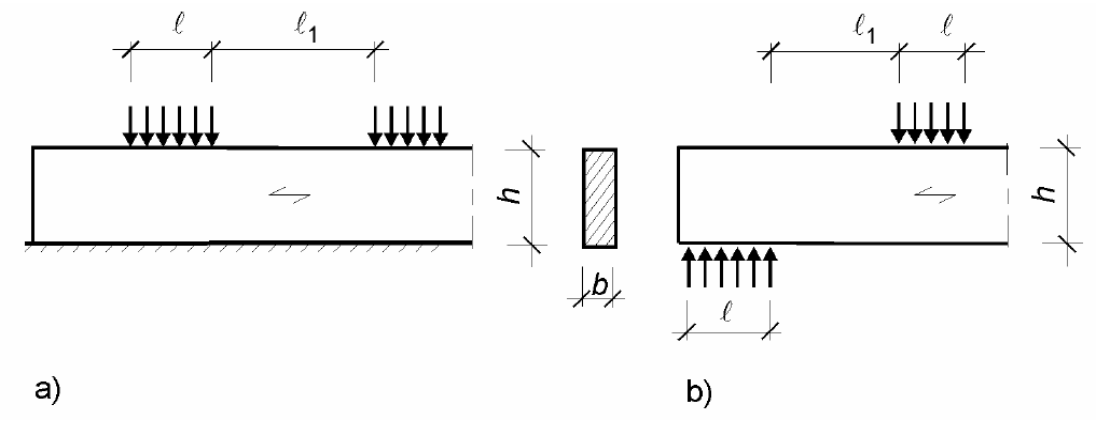

Figure 3.15 Determination of the effective lengths for, (a), a member on a continuous support and a member with a discrete support (b), [5]

1) The following expression shall be satisfied:

$$\frac{\sigma_{c,90,d}}{k_{c,90} \cdot f_{c,90,d}} \leq 1 \tag{3.11}$$

with:

$$\sigma_{c,90,d} = \frac{F_{c,90,d}}{A_{ef}} \tag{3.12}$$

A_{ef} is the area of the effective surface of applied load in compression perpendicular to the grain

$k_{c,90}$ is a factor taking into account the unload length effect

To calculate the area of the effective area of the applied load in compression perpendicular to the grain, A_{ef}, it is possible to increase the length of the surface of the applied load along the direction of the grain up to 30 mm on both sides.

For the value of the factor $k_{c,90}$ it is possible to assume the sequent values, for distances see Figure 3.15 (a) and (b):

$k_{c,90} = 1{,}0$ for plain timber and for glue-laminated timber with $l_1 < 2h$ as well as for hardwood

$k_{c,90} = 1{,}25$ for plain timber with $l_1 \geq 2h$ with a compressed tie (sill)

$k_{c,90} = 1{,}5$ for glue-laminated timber $l_1 \geq 2h$ with a compressed tie as well as for plain timber with $l_1 \geq 2h$ and with $l < 400mm$

$k_{c,90} = 1{,}75$ for glue-laminated timber with $l_1 \geq 2h$ and with $l < 400mm$

3.4.3 Italian code (CNR-DT 206:2006)

The Italian code treats the unloaded length as follows, [9]:

The following expression must be satisfied:

$$\sigma_{C,90,d} \leq f_{C,90,d} \tag{3.13}$$

With:

$$\sigma_{C,90,d} = \frac{F_{90,d}}{b \cdot l_{ef}} \tag{3.14}$$

Where:

l_{ef} is the effective length determined considering the distribution of the stress field parallel to the grain with an inclination equal to 1/3. The effective length must respect the following limitations; see equation (3.13) and Figure 3.16:

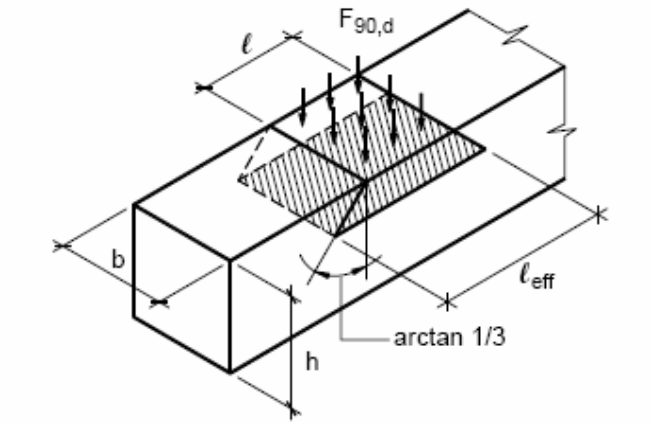

Figure 3.16 Definition of the effective length, [9]

$$l_{ef} \leq l + 1/3h \qquad l_{ef} \leq 2l \tag{3.15}$$

However, it is possible to use a value of more than 1.5 times the strength when it is allowed to have high deformations perpendicular to the grain.

3.4.4 Swedish code (BKR:2003)

The Swedish code treats the unloaded length as follows, [6]:

The following condition governs the resistance in compression perpendicular to the grain:

$$R_{c90d} = \kappa_{c90} \cdot f_{c90d} \cdot A \tag{3.14}$$

Where:

f_{c90d} is the design value of compressive strength

A is the cross sectional area of the member

κ_{c90} is the magnifying factor which, for example, takes into account the loaded length and is defined according to Eurocode 5, see above.

In practice the use of κ_{c90} is normally not applied and can therefore be put to 1.

3.4.5 Comparison viewed in an example

In this paragraph an example is shown of calculation with different codes of the characteristic capacity in compression perpendicular to the grain. The example uses the same geometry as the test specimens discussed in Chapter 5. The type of glue-laminated timber used in the calculation are GL32 for German code, L40 for Swedish code and GL32 for European code and Italian code according to standard UNI EN 1194:2000. The chosen classes have about the same bending strength and are therefore in theory representing the same glue-laminated timber. The values of f_{c90k} can be summarized in the sequent table, see Table 3.2:

Table 3.2 Compressive strength according to different codes

Codes	$f_{c,90,k}$ [MPa]	Strength class
German	3.3	GL32
Swedish	8.0	L40
European and Italian	3.3	GL32

The geometry of the specimen is as described earlier and can be seen in Figure 3.17. However, the plate is assumed to be 200 x 215 mm in order to neglect the small gaps of 7.5 mm on both sides of the plate. In this example the height, *h*, is considered as half the total height of the specimen (900/2 = 450 mm).

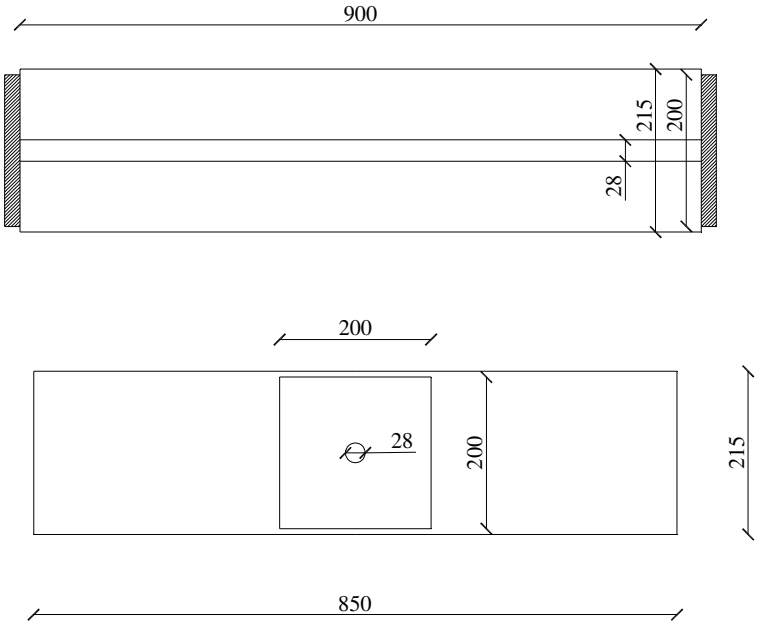

Figure 3.17 Geometry of the specimen used in this example

- *Eurocode 5 (prEN 1995-1-1:2004)*

Member with a depth h > 2,5 b loaded with a concentrated compressive force on two opposite sides must be considered in this case, so the factor $k_{c,90}$ is given by:

The total characteristic capacity is then equal to:

$$F_{c,90,k} = A \cdot k_{c,90} \cdot f_{c,90,k} = \left(200^2 - \frac{\pi \times 28^2}{4} \right) \times 2.5 \times 3.3 = 325 \quad kN$$

- *German code (DIN 1052:2004)*

The effective area, A_{ef}, must be accounted for, so the length of the surface of the applied load along the direction of the grain increase up to 30 mm on both sides. The factor $k_{c,90}$ is given for the case of:

$$l_1 = \infty \geq 2h = 900mm, \text{ with } l = 200mm < 400mm \quad \rightarrow \quad k_{c,90} = 1.75$$

Where the total characteristic capacity is then equal to:

$$F_{c,90,k} = A_{ef} \cdot k_{c,90} \cdot f_{c,90,k} = \left[200 \times (200 + 2 \times 30) - \frac{\pi \times 28^2}{4} \right] \times 1.75 \times 3.3 = 297 \quad kN$$

- *Italian code (CNR-DT 206:2006)*

In the calculation of the effective length l_{ef} the limitation proposed are more restrictive than to consider the distribution of the stress field parallel to the grain with an inclination equal to 1/3:

$$l_{ef} = \min\left\{ 2 \cdot l \; ; l + \frac{1}{3} \cdot h \right\} = \min\left\{ 2 \times 200 \; ; 200 + \frac{1}{3} \times 450 \right\} = 350 \; mm$$

Where the total characteristic capacity is then equal to:

$$F_{c,90,k} = \left(b \cdot l_{eff} - A_{hole} \right) \cdot f_{c,90,k} = \left(200 \times 350 - \frac{\pi \times 28^2}{4} \right) \times 3.3 = 229 \quad kN$$

- *Swedish code (BKR:2003)*

The calculations are the same as for Eurocode 5 with the only difference in the values of characteristic strength in compression perpendicular to the grain for glue-laminated timber, type L40. Therefore, the total characteristic capacity is equal to:

$$F_{c,90,k} = A \cdot k_{c,90} \cdot f_{c,90,k} = \left(200^2 - \frac{\pi \times 28^2}{4} \right) \times 1 \times 8.0 = 315 \quad kN$$

It can easily be noticed that the different codes differs a lot in terms of total characteristic capacity for the same material in question. The calculations based on the Italian code results in the lowest capacity, whereas, the highest is obtained by using Eurocode 5. In the case of the Swedish code the suggested value on $f_{c,90,k}$ is very high but here compensated by the fact that the capacity is not further increased by the unloaded length effect. It will be shown later in this thesis whether the characteristic strength in compression perpendicular to the grain suggested by these codes can be regarded as realistic or not.

4 Reinforcement with full-threaded screws

4.1 General description

Screws can be used as a method of reinforcement in numerous different situations, wherever there is a risk of high compression stress perpendicular to the grain. Normally full-threaded screws are used since they prove to have a higher withdrawal capacity than screws that are partially threaded. When screws are loaded in compression parallel to the axis of the screws, two different failure modes concerning the screw can occur. These two failure modes are buckling of the screw and the screw being pushed in.

4.1.1 Collins method

Francois Collins, [3], developed a model based on test results of glue-laminated timber subjected to compression perpendicular to the grain. Collins separated the behaviour into three different categories in order to understand the whole behaviour of the reinforced specimen. Tests were made on un-reinforced specimens to acquire the strength of these, tests were made on the screws only to obtain the load bearing capacity of the screws and finally tests were made on reinforced specimens to obtain the total capacity of these. With these results Collins could formulate a relation between the un-reinforced specimens and the reinforced specimens, and the final equation could be derived, see equations (4.1-4.2).

$$F_{c,90} = F_{c,90,H} + k_A \cdot n_{ef} \cdot F_{D,S} \tag{4.1}$$

Where

$F_{c,90,H}$ is the capacity of the timber according EN 1193 [kN]

$F_{D,S}$ is the load bearing capacity of one screw [kN]

k_A is the coefficient depending on the material used for loading

$k_A = 1$ for hard materials like steel and concrete

$k_A = 0.75$ for soft materials like timber

n_{ef} is the effective number of screws [n_{ef} =1,2,3,..6,..]

$$n_{ef} = \min\begin{cases} 6 \\ \dfrac{b \cdot l_A}{450 \cdot d_s} \end{cases} \tag{4.2}$$

Where; $b \cdot l_A$ is the loading area [mm^2] and d_s is the diameter of the screw

4.1.2 Method developed in Karlsruhe

The model developed in Karlsruhe is an evolved version of the model by Collins where Blass and Bejtka, [2], by means of tests developed a new model that can more accurately consider the effect of screws as reinforcement. Focus was put into understanding the behaviour of buckling of the full-threaded screws, see Chapter 4.3 for detail. During the tests they could distinguish three different failure modes and the consequences of these are taken into account in the following design equations, see equations (4.3-4.6).

Design equations for reinforced beam supports:

$$R_{90,d} = \min\begin{cases} n \cdot R_d + k_{c,90} \cdot l_{ef,1} \cdot b \cdot f_{c,90,d} \\ b \cdot l_{ef,2} \cdot f_{c,90,d} \end{cases} \tag{4.3}$$

Where (4.4)

$$R_d = \min\{R_{ax,d}; R_{c,d}\}$$

$$R_{ax,d} = d \cdot l_s \cdot f_{1,d}$$

$$R_{c,d} = \kappa_c \cdot \frac{N_{pl,k}}{\gamma_M} \qquad with \quad \gamma_M = 1{,}1$$

$$\kappa_c = 1 \qquad for \quad \overline{\lambda_k} \le 0{,}2$$

$$\kappa_c = \frac{1}{k + \sqrt{k^2 - \overline{\lambda^2}_k}} \qquad for \quad \overline{\lambda_k} > 0{,}2$$

Where

$$k = 0{,}5 \cdot \left[1 + 0{,}49 \cdot \left(\overline{\lambda_k} - 0{,}2\right) + \overline{\lambda^2_k}\right] \tag{4.5}$$

$$\overline{\lambda_k} = \sqrt{\frac{N_{pl,k}}{N_{ki,k}}} \qquad with \quad N_{pl,k} = \pi \cdot \frac{(0{,}7 \cdot d)^2}{4} \cdot f_{y,k} \tag{4.6}$$

and

d	is the screw diameter
n	is the number of screws
l_s ; b; $l_{ef,1}$; $l_{ef,2}$	According to Figure 4.1
$f_{1,d}$	is the design value of the withdrawal capacity parameter
$f_{c,90,d}$	is the design value of the compressive strength perpendicular to the grain
$f_{y,k}$	is the characteristic yield strength (for conventional screws: $f_{y,k}$ = 400 N/mm^2)
$k_{c,90}$	is the coefficient $k_{c,90} \in [1\,;1{,}75]$ for the load distribution

$N_{ki,k}$ is the characteristic buckling load for a screw taking into account the elastic foundation perpendicular to the screw axis, a triangular normal load distribution along the screw axis as well as the support condition of the screw head.

Furthermore, Blass and Bejtka defines minimum spacing, end and edge distances when using screws as reinforcement, see Figure 4.1

$a_1 \geq 5 \cdot d$ $a_2 \geq 2{,}5 \cdot d$ $a_1 \cdot a_2 \geq 25 \cdot d^2$ $a_{1,c} \geq 5 \cdot d$ $a_{2,c} \geq 4 \cdot d$

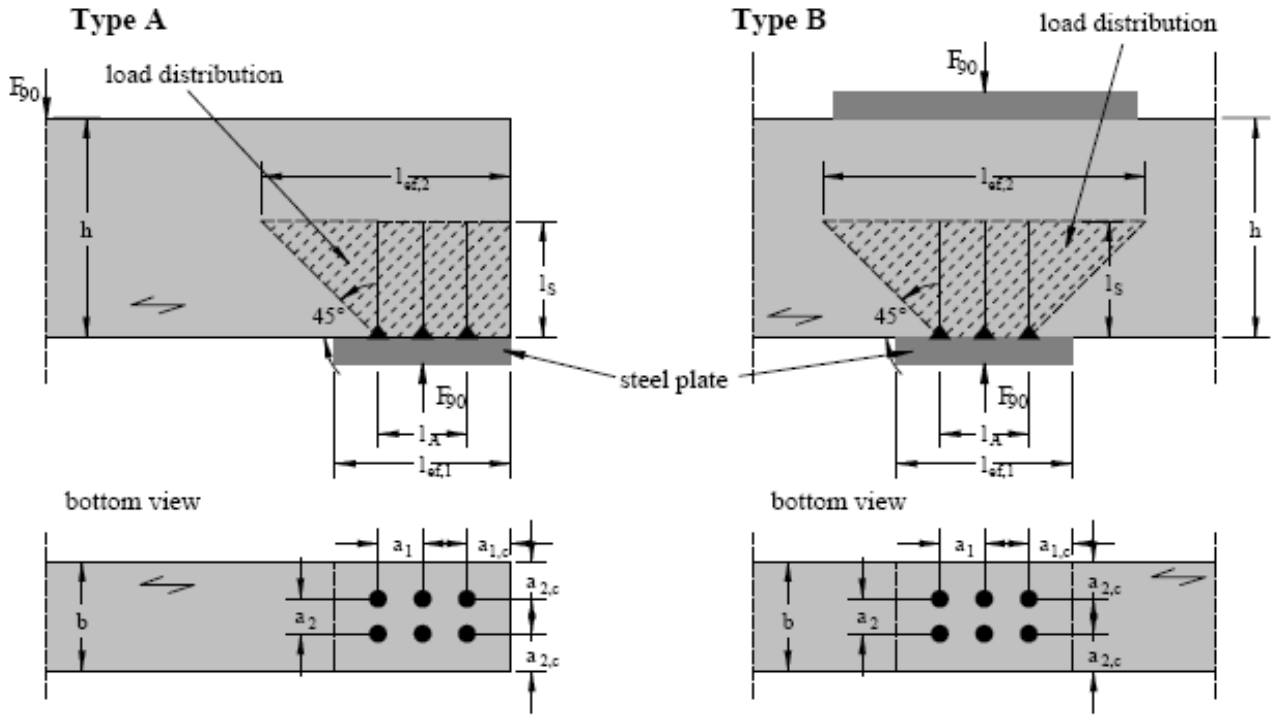

Figure 4.1, Supports that were used in the tests and suggested spacing, [2]

4.2 Pushing in capacity of the full-threaded screws

The pushing in effect is due to the fact that the bond strength between screw and timber has been reached and exceeded. This means that the interaction between the two materials has been lost and the screw can no longer transfer the load into the timber. This pushing in phenomenon corresponds to the withdrawal behaviour when the screw is being extracted out of the timber. The benefit of considering extraction is that the effect of buckling can be eliminated. The withdrawal capacity can be calculated using empirical data e.g. based on test results which are different in different building codes. Therefore a small variation can be noticed in results when using different codes. The withdrawal capacity according to the different codes is according to equations (4.8-4.12).

4.2.1 Eurocode 5 (prEN 1995-1-1:2004)

According to Eurocode 5, [7], the withdrawal capacity is linearly dependent on the effective number of screws and the withdrawal parameter f_{ax}, non-linearly dependent of the nominal diameter and the length of the screw.

$$R_{ax} = n_{ef} \cdot [\pi \cdot d \cdot (l_s - d)]^{0,8} \cdot f_{ax} \quad [N] \tag{4.8}$$

Where:

$n_{ef} = n^{0,9}$ is the effective number of the screws

f_{ax} is the characteristic withdrawal parameter dependent of the density of the timber in N/mm^2

$f_{ax} = 3.6 \cdot 10^{-3} \cdot \rho_k^{1,5}$

ρ_k is the characteristic density of the timber in kg/mm^3

4.2.2 German code (DIN 1052:2004)

According to the German code, [5], the withdrawal capacity is linearly dependent on the length of the screw, the nominal diameter and the withdrawal parameter f_1. This withdrawal parameter, f_1, is dependent on the density and the class of the screw.

$$R_{ax} = d \cdot l_s \cdot f_1 \quad [N] \tag{4.9}$$

Where:

d is the nominal diameter of the screw in mm

l_s is the threaded length of the screw in mm

f_1 is the withdrawal parameter dependent on the load capacity class of the screw and the density of the timber in N/mm^2

$f_{1,k} = 60 \cdot 10^{-6} \cdot \rho_k^2$ for screw with load capacity class 1

$f_{1,k} = 70 \cdot 10^{-6} \cdot \rho_k^2$ for screw with load capacity class 2

$f_{1,k} = 80 \cdot 10^{-6} \cdot \rho_k^2$ for screw with load capacity class 3

4.2.3 Italian code (CNR-DT 206:2006)

According to the Italian code, [9], the withdrawal capacity is linearly dependent on the effective number of screws and the withdrawal parameter f_{ax}, non-linearly dependent of the nominal diameter and the length of the screw.

$$F_{ax,\alpha,Rk} = n_{ef} \cdot \left[\pi \cdot d \cdot l_{ef}\right]^{0,8} \cdot f_{ax,\alpha,k} \quad [N] \tag{4.10}$$

Where:

$n_{ef} = n^{0,9}$ is the effective number of the screws

l_{ef} is the length of the threaded part in the point side element, in mm

$f_{ax,\alpha,k}$ is the characteristic withdrawal parameter dependent of the density of the timber and the angle between axis of the screw and the direction of the grain in N/mm^2

$$f_{ax,\alpha,k} = \frac{f_{ax,k}}{\sin^2 \alpha + 1.5 \cdot \cos^2 \alpha}$$

$f_{ax,k} = 3.6 \cdot 10^{-3} \cdot \rho_k^{1,5}$

ρ_k is the characteristic density of the timber, in kg/mm^3

4.2.4 Swedish code (BKR:2003)

According to Swedish code, [6], the withdrawal capacity is linearly dependent of the nominal diameter and the length of the screw.

$$R_{t,k} = 11 \cdot (2.5 + d) \cdot (l_g - d) \quad [N] \tag{4.11}$$

l_g is the threaded length of the screw in mm

d is the nominal diameter of the screw in mm

4.2.5 According to tests conducted by Bejtka

Bejtka, [8], improved the equations for calculating the withdrawal capacity after performing some tests.

$$R_{a,x} = d \cdot l_s \cdot f_{lx,new} \quad [N] \tag{4.12}$$

l_s is the threaded length of the screw in mm

d is the nominal diameter of the screw in mm

$f_{ax,new}$ is the characteristic withdrawal parameter according to test results in N/mm^2

$$f_{lx,new} = 0.61 \frac{\rho^{0,79}}{d^{0,47} \cdot l_s^{0,09}} \quad [N/mm^2]$$

4.2.6 Comparison

As an example to illustrate the differences in withdrawal capacity one screw type plus one timber density was chosen as follows:

$d = 10mm$

$\rho_k = 450kg/m^3$

This resulted in the following relationship where the capacities are plotted against the lengths of the screw, see Figure 4.2.

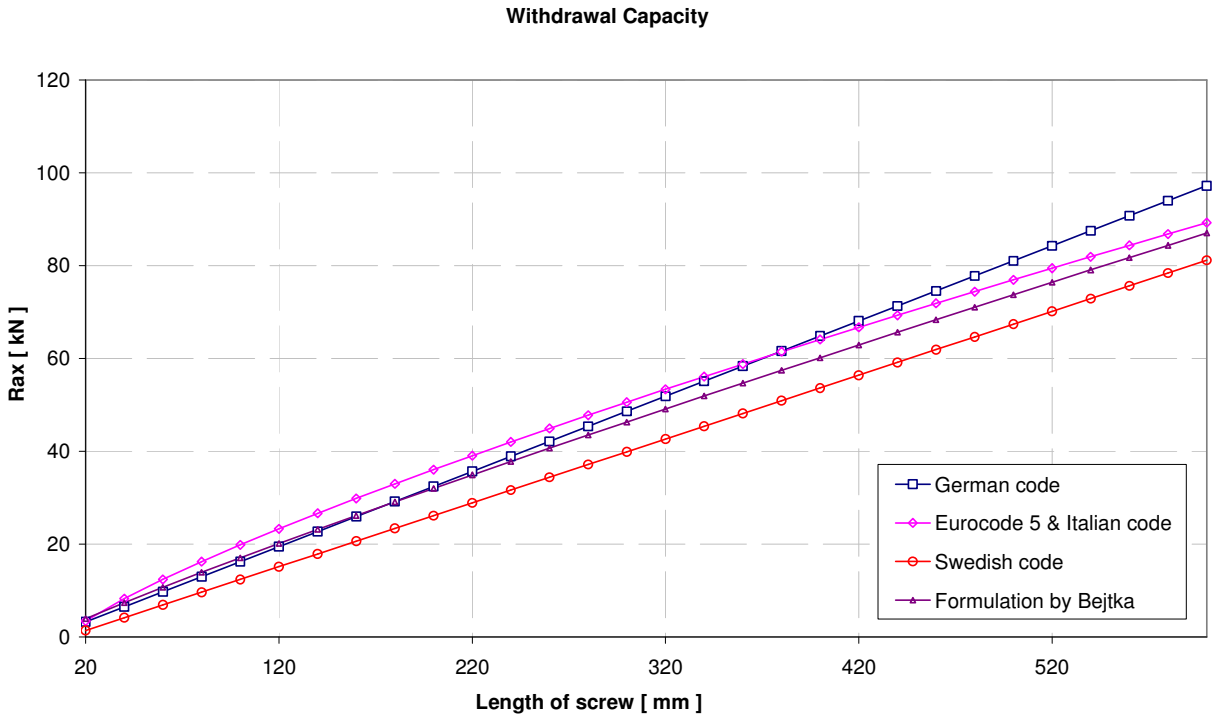

Figure 4.2 Plot of the differences in withdrawal capacity for different codes and lengths of the screw

According to these results it can be seen that the Swedish code is the most conservative and does not take into account the density of the timber. The highest characteristic withdrawal capacity is reached when using the German code; this is probably due to the fact that in the German code there is an option to choose the type of screw class that is appropriate for the current situation. In this example screw class 3 was chosen since the diameter of the screw is set to 10 mm. The Italian code and the Eurocode 5 have the same formulation when describing the withdrawal capacity.

4.3 Buckling of the full-threaded screws

4.3.1 Description

As described in paragraph 4.1.2, the load capacity of the reinforcement in compression perpendicular to the grain with self-tapping screws for the second mode of failure is dependent on the load carrying capacity perpendicular to the grain of the timber as well as the load carrying capacity of the screws due to buckling. To evaluate the load carrying capacity of the screws due to buckling some studies were performed at the University of Karlsruhe. The criterion for this study was that the load carrying capacity of the screws due to buckling was assumed equal to the critical load. Under this critical load the screws are in pure compression, as soon as the critical load is reached, buckling of the screws occur. The critical load can be determined with good approximation in an analytical or numerical way. In Figure 4.3 it is represented how a system of a slender screw used as reinforcement in compression perpendicular to the grain of the timber when the critical load N_k is applied.

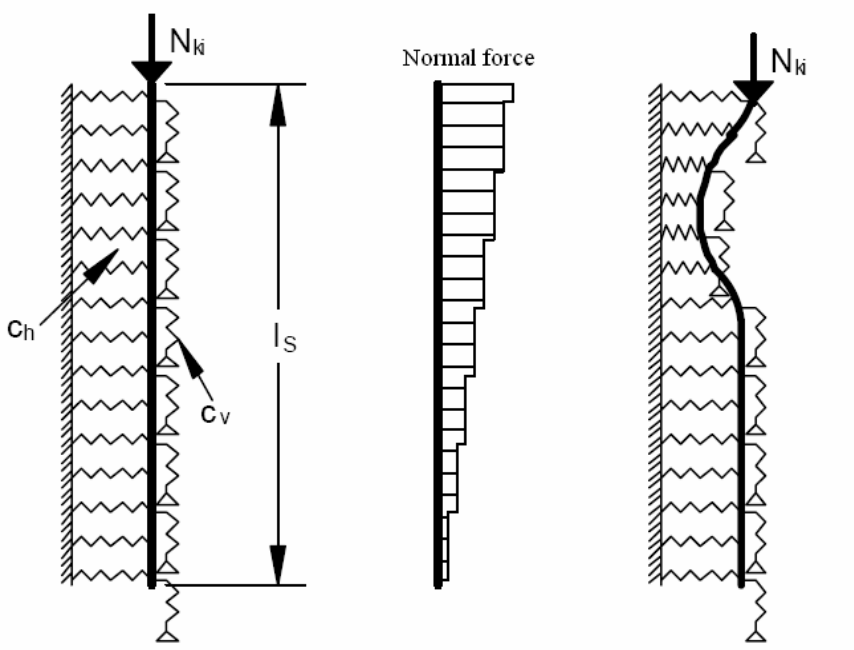

Figure 4.3 System of slender screw during buckling phenomena, [8]

The compression force on the head of the screw generates a normal force of compression along the screw's axes which is transferred into the timber across the threaded connection between timber and screw, also the timber offer a lateral stiffness to the screw. In this system, it is assumed that the interaction of the screw with the timber both in parallel and perpendicular direction can be considered as a distribution of independent springs along the screw axis if it is full-threaded. The stiffness of the bed of springs can be considered with the sequent coefficient c_h, see equation (4.13):

$$c_h = \frac{(0.22 + 0.014 \cdot d) \cdot \rho}{1.7 \sin^2 \alpha + \cos^2 \alpha} \tag{4.13}$$

Where:

d is the nominal diameter of the screw

ρ is the density of the timber in kg/m^3

α is the angle between the force F and the direction of the grain in the timber, see Figure 4.4

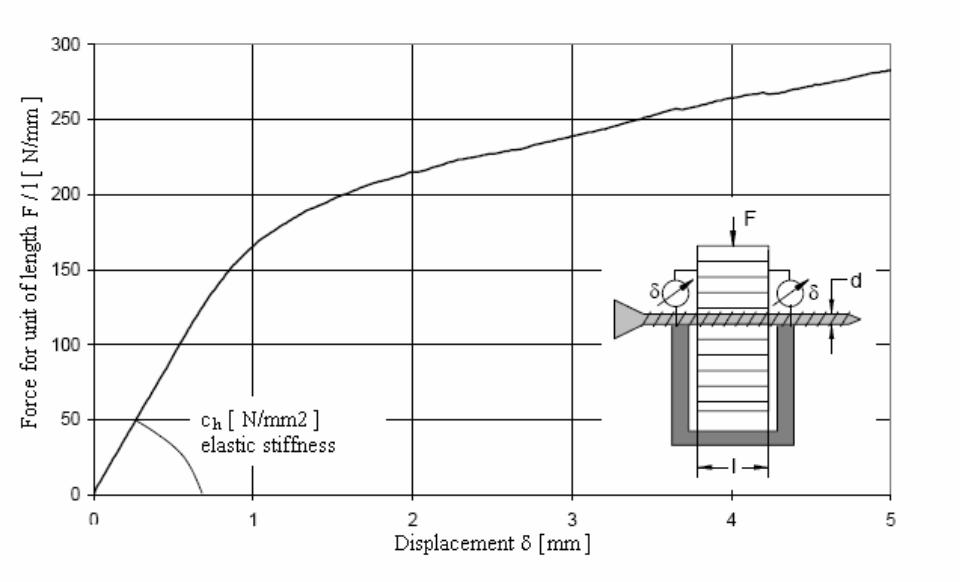

Figure 4.4 Tests performed to evaluate the stiffness coefficient, c_h, [8]

The stiffness coefficient, c_h, increases with the increase of the nominal diameter of the screw and the density of the timber, and also the critical load increases. The vertical stiffness can be considered with the sequent coefficient c_v, see equation (4.14):

$$c_v = 234 \cdot \frac{(\rho \cdot d)^{0,2}}{l_s^{0,6}} \tag{4.14}$$

Where:

d is the nominal diameter of the screw

ρ is the density of the timber in kg/m^3

l_s is the length of the screw

The magnitude of the vertical stiffness coefficient, c_v, interacts with the distribution of the normal force in the screw, however it does not influence the critical load. For small ratios of the elastic stiffness, c_v, and the axial stiffness, EA_s, the full-threaded screw can be assumed, with good approximation, to have a linear distribution of the normal force along the screw axis. The characteristic value of the critical load according to the elastic theory can be calculated in an analytical way by finding the numerical solution to the differential equation of fourth order. The amplitude and the deformed shape of the screw when it buckles are also dependent on in which way the load transfer zone is configured. When the reinforcement with screw is configured by using an arbitrary shape of the head of the screw, it is possible to calculate the critical load with the assumptions that the stiffness of the rotational spring placed in the zone of the applied load is equal to zero, K = 0, see Figure 4.5 on the right. This means that the head of the screw is allowed to rotate. If the reinforcement is configured by using a special steel plate, like shown in the Figure 4.6, the critical load can be calculated with the assumption that the stiffness of the rotational spring placed in the zone of the applied load are equal to infinity, K = ∞, see Figure 4.5 on the left. This means that the head of the screw is not allowed to rotate.

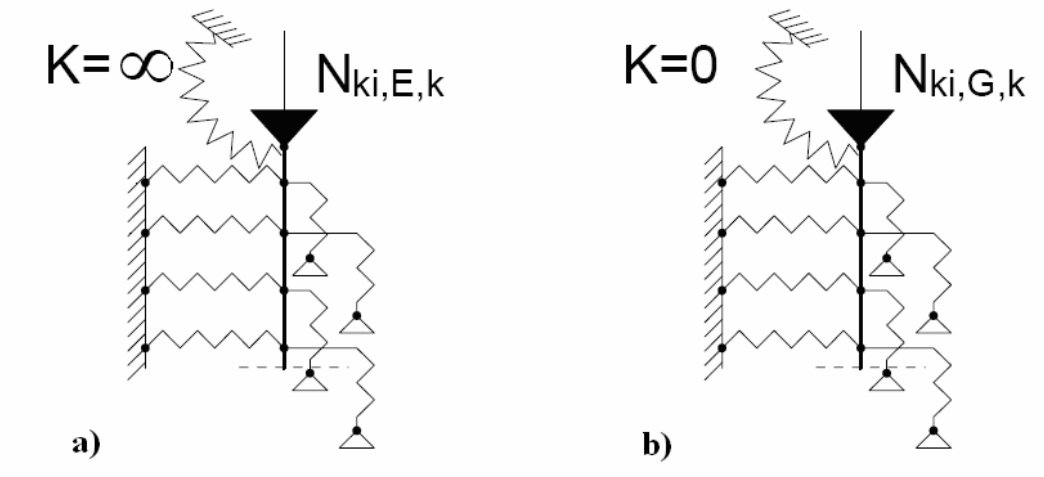

Figure 4.5 Bending springs placed in the zone of the applied load – a): fixed connection b): hinge, [8]

This special steel plate must have holes with the same shape as the heads of the screws, in this way the screw can be drilled in the timber after placing the special steel plate. The manufacturing of the reinforcement becomes more complex compared to the traditional case, however, the critical load becomes higher due the higher degree of constrain.

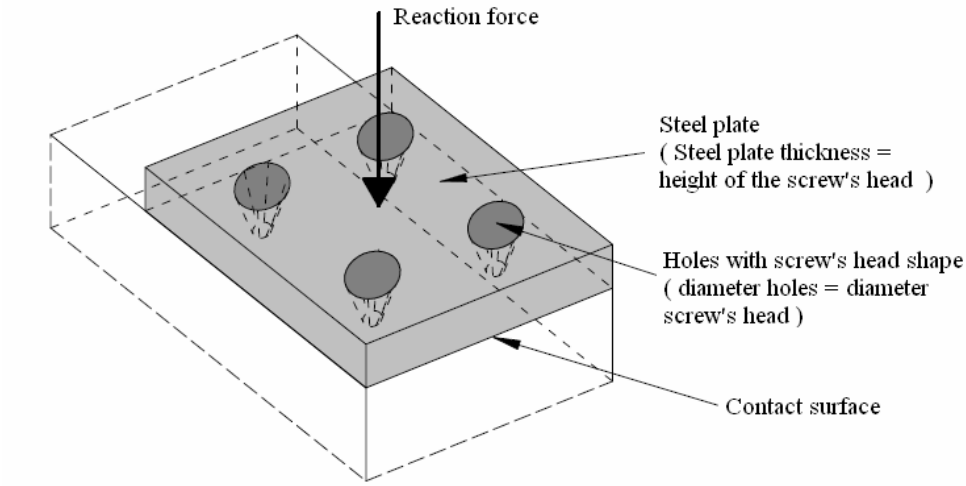

Figure 4.6 Reinforcement with special steel plate, K = ∞, [8]

Figure 4.7 illustrates the different deformed shapes and the relative characteristic critical load N_{ki} according to the elastic theory for different ratio of length l_s and nominal diameter d of the screw, both for the case of bending stiffness equal to zero, K = 0, and bending stiffness equal to infinity, K = ∞.

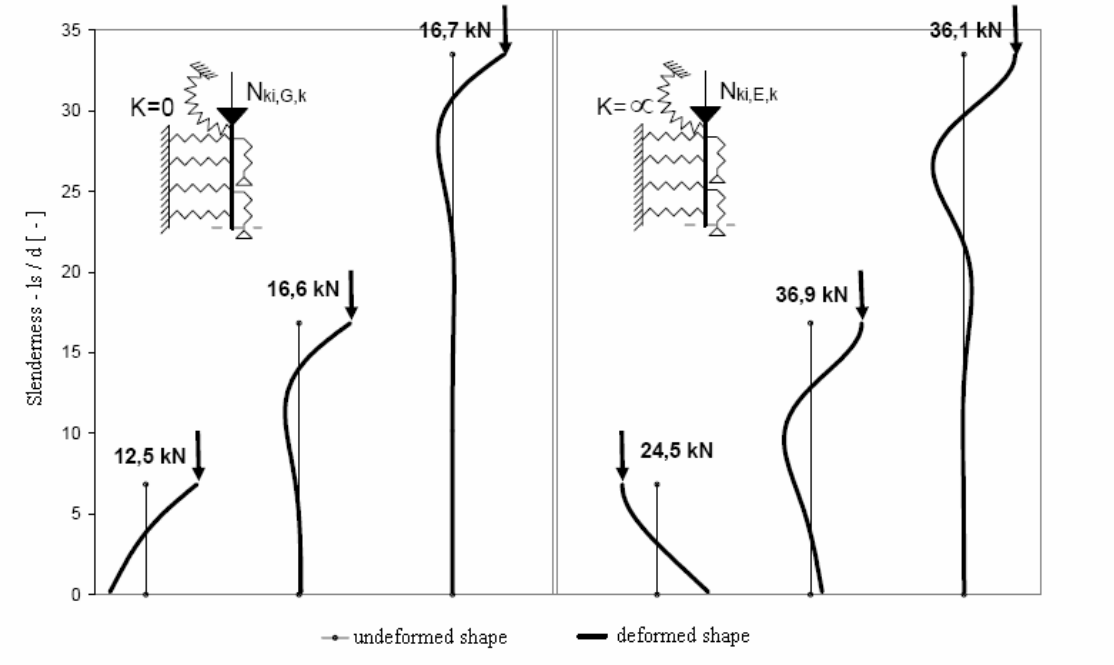

Figure 4.7 Deformed shapes of screws and characteristic buckling load for different slenderness and bending stiffness of the top of the screw, [8]

For the evaluation of the characteristic critical load, N_{ki}, according to the theory of elasticity for a fixed nominal diameter of the screw d, length of the screw l_s, characteristic density of the timber ρ_k and for the case K = 0 and K = ∞, it is possible to summarize the characteristic values in a table, see Table 4.1 and Table 4.2, where the intermediate values can be calculated by linear interpolation.

Table 4.1 Characteristic values of the critical load, $N_{ki,G,k}$ when K = 0, [8]

$N_{ki,G,k}$ [kN]		ρ_k = 310 kg/m3					ρ_k = 380 kg/m3					ρ_k = 410 kg/m3					ρ_k = 450 kg/m3				
		Screw diameter d [mm]					Screw diameter d [mm]					Screw diameter d [mm]					Screw diameter d [mm]				
		4	**6**	**8**	**10**	**12**	**4**	**6**	**8**	**10**	**12**	**4**	**6**	**8**	**10**	**12**	**4**	**6**	**8**	**10**	**12**
Screw length l_s in [mm]	**20**	4.0	4.5	5.0	5.4	5.8	4.9	5.5	6.1	6.6	7.1	5.2	6.0	6.5	7.1	7.7	5.7	6.5	7.2	7.8	8.4
	40	7.5	12.5	14.5	15.9	17.3	8.4	14.9	17.6	19.5	21.1	8.7	16.0	19.0	21.0	22.8	9.2	17.3	20.7	23.0	25.0
	60	7.4	16.4	24.2	28.3	31.2	8.3	18.4	28.7	34.3	38.1	8.6	19.2	30.5	36.8	41.0	9.1	20.2	32.7	40.1	44.8
	80	7.4	16.5	28.5	39.0	45.4	8.2	18.5	32.2	45.9	54.7	8.6	19.2	33.6	48.7	58.6	9.0	20.2	35.4	52.1	63.7
	100		16.6	29.0	43.9	56.9		18.6	32.5	49.7	66.7		19.3	34.0	52.1	70.6		20.3	35.8	55.0	75.4
	120	7.3		29.4	44.9	62.4	8.1		33.0	50.6	71.1	8.4		34.4	52.9	74.5	8.8		36.2	55.8	78.8
	140		16.7	29.7	45.7	64.2		18.6	33.2	51.4	72.5		19.3	34.6	53.7	75.9		20.3	36.4	56.7	80.2
	160				46.4	65.4				52.1	73.9				54.3	77.3				57.2	81.6
	180				46.8	66.5			33.3	52.4	75.0			34.7	54.7	78.4			36.5	57.6	82.7
	200			29.8		67.4					75.8					79.2					83.5
	220				47.1	68.1				52.7	76.4				55.0	79.7				57.8	84.0
	>240					68.6					76.9					79.7					84.4

Table 4.2 Characteristic values of the critical load $N_{ki,E,k}$,when $K = \infty$, [8]

$N_{ki,G,k}$ [kN]		ρ_k = 310 kg/m3					ρ_k = 380 kg/m3					ρ_k = 410 kg/m3					ρ_k = 450 kg/m3				
		Screw diameter d [mm]					Screw diameter d [mm]					Screw diameter d [mm]					Screw diameter d [mm]				
		4	**6**	**8**	**10**	**12**	**4**	**6**	**8**	**10**	**12**	**4**	**6**	**8**	**10**	**12**	**4**	**6**	**8**	**10**	**12**
Screw length l_s in [mm]	**20**	13.3	16.9	18.5	20.0	21.6	14.5	20.7	22.6	24.6	26.5	15.0	22.4	24.4	26.5	28.6	15.7	24.6	26.8	29.1	31.3
	40	16.2	24.5	36.1	39.1	42.2	19.1	28.2	44.2	47.9	51.7	20.3	29.8	47.7	51.7	55.8	21.7	32.0	50.8	56.8	61.2
	60	17.2	31.9	41.1	56.4	62.7	19.3	38.0	48.4	64.4	76.9	20.1	40.5	51.5	67.8	82.9	21.2	43.7	55.6	72.3	91.0
	80	17.2	36.6	51.2	61.7	76.5	19.1	41.2	61.4	73.3	89.1	19.8	43.0	65.6	78.2	94.5	20.8	45.3	71.2	84.8	102.0
	100		36.9	60.7	73.9	85.7		41.7	69.5	88.9	102.0		43.6	72.8	95.2	110.0		46.0	77.0	103.0	119.0
	120	15.6		62.1	86.8	99.8	17.3		70.5	102.0	120.0	17.9		74.0	108.0	129.0	18.8		78.4	115.0	140.0
	140		36.1	63.7	92.2	115.0		40.0	72.3	105.0	137.0		41.6	75.7	111.0	146.0		43.7	80.0	117.0	157.0
	160				94.5	126.0				108.0	145.0				114.0	153.0				121.0	163.0
	180			64.8	97.2	130.0			73.0	111.0	149.0			76.2	116.0	157.0			80.3	123.0	167.0
	200					134.0					154.0					162.0					172.0
	220				99.1	137.0				112.0	157.0				117.0	165.0				124.0	175.0
	>240					140.0					159.0					167.0					177.0

It is noticeable in the tables that the characteristic values of the critical buckling load can not be increased, in both case k=0 and k=∞, for values of slenderness ratio, l_s/d, larger than 20. For lengths of the screws more than 10 times the nominal diameter, the critical buckling load is independent of the length of the screw and can be approximated to be equal to $N_{ki,G/E,f}$, see equation 4.15, (Belluzzi 1949, Piazza and Turrini 1979), [4]:

$$N_{ki,G/E,f} = \left(c_h \cdot E \cdot J\right)^{0,5} \tag{4.15}$$

This buckling load corresponds to the case of elastically bedded beams without supports.

Where:

E is the modulus of elasticity of the screw equal to 210000 N/mm^2 (MPa)

J is the modulus of inertia of the screw considering the inner diameter (0,7 d) (mm^2)

For the case without vertical springs the normal force distribution on the screw is uniformly distributed along its axis, see Figure 4.8. In Appendix C the critical buckling load for such a case has been calculated and using the spring stiffness suggested above the critical buckling load results in:

$P_{crit,10} = 43.4\,kN$ for the screw with diameter d = 10 mm, l = 300 mm

$P_{crit,12} = 62.5\,kN$ for the screw with diameter d = 12 mm, l = 300 mm

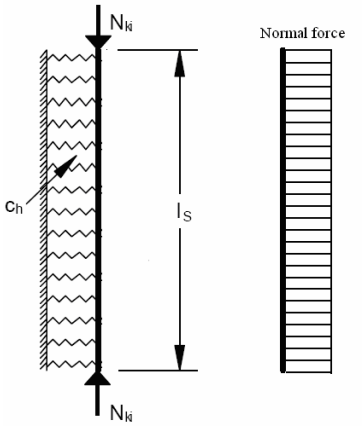

Figure 4.8 Embedded screw without vertical springs and uniform normal force distribution

When comparing the critical buckling load calculated for the case without vertical springs to the case with vertical springs it can be seen that the critical load is higher when using vertical springs. This is due to the fact that the normal force distribution is inclined and reaches a theoretical value of zero at the bottom of the screw, see Figure 4.3. In other words, the vertical springs increases the critical buckling load and in this generalised example, see Appendix C, the increase corresponds to 33.2 % and 38.2 %, respectively, see Table 4.3.

Table 4.3 Comparison between different buckling loads

	Without vertical springs	With vertical springs	Increase
$P_{crit,10}$	43.4 kN	57.8 kN	33.2 %
$P_{crit,12}$	62.5 kN	84.4 kN	38.2 %

4.3.2 Finite Element Analysis - University of Karlsruhe

To gain deeper understanding of the variation of characteristic critical load in dependence of the density, length and diameter of the screw according to the theory of elasticity, an analysis with Finite Elements program ANSYS were performed in the University of Karlsruhe. In this occasion the modulus of elasticity of the screw was taken equal to 210000 N/mm^2, the inner diameter of the screw was taken equal to d_k = 0.7 d. The analysis consisted of 6000 tests for both the cases where K=0 and K=∞, with the variation of the density of the timber (from ρ = 310 kg/m^3 to 450 kg/m^3 using 10 kg/m^3 steps), the nominal diameter of the screws (from d = 4 mm to 12 mm using 2 mm steps) as well as the length of full-threaded screws (from ls = 10 mm to 400 mm using 10 mm steps). In Figures 4.9 and 4.10 the results of the analyses are shown, the lines of the different results are in the same order as the legends in the figures.

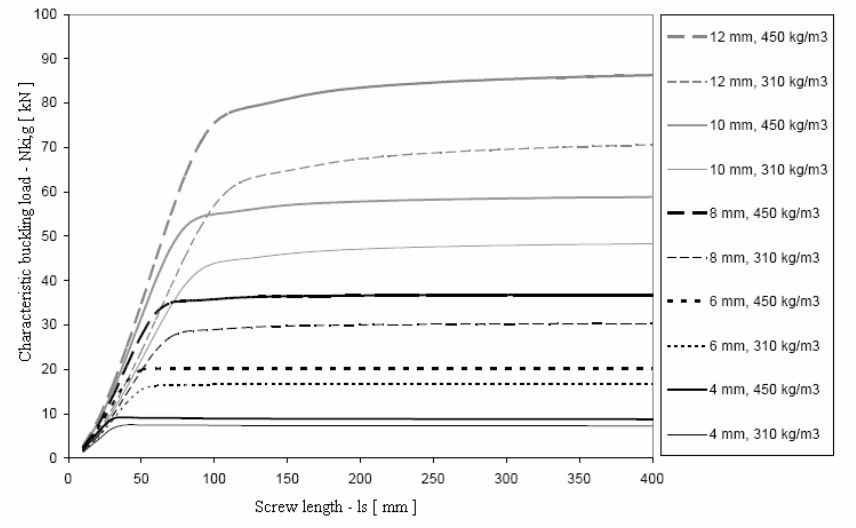

Figure 4.9 Characteristic buckling load $N_{ki,g}$,case K = 0, [8]

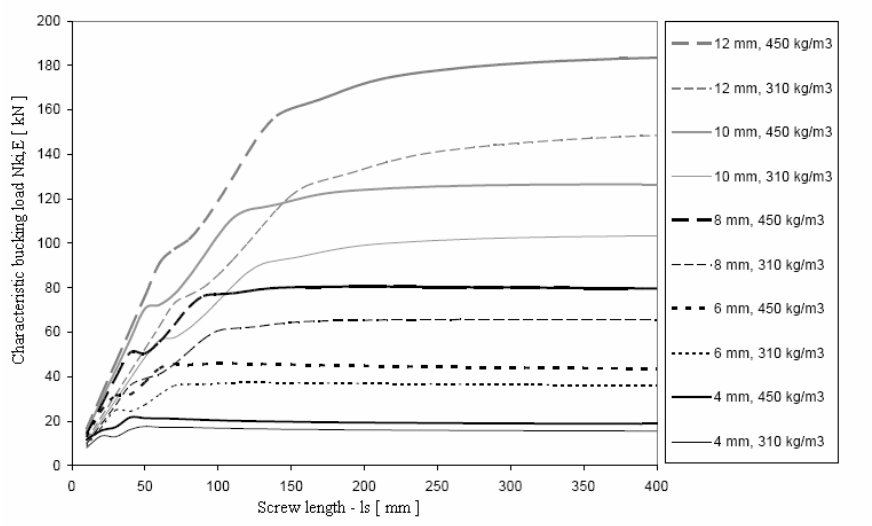

Figure 4.10 Characteristic buckling load $N_{ki,g}$,case K = ∞, [8]

It is possible to notice that, for both cases, with the increase of density and nominal diameter of the screws, the characteristic critical load increases as the length of the screws increase. However, at one specific slenderness ratio l_s / d or length of the screw, the characteristic critical buckling load does not increase further. In this case the deformed shape is identical and independent if the length of the screw is increased, c.f. Figure 4.7.

4.4 Influences of imperfections in assembling the screws

When assembling the screws some parameters are of importance since they govern the overall capacity of the reinforced element. Bejtka, [8], studied the influences of these parameters and here follows a short summary of the conclusions that he found.

The greatest precision is reached when using, as previously described, a custom steel plate which can take into account the exact shape of the heads of the screws, see Figure 4.11.

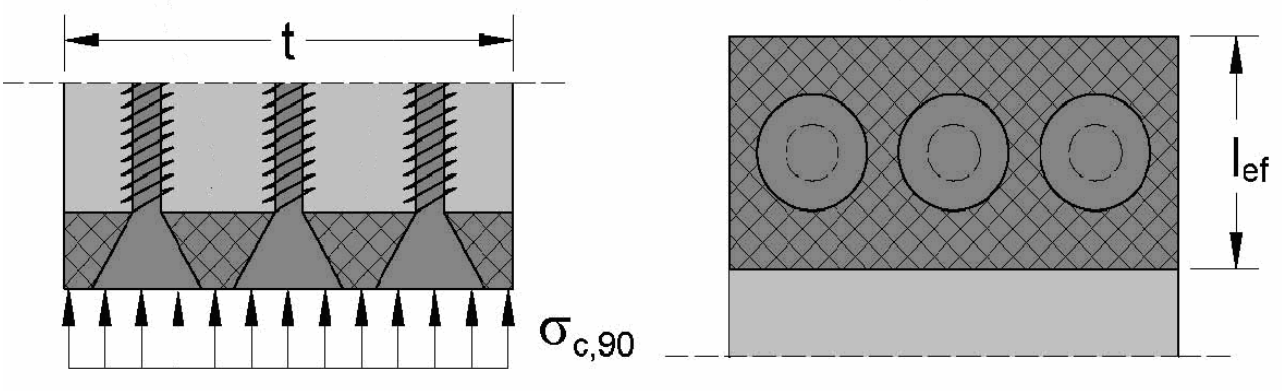

Figure 4.11 Configuration of the screws in the plate (left), View from the bottom (right), [8]

In this configuration, see Figure 4.11, the holes in the steel plate must have the same shape as the heads of the screws. With this it is possible to guarantee that all the screws are inserted into the timber with an inclination of 90° with respect to the direction of the grain and all positioned at the same level. If this type of special steel plate is not used, inaccuracy in the execution of the reinforcement can not be excluded. To be able to understand the effect of inaccuracy in the execution of the reinforcement 70 tests were performed at the University of Karlsruhe where different inaccuracies or imperfections of the self-tapping full-threaded screws were considered.

These types of inaccuracies were investigated:

A) Different sink of the screws into the timber. In this case a gap between the top of the screw and surface of the timber was considered. One of the screws was sunk with a 3 mm gap into the timber, the other was left at the timber surface (Type 3/0-0°), see Figure 4.12.

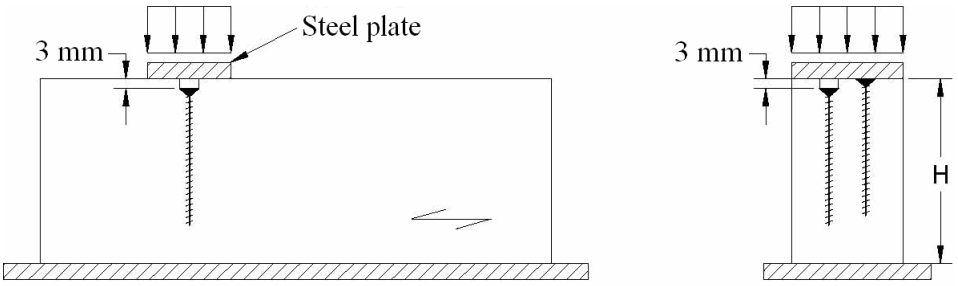

Figure 4.12 Variation in depth of the screw heads, [8]

B) In this configuration all screws were lowered equally so that the gap between the top of the screw and the timber, 3 mm, is consistent for all screws (Type 3/3-0°), see Figure 4.13.

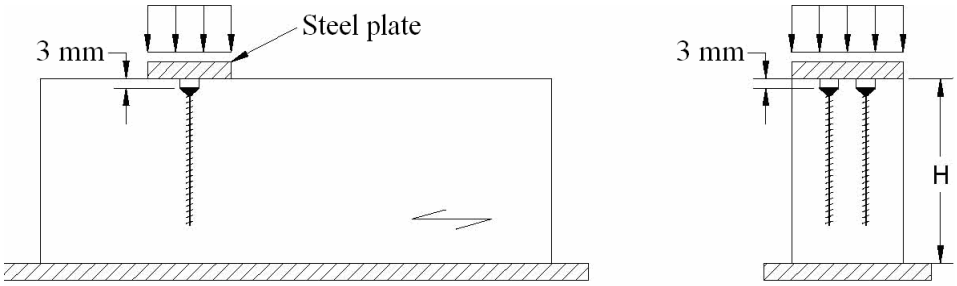

Figure 4.13 Equal gaps between top of the screws and the timber surface, [8]

C) Different inclination of the screws in the timber. In this case the angle was chosen between the screw axes and the axis perpendicular to the surface of the timber. The chosen angle was 10° (for 7,5 x 182 mm and 10 x 200 mm screws: Type 0/0-10°) and 5° (with 8 x 340 mm screws: Type 0/0-5°), see Figure 4.14.

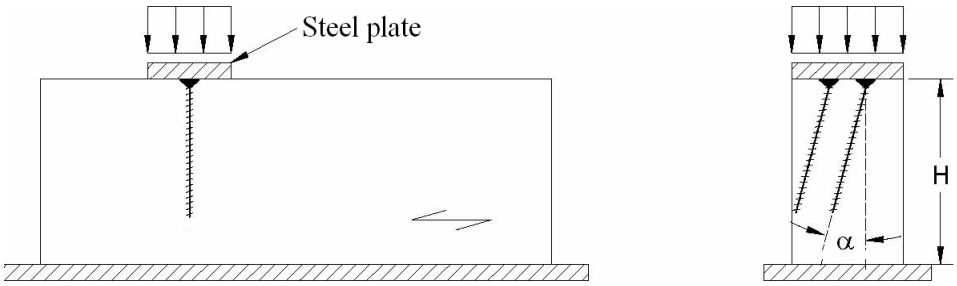

Figure 4.14 Inclined screws with respect to the perpendicular to the surface axis, [8]

D) Combination of inaccuracies A) and C), types (3/3-10° and 3/3-5°), see Figure 4.15.

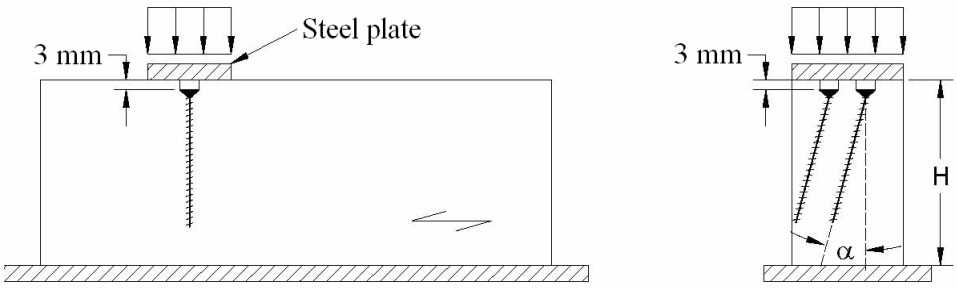

Figure 4.15 Combination of inaccuracies, [8]

For the quantitative evaluation of the effect of the inaccuracies that were tested also a configuration without imperfections (Type 0/0-0°) was considered. Furthermore, different types of screws were used in order to evaluate the influences of the inaccuracies in cases of different mode of failure (7,5 x 182 mm, 8,0 x 340 mm, 10 x 200 mm). All of the specimens were classified as GL28h glue-laminated timber according to DIN, and reinforced with two screws. The load was applied by a steel plate with a length of 80mm and the same width of the specimens, which is equal to 100mm. In Table 4.4 the results are gathered from the tests.

Table 4.4 Results from the tests regarding inaccuracies in assembling the screws, [8]

Type	**Depth – Depth** [mm]-[mm]	**Angle** [°]	**n°** [-]	**Load R_{90}** [kN]	**Deviation 0/0-0°** [%]	**E-Modulus E_{tot}** [N/mm^2]	**Density ρ** [kg/m^3]
Reinforcement with 2 screws 7,5 x 182 mm							
0/0-0°	0 - 0	0	5	96.1	0.0%	1050	460
3/0-0°	3 - 0	0	6	94.2	-2.0%	935	442
3/3-0°	3 - 3	0	5	101	5.5%	810	442
0/0-10°	0 - 0	10	5	99.6	3.6%	866	455
3/3-10°	3 - 3	10	7	88.7	-7.7%	624	434
Reinforcement with 2 screws 8 x 340 mm							
0/0-0°	0 - 0	0	5	98	0.0%	1350	425
3/0-0°	3 - 0	0	5	102	3.8%	1016	443
3/3-0°	3 - 3	0	5	114	16.0%	843	427
0/0-5°	0 - 0	10	5	99.6	1.6%	929	419
3/3-5°	3 - 3	10	6	108	9.7%	877	439
Reinforcement with 2 screws 10 x 200 mm							
0/0-0°	0 - 0	0	5	104	0.0%	1119	439
3/0-0°	3 - 0	0	5	99	-5.0%	761	438
3/3-10°	3 - 3	10	6	108	3.5%	656	432

In the column called deviation, see Table 4.4, it is stated how the performance is improved or decreased considering the inaccuracies. The type 0/0-0° is the reference cases which all other types are compared with. The greatest improvements are achieved if the screws are lowered 3 mm in relation to the surface. The most unfavourable cases are when the screws are inclined, since it results in both less load carrying capacity and loss in stiffness in the glue-laminated timber. A situation when the heads of the screws are on a different level is also unfavourable since it results in one screw being more loaded than the other, thus the efficiency of the whole reinforcement configuration being less.

In Figure 4.16 the comparison between timber in compression perpendicular to the grain and axially loaded screws can be noted. As soon as the strength of the timber is reached the stress of compression perpendicular to the grain is absorbed by the screws and distributed further

down in the timber. It must be noted that axially loaded screws behave similarly in both compression and tension.

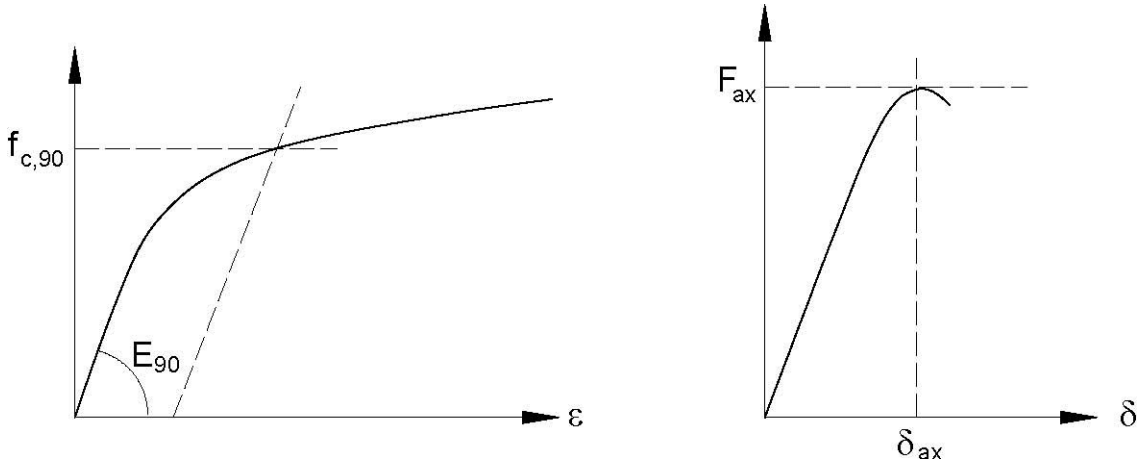

Figure 4.16 Compression perpendicular to the grain (left), Axially loaded screws in tension (right), [8]

4.5 Tests performed and conclusions

Several different studies have been performed concerning the effect of self-tapping screws used as reinforcement in timber structures. Self-tapping screws can be used both to reinforce against tensile failure and failure modes caused by compression. In this thesis the latter of the two types of reinforcement purposes is of interest.

4.5.1 Tests performed by Bejtka

A report presented by Blass and Bejtka, Reinforcements perpendicular to the grain using self-tapping screws, [2], was studied. Blass and Bejtka performed tests to compare the load-carrying capacity of reinforced and non-reinforced beam supports. As reinforcement they used self-tapping screws with continuous threads and the screws were placed at the beam supports, see Figure 4.1. The results Blass and Bejtka obtained showed an improvement of the load-carrying capacity of the reinforced beam supports between 131 % and 329 % compared to the non-reinforced beam supports. The difference depended on the type of screws that were used. In their study they could identify three different types of failure modes.

The three types of failure modes that were identified are:

1) The load-carrying capacity of the reinforced beam support was characterised by pushing the screws into the timber. Simultaneously, the compressive strength perpendicular to the grain at the beam surface was reached. For screws the pushing-in capacity is considered equal to the withdrawal capacity. This failure mode was observed at beam supports reinforced with slender screws.

2) The load carrying capacity of the reinforced beam support was characterised by buckling of the screws. Simultaneously, the compressive strength perpendicular to the grain at the beam surface was reached. This failure mode was observed at beam supports reinforced with slender screws, see figure 4.17.

3) The load-carrying capacity of the reinforced beam support was characterised by reaching the compressive strength perpendicular to the grain in a plane formed by screw points. This failure mode was observed at beam supports with short screws.

In Table 4.5 the test configuration is displayed together with the results from the tests performed by Bejtka. It is of interest also to notice the failure mode that was observed during the tests, e.g. specimen type A that was reinforced with short thin screws caused a failure in the timber in stead of the screw being pushed into the timber. This is likely due to the low capacity in the timber.

Table 4.5 Test configuration and results, [2]

Specimen		Screws				Beam support		Capacity	Load increase	Mode of failure
Type [mm]	n°	ϕ [mm]	l_s [mm]	l_{eff} [mm]	n°	b [mm]	L [mm]	$F_{c,90}$ [kN]	[%]	
A	10	-	-	-	-	120	90	57,1	-	-
A	10	6,5	160	220	6	120	90	132	131%	3
B	3	-	-	-	-	120	90	56,4	-	-
B	3	7,5	180	390	6	120	90	195	246%	1/3
B	3	8	260	550	6	120	90	228	304%	2
B	3	8	400	830	6	120	90	242	329%	2

Figure 4.17 Buckling of the full-threaded screws, [8]

The main conclusions that can be drawn from the study by Blass and Bejtka, is that using self-tapping screws as a way to reinforce timber elements perpendicular to the grain, is a simple and an efficient method to improve the timber elements capacity to withstand compression forces.

4.5.2 Tests performed by Nilsson

Karin Nilsson treats the subject concerning reinforcement perpendicular to the grain using self-tapping screws in her master thesis at Lunds Tekniska Universitet, [3]. The aim of her study was to distinguish the differences in the behaviour of timber, subjected to a compressive load perpendicular to the grain, when both reinforced with screws and without reinforcement. Furthermore, the influence of the lengths of different types of screws was of interest. This reinforcement effect was to be studied by using a model presented by Colling, 2000, [3], see equation (4.1).

The screw that was used in her study was of type WT-T-8.2 with varying lengths of 160, 220 and 300 mm. The test was performed on glue-laminated specimens with strength class L40, which corresponds to a GL32 according to EN 1193. The dimension of the specimens that were tested was 90 x 315 x 500 mm. The load was applied both by a steel plate and a timber plate perpendicular to the grain. The dimensions of the plates were 90 x 150 x 10 mm for the steel plate and 90 x 150 x 16 mm for the timber plate.

The first tests were conducted to determine the influence of each screw concerning the load bearing capacity perpendicular to the grain. 18 screws were loaded using a Torx-socket, T40, since it proved to be most suited for these types of tests. The screws were placed in groups of three with the same spacing in between. The results that were obtained from these tests showed that both the 220 mm and the 300 mm screws buckled when subjected to the load. The buckles occurred about 20 mm below from the head of the screws. The shorter 160 mm screw did not buckle but was pushed into the wood. The highest capacity was reached by the 220 mm screw before buckling.

The second test treated the influence of the plates. These tests were done separately in order to be able to use the Colling model. Values of $F_{c,90,timber}$ were obtained. The load was applied until 10 mm of deformation was reached which exceeds the proportionality limit of about 1 mm.

In the third test the load was applied via a steel plate and a timber plate onto the screws and group of screws. These tests represent the actual reinforcement of the glue laminated timber

and will correspond to the sum of test one and test two in the Colling model, $F_{c,90}$, with some modifications.

When the third test was conducted Nilsson, [3], noticed no visual crack initiation or other types of defects in the wood. When the load was applied via a wood plate onto the screws Nilsson noticed that the screw head penetrated the wood plate and made an imprint into the plate. Moreover she did a study of groups of screws loaded by a steel plate and a wood plate. When the group of screws were loaded via the steel plate, it could be noticed that deformations in the glue-laminated timber were introduced at the tips of the screws. Nilsson also noticed a bump on both sides of the glue-laminated specimen. As the load was applied via the wood plate onto the screws the same phenomenon as before presented itself as the screw heads penetrated the wood plate but this time the stress concentration was to be found about 20-30 mm below the point of loading. Also in this case deformations occurred on both sides of the glue-laminated specimens. The results from the tests can be seen in Table 4.6 and the model presented in equation (4.17).

Table 4.6 Results from the tests conducted by Nilsson

Configuration	Steel plate, F_{c90}	Timber plate, F_{c90}
Un-reinforced	76 kN	86 kN
4Φ8.2x220 mm screws	141 kN	96 kN
6Φ8.2x220 mm screws	159 kN	98 kN
8Φ8.2x220 mm screws	140 kN	108 kN

Model presented:

$$F_{c,90} = F_{c,90,timber} + k \times n \times F_{D,S} \tag{4.16}$$

Total capacity = Capacity of timber + Capacity of screws

Where:

$F_{c,90}$ is the compression strength with the given configuration of screws [kN]

k Coefficient

n is the number of screws

$F_{D,S}$ is the maximum buckling capacity of the screws tested with the torx-socket [kN]

In order to obtain the value of the coefficient k the results from the three tests were added into the Colling model and the value of the coefficient could be solved. By doing this an approximation of the influence of the different types of plates were done. The final model that these tests led to is as follows; see equations (4.17-4.18):

Reinforcement with timber steel plate, $k = 0{,}5$:

$$F_{c,90} = F_{c,90,timber} + 0{,}5 \times n \times F_{D,S} \quad (4.17)$$

Reinforcement with timber plate, $k = 0{,}1$:

$$F_{c,90} = F_{c,90,timber} + 0{,}1 \times n \times F_{D,S} \quad (4.18)$$

In the results Nilsson concludes that by using self-tapping screws as a way to reinforce glue-laminated timber a significant improvement is reached compared to non-reinforced glue-laminated timber. When Nilsson studied the different lengths it was observed that the 160 mm screw proved to be the best when subjected to a direct load. The 220 mm screw showed best performance when the load was applied by wood plate since it allowed the screw head to penetrate the wood plate and stabilise the screw.

The conclusions that can be made after studying the master thesis by Karin Nilsson is that she has noticed that an improvement of the compression load capacity can be obtained by using screws as a method of reinforcing. She also observes the different types of failure mode that can occur, screws being pushed in (withdrawal failure), buckling of the screw and compression failure in the wood at the tip of the screw. By using a group of screws and a steel plate transferring the load onto the screws the capacity is improved the most.

4.5.3 Tests performed by Reichegger

Reichegger, [11], performed tests to understand the effect of the reinforcement of timber in compression perpendicular to the grain with self-tapping screws. The tests were made as a comparison with the analytical solution of the load carrying capacity of reinforced glue-laminated timber, proposed by the University of Karlsruhe, see Chapter 4.1.2. Furthermore, the un-reinforced configuration was taken into account to evaluate the real advantages of the reinforcement, also different types of screws and different configurations of plates were taken into account.

The specimens that were tested were made in glue-laminated timber of class BS24h and BS28h in accordance to the German code (DIN 1052:2004), [5]. The dimensions were of two types; 400x120x200mm and 600x120x200mm. The dimensions of the applied load were chosen accordingly to the prescriptions of the minimum distances of the self-tapping screws from the edge and between themselves, that is 80x120mm and 120x120mm, respectively. The plates used were of two different types, one in steel and the other in timber of class BS11 according to the German code. The self-tapping screws used in the reinforcement were of two different types, WT-T SFS and SPAX-S screws of different length and diameter. All the different types of tests made are summarised in the sequent table, see Table 4.7:

Table 4.7 Test configuration of the tests performed by Reichegger, [11]

n°	Specimens	Dimension [mm]	Screws (n°=4)	Plate	Dimension [mm]
2	Unreinforced	400x120x200	-	steel	120x80
1	Unreinforced	400x120x200	-	timber	120x80
1	Unreinforced	600x120x400	-	steel	120x120
1	Reinforced	400x120x200	WT-T SFS Φ6.5/160	timber	120x80
3	Reinforced	400x120x200	WT-T SFS Φ 6.5/130	steel	120x80
2	Reinforced	400x120x200	WT-T SFS Φ 6.5/160	steel	120x80
3	Reinforced	400x120x200	WT-T SFS Φ 8.2/160	steel	120x80
2	Reinforced	600x120x400	WT-T SFS Φ 8.2/220	steel	120x120
1	Reinforced	600x120x400	SPAX-S Φ 8/200	steel	120x120
1	Reinforced	600x120x400	SPAX-S Φ 8/200	timber	120x120

In the following figures, see Figures 4.18-4.19, the test results are presented regarding the test results on the configuration seen in Table 4.7.

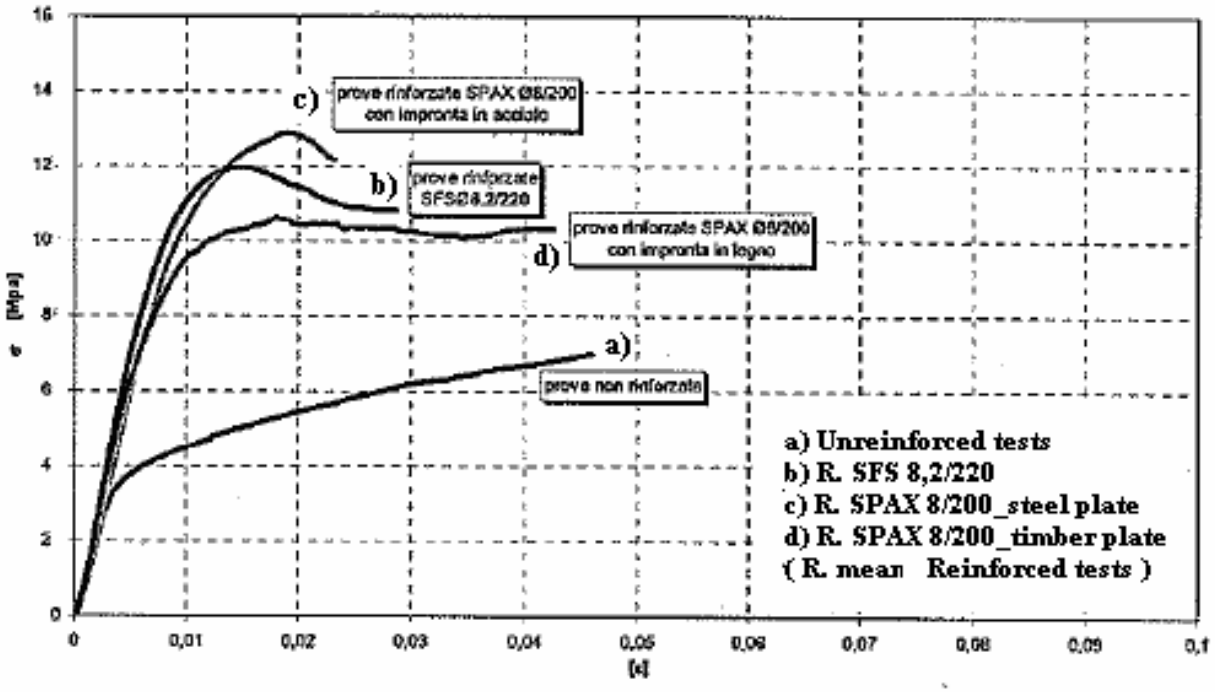

Figure 4.18 σ–ε Relationship of mean values of tests results for [600x120x400] specimens reinforced with 4 screws with [120x120] surface of applied load, [11].

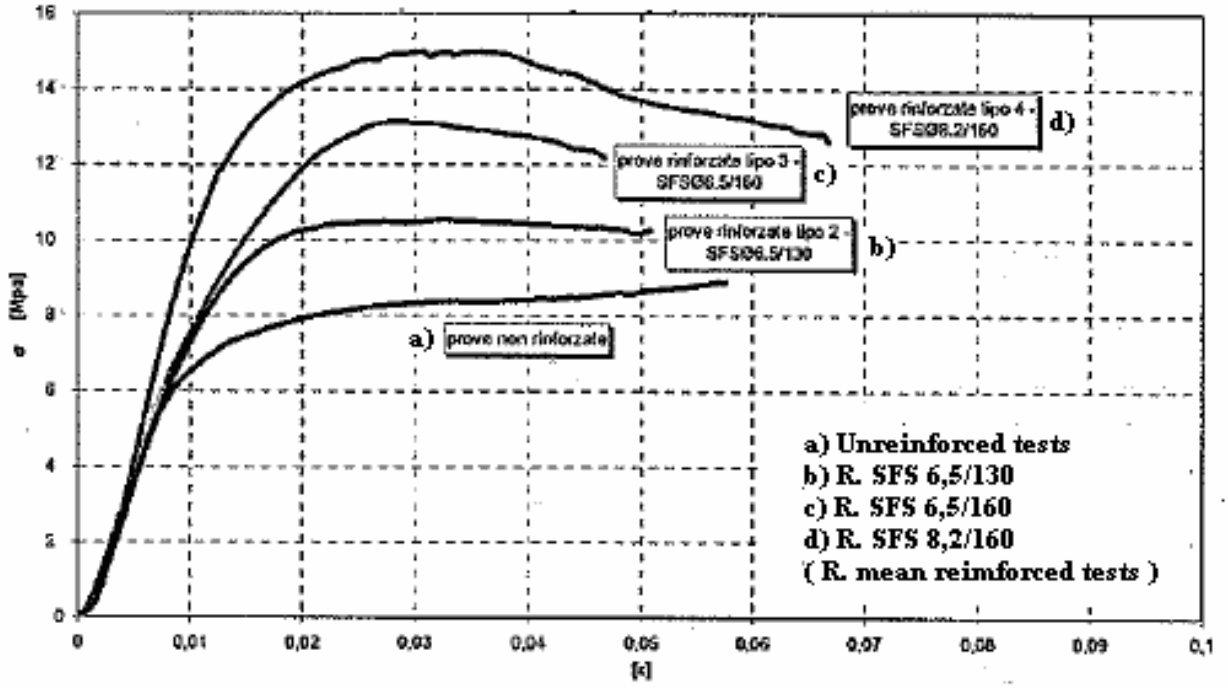

Figure 4.19 σ–ε Relationship of mean values of tests results for [400x120x200] specimens reinforced with 4 screws with [80x120] surface of applied load, [11].

The analysis of the test result was performed so that the characteristic strength of the timber in compression perpendicular to the grain according to European standard UNI EN 1193 could be

calculated. These values can be compared to the calculations according to the model proposed by university of Karlsruhe, see Chapter 4.1.2. In the sequent table, see Table 4.8, the calculations made on BS24h and BS28h are summarized.

Table 4.8 Summary of the capacities from the tests, $F_{C,90,k}$, and the analytical values according to the model of Karlsruhe, [11]

Specimen	**Screws**				**Applied load**		**Model of Karlsruhe**		**$F_{c,90,k}$**	
Dimension [mm]	**Type**	**d [mm]**	**l_s [mm]**	**N°**	**b [mm]**	**L [mm]**	**GL24h [kN]**	**GL28h [kN]**	**EN 1193 [kN]**	**[%]**
400x120x200	-	-	-	-	120	90	53.5	59.4	76.3	-
400x120x200	WT-T SFS	6.5	130	4	120	90	86.4	100.8	101.5	+33
400x120x200	WT-T SFS	6.5	160	4	120	90	95.6	108.0	123.7	+62
400x120x200	WT-T SFS	8.2	160	4	120	90	104.3	118.2	136.3	+79
600x120x400	-	-	-	-	120	120	72.9	81.0	65.7	-
600x120x400	WT-T SFS	8.2	220	4	120	120	136.2	152.9	173.1	+63
600x120x400	SPAXS-S	8.0	200	4	120	120	141.4	155.9	175.8	+167

It is possible to see in the Figures 4.18-4.19 that there is always an increase of capacity when the specimens are reinforced with full-threaded screws, except when the load is applied with a timber plate and the head of the screws are too thin like the SPAX-S screws. In that case the screw heads are penetrating the timber plate.

As a conclusion Reichegger found that the model of University of Karlsruhe is a good predictor of the load carrying capacity in the case of reinforcement of compression perpendicular to the grain with full-threaded screws, see Table 4.8. Furthermore, the failure modes were correctly predicted by the model. In fact, for the for the screws WT-T SFS Φ6.5/130, WT-T SFS Φ 6.5/160 and WT-T SFS Φ 8.2/160 the mode of failure was the pushing in of the screws, instead of the screws WT-T SFS Φ 8.2/220 and SPAX-S Φ 8/200 the mode of failure was the buckling of the screws.

The specimens loaded with the steel plate, reinforced with four screws showed an increase of capacity from 33% to 167%, see Table 4.8. The difference in the type of screw heads has a negligible influence.

4.5.4 Comparison between Collins model and the model of Karlsruhe

In order to be able to compare the two different models and the test results obtained by Nilsson the model of Karlsruhe needs to be refined by removing all the safety factors. The tested specimens with their properties are to be inserted into the model from Karlsruhe and then compared with the test results obtained by Nilsson.

In this study the timber plate is disregarded due to its poor performance in the tests, thus the model of Karlsruhe does not treat the case with a timber plate.

The first observations made were that the capacity according to the model of Karlsruhe and the Colling model varies linearly with the number of screws. In the tests performed by Nilsson it was shown that the capacity relationship is not linear with the number of screws, see Figure 4.21. In fact when the numbers of screws are increased the contribution of each screw in the group of screws may be decreased, this is most likely due to lack of distance between the screws.

Colling considers the reduction depending on the loading material with a constant coefficient *k*, see Chapter 4.1.1 whereas the model of Karlsruhe do not consider this fact. However, the

model of Karlsruhe considers two types of failure modes of the screw separately. The model of Karlsruhe distinguishes between buckling of the screw and the screw being pushed in. This is to be compared to the Colling model that only considers an ultimate capacity of the screw independently of how it fails.

This means that the interaction between the screws and the timber is only considered in the model of Karlsruhe. At the head of the screw two theoretical spring stiffness situations are considered, one assuming that the rotational spring stiffness at the head of the screw being, $K_{spring} = 0$ and the other where K_{spring} = infinity. The first assumption that the spring stiffness k= 0 is on the safe side and the reality is somewhere in between these extreme values. A sensitivity study of this stiffness parameter showed that the influence of these two extremes on the total buckling capacity is about 16 %, which can be regarded as negligible.

In the comparison four calculations were done with the model of Karlsruhe; 1 screw loaded by a steel plate, 4 screws loaded by steel plate, 6 screws loaded by steel plate and 8 screws loaded by a steel plate. These analytical results were to be compared to the test results performed by Nilsson. The value of $f_{c,90,k}$ in the model of Karlsruhe is taken as 3.3 MPa according to the German code (DIN 1052:2004), [5]. The results from the comparison can be seen in Table 4.9.

Table 4.9 Comparison between the analytical model of Karlsruhe and test results by Nilsson

Configuration	Total capacity		Deviation from test
	Test results by Nilsson (mean values of the tests)	Model of Karlsruhe ($f_{c,90,k}$ = 3.3 MPa)	
1Φ8.2x220 mm screws Steel plate	70 kN	58.3 kN	-17 %
4 Φ8.2x220 mm screws Steel plate	141 kN	99.7 kN	-29.8 %
6 Φ8.2x220 mm screws Steel plate	159 kN	127.3 kN	-19 %
8 Φ8.2x220 mm screws Steel Plate	140 kN	148.5 kN	+6 %

The results of the comparison between the different models and the test results from Nilsson's master thesis are shown in Figure 4.21. The value of $f_{c,90,k}$ used in the both models was chosen to be 3.3 MPa according to the German code (DIN 1052:2004), [5]. The capacity of the screws used in the model by Colling, $F_{D,S}$, was taken from the tests by Nilsson and is 27.5 kN. It can be seen in Figure 4.21 that the model by Colling adapts best to the test results by Nilsson and when compared to the model of Karlsruhe. This is probably due to the fact that the capacity of the screws that is to be inserted into the model by Colling is taken from the tests by Nilsson. However, the fact that the capacity of the screws is an empirical parameter and can not be

calculated is a great weakness in the model. Hence, for a given screw in a given configuration the capacity of that particular screw must be known in order for the calculations to be useful. The model from Karlsruhe proves to be conservative and on the safe side except for the case when eight screws was used in the tests by Nilsson. However, the drop in capacity could be related to the fact that the distance between the screws in the tests does not respect the distances given by the recommendations in the model by Karlsruhe.

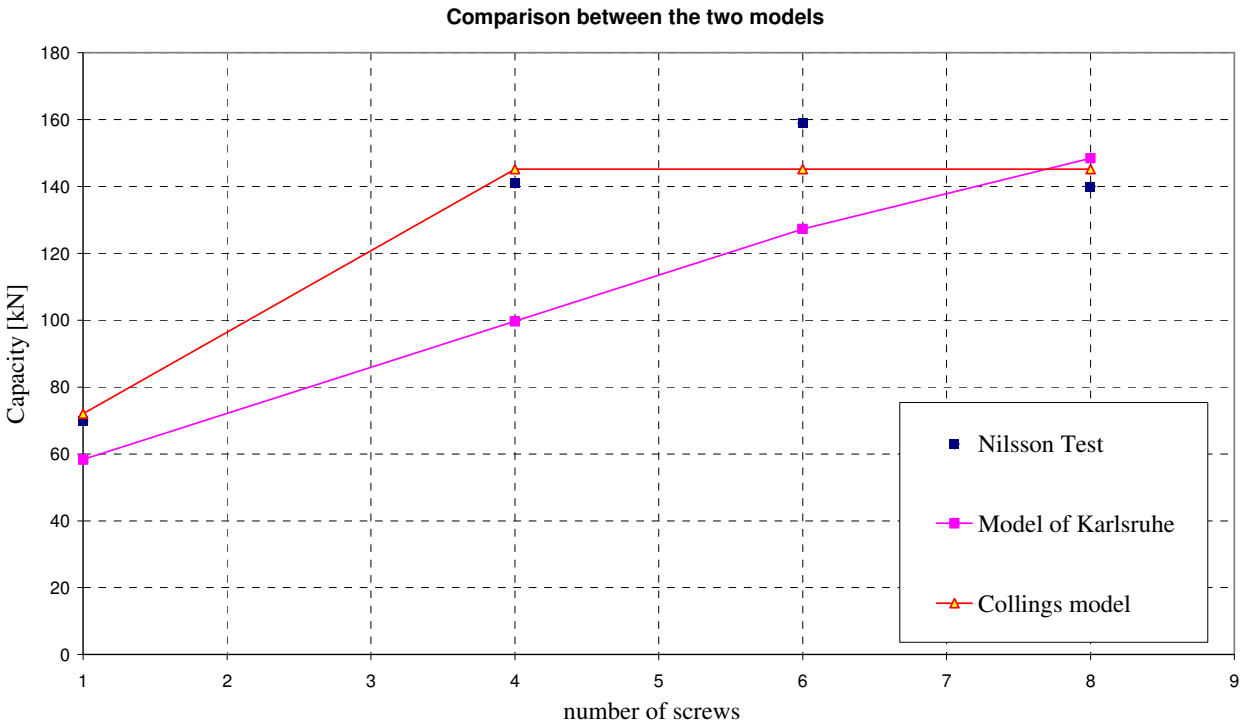

Figure 4.21 Comparison between different models and the test results by Nilsson.

5 Laboratory tests

5.1 Description

The aim of the tests was to find out if the load carrying capacity corresponds to the values suggested by the different codes thus verifying the FE-model. Furthermore, it was of interest to note the behaviour of the reinforced specimens and if the failure modes present themselves as described in theory. The number of test specimens does not give a statistically good representation of how glue-laminated timber behaves in compression perpendicular to the grain. However, the tests gives a hint on the influences of different anchorage configuration and whether reinforcement using screws can be regarded as an effective method of reinforcing.

5.1.1 Design of test specimens and required components

The test specimens were designed to withstand a tensile of 300 kN in the pre-stressing bar. Special attention was put into designing the plates and the washer that were to transfer the load from the bar onto the timber. The calculations can be seen in Appendix E. The result of these calculations can be seen in Table 5.1.

The choice of screws was determined from analytical calculations using the model presented in Karlsruhe, see Chapter 4. In order to optimize the tested elements lengths and diameters had to be chosen so that withdrawal failure would not occur. In fact, as can be seen in Chapter 4, by increasing the length after a certain value only has an influence on the withdrawal capacity. Therefore fixing a length to a value that is big enough to exclude the pushing in failure mode was considered appropriate.

The specimens were divided into two categories. The first category regards the ultimate load-carrying capacity and the second category considers the long-term behaviour including the loss of pre-stressing force in the specimens due to creep in the timber and relaxation of the steel. Moreover, the long term tests were also performed to monitor the behaviour of the glue-laminated timber when subjected to change in temperature and moisture content. Ten L40 glue-laminated timber specimens were manufactured by Moelven with the dimensions as seen in the Figures below. The specimens were pre-drilled by the manufacturer with the diameter of 28-30 mm. This was done to be able to insert the pre-stressing bar which has a diameter of 20 mm. Figure 5.1 illustrates the geometry of the test specimens and Figure 5.2 displays all the components that were used to assemble the different anchorage configurations.

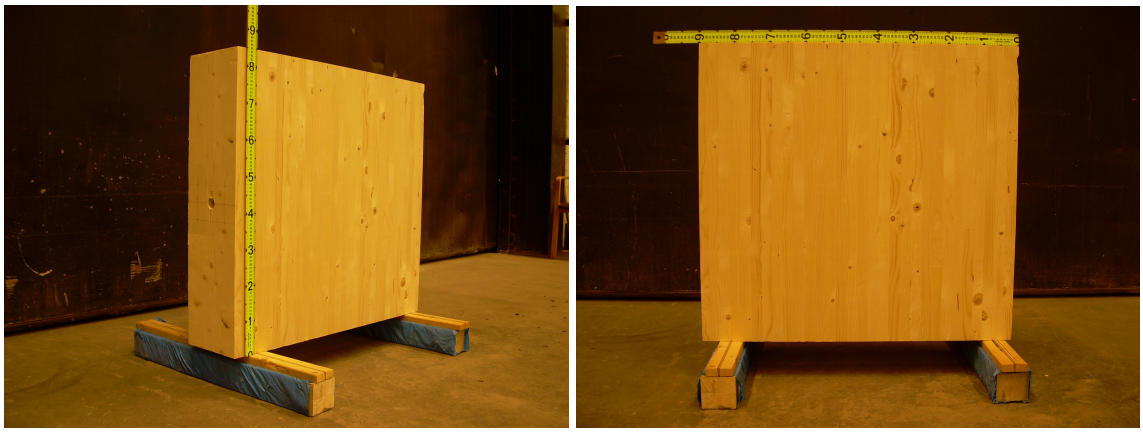

Figure5.1 Specimen 900x850x215 mm

Figure 5.2 Components included in the different anchorage configurations

The different dimensions of the components included in the tests can be seen in Table 5.1. Due to production inaccuracies the dimensions described in Table 5.1 does not apply for all specimens but can be considered as mean values of all specimens and components.

Table 5.1 Different components included in the laboratory tests

Part	**Length**	**Width**	**Height**	**Hole diameter**
Glue-laminated timber	900 mm	850 mm	215 mm	28-30 mm
Hardwood plate, $\rho \approx 1000\ kg/m^3$	205 mm	200 mm	40-43 mm	45 mm
Square Steel plate	200 mm	200 mm	15 mm	40 mm
Square Steel plate	200 mm	200 mm	20 mm	30 mm
Hexagonal Nut	36 mm	36 mm	70 mm	20 mm
	Outer diameter	**Thickness**	**Hole diameter**	
Steel Washer	100 mm	10 mm	26 mm	
Circular aluminium plate	200 mm	20 mm	26 mm	

The bar that was used to apply the pre-stressing force was a Dywidag reinforcement bar with the diameter of 20 mm and length of 2.5 m. The Dywidag bar has the design strength values as follows:

$f_{yd} = 900 \quad MPa$

$f_{ud} = 1100 \quad MPa$

Two types of screws were chosen both from the manufacturer SPAX. The chosen screws were the full-threaded self-tapping 300Φ10 mm and 300Φ12 mm screws, see Figure 5.3.

Figure 5.3 SPAX Full-threaded self-tapping screws, length 300 mm diameters 10-12 mm

5.1.2 Preparation of the test specimens

The test specimens were delivered without pre-drilled holes for the screws and the holes for the pre-stressing bars were not perfectly straight. Regarding the specimens that were to be subjected to long term load it was crucial that the holes for the pre-stressing bars had to be big enough thus straight. This issue was resolved by drilling the holes with a $d = 30mm$ drill thus enlarging the diameter in order to have a good clearing for the bars.

Considering the specimens that were to be reinforced extra attention were put into inserting the screws so that they are straight. The choice was made to pre-drill holes since the equipment needed to insert the screws without pre-drilling was missing. Two different drills were chosen, see Figure 5.4. The first drill was chosen to pre-drill holes for the d = 12 mm screws and the second drill for the d = 10 mm screws, with approximate drilling lengths of 150 mm and 80 mm, respectively.

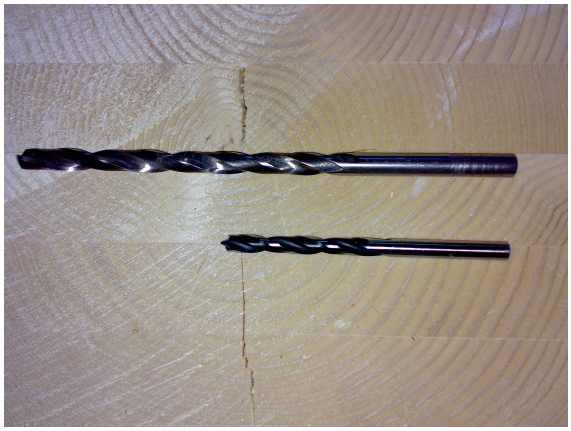

$l_1 = 162mm, \quad d_1 = 7.2mm$

$l_2 = 93mm, \quad d_2 = 6mm$

Figure 5.4 Drills that were used for pre-drilling the holes of the screws

The first centimetres of the screws were inserted manually to ensure a straight angle between the screw axis and the specimens, and then driven into the timber using a drilling machine combined with the T50 torx socket. To avoid the imperfections described in chapter 4.4 the screws were lowered 2-3 mm into the specimens ensuring equal loading on the screws. In Figure 5.5 the pre-drilling procedure is visualized together with the end result of four screws being inserted.

a)  b) 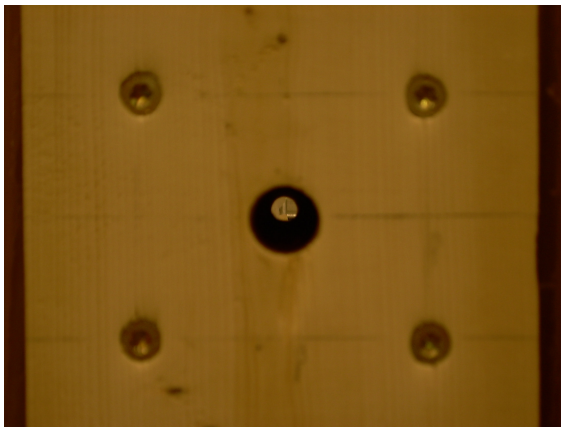

Figure 5.5 Pre-drilling a), Screw reinforced specimen b)

The distances that were used between screws and edge distances to screws are in accordance to the suggested values by Bejtka, see Chapter 4.1.2 and Figure 5.6. These distances were calculated using $d = 10mm$ and also used for the $d = 12mm$ screws.

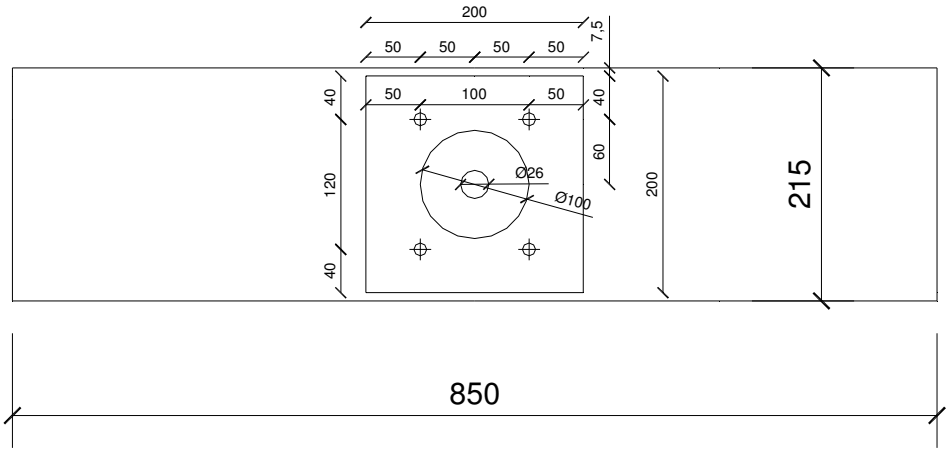

Figure 5.6 Distances of the reinforced specimen

In order to monitor the change in load of the bar when considering the specimen that were subjected to long-term loading some arrangement had to be made. First holes needed to be drilled in the specimens so that a wire connected to the strain gauges could be inserted. The strain gauges were applied on the Dywidag bars using glue and covered by applying tape so that the strain gauges remain in position when inserting them into the specimens. Figure 5.7 displays the assembly process of the strain gauges.

a) 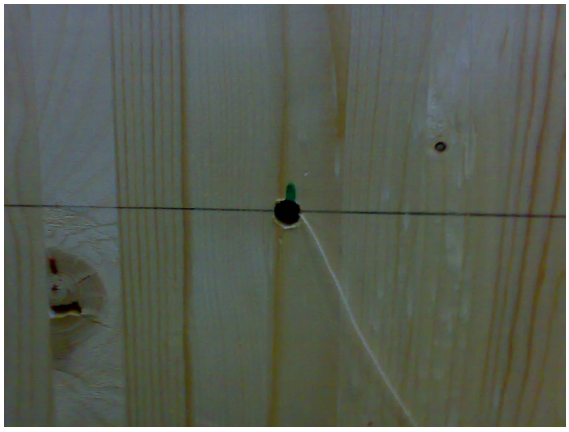 b) 

Figure 5.7 Drilled hole for the wire connected to the strain gauge a), Strain gauge connected to the Dywidag bar b)

5.2 Ultimate load carrying capacity

The ultimate load carrying capacity was determined by subjecting the test specimens to a uniform compression load, see Figure 5.8. This method of loading was necessary since the hydraulic jack lacks the ability to reach load that would cause failure of the test specimens, c.f. 1.2 in Appendix K. The consequence of loading the specimens by using this method is that it does not represent the real loading of the specimens when used in field. However, it was considered to be of more importance to be able to load the specimens to failure in a controlled approach than simulating the loading in field. Equipment used in these tests together with the calibration of the hydraulic jack is described in Appendix K.

Figure 5.8 Loading of the test specimen

5.2.1 Test configurations

The test configuration of the specimens that were loaded until failure is divided into two different types. One type consists of un-reinforced specimens and the other of specimens reinforced with four screws in different manner. The following test configurations were used when testing the ultimate load carrying capacity of the specimens, see Table 5.2 and Table 5.3.

Table 5.2 List of parts that is included in the different test configurations

Type of test	Parts included in the configuration		
Un-reinforced	Steel plate	-	-
Traditional	Hardwood plate	Aluminium plate	Steel washer
Reinforced	4 Screws	Steel plate	Steel washer

Table 5.3 Test configurations of the tests regarding the ultimate load carrying capacity

Specimen	Date	Type of test	Type of screws	Configuration
pl40	2006-12-15	Un-reinforced	-	Steel plate 40 mm
plHW	2006-12-15	Traditional	-	Hardwood plate
S10pl15	2006-12-18	Reinforced	4x300Φ10	Steel plate 15 mm
S12pl15	2006-12-18	Reinforced	4x300Φ12	Steel plate 15 mm
S10pl20	2006-12-18	Reinforced	4x300Φ10	Steel plate 20 mm
S12pl20	2006-12-18	Reinforced	4x300Φ12	Steel plate 20 mm

The first specimen, pl40, was tested by using the default thick steel plate included in the testing equipment. The difference between this specimen and the traditional, plHW, is that the traditional considers the influence of the hardwood plate, the circular aluminium plate and the steel washer. The specimen plHW was also un-reinforced as the specimen pl40 but with different configuration, see Tables 3.2 and 3.3.

5.2.2 Test procedure

The loading rate is of importance when testing; in this case where the testing was done by displacement control the loading rate decides the amount of applied displacement per minute. In these tests the choice was made to load with a velocity of 1.2 mm/min.

The specimens were first loaded to 100 kN and then unloaded back to 0 kN to be loaded again to failure. The first phase were the specimens were loaded to 100 kN was done in order to verify the elastic region of the specimen and to let the different components in the assembly settle in a good manner.

After failure had been reached the specimens were unloaded, the only deformations that remain after this procedure are the plastic deformations which now could be measured.

5.3 Long term behaviour

The long term tests were performed in order to understand the loss of pre-stressing force and to observe and approximate the creep in the timber over time. The tests were conducted in a controllable climate where the relative humidity and temperature can be adjusted. The equipment needed for these tests can be seen in Appendix K.

5.3.1 Test configurations

The following test configurations were used when investigating the long term behaviour; see Table 5.4 and Figure 5.9. The traditional and the reinforced configurations have the same properties as can be seen in Table 5.2 and Table 5.3. Furthermore, all configurations listed below includes the Dywidag bar, d = 100 mm steel washer and nuts locking the configurations.

Table 5.4 Test configurations of the test specimens subjected to long term loading

Specimen	Date	Type of test	Type of screws	Configuration	Moisture content
plHW-LT	2007-02-1	Un-reinforced	-	Hardwood plate	11.5 %
S10pl15-LT	2007-02-1	Reinforced	4x300Φ10	Steel plate 15 mm	11.3 %
S12pl20-LT	2007-02-1	Reinforced	4x300Φ12	Steel plate 20 mm	11.4 %
S10pl20-LT	2007-02-1	Reinforced	4x300Φ10	Steel plate 15 mm	11.1 %

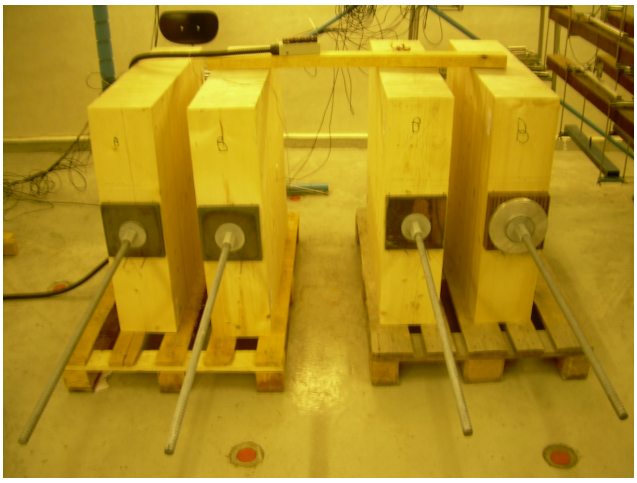

Figure 5.9 Specimens subjected to long-term loading

5.3.2 Procedure

The specimens were placed in a climate room, and then the different configurations where tightened by hand in order to ensure that the plates were centred. After mounting the hydraulic jack on to the bars a backnut was placed on the bar, as can be seen in Figure 5.10, consequently locking the translation of the hydraulic jack when pre-stressing. The pre-stressing force of 230 kN was reached by applying a hydraulic pressure equivalent of 560 bars in the compressor. When desired load was reached the nut locking the configuration was tightened hence storing the pre-stressing force within the test specimens. The strain of the bars was recorded and

monitored in the logging machine with different time intervals. An interval of one reading per second was used during the first 1h 30 min and then one reading per minute was recorded during 17 min and finally one reading per hour was recorded during 260 hours. With the recorded data from these strain gauges the loss of pre-stressing force over time could easily be calculated and displayed as seen in Chapter 5.3.4, Results. The climate in the climate room where set to 23 ˚ C and RH = 58 %.

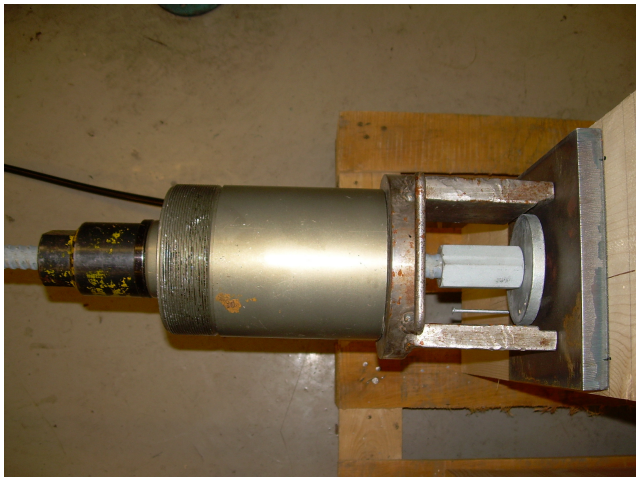

Figure 5.10 Assembly of the hydraulic jack

5.3.3 Long-term results

All the data that are obtained from the strain gauges are analysed and transformed into pre-stressing force as follows in the sequent equation:

$$N = \varepsilon \cdot A_{bar} \cdot E_{bar} \qquad (5.1)$$

Where,

N is the pre-stressing force in the bar

ε is the strain

A_{bar} is the cross section area of the bar equal to 314.2 mm^2 (diameter = 20 mm)

E_{bar} is the E-modulus of the bar equal to 210000 MPa

For each time interval the mean value of the strain in the bar was used. In the following figure, see Figure 5.11, it is possible to see the time-strain relationship that is obtained from one strain gauge during the loading procedure. Tree cycles of pre-stressing and re-stressing were applied in order to reach the prescript pre-stressing force equal to 230kN.

Table 5.5 Initial loss of pre-stressing force due to locking of the nut, a) S10pl15-LT, b) S12pl20-LT, c) S10pl20-LT, d) plHW-LT

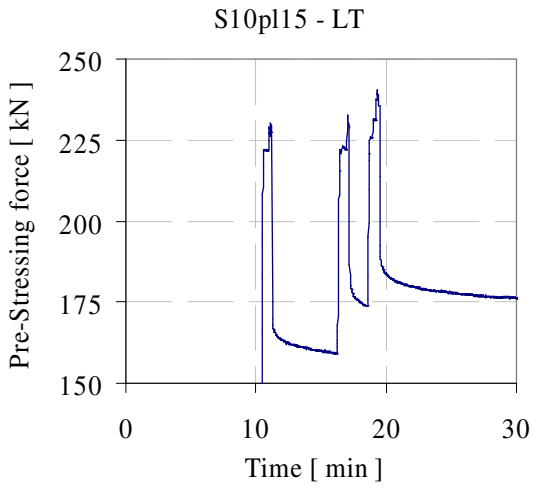

a)

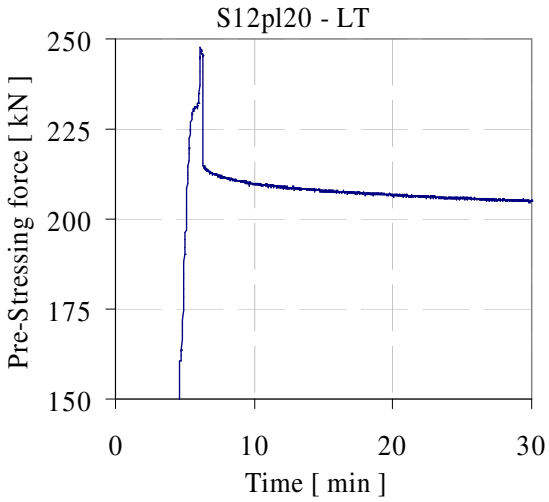

b)

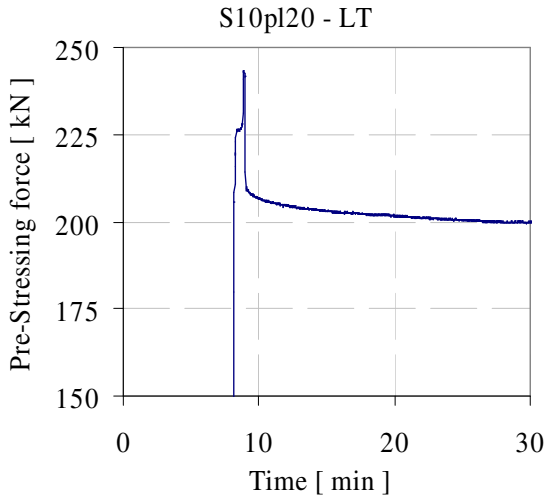

c)

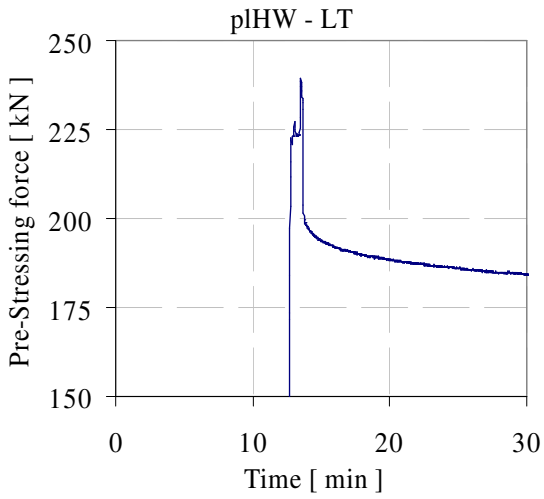

d)

It is possible to notice the loss due to the locking of the nut in all three cases and this effect is not negligible even when conducting more than one pre-stressing procedure as can be seen in Table 5.5 a). When considering this, in order to evaluate and compare the loss of pre-stressing force in the bars, the initial value was chosen at the moment of release of the hydraulic jack and the locking of the nut, as represented in the sequent simplified schematic figure, see Figure 5.11.

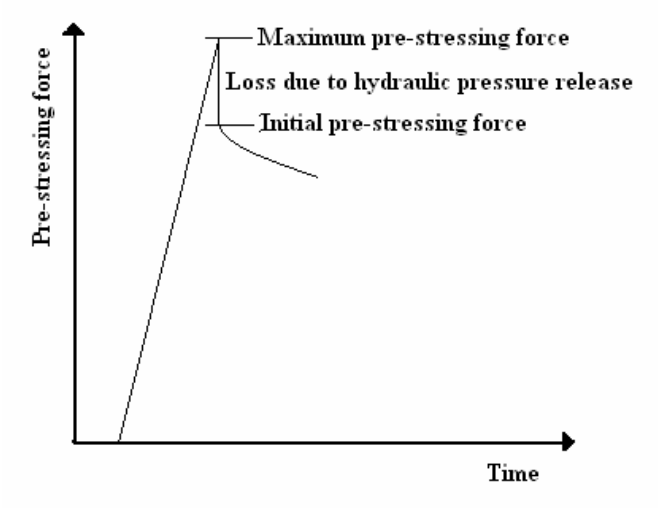

Figure 5.11 Pre-stressing time – force relationship and definition of initial pre-stressing force

In the following figure, see Figure 5.12, the relationship between the ratio of initial pre-stressing force and the time is represented.

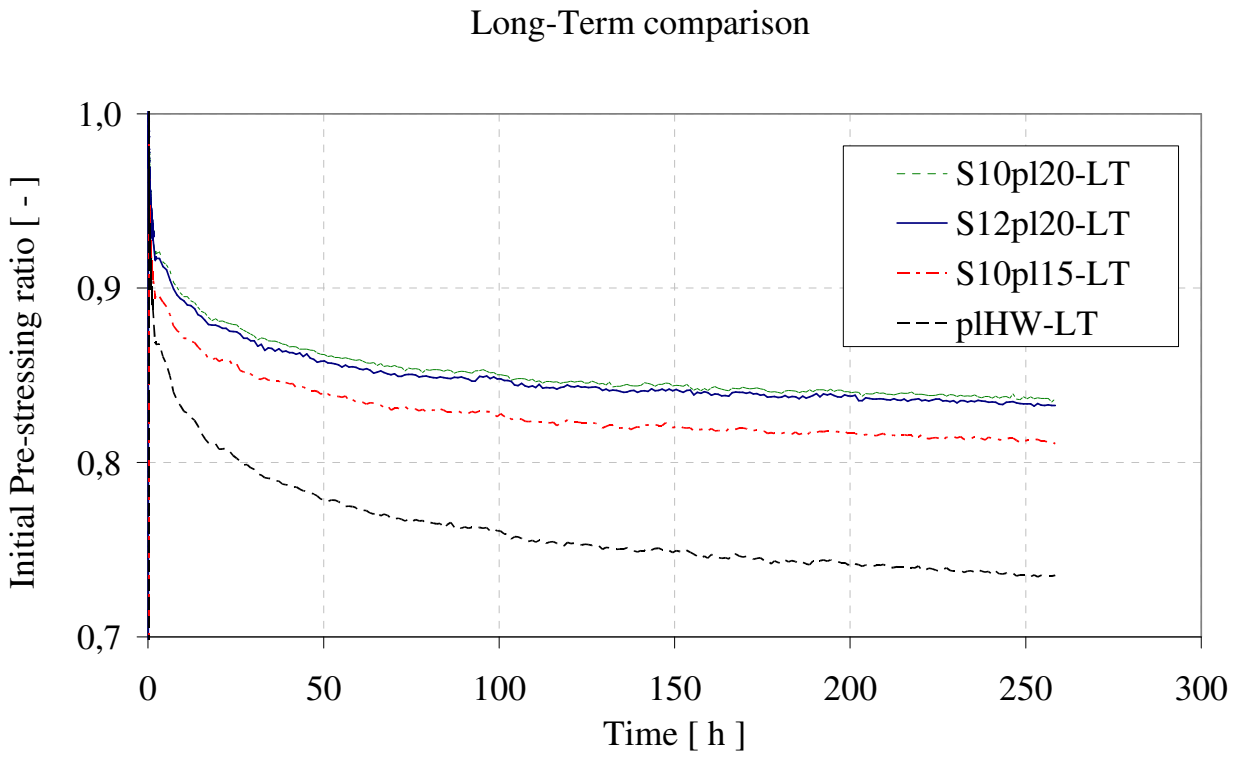

Figure 5.12 Relationship between time and ratio of initial pre-stressing force, the legend and the series are in the same order

In Figure 5.12 it is clearly seen that the greatest loss of pre-stressing force takes place in the un-reinforced specimen, plHW, whereas the use of the thicker steel plate, 20 mm, is most beneficial. The 15 mm plate bended during loading which can be considered as failure since bending of the plate drastically reduces the pre-stressing force initially, 25-30 % reduction, and the specimen was due to this reason re-stressed three times in order to have the same starting value as the other, see Figure 5.14 b) and c.f. 5.11. The hardwood plate cracked during loading

but this is not considered as failure of the plate but normal behaviour during these circumstances; see Figure 5.13 a). Furthermore, it is noticeable that the diameter of the screw has no significant influence on the performance between the different reinforced specimens but increases the performance considerably comparing to the un-reinforced. After 260 h of loading the moisture content had changed to 11.9 % in all specimens. The actual pre-stressing force and the percentage loss of pre-stressing force with respect to the maximum and the initial is gathered in Table 5.6 and 5.7, respectively.

Table 5.6 Pre-stressing force and the loss of pre-stressing force due to locking of the nut

Pre-stressing force and loss	Max [kN]	Initial [kN]	loss [%]
S12pl20-LT	247.6	215.4	13.0
S10pl20-LT	243.4	209.3	14.0
S10pl15-LT	240.6	188.1	21.8
plHW-LT	239.3	198.7	17.0

Table 5.7 Pre-stressing force and the loss of pre-stressing force over time compared to initial, maximum and design value

Pre-stressing force	Initial	50 h		100 h		150 h		200 h		250 h	
and loss	[kN]	[kN]	[%]	[kN]	[%]	[kN]	[%]	[kN]	[%]	[kN]	[%]
S12pl20-LT	215.4	184.9	14.2	182.7	15.2	181.4	15.8	180.5	16.2	179.6	16.6
S10pl20-LT	209.3	180.4	13.8	178.0	15.0	176.7	15.6	175.8	16.0	175.1	16.3
S10pl15-LT	188.1	158.2	15.9	155.8	17.2	154.4	17.9	153.6	18.3	152.9	18.7
plHW-LT	198.7	154.7	17.7	151.1	19.7	148.9	20.8	147.6	21.5	146.2	22.3

Pre-stressing force	Max	50 h		100 h		150 h		200 h		250 h	
and loss	[kN]	[kN]	[%]	[kN]	[%]	[kN]	[%]	[kN]	[%]	[kN]	[%]
S12pl20-LT	247.6	184.9	25.3	182.7	26.2	181.4	26.7	180.5	27.1	179.6	27.5
S10pl20-LT	243.4	180.4	25.9	178.0	26.9	176.7	27.4	175.8	27.8	175.1	28.1
S10pl15-LT	240.6	158.2	34.3	155.8	35.3	154.4	35.8	153.6	36.2	152.9	36.5
plHW-LT	239.3	154.7	35.3	151.1	36.8	148.9	37.8	147.6	38.3	146.2	38.9

Pre-stressing force	Design	50 h		100 h		150 h		200 h		250 h	
and loss	[kN]	[kN]	[%]	[kN]	[%]	[kN]	[%]	[kN]	[%]	[kN]	[%]
S12pl20-LT	230.0	184.9	19.6	182.7	20.6	181.4	21.1	180.5	21.5	179.6	21.9
S10pl20-LT	230.0	180.4	21.6	178.0	22.6	176.7	23.2	175.8	23.6	175.1	23.9
S10pl15-LT	230.0	158.2	31.2	155.8	32.3	154.4	32.9	153.6	33.2	152.9	33.5
plHW-LT	230.0	154.7	32.7	151.1	34.3	148.9	35.2	147.6	35.8	146.2	36.5

The greatest loss of pre-stressing force occurs within the two first days of loading as can be seen in Tables 5.6 and 5.7. This is due to the fact that the most creep occurs shortly after loading and therefore reducing the strain in the bar. The influence of moisture content is not relevant due to the small variation in this test (from 11.3 to 11.9 %, mean value of the specimens).

a)  b) 

Figure 5.13 a) Hardwood crack due to pre-stressing force (plHW); b) Bending of the 15 mm plate due to pre-stressing force (pl15)

5.4 Results of tests on ultimate load carrying capacity

5.4.1 Summary of test results

The test results can be summarized, as seen in Figure 5.14, displaying force-strain curves of the different test configurations. At first it is possible to notice that the 20 mm thick plate performed better than the 15 mm thick plate due to bending of the plate. The 12 mm screws performed better than the 10 mm screws as expected.

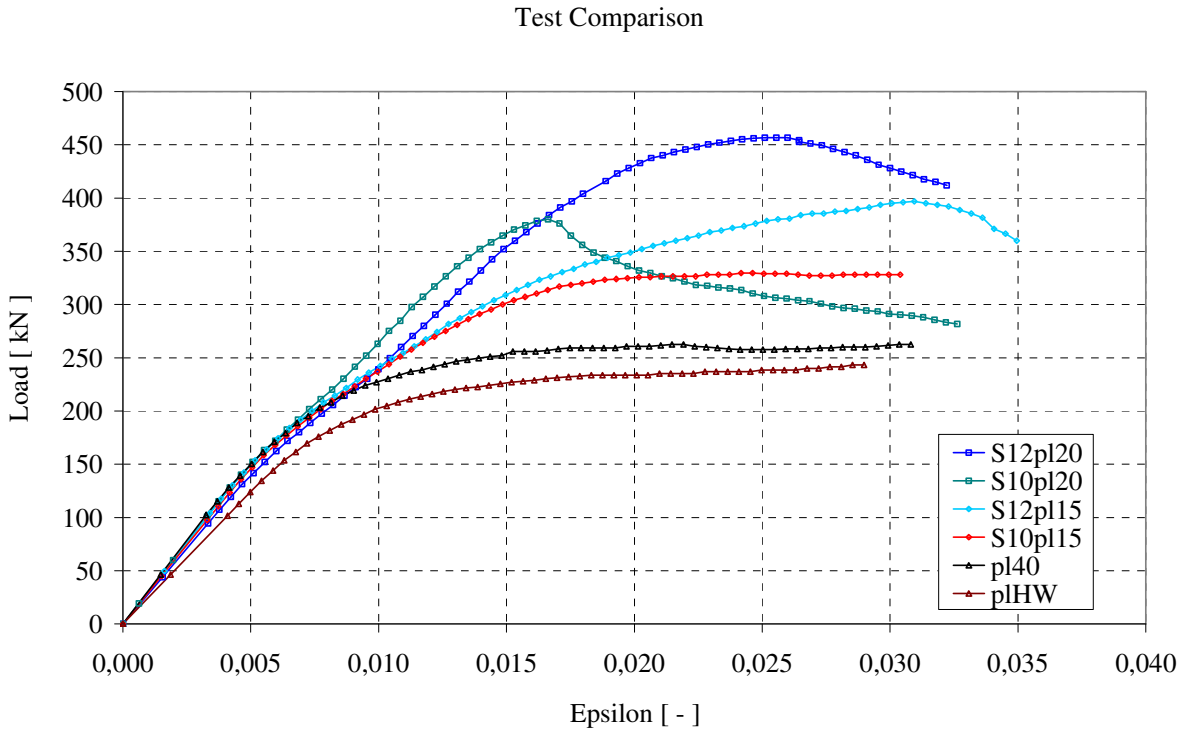

Figure 5.14 Load-Strain relationships from the tests of ultimate load carrying capacities

The un-reinforced curves present the typical behaviour of timber in compression perpendicular to the grain as seen in Chapter 3. The steel plate in this case performed better than the configuration with the hardwood plate. For the cases with reinforcement with screws, it is possible to notice that the curves can be divided into three steps. The different steps are as follows, see Figure 5.15:

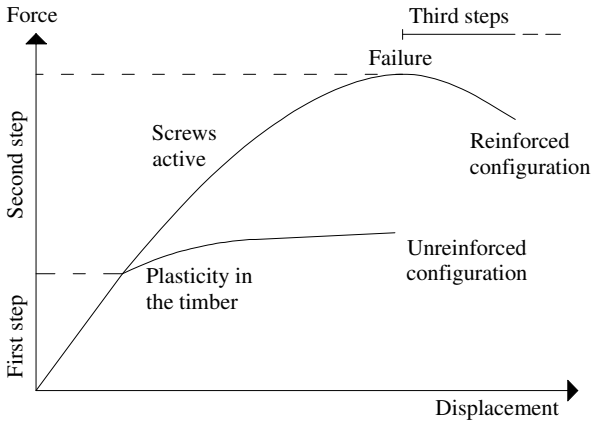

Figure 5.15 Illustration of the different steps identified

First step: From the start of loading to the end of the elastic behaviour of the timber the stiffness of the reinforced cases is the same as of the un-reinforced cases due to the fact that only the timber is active. In this range the screws are not contributing to the stiffness since the magnitude of the deformation is not sufficient to activate the screws.

Second step: From the end of the elastic range of the timber to the maximum capacity reached the screws are activated until their failure.

Third step: In the range after the maximum capacity the load can not be increased further and only when applying displacement control a reduction of stiffness can be viewed.

Different stiffness is displayed in the second step when comparing the 15 mm thick plate to the 20 mm thick plate. This is due to the plate bending effect that is treated in detail in the following chapters.

5.5 Test evaluation and comparison with the analytical solutions

5.5.1 Evaluation of the capacities according to UNI EN 408

In order to evaluate the characteristic capacity in compression perpendicular to the grain, $F_{c,90}$, of the tests performed the standard method proposed by the normative was applied, UNI EN 408, see Chapter 3.2. The capacities obtained can be seen in the following table, see Table 5.8.

Table 5.8 Summarized test results according to UNI EN 408

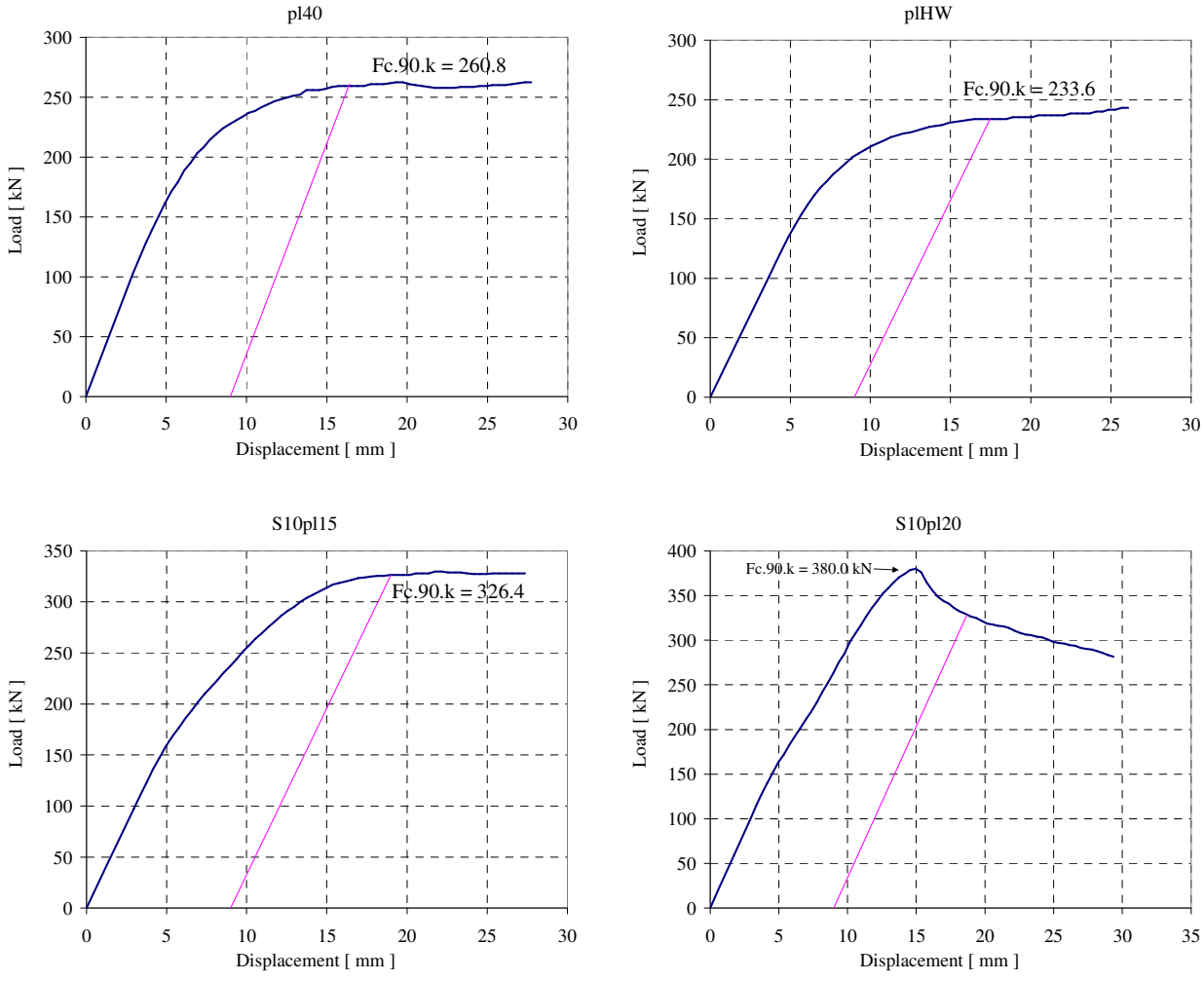

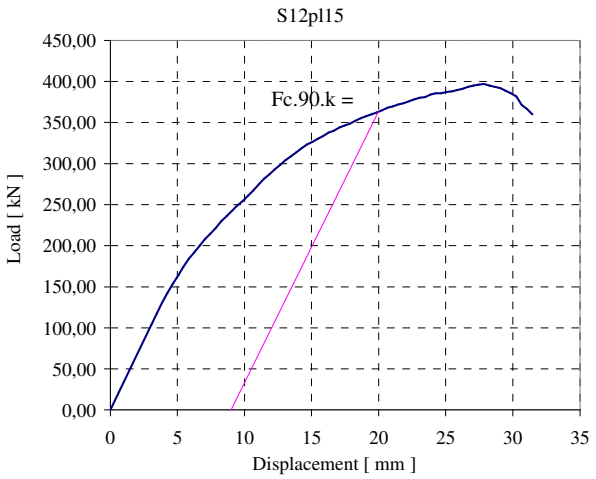

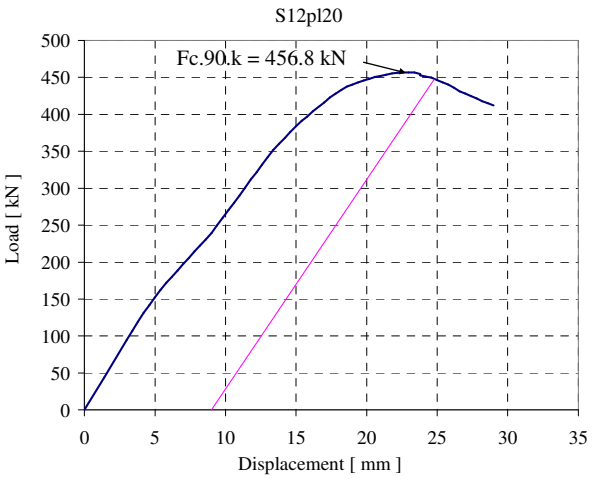

For the cases S10pl20 and S12pl20 the capacity was taken at the point of failure since the maximum point occurred before the calculated point when using the UNI EN 408 standard. In Table 5.9 All the values of the capacities are gathered and the different configurations are compared to the mean value of the capacity of the un-reinforced and the traditional configurations.

Table 5.9 Capacities and effects of the reinforcement regarding the ultimate load carrying capacity

Specimen	Type of test	Capacity UNI EN 408	Increase
pl40	Un-reinforced	260.8 kN	Mean value:
plHW	Traditional	233.6 kN	247.2 kN
S10pl15	Reinforced	326.4 kN	+ 32.0 %
S12pl15	Reinforced	362.9 kN	+ 46.8 %
S10pl20	Reinforced	380.0 kN	+ 53.7 %
S12pl20	Reinforced	456.8 kN	+ 84.8 %

5.5.2 Evaluation of test results and comparison to the analytical solution

The evaluation, configuration by configuration, and the analytical capacities according to the different codes are introduced in this paragraph. Moreover, the failure modes that are of interest are described more in detail. The following figures show the load-strain curves and the imprints caused by the plate and in some cases specific failure modes of the tested specimen, see Figures 5.16 to 5.27. As can be seen in the figures regarding the imprints the loading was not symmetric and the failure only occurred on the weaker side of the specimen.

- pl40

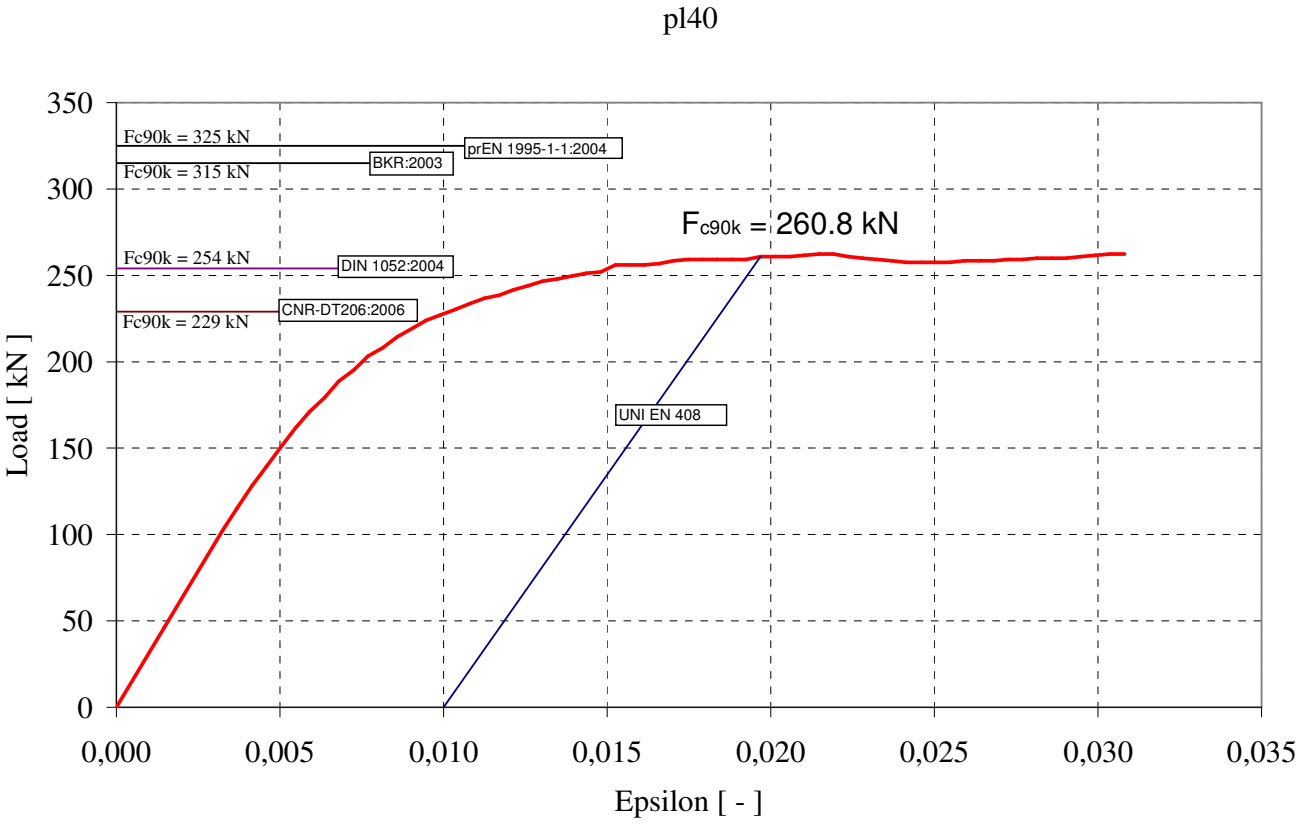

Figure 5.16 F-ε relationship of the un-reinforced test specimen loaded by a 40 mm steel plate

Figure 5.17 Imprint in the specimen representing the remaining plastic deformations, pl40

- plHW

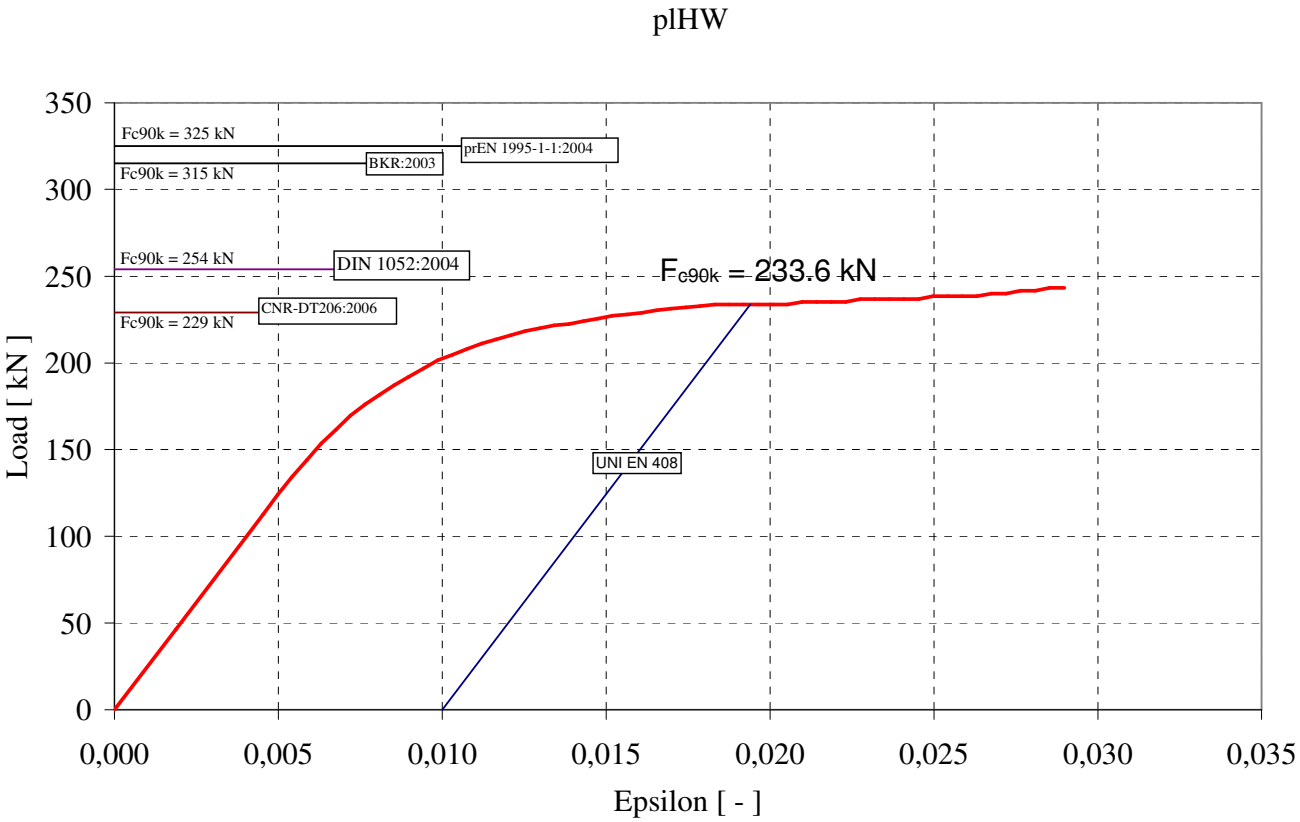

Figure 5.18 F- ε relationship of the un-reinforced specimen, plHW

Figure 5.19 Remaining plastic deformations and the imperfection due to mal-production, plHW

- S10pl15

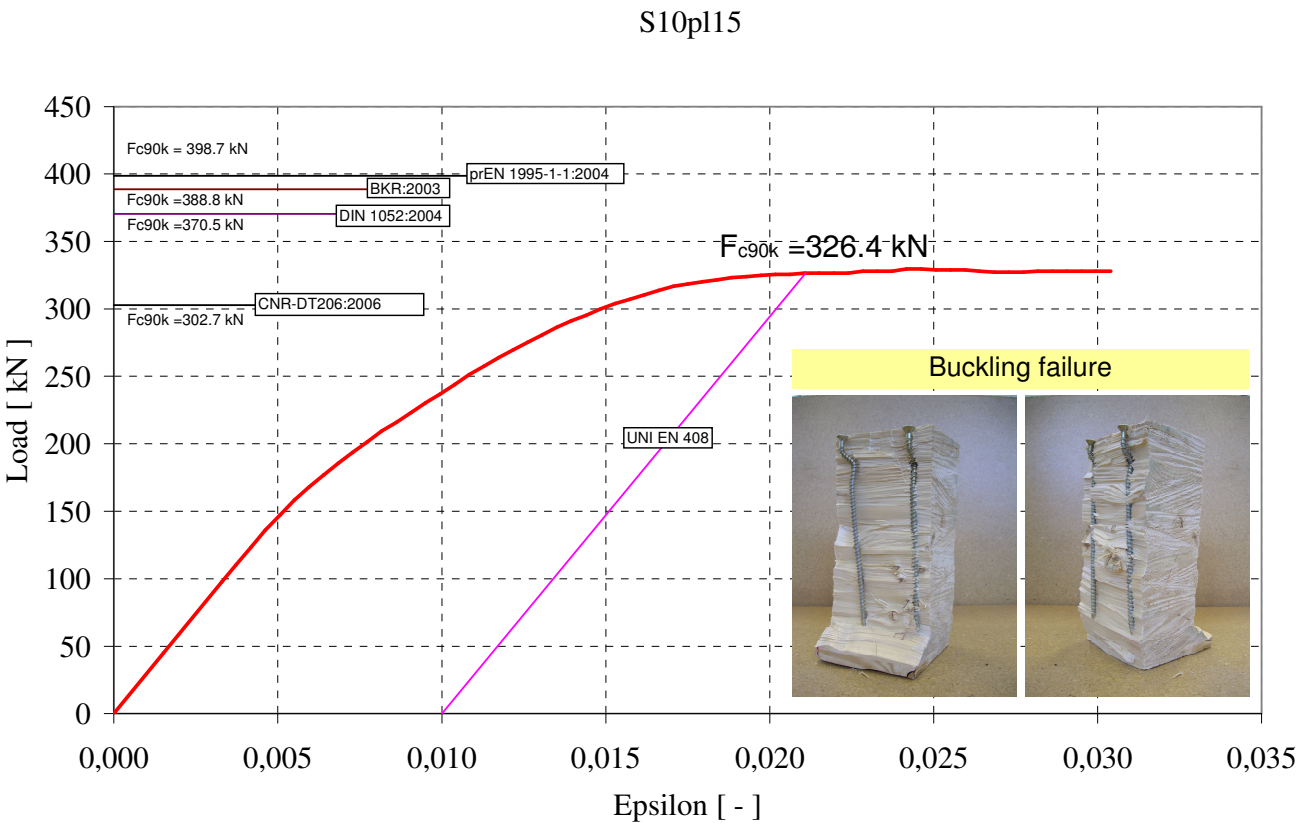

Figure 5.20 F- ε relationship of the reinforced specimen, S10pl15

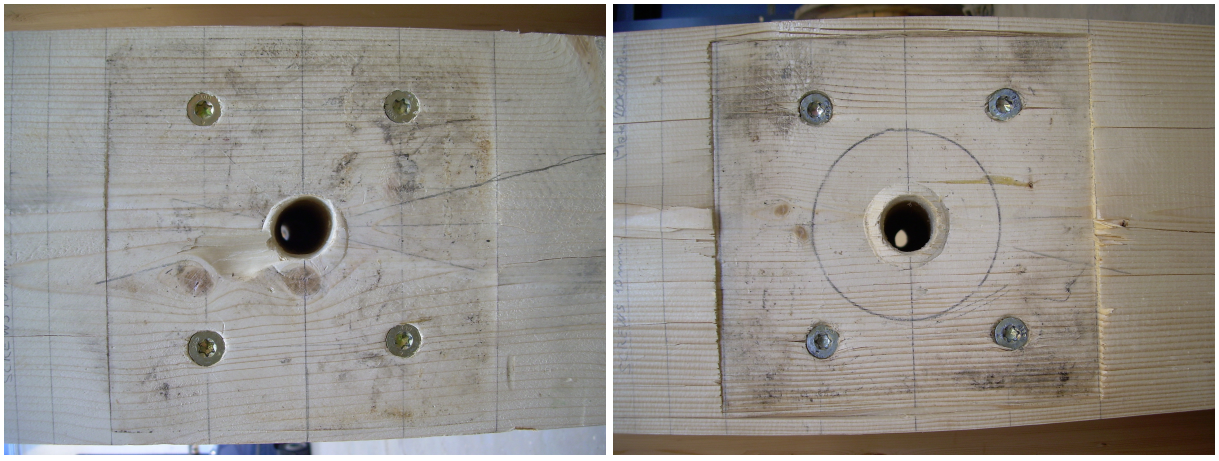

Figure 5.21 Imprint on the specimen, S10pl15

During the test the plate bended and the head of head of the screws followed the rotation of the plate.

- S10pl20

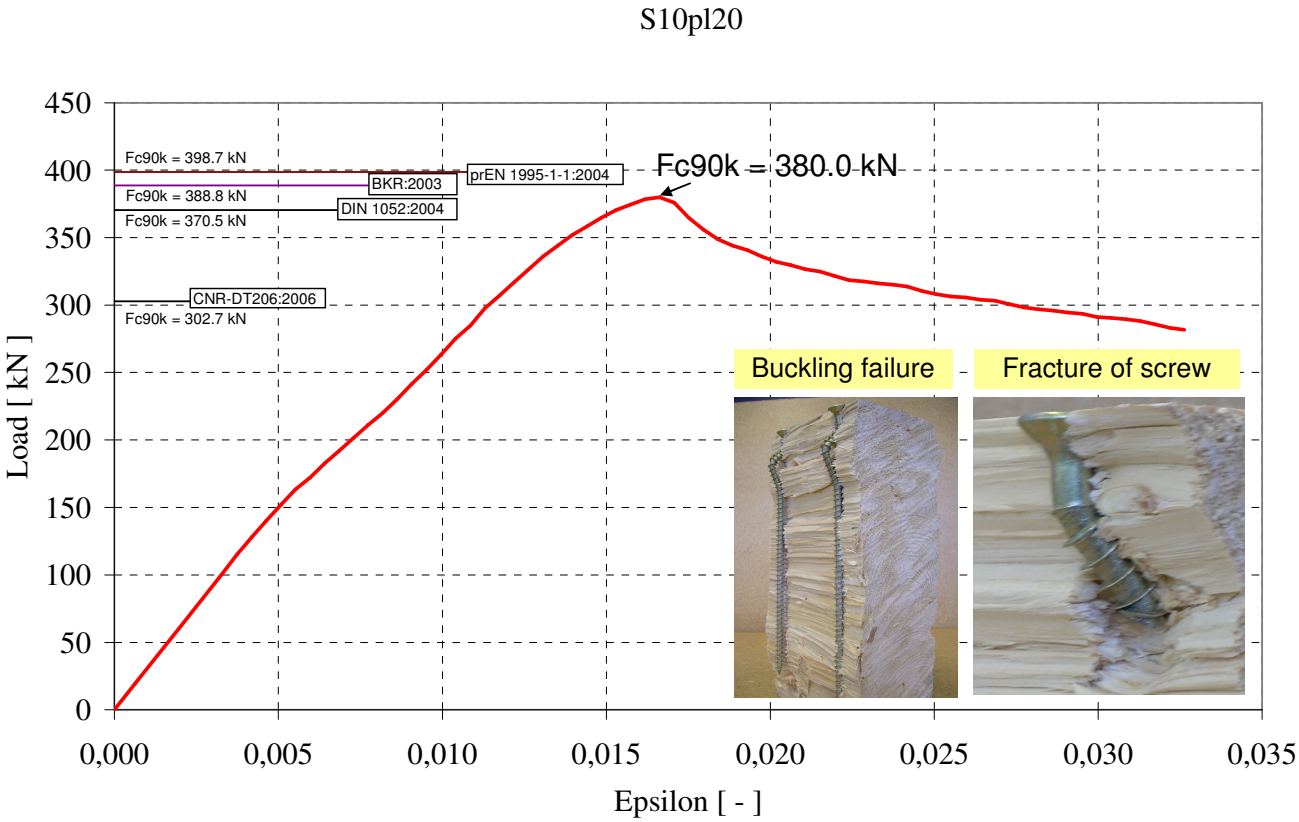

Figure 5.22 F- ε relationship of the reinforced specimen, S10pl20

Figure 5.23 Imprint of the plate and the vertical displacement of the screws, S10pl20

The brittle failure that occurred in this test was premature due to the fracture of the screw as seen in Figure 5.22. The fracture appeared in one screws and was caused by the excessive yielding and bending after buckling of the screw.

- S12pl15

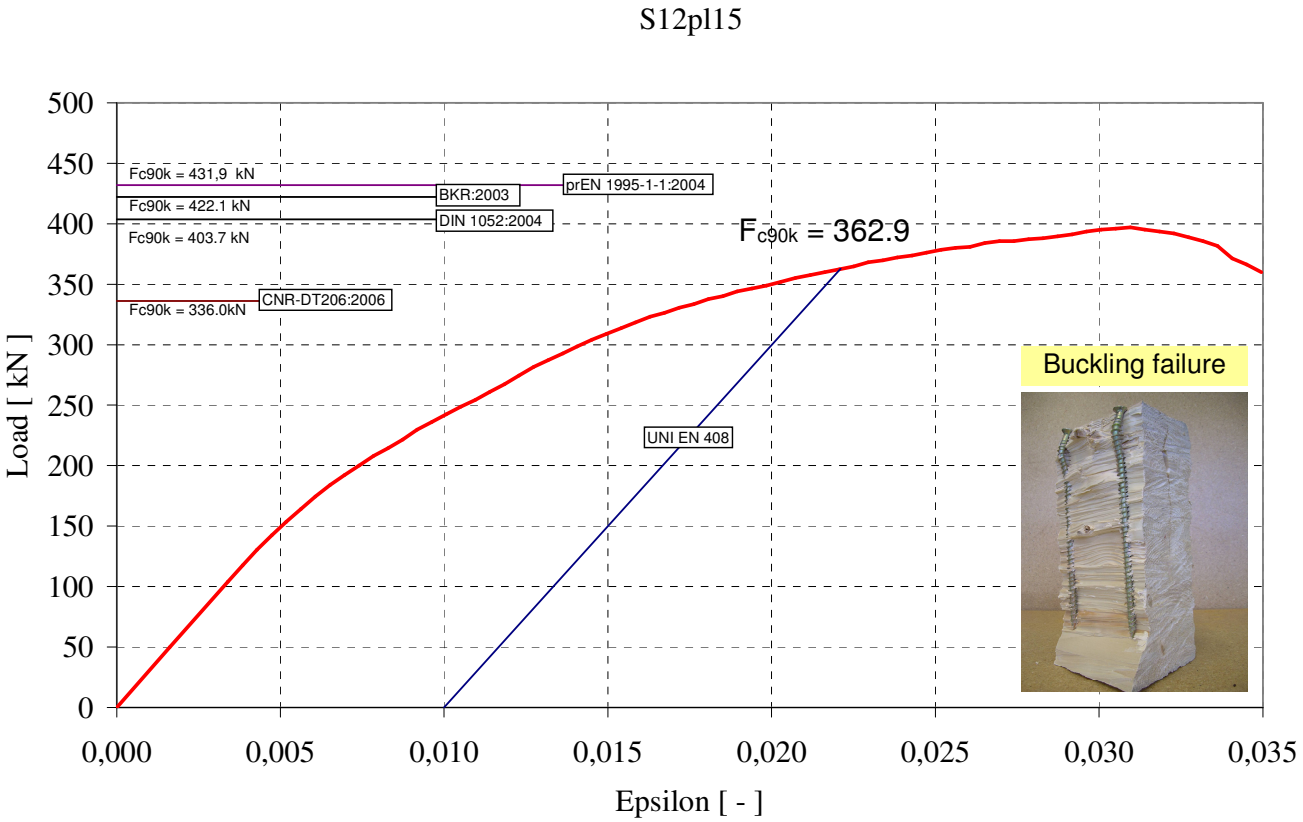

Figure 5.24 F- ε relationship of the reinforced specimen, S12pl15

Figure 5.25 Remaining plastic deformations in the timber, S12pl15

During the test the plate bended and the head of head of the screws followed the rotation of the plate.

- S12pl20

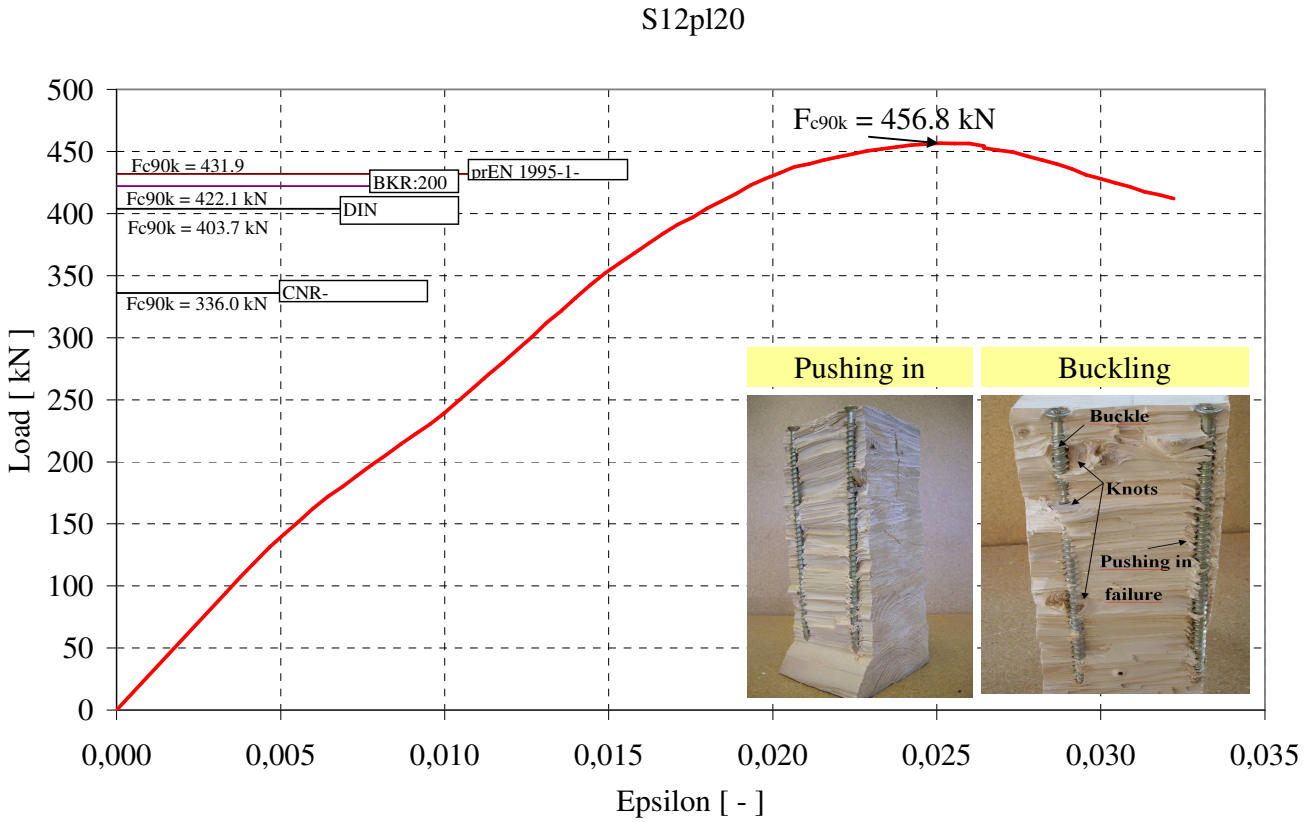

Figure 5.26 F-ε relationship of the reinforced specimen, S12pl20

Figure 5.27 Remaining plastic deformations of the reinforced specimen, S12pl20

The failure occurred in the test was primarily pushing in failure of the screws except for one screw that was drilled trough three knots and buckled, as seen in Figure 5.26. The presence of knots changed the failure mode from pushing in failure to buckling failure, this is due to the increased interaction between screw and timber in the knot and therefore pushing in was prevented. From this point and forward the stiffness depends on the performance of the screws. When the screw has been pushed in the interaction between screw and timber is lost and the screws no longer transfer the load.

5.5.3 Cracks and plate bending

Cracks appear on the timber surface due to high local tension stresses at the surface of the loading, next to the loading plate. Hence, the stresses exceed the tension capacity perpendicular to the grain, $f_{t,90,k}$. The need for the timber to expand due to local compression creates these stresses according to the Poisson theory. The different codes suggests a value of the characteristic tension capacity, $f_{t,90,k}$, equal to 0.5 MPa and according to the FE models the tension stresses at the edge of the plate span between 2-5 MPa, hence cracks in all models and cracks in the tests. In Figure 5.28 the surface crack can be seen and the propagation of that crack down the short edge of the specimen.

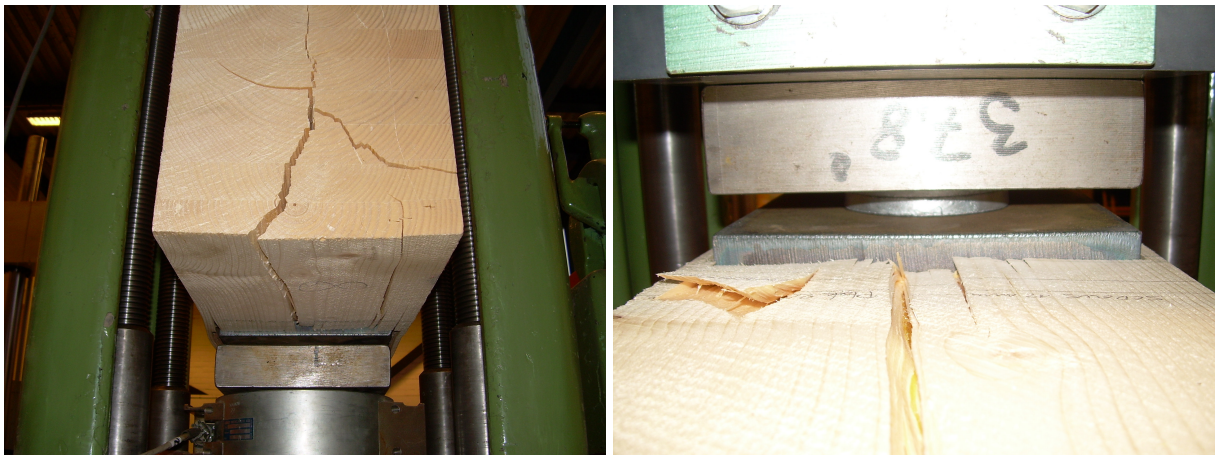

Figure 5.28 Surface crack propagated down the short edge of a test specimen

Plate bending is likely to occur when using a thinner plate. Bending of the plate occurs when the moment caused by force applied on the plate and the reaction forces under plate exceeds the yield moment of the plate. In Figure 5.30 and equations (5.2-5.4) the general theory and equations that governs the plate bending phenomena are displayed. Plate bending in the case of the tested specimens can be considered as unfavourable phenomena since it decreases the loaded area and increases the local stresses under the plate and the loading of the screws becomes eccentric. In the case below the calculated values regards a plate thickness of 15 mm and design load of 230 kN thus design yield strength of the plate equal to 287.9 MPa. This corresponds to the configurations tested with 200x200x15 mm plates and d = 100 mm washers.

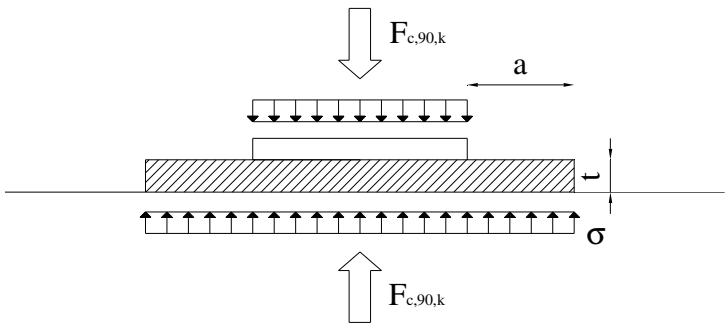

Figure 5.29 Static configuration of the plate

$$M_{S,\max} = \frac{\sigma \cdot a^2 \cdot b}{2} = \frac{5.90 \times 10^6 \times 0.05^2 \times 0.2}{2} = 2949\ Nm \tag{5.2}$$

$$\sigma = \frac{F_{c,90,k}}{A} = \frac{230\ kN}{0.039\ m^2} = 5.90\ MPa \tag{5.3}$$

$$M_Y = \frac{f_Y \cdot b \cdot t^2}{6} = w \cdot f_Y = \frac{287.9 \times 10^6 \times 0.2 \times 0.015^2}{6} = 2159\ Nm \quad (5.4)$$

$M_{S,\max} > M_Y$ → Plate bending

Where

$F_{c,90,k}$ is the applied load

A is the area under the plate

a is the cantilever distance

b is the width of the plate perpendicular to a

t is the thickness of the plate

f_Y is the yield limit of the plate

In Figure 5.30 the plate bending phenomena during the test and after the test with the bended plate can be viewed. The figure displays a plate with dimensions 200 x 200 x 15 mm.

a)  b) 

Figure 5.30 Bending of the plate a), the plastically deformed plate after test b)

5.5.4 Comparison with the analytical solutions

The comparison is done by comparing the test results from the un-reinforced configuration with the capacities given by the codes. The codes does not provide methods to calculate the capacities when the specimens are reinforced, therefore the comparison is done by comparing the test results with the suggested analytical model presented in Karlsruhe, see Chapter 4. The glue-laminated timber class is L40 and calculated as such when using the Swedish code; however this class is interpreted as GL32 according to UNI EN 1194:2000 and used when calculating the capacities with the other codes. The calculations of the characteristic capacities can be seen in Appendix I.

The calculated values of the capacities perpendicular to the grain suggested by the codes for the un-reinforced specimen can be seen in Chapter 3 and summarized in Table 5.10 together with the test results.

Table 5.10 Comparison of the un-reinforced perpendicular to grain capacities

Unreinforced	Characteristic capacity	Increase
UNI EN 408 (test-mean value)	247.2 kN	-
prEN 1995-1-1:2004	325 kN	+31.5 %
DIN 1052:2004	254 kN	+ 2.8 %
CNR-DT206:2006	229 kN	- 7.4 %
BKR:2003	315 kN	+ 27.4 %

It can be seen in Table 5.10 that the capacities according to the German and the Italian code corresponds best with the capacity obtained from the test. The Swedish code, BKR:2003, [6], and Eurocode 5 overestimates the compressive strength and are on the un-safe side.

In the table, see Table 5.11, the capacities has been calculated according to different codes only for the two reinforced configurations with 20 mm thick plate. The other two reinforced configurations, that have a plate thickness of 15 mm, are not considered due to the bending of the plate that can not be treated by the model of Karlsruhe. In fact, the model assumes that the plate is uniformly displaced when the load is applied. When the plate has bended the loading area changes and the loading on the screws has not the same behaviour as described and assumed by the model of Karlsruhe.

Table 5.11 Reinforced characteristic capacities compared to test values

Reinforced tests	UNI EN 408	prEN 1995-1-1:2004	DIN 1052:2004	CNR-DT206:2006	BKR:2003
S10pl20	380.0 kN	398.68 kN (4.9 %)	370.5 kN (-2.5 %)	302.73 kN (-20.3 %)	388.8 kN (2.3 %)
S12pl20	456.8 kN	431.91 kN (-12.7 %)	403.74 kN (-18.9 %)	335.97 kN (-33.7 %)	422.1 kN (-14.9 %)

The failure when using the d=10 mm screw was premature and brittle as seen in the figure, see Figure 5.23. Since the failure was brittle no general conclusions can be drawn whether the model has a good agreement even though the table above suggests it. The analytical solution predicts buckling of the screw in both configurations with 20 mm thick plate but in the test only the d = 10 mm screw buckled whereas for the d = 12 mm screws pushing in failure was dominant.

6 FE-Modelling

An FE-analysis was used as a complimentary tool to the laboratory tests performed. The models that were analysed with finite elements were split into to two branches were each branch represents a field of study. The first branch represents the un-reinforced and the reinforced cases of the laboratory test specimens. The second branch represents the study of the effect of the unloaded length and how it is treated in ABAQUS, this branch is to be compared to tests performed by Reichegger, [11], in Trento, Italy, who studied this phenomena. These test results can be seen in Chapter 3.

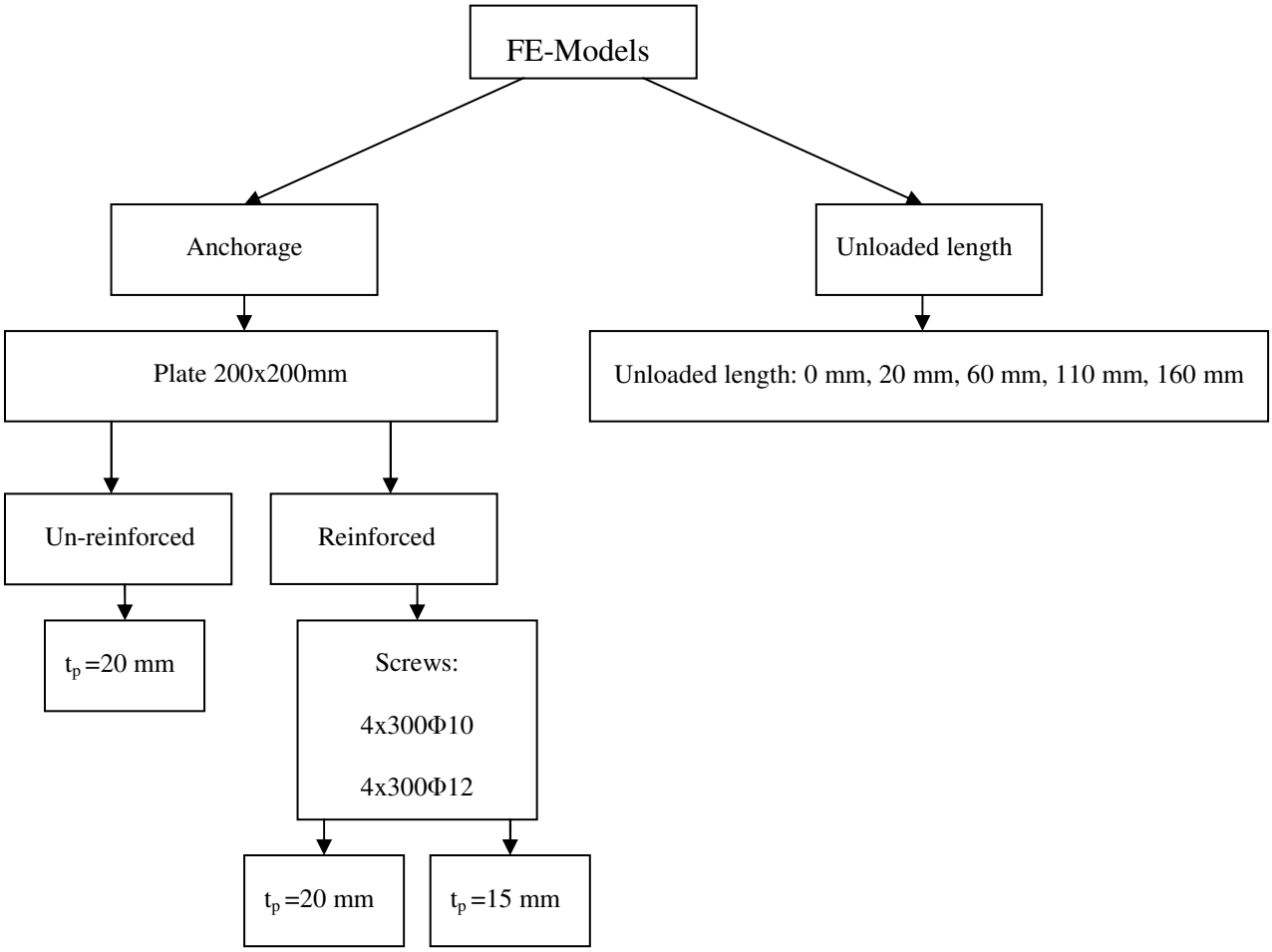

Figure 6.1 Model tree and the different branches

In Figure 6.1 it is shown how the main branches of the model are built up, the model configurations in the branch that regards the anchorage corresponds to the same configurations that were used in the laboratory tests.

The un-reinforced and the reinforced models have numerous components in common and is therefore not described separately, however where the two models differ it is described in detail.

6.1 Assumptions and limitations of the FE-model

The reality is often difficult to model exactly, especially if the model treats materials such as timber which is highly inhomogeneous and each specimen differs from the other. The presences of knots as an example are not modelled. Even when glue-laminated timber is considered, which is less inhomogeneous than plain timber, there are still variables in the modelling that has to be neglected in order to make the model simple and efficient.

6.1.1 Assumptions regarding the glue-laminated timber

The glue-laminated timber specimen is modelled as one element, neglecting the different layers of lamellas. This is due to the fact that it is assumed that each lamella in the specimen shares the same material properties, and therefore can be modelled as a solid. The second assumption concerns the plastic behaviour of the timber. The plastic properties are modelled as isotropic which can be understood as a fixed 3D boundary of the stress limit in the timber. The effect or consequence of this is that when the stresses reach this limit the behaviour in the timber is regarded as plastic, regardless of whether the stresses act in tension or in compression. The reason why this assumption is made is due to the complicity in treating plastic behaviour in an orthotropic way.

6.1.2 Assumptions regarding the screws

The buckling of the screws is not modelled specifically in ABAQUS, this due to the fact that it increases the total complexity of the model. Furthermore, the interaction between the timber and the screws is also a complex phenomenon in reality and the chosen approach was to model it with linear elastic springs in the three main directions.

6.1.3 Assumptions regarding the loading

When performing a non-linear analysis the loading sequence is of importance. The load was applied in the model as assumed displacement rather than an applied force. This method is called displacement control and has several benefits compared to the load control method. One of these benefits concerns the increased probability of finding convergence during analysis, see Figure 6.2.

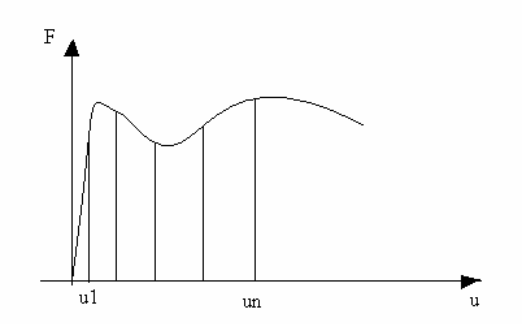

Figure 6.2 Example of the displacement control method

Another benefit when using the displacement-control method is that the loading can be applied in an indirect way and in this case more realistic since the displacement is applied on the pre-stressing bar simulating the bar compressing the timber due to tension, as the case in the laboratory tests considering the long-term loading.

6.2 Modelling laboratory test specimens

6.2.1 Elements and assembly

When modelling the un-reinforced and reinforced laboratory test specimens symmetry was used so that only one half of the test specimens was modelled, hence only one anchor modelled. The un-reinforced model consists of five different parts all modelled as 3D Solid Extrusion Elements. The five different parts that were included in the model are; the glue-laminated timber, the steel plate, the steel washer, the pre-stressing bar and the nut, see Figure 6.3. Since the reinforced model is reinforced with screws it has a further contribution of screws modelled as Beam Elements.

The geometry of the basic model represents the geometry of one side of specimens that were used in the laboratory tests. For more details on the dimensions of each part see Chapter 5.

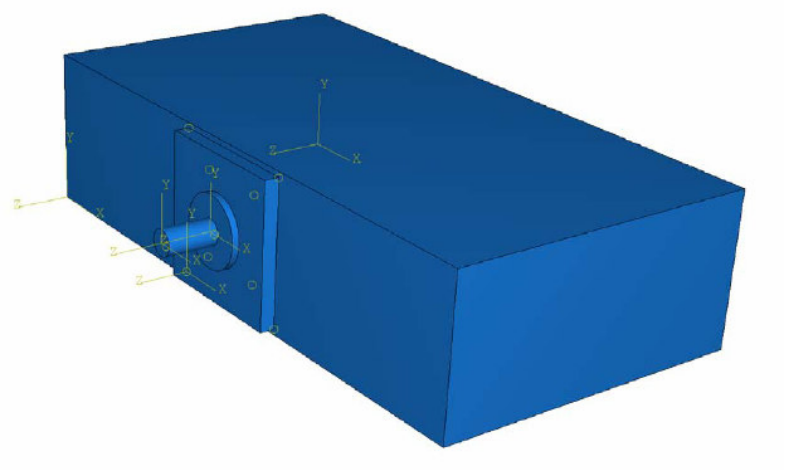

Figure 6.3 Assembly of the un-reinforced model

6.2.2 Material properties

The material properties that were used in the model are divided into two parts, one part which consists of pre-test properties of the glue-laminated timber and the other part which consists of calibrated properties of the glue-laminated timber according to the results from the tests. This is due to the fact that it is difficult to predict and model accurate properties of the glue-laminated timber and therefore the FE-model had to be calibrated after the tests.

In the model the glue-laminated timber is modelled as orthotropic elastic isotropic plastic which means that it has material properties defined in each direction in the elastic region. The elastic properties of the glue-laminated timber in each direction are well described in the doctoral thesis by Kent Persson, [10]. Persson suggests values for the stiffness of spruce at 12% moisture content. These suggested values can be seen in Table 6.1.

Table 6.1 Showing the suggested stiffness values and values of the Poisson's ratio of spruce at 12% moisture content according to Persson, [10]

Parameter	Measurements
$E_{L,}$ MPa	13500-16700
$E_{R,}$ MPa	700-900
$E_{T,}$ MPa	400-650
$G_{LR,}$ MPa	620-720
$G_{LT,}$ MPa	500-850
$G_{RT,}$ MPa	29.0-39.0
υ_{RL}	0.018-0.030
υ_{TL}	0.013-0.021
υ_{TR}	0.24-0.33

Considering the fact that our test specimens are graded as L40 according to the Swedish glue-laminated timber standard the stiffness values according to Table 6.1 are interpolated into suitable values so the model shows a good stiffness representation of the general L40 glue-laminated timber. The properties are further calibrated to represent the values of the actual test specimens.

The interpolation of the suggested values as shown in Table 6.1 was obtained by using the stiffness modulus in the longitudinal direction, $E_{L,}$ according to the Swedish code, BKR:2003, [6], as a start value. According to BKR:2003 the MOE of L40 glue-laminated timber in the longitudinal direction is set to 13000 MPa. The interpolated values and the calibrated values can be seen in Table 6.2 and Figure 6.4.

Table 6.2 Interpolated values for L40 glue-laminated timber

Parameter	Interpolated values for L40 glue-laminated timber	Calibrated values according to test results
$E_{L,}$ MPa	13000	11750
$E_{R,}$ MPa	699	591
$E_{T,}$ MPa	361	263
$G_{LR,}$ MPa	604	565
$G_{LT,}$ MPa	405	309
$G_{RT,}$ MPa	27	24
υ_{RL}	0.016	0.011
υ_{TL}	0.012	0.009
υ_{TR}	0.226	0.191

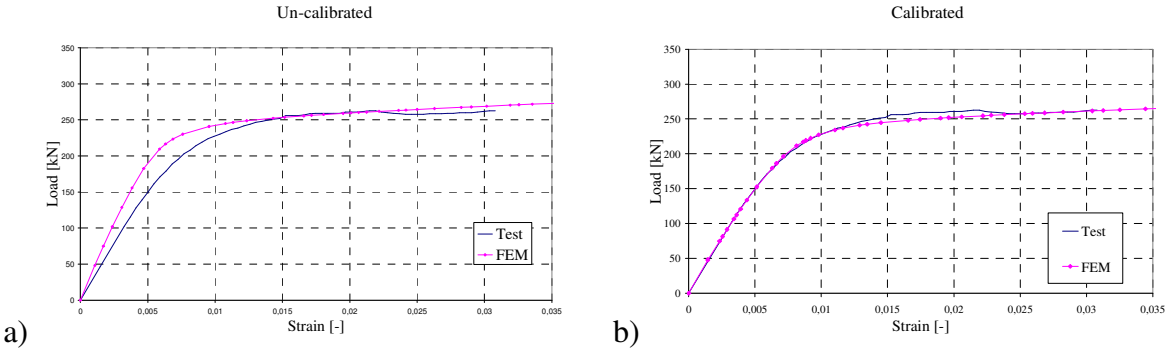

Figure 6.4 Schematic view of the difference in un-calibrated values (a) and calibrated values (b)

As the values of the stiffness and Poisson's ratios are known the following proportions (6.1) can be used for the symmetric stiffness matrix.

$$\frac{\upsilon_{RL}}{E_R} = \frac{\upsilon_{LR}}{E_L}, \quad \frac{\upsilon_{TL}}{E_T} = \frac{\upsilon_{LT}}{E_L}, \quad \frac{\upsilon_{TR}}{E_T} = \frac{\upsilon_{RT}}{E_R} \tag{6.1}$$

When these proportions are know the following conversions (6.2) were made according to the ABAQUS Users Manual.

$$D_{1111} = E_1 \cdot (1 - \nu_{23} \cdot \nu_{32}) \cdot \Gamma \tag{6.2}$$

$$D_{2222} = E_2 \cdot (1 - \nu_{13} \cdot \nu_{31}) \cdot \Gamma$$

$$D_{3333} = E_3 \cdot (1 - \nu_{12} \cdot \nu_{21}) \cdot \Gamma$$

$$D_{1122} = E_1 \cdot (\nu_{21} + \nu_{31} \cdot \nu_{23}) \cdot \Gamma = E_2 \cdot (\nu_{12} + \nu_{32} \cdot \nu_{13}) \cdot \Gamma$$

$$D_{1133} = E_1 \cdot (\nu_{31} + \nu_{21} \cdot \nu_{32}) \cdot \Gamma = E_3 \cdot (\nu_{13} + \nu_{12} \cdot \nu_{23}) \cdot \Gamma$$

$$D_{2233} = E_2 \cdot (\nu_{32} + \nu_{12} \cdot \nu_{31}) \cdot \Gamma = E_3 \cdot (\nu_{23} + \nu_{21} \cdot \nu_{13}) \cdot \Gamma$$

$$D_{1212} = G_{12}$$

$$D_{1313} = G_{13}$$

$$D_{2323} = G_{23}$$

E_1	E_L
E_3	E_R
E_2	E_T
G_{13}	G_{LR}
G_{12}	G_{LT}
G_{32}	G_{RT}
υ_{31}	υ_{RL}
υ_{21}	υ_{TL}
υ_{23}	υ_{TR}
υ_{13}	υ_{LR}
υ_{12}	υ_{LR}
υ_{32}	υ_{RT}

where;

When these parameters are known the symmetric stiffness matrix for the orthotropic elastic material can be assembled in ABAQUS, as can be seen in Figure 6.5.

$$\begin{Bmatrix}\sigma_{11}\\ \sigma_{22}\\ \sigma_{33}\\ \sigma_{12}\\ \sigma_{13}\\ \sigma_{23}\end{Bmatrix} = \begin{bmatrix} D_{1111} & D_{1122} & D_{1133} & 0 & 0 & 0 \\ & D_{2222} & D_{2233} & 0 & 0 & 0 \\ & & D_{3333} & 0 & 0 & 0 \\ & & & D_{1212} & 0 & 0 \\ & sym & & & D_{1313} & 0 \\ & & & & & D_{2323} \end{bmatrix} \begin{Bmatrix}\varepsilon_{11}\\ \varepsilon_{22}\\ \varepsilon_{33}\\ \gamma_{12}\\ \gamma_{13}\\ \gamma_{23}\end{Bmatrix}$$

Figure 6.5 Symmetric elastic stiffness matrix, D, for orthotropic materials in ABAQUS

The value of the plasticity behaviour of the glue-laminated timber was only considered in the direction perpendicular to the grain in order to simplify the model. The glue-laminated timber was assumed to behave as elastic until the stresses exceeded 3 MPa. The density of the timber was set to 450 kg/m^3.

The parts in steel were modelled as isotropic materials and were given an E-modulus of 210 GPa and a Poisson's ratio of 0.3. The density of the steel was set to 7800 kg/m^3.

In Table 6.3 it is shown how the different parts of the model were created and what material properties these were given.

Table 6.3 Different parts and their element types along with the properties

Part	**Glue-laminated timber**	**Steel plate** Various sizes	**Steel washer**	**Bar**	**Nut**	**Screws** d=10mm, d=12mm
Element type	3D solid extrusion	3D solid extrusion	3D solid extrusion	3D solid extrusion	3D solid extrusion	Wire-beam elements
Material	Orthotropic-elastic Isotropic-plastic	Isotropic-elastic (steel)	Isotropic-elastic (steel)	Isotropic-elastic (steel)	Isotropic-elastic (steel)	Isotropic-elastic (steel)

6.2.3 Interactions

The different parts of the model were coupled together using primarily the tie constraint. The tie applies for connecting the plate to the timber, washer to plate, nut to washer and nut to bar.

The second interaction that was applied in the model regards the reinforced model and the interaction between the head of the screws and the timber. The interaction element that was used is a user-defined connector element in ABAQUS CAE. This interaction is motivated by the fact that in order to simulate displacement of the screws being governed by the vertical displacement of the steel plate, the screws ability to penetrate the steel plate had to be restricted. The connector element is a "Join + Align" type element, see Figure 6.6, which restricts all types of motion in all directions.

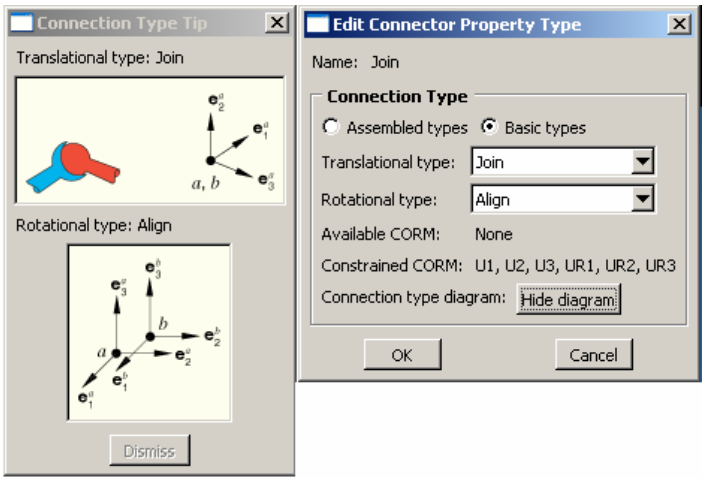

Figure 6.6 Join+Align type connection

The third interaction that was modelled regards the interaction between the screws and the glue-laminated timber in the reinforced model. This interaction was done by using linear-elastic spring elements in order simulate the stiffness and the bond strength of the screws in timber. The amounts of springs that were used are dependent on the size of the mesh of the glue-laminated specimen. This is due to the fact that each node on the beam element (screw) had to have a corresponding node in the glue-laminated timber element with the same coordinates in order to be able to connect the two points with spring elements. Each node has three springs acting in the three different directions.

For convenience only one spring per screw is created in ABAQUS CAE, connected to an arbitrary node in the glue-laminated timber element, see Figure 6.7. These timber nodes were later modified in the input file so that they have the same coordinates as the nodes in the screws. The remaining springs with their corresponding nodes in the glue-laminated timber were programmed in the input file. As a result, the spring configuration of the reinforced model with four screws includes a total of 132 springs. This applies when the global mesh size was chosen to 30 mm in element height.

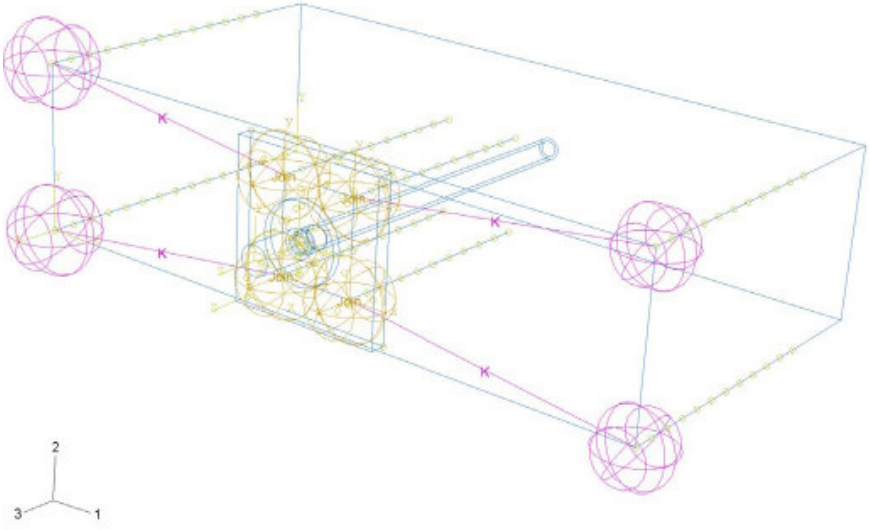

Figure 6.7 Springs connected from the screws to an arbitrary node in the glue-laminated timber element

The different springs stiffness in the different directions are described by Bejtka, [8] in his Ph.D. Thesis were obtained by tests on different screws with different lengths and diameters. Bejtka also defined an expression of how this interaction can be calculated with a good

correlation between the tested values and calculated values. These equations can be seen in equations (6.3-6.4).

Horizontal direction, corresponds to the 1 and 2 direction in the FE-model

$$c_H = \frac{(0.22 + 0.014 \cdot d) \cdot \rho}{1.17 \cdot \sin^2 \alpha + \cos^2 \alpha} \qquad \left[\frac{N}{mm^2}\right] \tag{6.3}$$

Note that the angle, α, changes depending on the direction 1 and 2, see Figure 6.8.

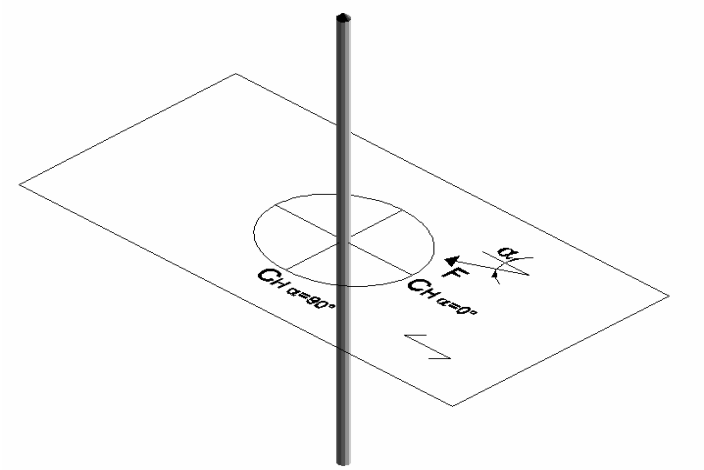

Figure 6.8 Illustration of how the angle α is considered

Vertical direction, corresponds to the 3 direction in the FE-model

$$c_V = 234 \cdot \frac{(\rho \cdot d)^{0,2}}{l_s} \qquad \left[\frac{N}{mm^2}\right] \tag{6.4}$$

Where,

c_H is the horizontal spring stiffness

c_V is the vertical spring stiffness

α is the angle between the force and direction of the grain

d is the diameter of the screw in mm

ρ is the density of the timber in kg/m^3

l_S is the active length of the screw in the timber

In ABAQUS the stiffness equations (6.3-6.4) are applied on every node on the screws and in order to do that they have to be converted to N/m. Furthermore, the spring stiffness is adjusted so that the stiffness of a spring is re-calculated into a stiffness that takes into account the distance between the nodes.

An example of how the stiffness coefficients are interpreted is shown here. The total length of the screw is l_s (in mm) divided with an arbitrary number, *i*, causing the screw to be split into $n = \frac{l_S}{i}$ number of segments is given. Then the number of nodes will be $n+1$ and the distance between the nodes is $\Delta l_s = \frac{l_S}{n}$ in mm. This gives the following vertical spring stiffness for each node, see equation (6.5)

$$c_V \cdot \Delta l_S = 234 \cdot \frac{(\rho \cdot d)^{0,2}}{l_s} \cdot \Delta l_S \cdot 1000 \quad in \quad \frac{N}{m} \tag{6.5}$$

Regarding the horizontal spring stiffness in each node the expression is independent of the distances between the nodes and has been converted as can be seen in equation (6.6)

$$c_H \cdot d = \frac{(0.22 + 0.014 \cdot d) \cdot \rho}{1.17 \cdot \sin^2 \alpha + \cos^2 \alpha} \cdot d \cdot 1000 \quad in \quad \frac{N}{m} \tag{6.6}$$

The calculations of the spring stiffness in different directions and appropriate ABAQUS syntax can be seen in APPENDIX D

6.2.4 Mesh

The mesh is the decisive factor that influences the accuracy of the results obtained by the FE-model. The different parts were meshed differently depending on their geometry and importance in the model. Quadratic element types have been chosen for all parts in the model since they prove to give more accuracy in the calculations when compared to linear elements.

Regarding the un-reinforced model the glue-laminated timber has been modelled with a hexagonal mesh with the size of 0.03. This result in an element size of 30x30x27.4 mm and 3660 elements created on the glue-laminated specimen. The steel plate was meshed with the same type of mesh only given a finer mesh size, 0.01, and it resulted in 808 elements created on the steel plate. Regarding the circular parts of the model it was shown to be more beneficial to use the tetrahedral mesh type so that the rounded edges could be modelled properly. The mesh size for these parts, steel washer, pre-stressing bar and the nut, were all given the value of 0.01 and resulted in 673, 732 and 567 elements created on the parts, respectively, see Figure 6.9.

The screws had to be meshed with the same size as the glue-laminated timber element consequently creating 10 elements on each screw.

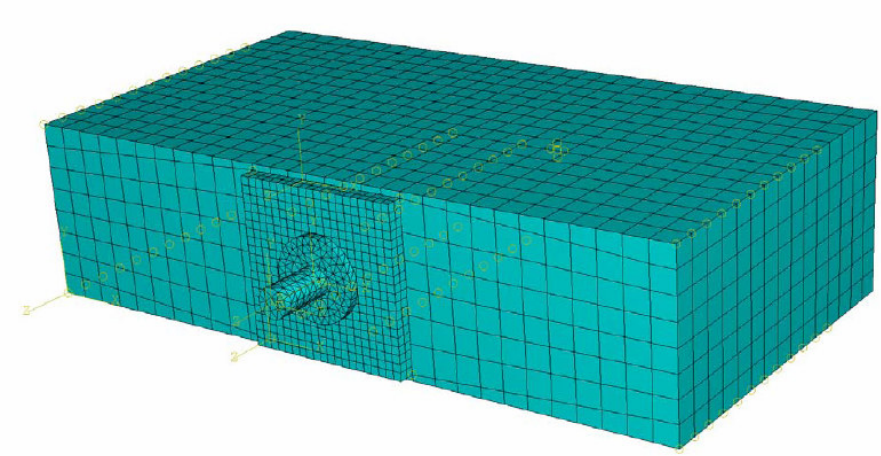

Figure 6.9 Description of mesh configuration

6.2.5 Step

In the step module it is specified what type of analysis ABAQUS is to perform, i.e. static general. The un-reinforced model has a different loading sequence compared to the reinforced model. This is due to the fact that the un-reinforced model has a distinct phase when it behaves linear-elastically and can therefore due to time saving arguments be modelled in two steps. The first step is considered fully elastic and can be calculated using one increment. The next step where the model goes from being elastic to plastic successively needs a lot of iterations and is therefore divided into 100-300 increments. Both of these were done using the step Static, General.

Considering the reinforced model it is more difficult to judge whenever the behaviour is elastic or not, therefore the whole loading sequence is done in one step but with a large amount of increments in order to find convergence. This is a rather time consuming method but necessary in this case. The step that was used here were Static, Riks which uses the arch length method to find convergence.

In order to find convergence when analysing the reinforced case some alterations had to be made in the ABAQUS input file. The following commands were entered in the input file:

```
*Controls, analysis=discontinuous

*Controls, parameters=field, field=global
3e1, 3., , , , , ,
```

A controls command lets the user define and set limits to the solver and guide it to what is the best way to treat the problem. In this case the controls command, analysis = discontinuous tells ABAQUS that severe discontinuous problems can occur in the solution process and with that information ABAQUS can treat discontinues more efficiently. The second command that was applied regards the possibility of finding convergence. This command proved to be crucial regarding the reinforced model. By default ABAQUS uses very strict limits for the residuals when performing iterations and for the case with the reinforced model these residuals and the tolerances set for these were set too strictly. In order to increase the chance of convergence the tolerance levels had to be slightly altered from their default values so that the solution could converge.

6.2.6 Loads and boundaries

When loading the specimen in the FE-model the aim was to simulate the loading situation in the most realistic way as possible. This means that in stead of applying a pressure at the surface of the glue-laminated model the load was applied onto the bar as displacement. By using this method the load could be controlled by measuring the strain in the bar. Further advantages are as described in the previous chapter. The load that was applied corresponds to 20 mm of displacement of the pre-stressing bar. This displacement was manually applied in the input file and the syntax governing this can be seen below.

```
*BOUNDARY,  OP=MOD,  TYPE=DISPLACEMENT
        Bar-1.1,    3,  ,   -2E-2
```

In order to analyse the model some parts of the model had to be constrained to prevent translation and rotation, this also to simulate the situation as well as possible. The glue-laminated specimen was restricted to move in the vertical direction thus the rotation was prevented around the two horizontal axes at the symmetry line. Furthermore, one point was selected in the glue-laminated timber and was fully fixed; this was to prevent the whole specimen from sliding in the horizontal plane.

In order to control the motion of the bar so that it only moves in the vertical direction one point was selected and all but the vertical degrees of freedom were locked. The configuration of the boundaries can be seen in Figure 6.10.

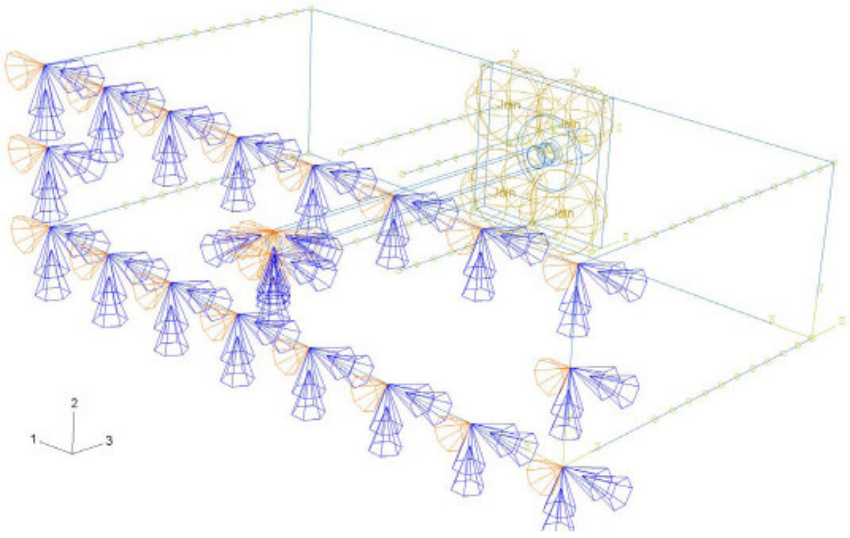

Figure 6.10 Configuration of the boundaries

6.3 FE-analysis results

The results from the FE analysis are presented and summarized in a relationship; see Figure 6.11. In Table 6.4 the different configurations are compared to each other in terms of capacities calculated according to the UNI EN 408 standard. The different configurations are also described and presented in more detail in two different categories. Category one represents the un-reinforced model and two the reinforced models, respectively.

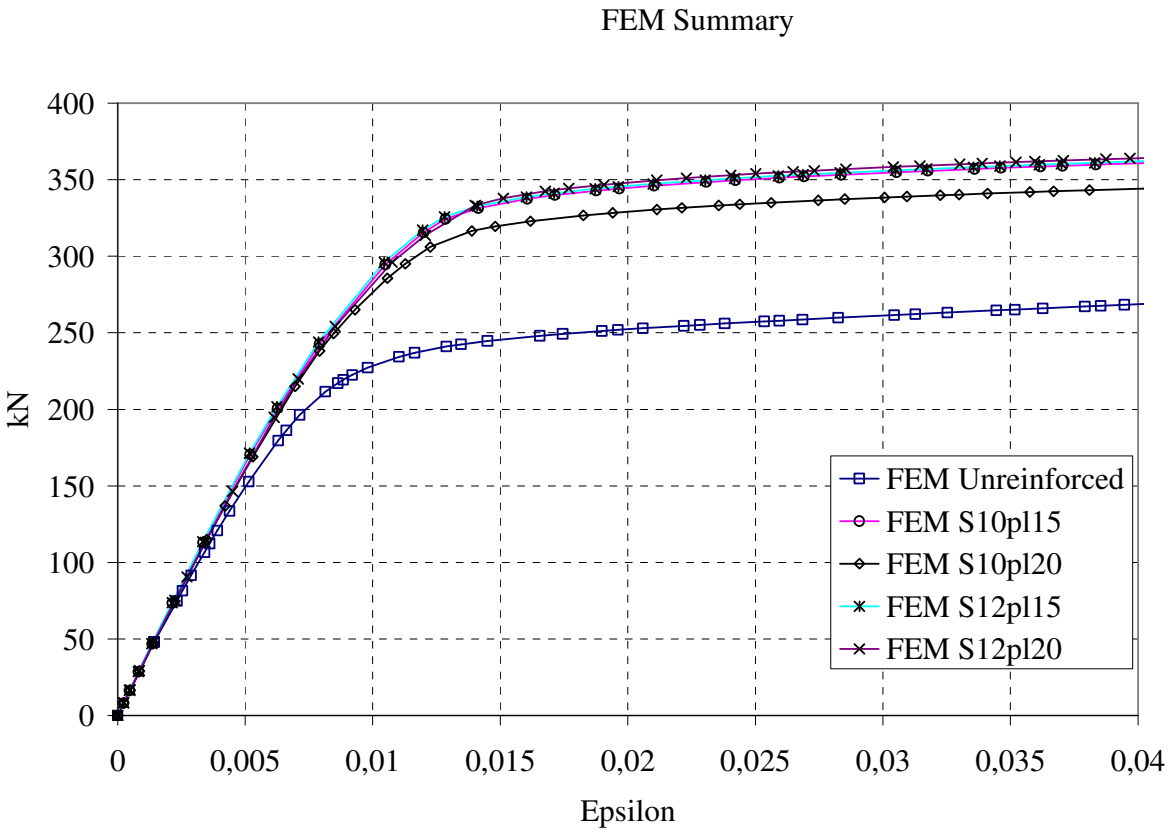

Figure 6.11 Summary of the FE results

Table 6.4 Capacities according to the UNI EN 408 standard and increase of capacity compared to the un-reinforced model

FEM Model	Capacity [kN]	Increase [kN]	Increase [%]
Un-reinforced	251.2	- -	-
S10pl15	348.4	97.2	+38.7
S10pl20	330.5	79.3	+31.6
S12pl15	358.2	107.0	+42.6
S12pl20	351.0	99.8	+39.7

6.3.1 Un-reinforced

The *F-ε* relationship of the un-reinforced model and its capacity according to the UNI EN 408 standard is displayed in Figure 6.12. The maximum capacity reached is 251.19 kN.

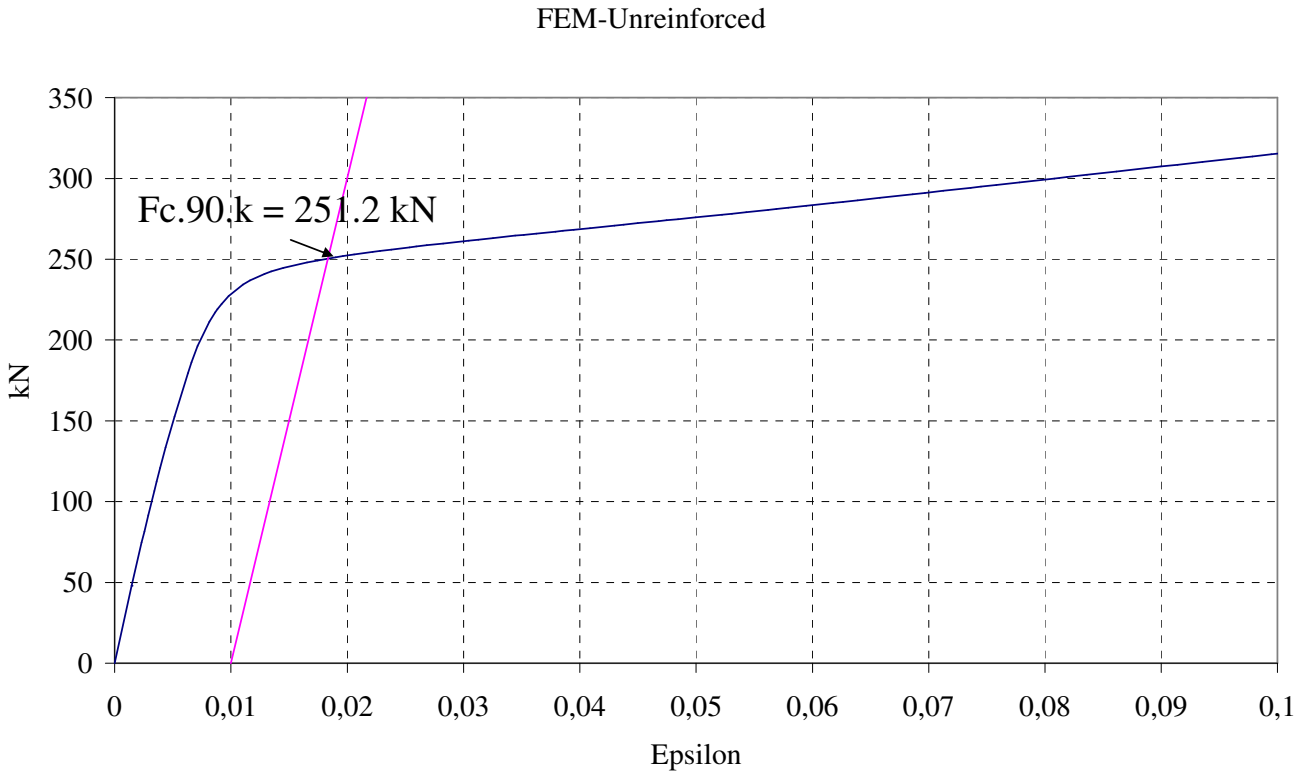

Figure 6.12 Capacity according to the UNI EN 408 standard

Figure 6.13 shows the deformed shape and displacement at the point of maximum capacity. According to the FE model the displacement at 251.19 kN is 8.54 mm.

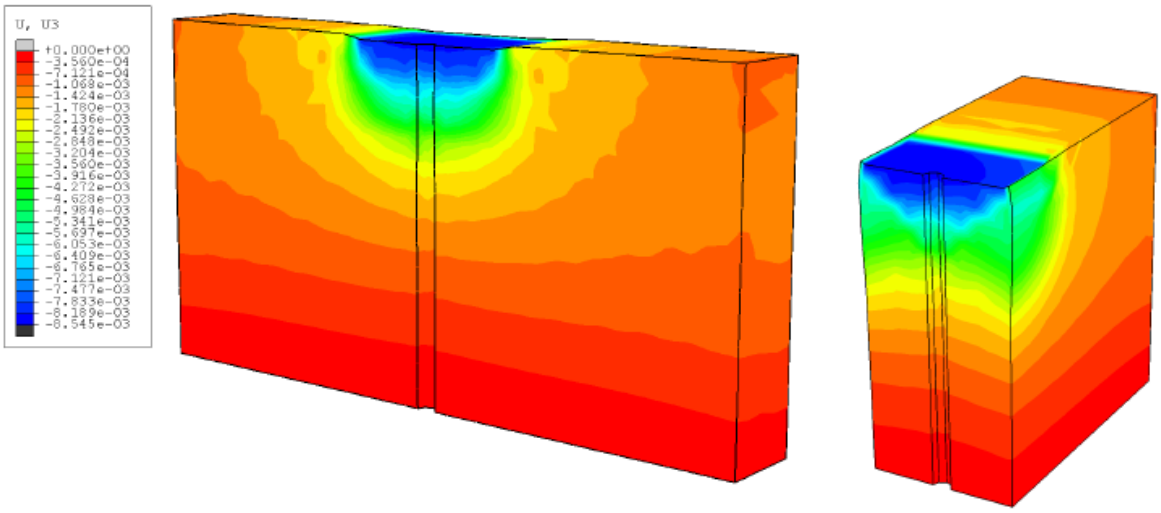

Figure 6.13 Displacement and deformed shape at 251.19 kN of loading of the un-reinforced model

In Figure 6.14 the stress field of the un-reinforced model is displayed. Worth to notice is that the highest stress concentration appears at the edges of the plate. The stresses are then

distributed down the model and can be assumed uniformly distributed at a distance of 140 mm from the bottom edge. The maximum stress reached at 251.19 kN of loading is 5.36 MPa in compressive stress.

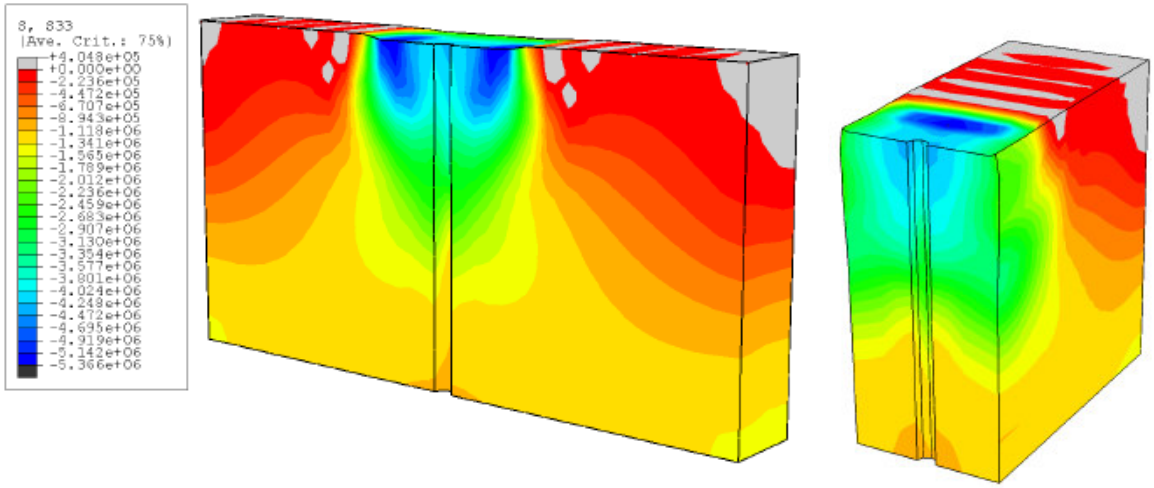

Figure 6.14 Stress field of the un-reinforced model at 251.19 kN of loading

6.3.2 Reinforced

- S10pl15

Figure 6.15 displays the *F-ε* relationship of the model reinforced with the thinner d = 10 mm screws and the plate thickness of 15 mm, S10pl15. The capacity according to the UNI EN 408 standard is 348.4 kN.

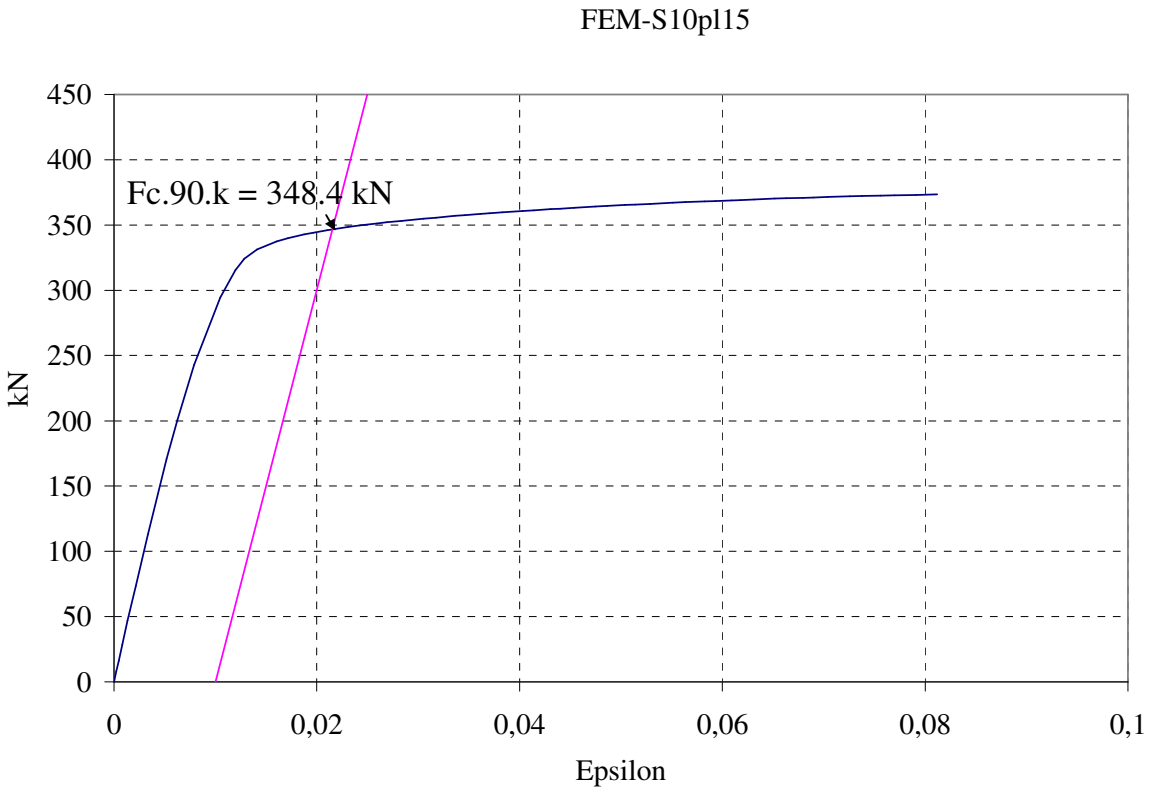

Figure 6.15 Capacity according to the UNI EN 408 standard, S10pl15

In Figures 6.16-6.17 the displacement in vertical direction is showed for both a cut at the centre of the specimen and at the level of the screws. The displacement viewed only regards the displacement of the timber. It is of interest to note that the vertical displacement of the timber in close vicinity to the screws is higher than far from the screws. This is due to the fact that the steel plate governs the vertical displacement of the screws and the bond between the screws and the timber require the timber to follow this displacement. The maximum displacement at 348.4 kN is 10.3 mm.

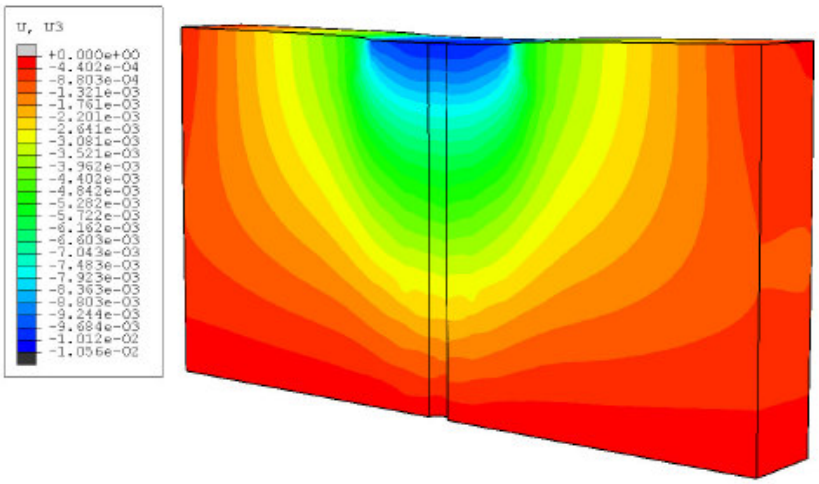

Figure 6.16 Displacement at the centre of the specimen, S10pl15

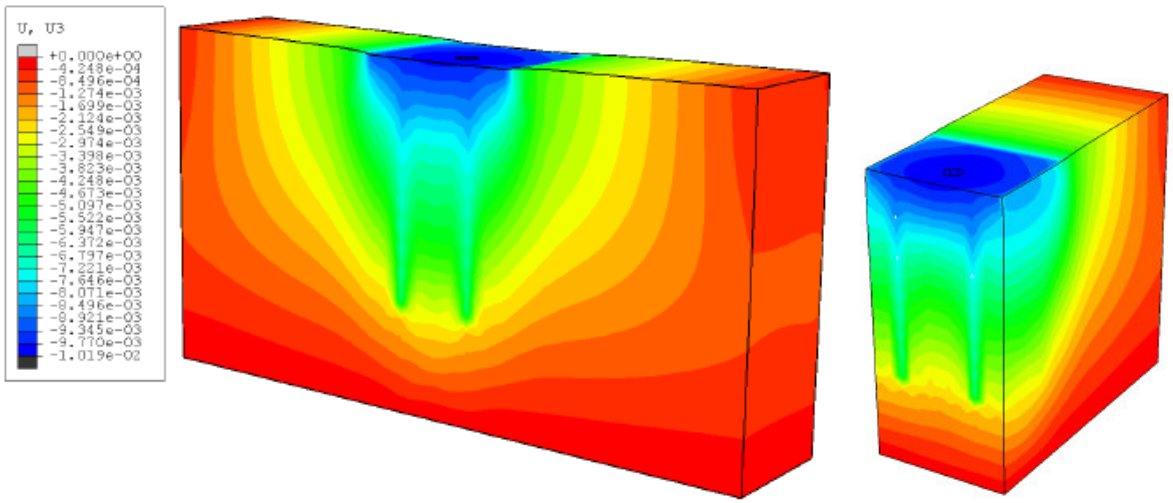

Figure 6.17 Displacement at the level of the screws, S10pl15

The stress field of the S10pl15 model at screw level can be seen in Figure 6.18. Higher stresses are obtained due to the increase in load compared to the un-reinforced model. This ability to take higher loads is due to the effect of the screws transferring the loads deeper into the specimen and therefore reducing the high stress concentration that otherwise appears beneath the plate, c.f. 6.14. This effect does however induce high tension stresses at the bond region around the screws and is very visible in Figure 6.18. However, even though increased distribution of stresses high local stresses appears at the edges of the plate. The maximum stress that appears in this model is due to the local concentration of stresses at the edges and has a magnitude of about 20 MPa.

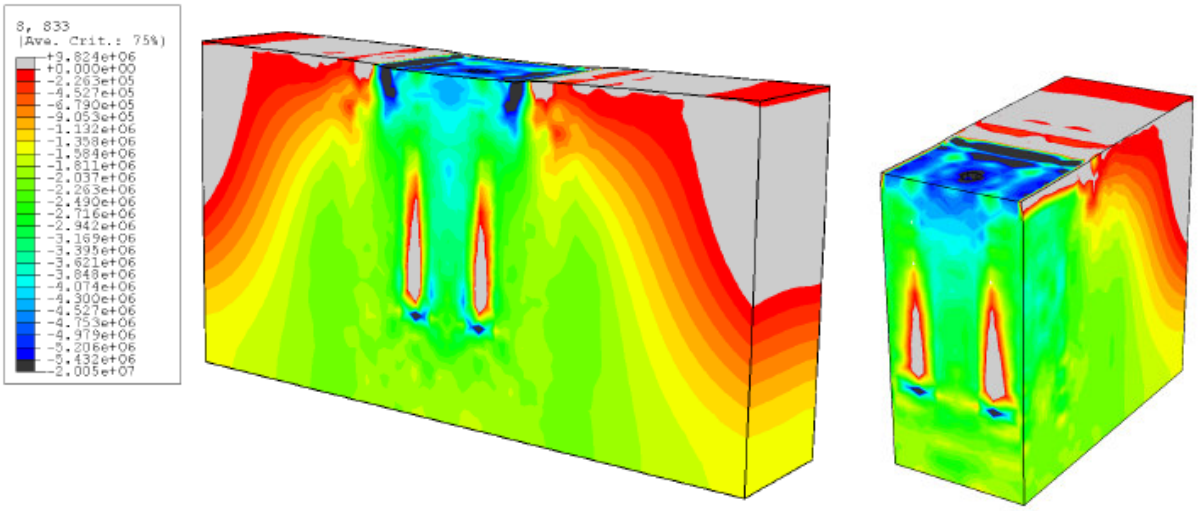

Figure 6.18 Stress field at the level of the screws, S10pl15

- S10pl20

The results from the model with the thicker plate, S10pl20, show similar behaviour as S10pl15 but with slightly less capacity, see Figure 6.19. The resulting capacity according to the UNI EN 408 standard is 330.5 kN.

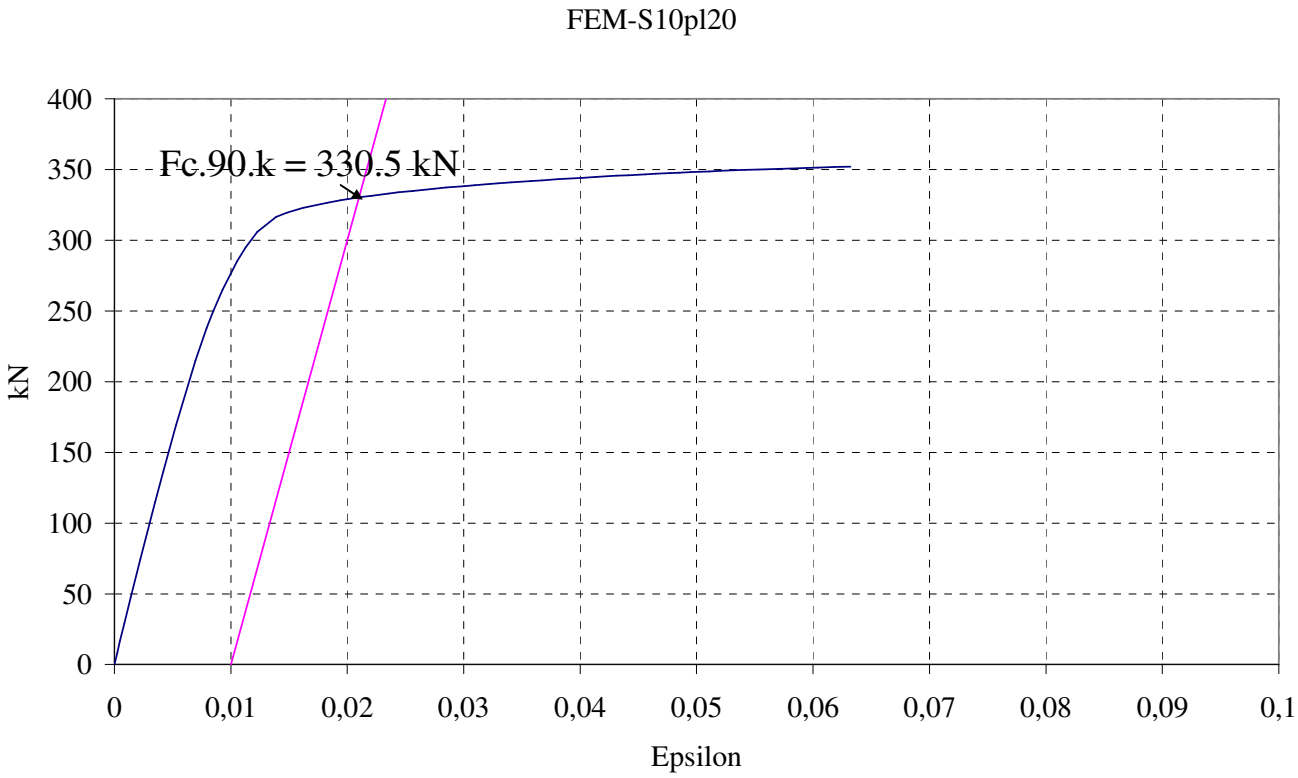

Figure 6.19 Capacity according to the UNI EN 408 standard, S10pl20

The displacement and deformation is displayed in Figures 6.20-21 and the maximum displacement at the ultimate capacity is 9.1 mm. The same phenomenon as described earlier is true for this model regarding the displacement in the vicinity of the screws.

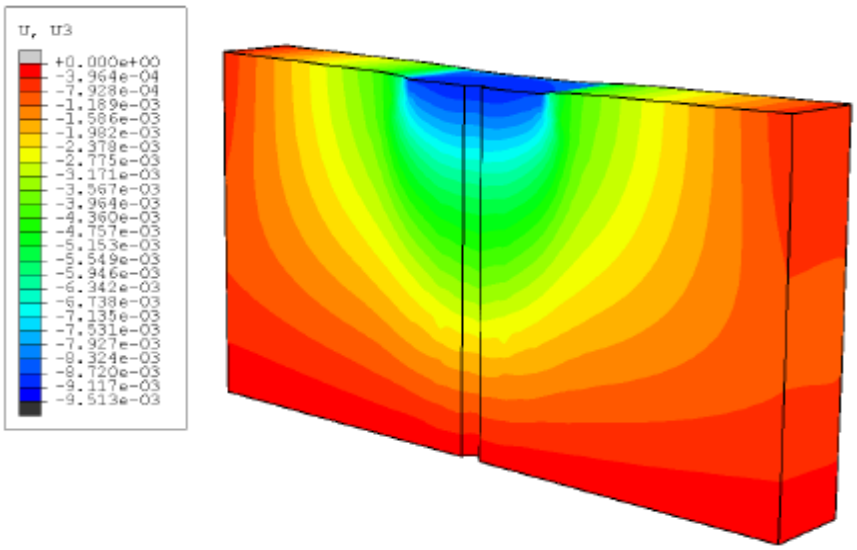

Figure 6.20 Displacement at the centre of the specimen, S10pl20

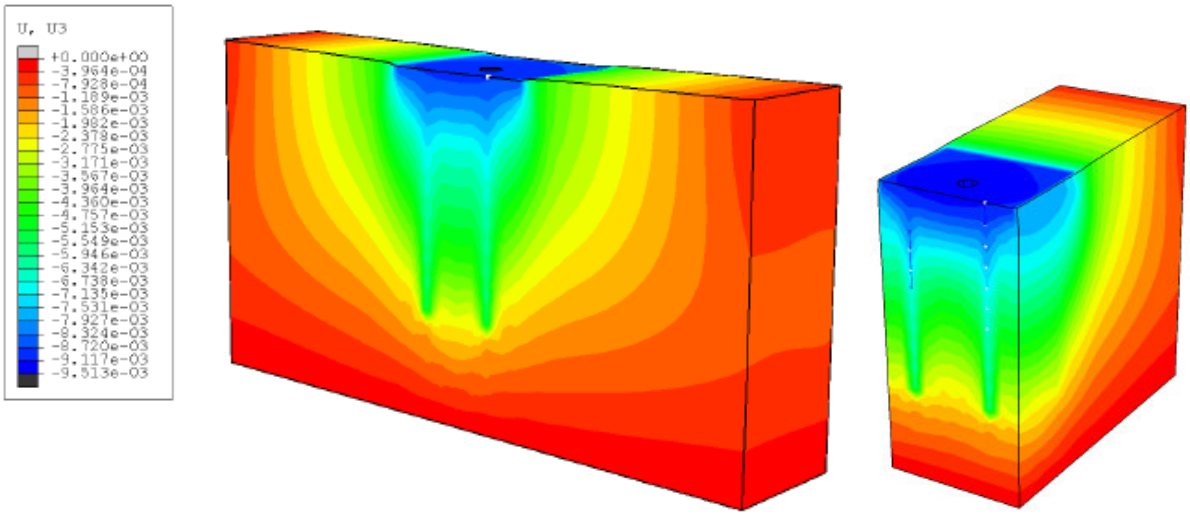

Figure 6.21 Displacement at the level of the screws, S10pl20

The stress field can be viewed in Figure 6.22 and the maximum stress occurring at 330.5 kN is about 19 MPa and is positioned at the edges of the plate.

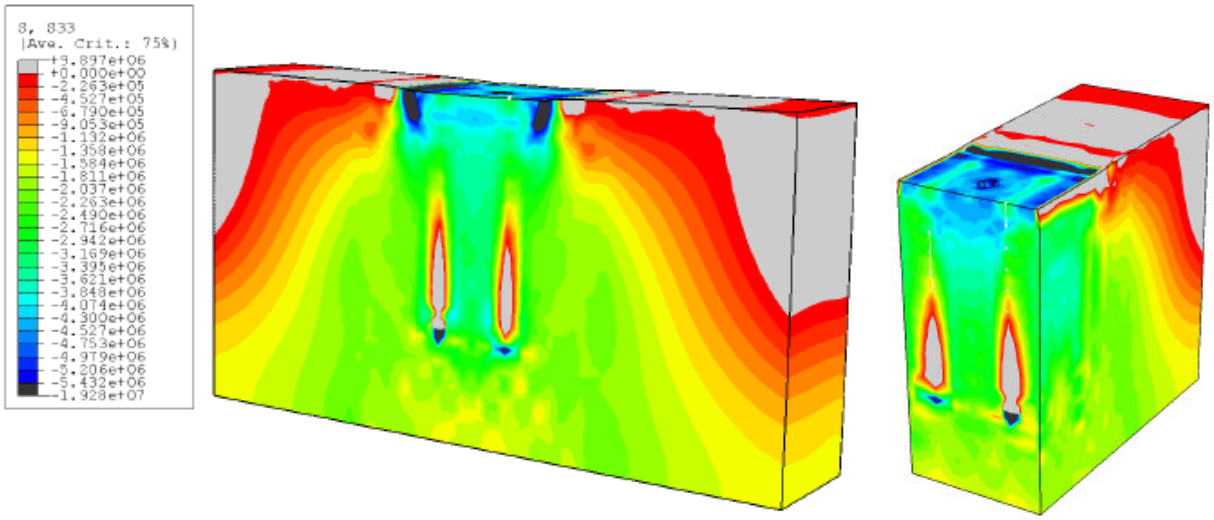

Figure 6.22 Stress field at the level of the screws, S10pl20

- S12pl15

In Figure 6.23 the *F-ε* relationship of the model with *d*= 12 mm screws and 15 mm thick plate is plotted, S12pl15. The capacity reached using the UNI EN 408 standard is 358.2 kN and the corresponding displacement at that load is about 15 mm.

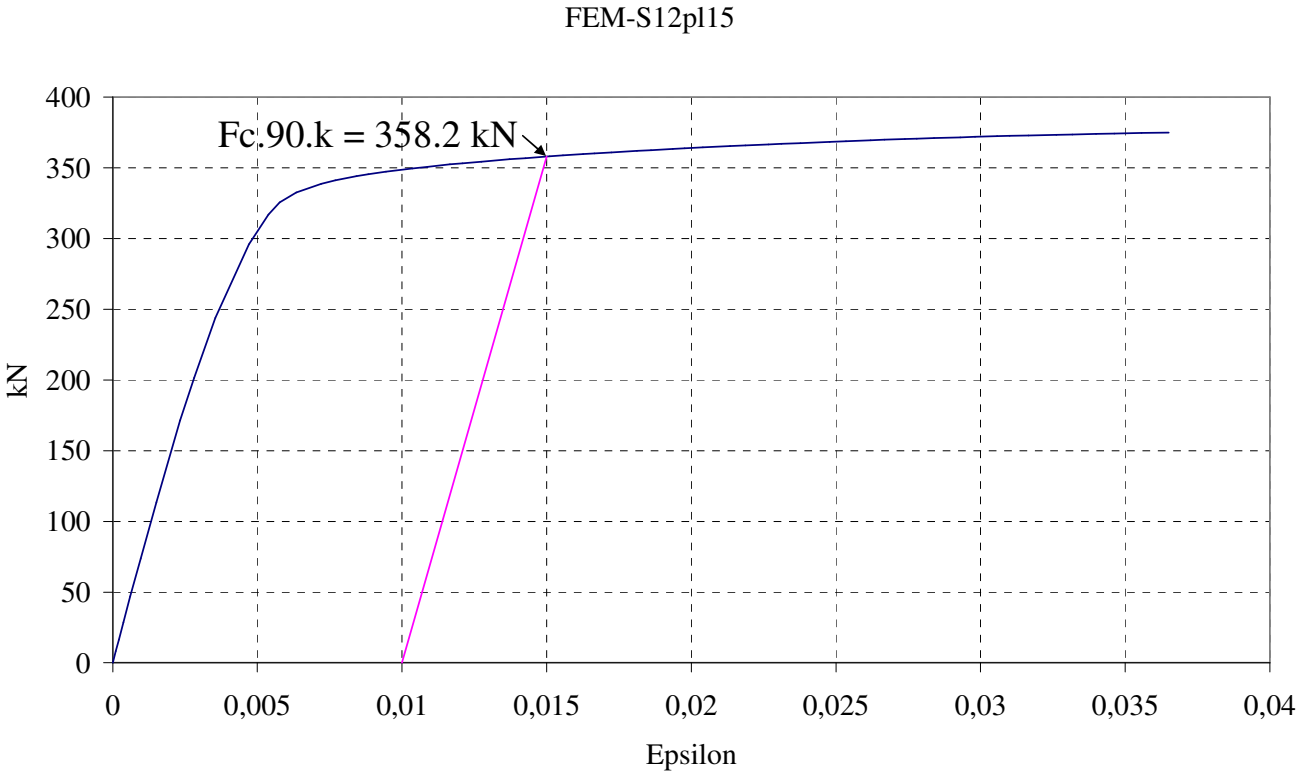

Figure 6.23 Capacity according to the UNI EN 408 standard, S12pl15

Figures 6.24-6.25 shows the vertical displacement at the centre of the specimen and at the level of the screws, respectively. The same argument is true for this specimen as discussed above.

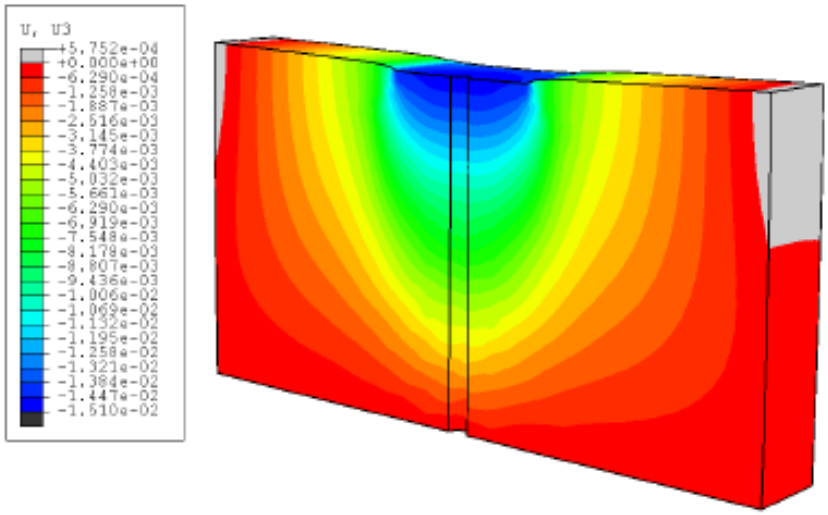

Figure 6.24 Displacement at the centre of the specimen, S12pl15

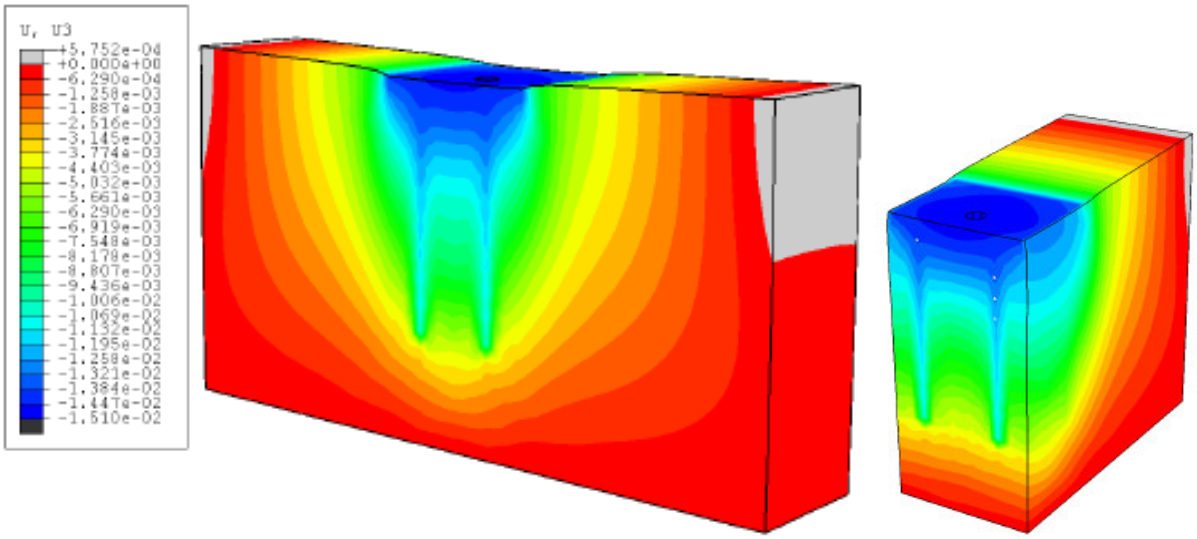

Figure 6.25 Displacement at the level of the screws, S12pl15

Regarding the stress field of the model, S12pl15, it shows similar behaviour as the previous reinforced models described, see Figure 6.26. Since the load carrying capacity has increased hence the stresses has increased at the edges of the plate. In this case the maximum stresses at the edges are in the region of 26 MPa. The stresses can not be assumed to be uniformly distributed at the bottom of the specimen.

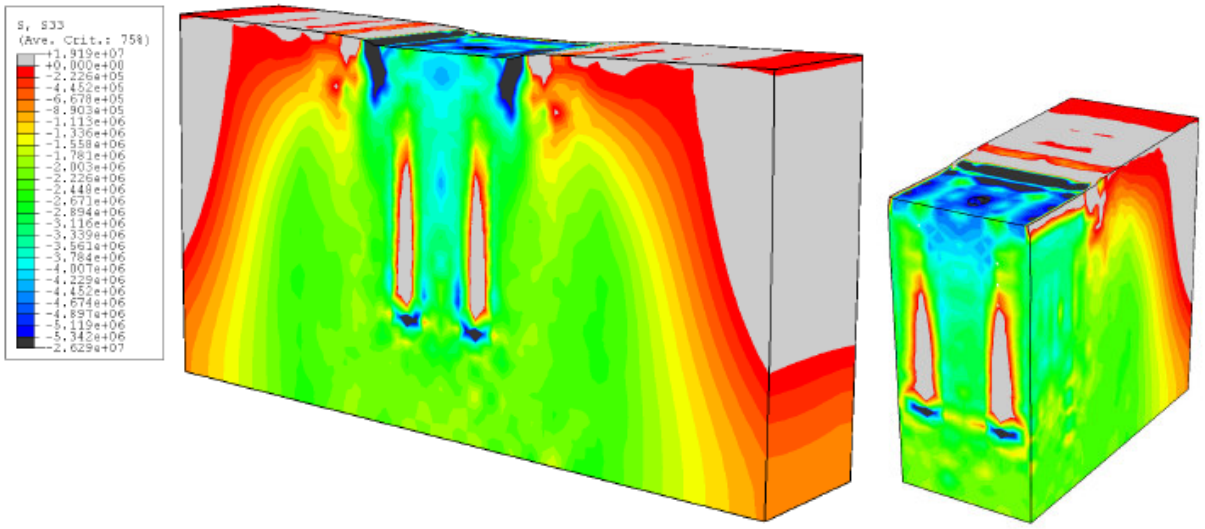

Figure 6.26 Stress field at the level of the screws, S12pl15

- S12pl20

Figure 6.27 represents the case where the diameter of the screw is set to 12 mm and the plate thickness set to 20 mm. The load carrying capacity according to UNI EN 408 is 351 kN with corresponding deformation of about 10 mm.

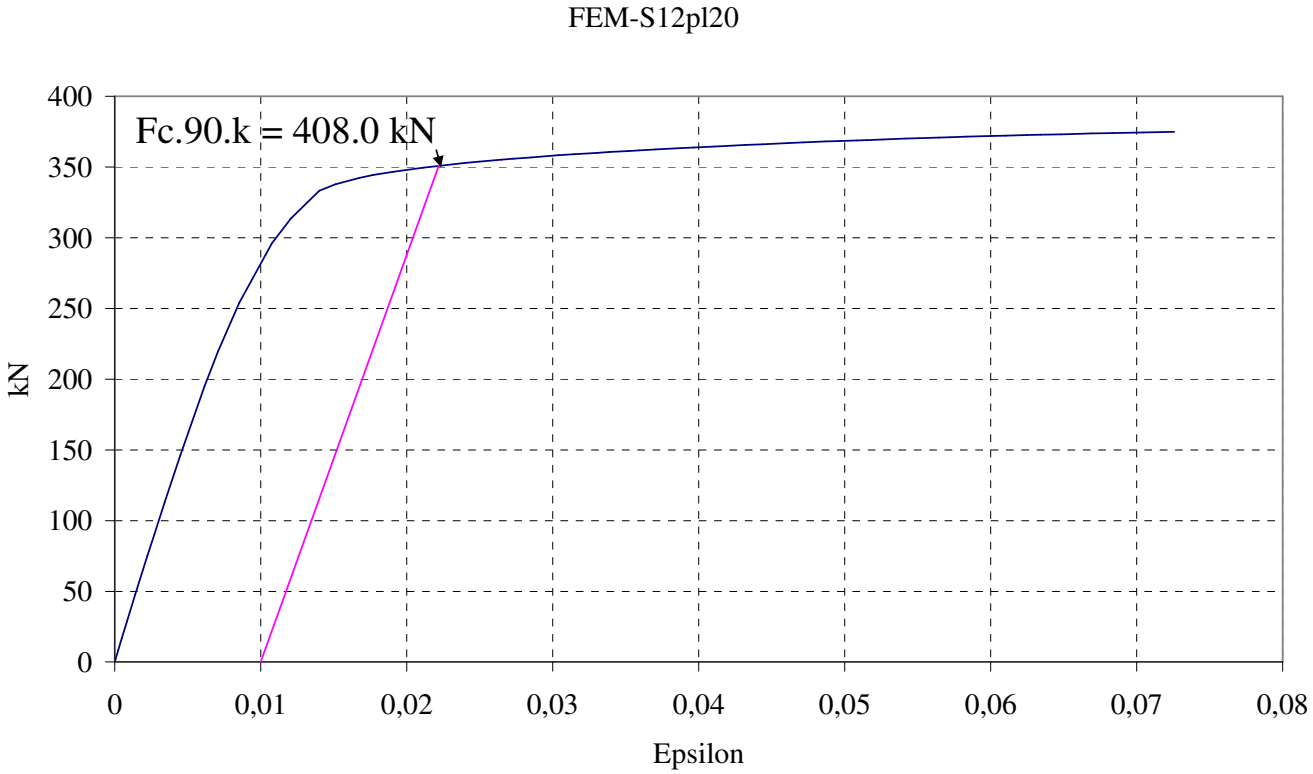

Figure 6.27 Capacity according to the UNI EN 408 standard, S12pl20

Figures 6.28-6.29 displays the deformation at the centre of the specimen as well as at the level of the screws.

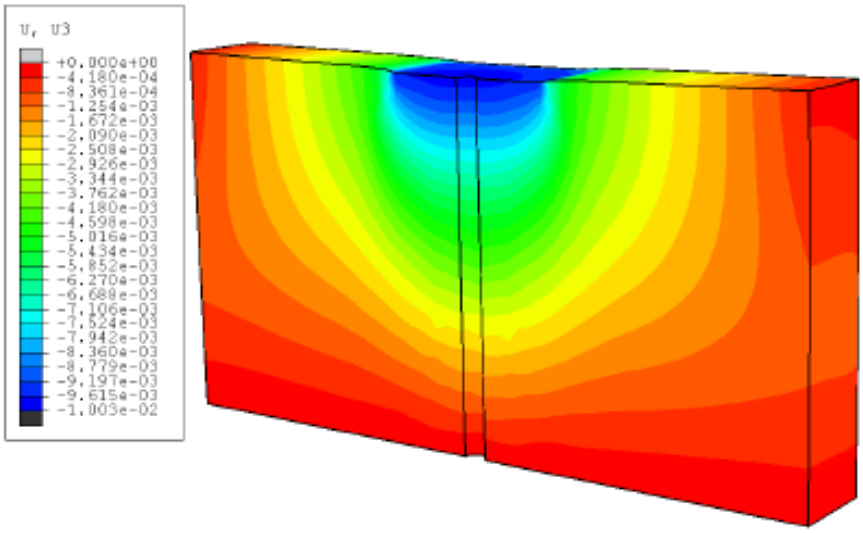

Figure 6.28 Displacement at the centre of the specimen, S12pl20

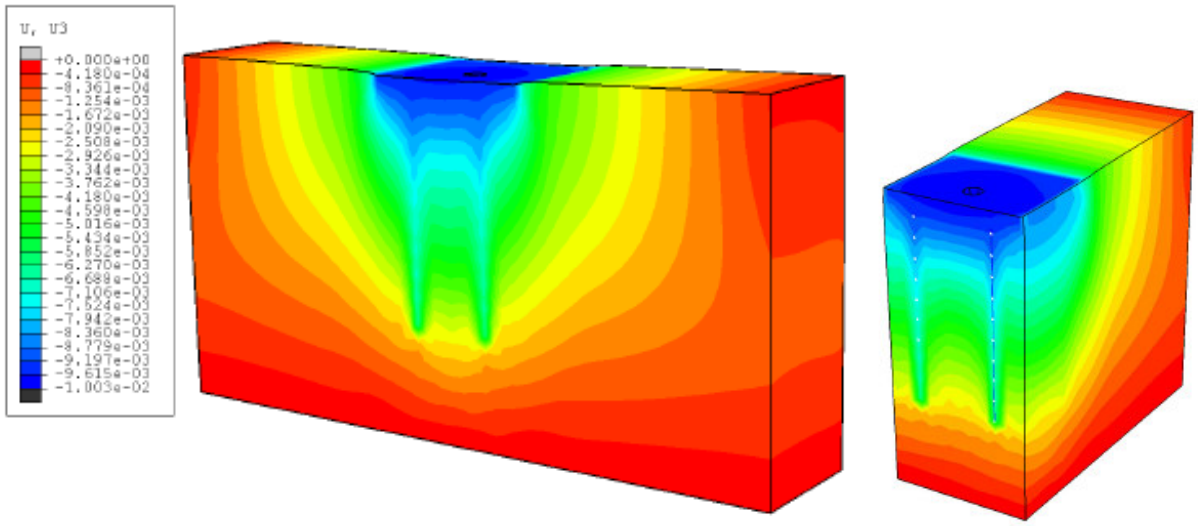

Figure 6.29 Displacement at the level of the screws, S12pl20

The stress field can be viewed in Figure 6.30 and maximum stresses occurring at the edges of the plate is approximately 22 MPa. The stresses can be assumed to be uniformly distributed at the bottom part of the specimen.

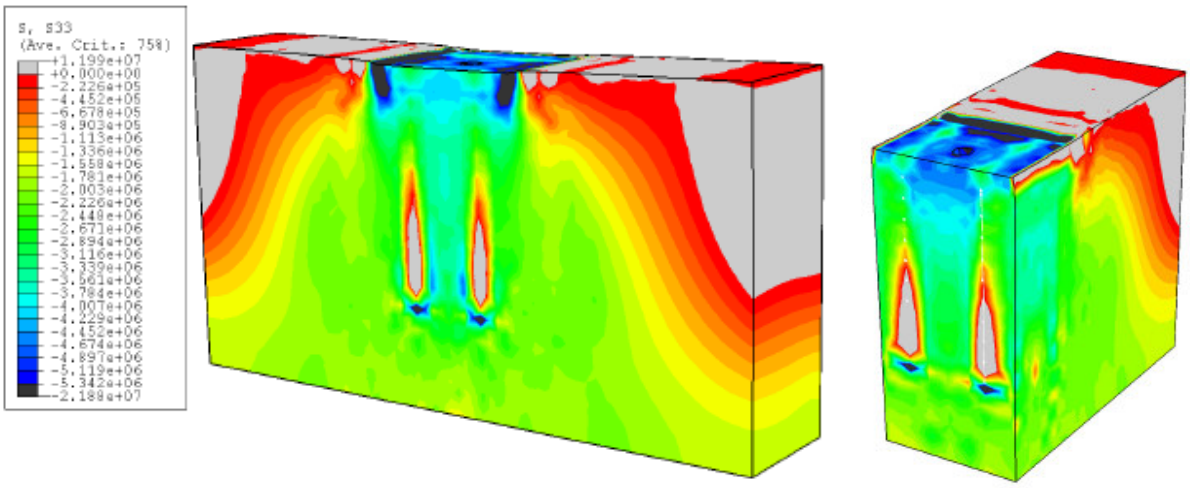

Figure 6.30 Stress field at the level of the screws, S12pl20

6.3.3 Comparison with test results and analytical solutions

By comparing the test results to the FE-model it is easy to notice the real behaviour compared to the theoretical behaviour and phenomenon that occurs in reality becomes more distinct when comparing to the FE-results. In Table 6.5 the overall comparison between the FE-models and the tests are displayed as a matrix where the diagonal represents the configurations that corresponds to each other. In an ideal case the diagonal would be zero but since there is a deviation between the FE-results and the test results the diagonal is different from zero. Moreover, in the ideal situation the values under the diagonal should be negative, since in the comparison those values represent a "weaker" configuration comparison. However, the performance of the configurations with the 20 mm plate in the FE-analysis did not differ much from the configurations with the 15 mm plate and proved to have a capacity less than the tests with the 15 mm plate. Hence the reason to the positive values under the diagonal, marked as grey cells in Table 6.5.

Table 6.5 Comparison between different configurations and percentage greater or less capacity in the tests compared to the FE models

Percentage of capacity in the tests compared to the FE model *(+: greater capacity, -: less capacity)*						
FEM \ Test	pl40	plHW	S10pl15	S10pl20	S12pl15	S12pl20
Unreinforced	**3.8%**	**-7%**	*30%*	*+51.3 %*	*+44.5 %*	*82%*
S10pl15	*-25.1%*	*-33%*	**-6.3 %**	*+9.1%*	*+4.1 %*	*+31.1 %*
S10pl20	*-21.1 %*	*-29.3 %*	*-1.2 %*	**15%**	*+9.8 %*	*+38.2 %*
S12pl15	*-27.2 %*	*-34.8 %*	*-8.9 %*	*+6.1 %*	**+1.3 %**	*+27.5 %*
S12pl20	*-25.7 %*	*-33.4 %*	*-7%*	*+8.3 %*	*+3.4 %*	**+30.1 %**

Overall the agreement between the FE-results and the test results is good, except for the cases when the plate thickness in the FE-model is 20 mm. In these cases the deviation is 15 % and 30.1 % for S10pl20 and S12pl20, respectively. This can be explained by the influences of the plate thickness is not modelled properly. The plates are constrained in the FE-model with a tie to the timber surface, therefore the phenomena that occurred in the tests with plate bending resulting in an decreased contact area between plate and timber is not present in the FE-results.

None of the FE models, except for the S10pl15 case, reaches the capacity of the tests performed and this is partly due to the fact, as discussed earlier, that the plate bending was not properly considered. Plate bending can be considered by changing the interaction between the

plate and the timber. However, such a modification of the FE-model demands much more focus on the non-linear behaviour of the details regarding the contact. Furthermore, the difference in spring stiffness has a greater influence than predicted. The stiffer the springs the more increase of capacity. In the FE-model homogeneous material is assumed which creates constant spring stiffness since the stiffness of the springs is dependent of the density of the material. In the reality however the "spring stiffness" is not constant due to local imperfections in the material at the screws. Moreover, the FE-model does not consider the cutting of the fibres as the plate is being pushed into the timber, this phenomena could be explained, in the tests as a reduction of stiffness, occurs generally for the thicker 20 mm plate. The FE-model, as previously mentioned does not consider buckling of the screws which also has great influence on the capacity obtained by the FE-analysis.

In Figures 6.31-6.35 the test results and the results obtained from each configuration in the FE model is displayed together with the results from the analytical solutions.

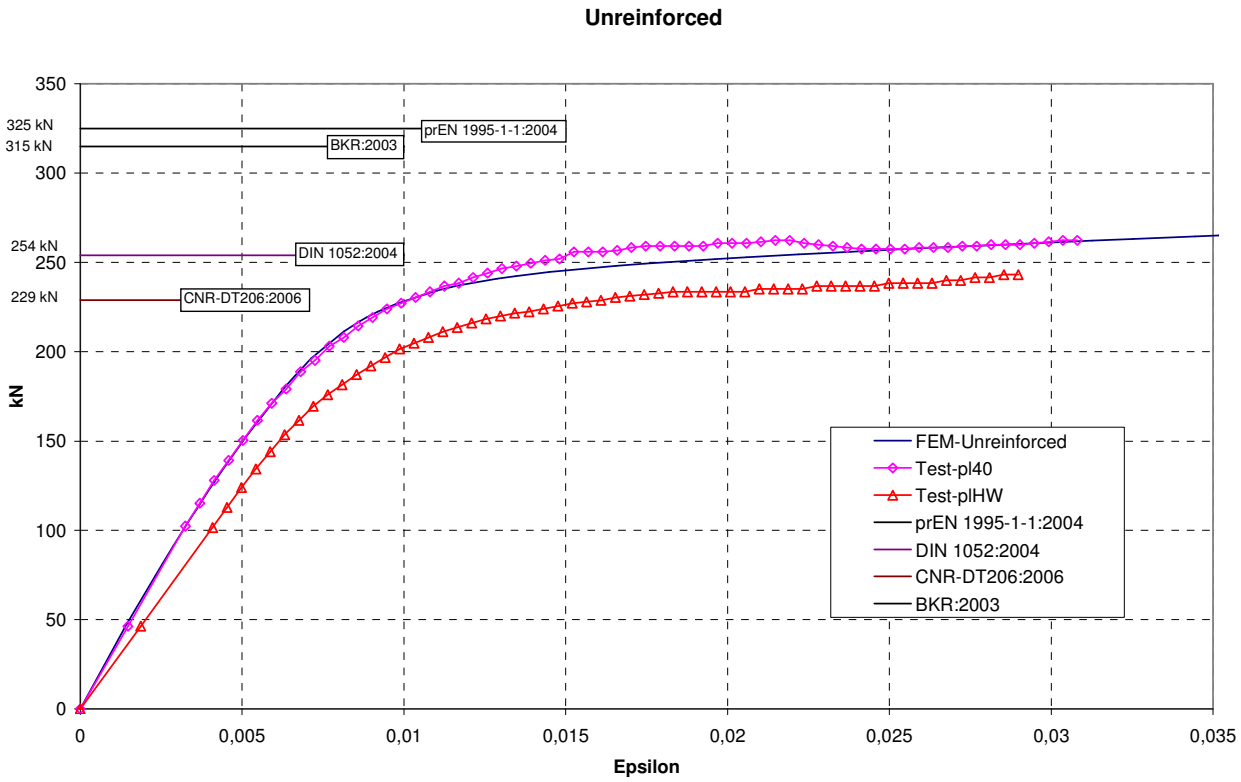

Figure 6.31 FE-Unreinforced together with the test results of the un-reinforced specimen with a thick steel plate and the traditional configuration and the characteristic values suggested by the codes

In Figure 6.31 the comparison between the un-reinforced FE-model and the two un-reinforced test specimens is displayed together with the analytical solutions. It can be noticed that the agreement between the FE-model and the un-reinforced test specimen with the thicker plate is good. This is due to the fact that no plate bending occurs. Regarding the traditional configuration the stiffness is slightly less, therefore also less capacity. The lesser stiffness can be explained by imperfections in the test specimen and the fact that the material in these two specimens does not share the same properties. Furthermore, the German code predicts the capacity best and both Eurocode 5 and the Swedish code seem to overestimate the capacity. The Italian code is conservative and slightly on the safe side.

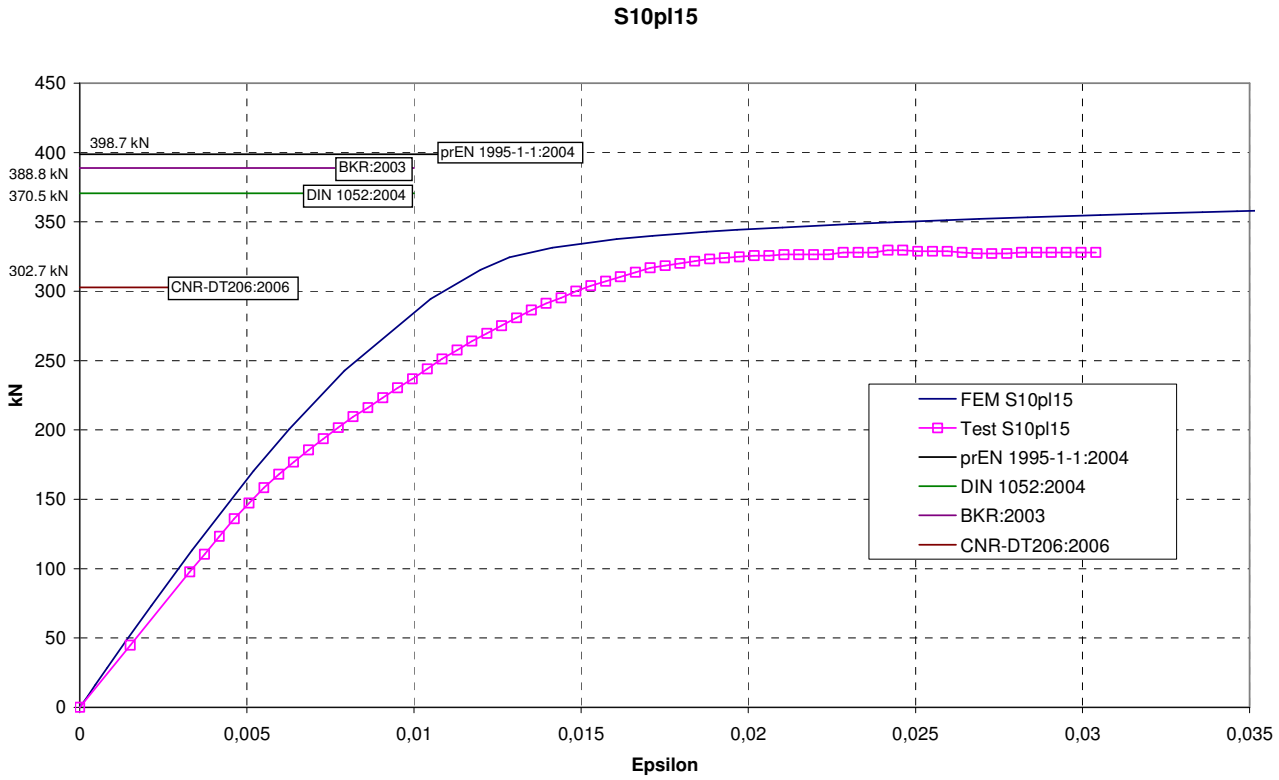

Figure 6.32 Reinforced FE-model and test results together with the analytical solution for the case with d = 10 mm screws and a 15 mm steel plate

In Figure 6.32 the results of the reinforced case with d = 10 mm and plate thickness equal to 15 mm is displayed. Since the FE-model does not take into account bending of the plate in the most desirable way the stiffness and the ultimate capacity is slightly higher when compared to the test results. In the tests the screw buckled which ultimately led to failure; this was not captured by the FE-model. It can be seen that the loss of stiffness in the test results occurs at about 150 kN which corresponds to the start of plate bending. Moreover, due to lack of test quantities the results can not be considered as the general behaviour, however it gives an indication of the general behaviour. The best agreement with the test results and the FE-model is reached when using the Italian code. The other codes that where used in this comparison all generates results that overestimates the capacity. It must be noted again that the analytical model does not consider the thickness of the plate and can therefore not predict the bending of the plate which reduces the overall capacity.

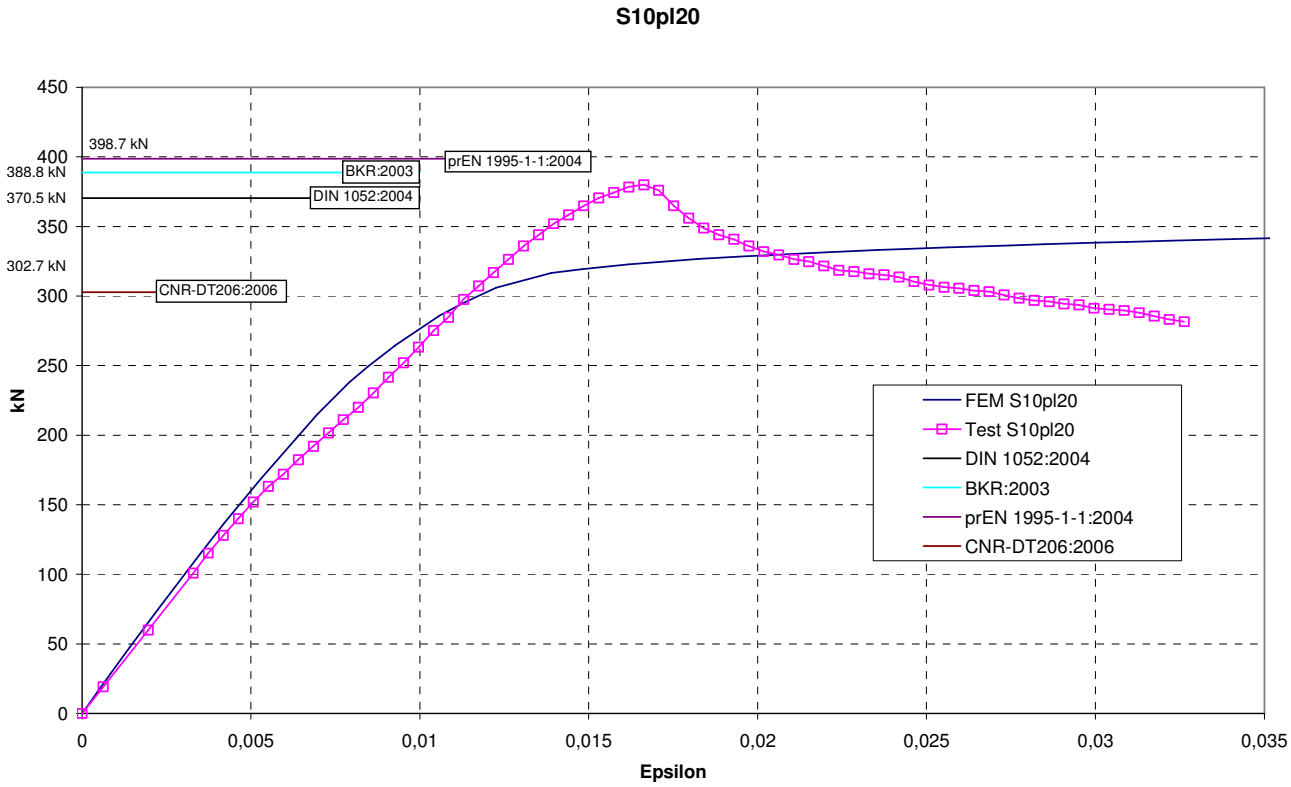

Figure 6.33 Reinforced FE-model and test results together with the analytical solution for the case with d = 10 mm screws and a 20 mm steel plate

Figure 6.33 displays the reinforced case where the diameter of the screws is set to 10 mm and the plate thickness is 20 mm. In this comparison between the FE-model and the test results the agreement is not satisfactory; this is due to the fact that the screws in the test performed better than predicted in the FE-model even though failure at 380 kN. The stiffness agreement can be considered as good, however, when the plate in the test is pressed into the timber it generates a loss in stiffness in the timber, hence the slight change of stiffness in the test curve at approximately 150 kN. The analytical solutions generally agree with the test results except Eurocode 5 which overestimates the capacity slightly. The fact that the analytical solutions performs so well can be related to the fact that they have the ability to predict buckling of the screws. The Italian code generates a capacity that is on the safe side and significantly less than the other codes used in this evaluation.

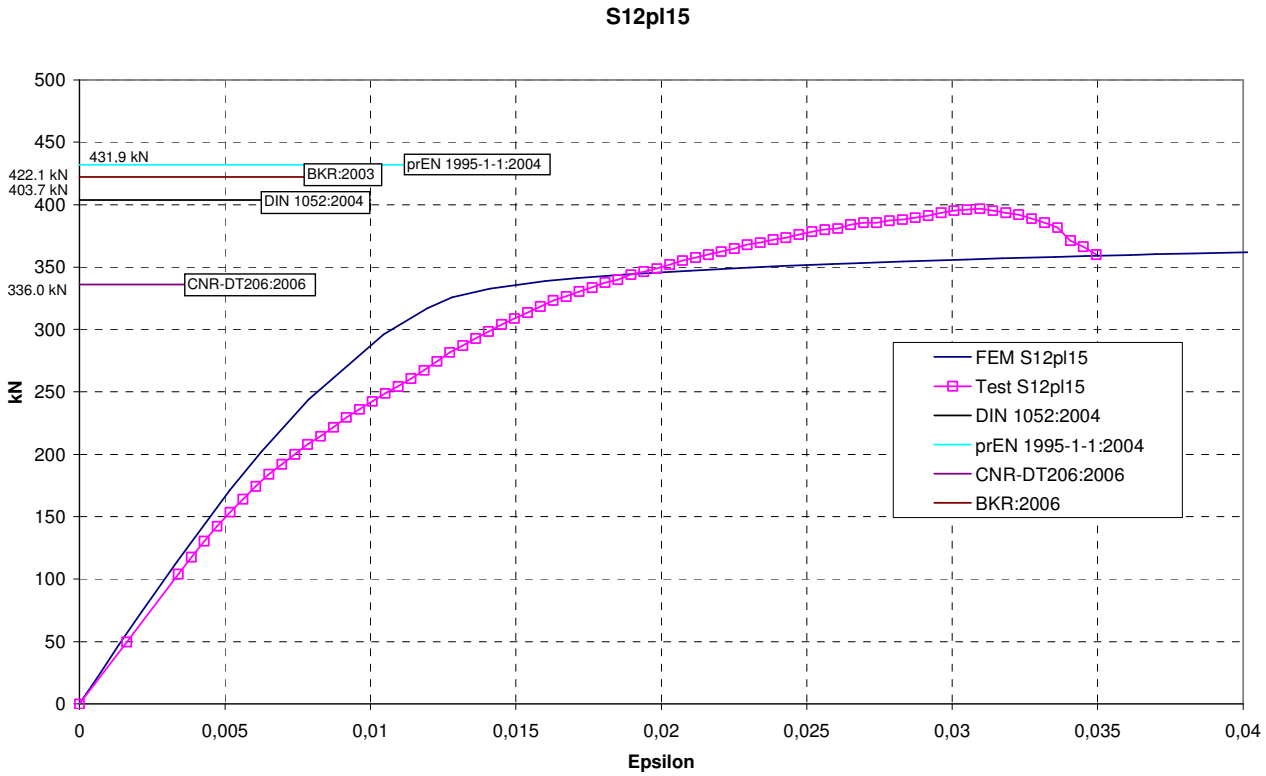

Figure 6.34 Reinforced FE-model and test results together with the analytical solution for the case with d = 12 mm screws and a 15 mm steel plate

Figure 6.34 shows the load-strain diagram of the test results along with the FE-result and the analytical results for the reinforced case with d = 12 mm screws and a plate thickness of 15 mm. The behaviour is similar to the S10pl15 case for small loads. However, the d = 12 mm screws proves to generate stiffer response to the loading and therefore increased capacity compared to S10pl15. Plate bending occurs at about 150 kN and the stiffness is reduced from that point. The increased capacity and the less stiffness compared to the FE-model results in a conclusion that the agreement between the FE-model and the test is not satisfactory, even though the ultimate capacity is similar. The Italian code proves to predict the capacity best since the other codes in this evaluation overestimates the capacity.

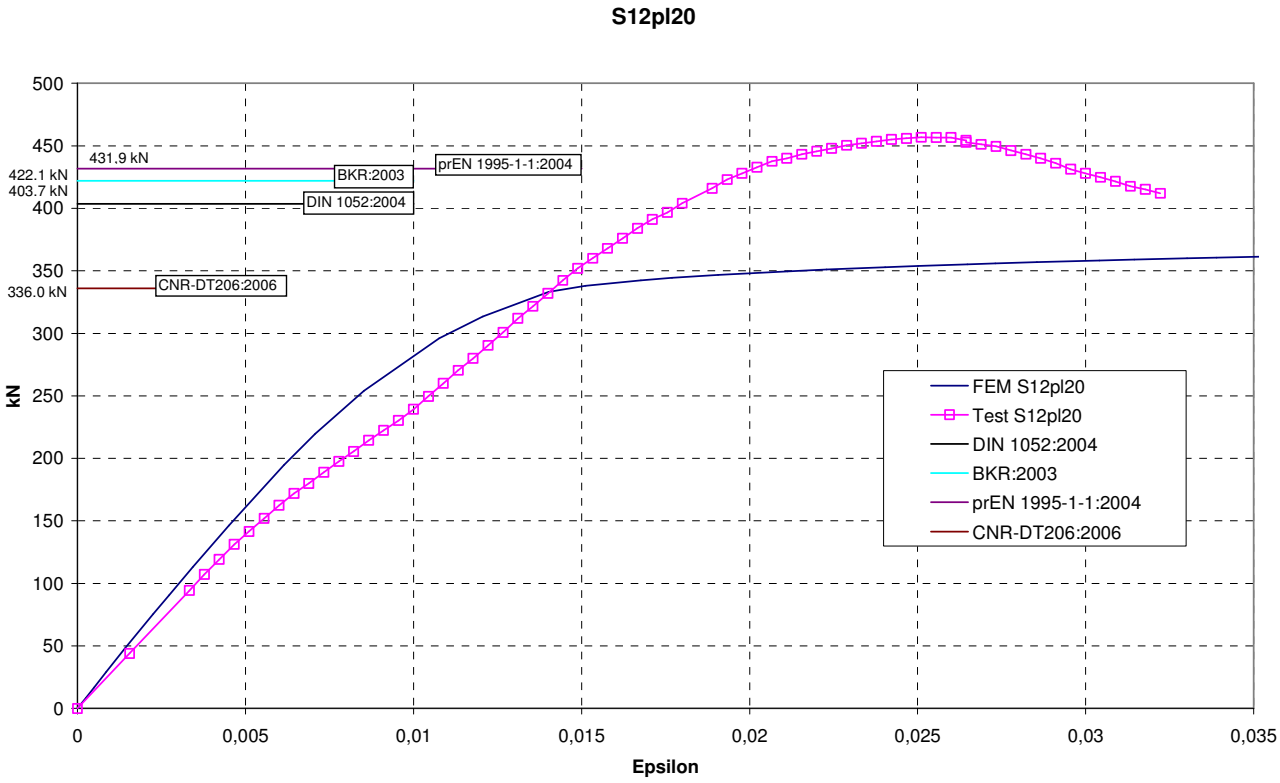

Figure 6.35 Reinforced FE-model and test results together with the analytical solution for the case with d = 12 mm screws and a 20 mm steel plate

Figure 6.35 displays similar behaviour as the S10pl20, Figure 6.33. This is due to the thicker plate being pushed into the timber, leaving a depression which reduces the stiffness in the timber. Moreover, the d = 12 mm screws increases the capacity significantly compared to the FE-model and the overall conclusion is that the agreement is not satisfactory between the two curves. The analytical solution using different codes all underestimates the capacity, but Eurocode 5 assumes the closest value. Again, the test result gives no accurate conclusion regarding the ultimate capacity, however, good guidance and hints on the effect of this configuration is gained.

6.4 Modelling the effect of the unloaded length

6.4.1 Element and assembly

When modelling the effect of the unloaded length both the entire specimen and one fourth of it were modelled for each loading configuration. The first type was used to better investigate the global behaviour and the second type to optimize the analysis in terms of mesh size consequently resulting in better accuracy. The specimens consists of two parts modelled as 3D solid extrusion elements, one for the timber specimen and the other for the steel plate, see Figure 6.36

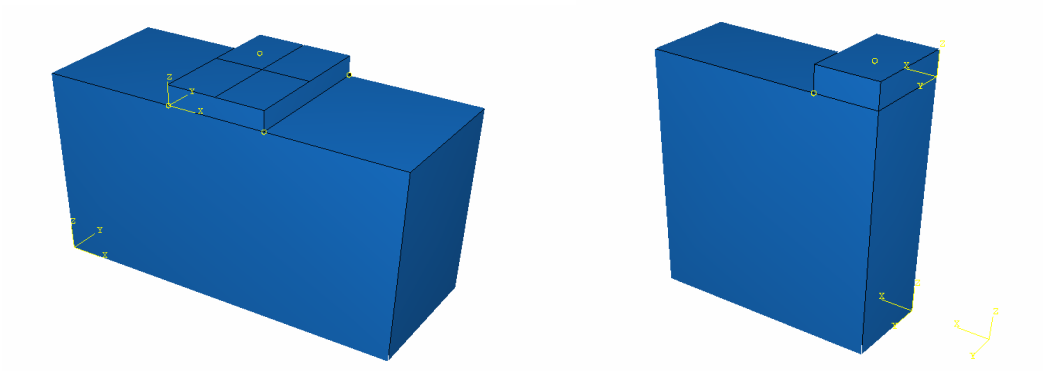

Figure 6.36 Assembly of models: global and symmetric model (case 300x120x200)

The geometry of the models are the same as of the tests performed by Reichegger [11], see Chapter 3.2

6.4.2 Material property

The material property that were used in the model are obtained with the same procedure done for the model of the laboratory test specimens, see Chapter 6.2.2. In this case the type of glue-laminated timber used were GL24 and the interpolated values of the orthotropic coefficients can be seen in the Table 6.6.

Table 6.6 Interpolated values for GL24 glue-laminated timber

$E_{L,}$	11600	[MPa]
$E_{R,}$	581.25	[MPa]
$E_{T,}$	251.56	[MPa]
$G_{LR,}$	560.63	[MPa]
$G_{LT,}$	292.19	[MPa]
$G_{RT,}$	23.06	[MPa]
υ_{RL}	0.01	
υ_{TL}	0.01	
υ_{TR}	0.19	

It was consider also a plastic behaviour of the timber in the model. The type of hardening chosen is isotropic and the value of yield strength was varied from 3.0 MPa to 4.5 MPa.

The parts in steel were modelled as isotropic materials and were given a Young's modulus of 210 GPa and a Poisson's ratio of 0.3. The density of the steel was set to 7800 kg/m^3.

6.4.3 Interactions

The two parts of the model were coupled together using the surface to surface tie constraint, in this way the contact between steel plate and the timber does not allow any slip of the plate.

6.4.4 Mesh

The two parts were meshed with the same sizes and type. Quadratic elements have been chosen since they prove to give more accuracy in the calculations when compared to linear elements. The global model has been modelled with hexagonal mesh with the size of 0.01, instead of the symmetric model has been modelled with a mesh equal to 0.005, see Figure 6.37.

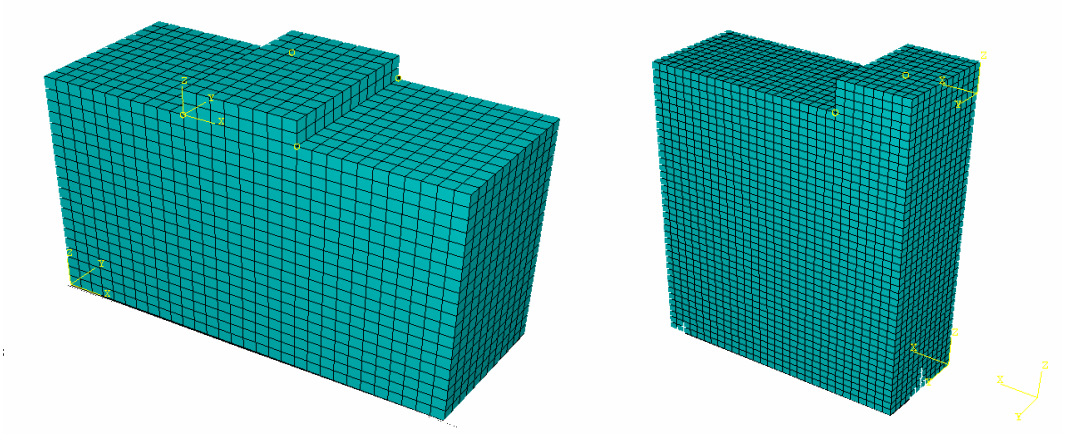

Figure 6.37 Description of mesh configuration (case 300x120x200)

6.4.5 Step

The type of analysis was chosen as Static, Riks procedure which uses the arch length method to find convergence. This choice was done due to the non-linear behaviour of the timber when it enters the plastic field. The maximum number of increment was fixed equal to 100 and the minimum and maximum arch length was fixed equal to 0.00001 and 0.1 with the initial value equal to 0.01.

6.4.6 Loads and boundaries

Since the exact configuration of the applied load in the tests performed by Raichegger, [11], were not completely known some approximations were done in the FE-model. This means that the load was applied as a displacement in the centre point at the top of the steel plate. The chosen applied displacement was equal to 20 mm for specimen with height equal to 200 mm and 10 mm for specimens with height equal to 100 mm. In the global model the load was applied by partitioning the upper surface of the steel plate in order to select the centre point.

The bottom face of the specimen was completely constrained in order to simulate the contact of the specimen with the support. In this case the effect of friction was neglected since this aspect does not influence the result.

In the symmetric model the two horizontal axes of symmetry were utilized, so the translation in the direction perpendicular to the plane and the rotation along the axes in the plane of symmetry were constrained, all the other degrees of freedom were available. The configuration of the boundaries can be seen in Figure 6.38.

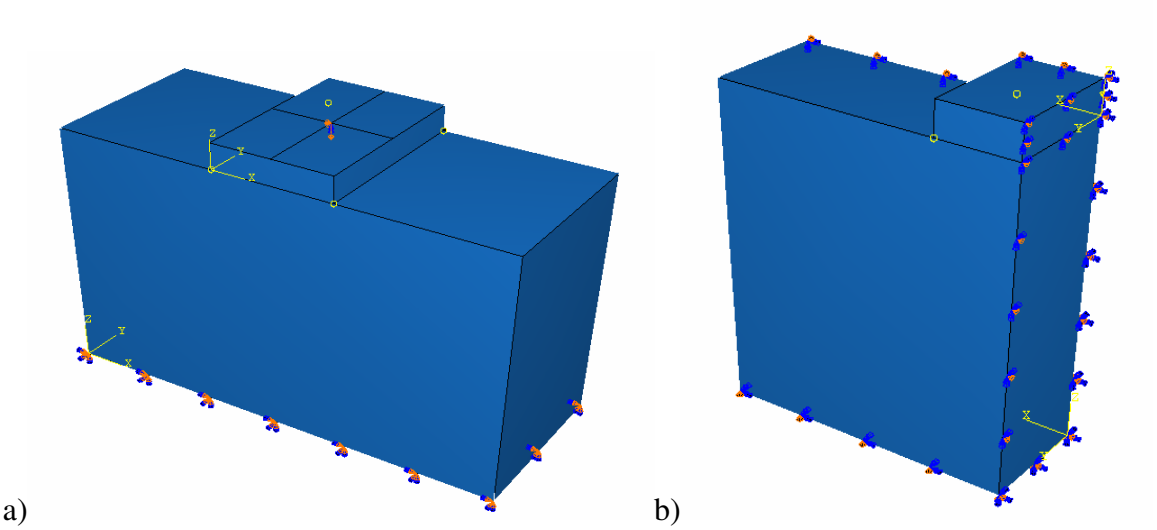

a) b)

Figure 6.38 Configuration of the boundaries (case 300x120x200) for global model, a), and symmetric model b)

6.4.7 FE Analyses

A series of FE analyses were performed as described in the sequent table, see Table 6.7:

Table 6.7 Table of the analyses performed

Name	Timber Specimen	Model	Yield stress
G80	[80x120x100]	Global	3.0 MPa
G120	[120x120x200]	Global	3.0 MPa
G200	[200x120x200]	Global	3.0 MPa
G300	[300x120x200]	Global	3.0 MPa
G400	[400x120x200]	Global	3.0 MPa
S80 (0) (1) (2)	[80x120x100]	Symmetric	(3.0) (3.5) (4.0) MPa
S120 (0) (1) (2)	[120x120x200]	Symmetric	(3.0) (3.5) (4.0) MPa
S200 (0) (1) (2)	[200x120x200]	Symmetric	(3.0) (3.5) (4.0) MPa
S300 (0) (1) (2)	[300x120x200]	Symmetric	(3.0) (3.5) (4.0) MPa
S400 (0) (1) (2)	[400x120x200]	Symmetric	(3.0) (3.5) (4.0) MPa

The only parameter that changes in the analyses performed is the yield stress.

6.4.8 Results and comments

After the FE analysis some significant results are reported in this paragraph to illustrate and comment the effect of unloaded length. Preliminarily it is of interest to show how the timber deformation changes with the increment of the unloaded length. This study was performed with the global models and the case with vertical displacement equal to zero has been neglected since it shows no difference in behaviour between the models. The sequent figure, see Figure 6.39, shows the displacement field U3 when the sink of the steel plate into the timber is equal to 15 mm. The other studied loading cases can be seen in Appendix G.

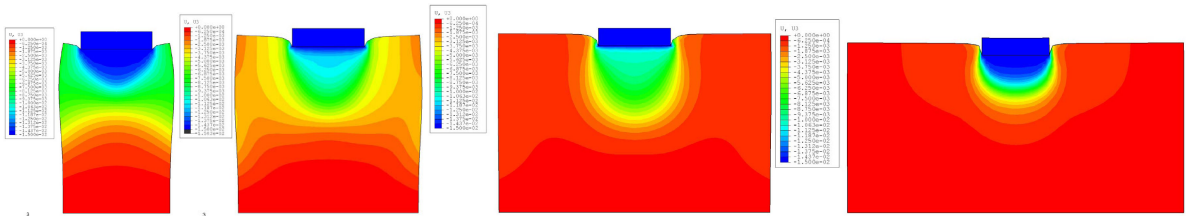

Figure 6.39 Displacement field at the centre of the models at 15 mm of deformation

It is possible to see in the figures, see Appendix G, which with the increasing deformation of the steel plate into the timber after the elastic behaviour there is a plastic deformation. In the elastic field, there is a zone under the steel plate where the loads are spread into the timber and at a certain depth the deformation and the stress field becomes uniform, as mentioned in the St Venant theory. This effect is less visible with the increment of the unloaded length, due to the fact that the zones at the edges are too far from the position of the applied load. When the timber becomes plastic, the permanent deformation is concentrated under the steel plate and it increases with the increment of the sink of the steel plate and the load applied can not be increased further. For an unloaded length longer than a certain length the plastic deformation is not affected of the length of the timber, thus the behaviour is the same as the case of an infinitely long unloaded length.

As the analyses are in displacement control the total load applied is calculated for each increment as the sum of the reaction forces at the nodes on the bottom face of the timber element, vertical direction RF3. In this way it is possible to print the force-displacement relationship and stress-deformation relationship. The node chosen to measure the displacement and deformation is at the same position as the point of measurement in the tests conducted by Reichegger, [11]. It corresponds to the edge point at the centre of the upper timber face. The force-displacement curve and the stress -strain curve for each configuration is shown in the sequent table, see Table 6.9. In the relationships regarding the stress-strain curve the test results conducted by Reichegger, [11], is also introduced.

Table 6.9 Force – Displacement and Stress –Strain Curves of the model

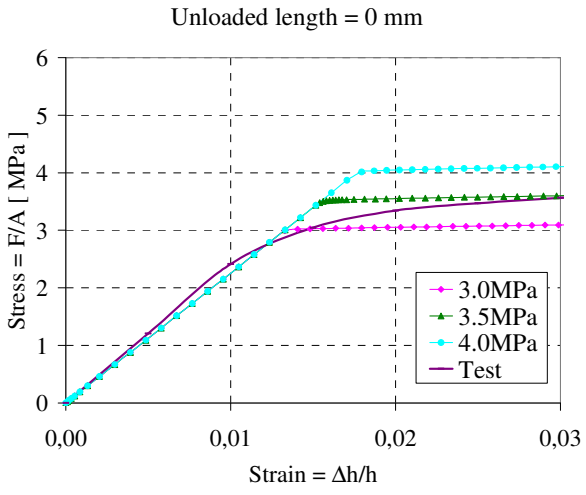

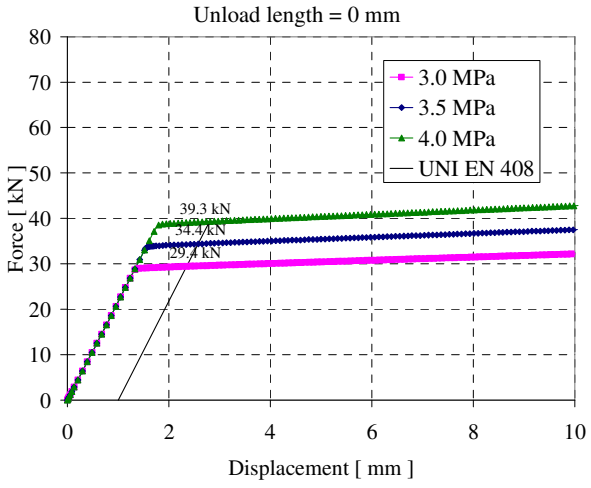

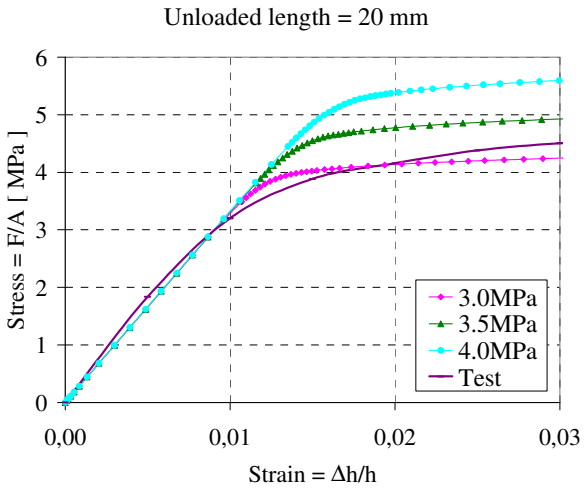
Unloaded length = 20 mm
Stress = F/A [MPa]
Strain = Δh/h
3.0MPa
3.5MPa
4.0MPa
Test

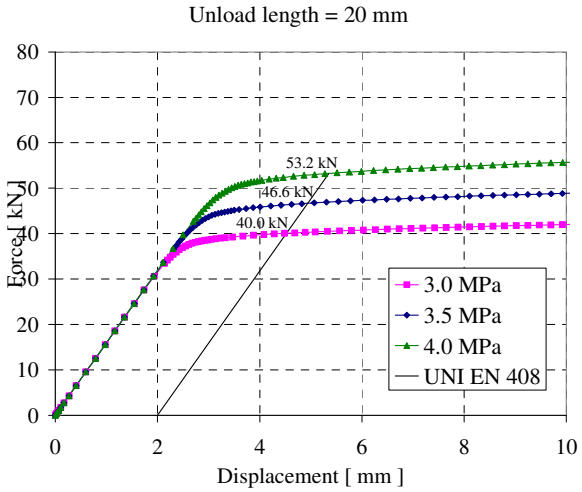
Unload length = 20 mm
Force [kN]
Displacement [mm]
53.2 kN
46.6 kN
40.0 kN
3.0 MPa
3.5 MPa
4.0 MPa
UNI EN 408

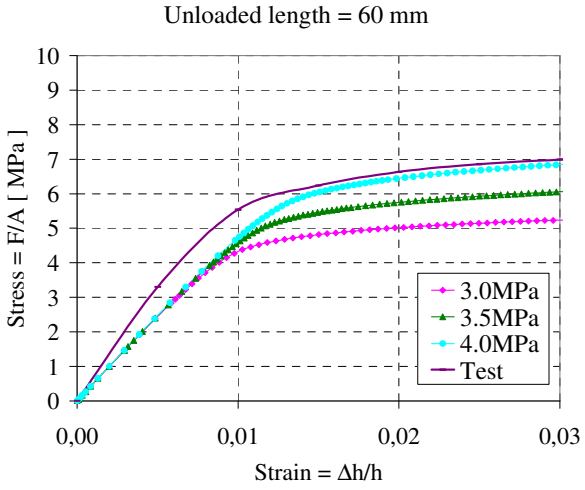
Unloaded length = 60 mm
Stress = F/A [MPa]
Strain = Δh/h
3.0MPa
3.5MPa
4.0MPa
Test

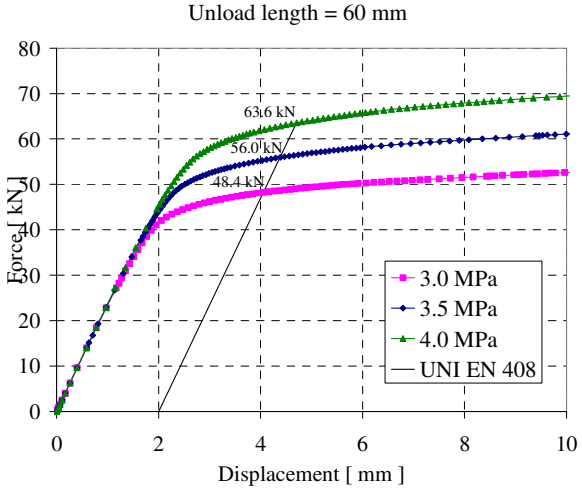
Unload length = 60 mm
Force [kN]
Displacement [mm]
63.6 kN
56.0 kN
48.4 kN
3.0 MPa
3.5 MPa
4.0 MPa
UNI EN 408

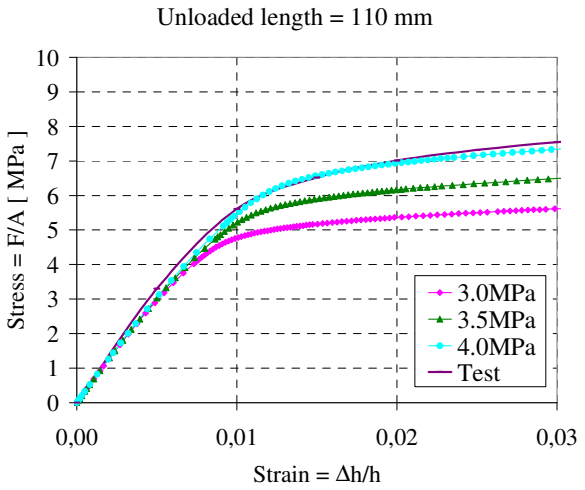
Unloaded length = 110 mm
Stress = F/A [MPa]
Strain = Δh/h
3.0MPa
3.5MPa
4.0MPa
Test

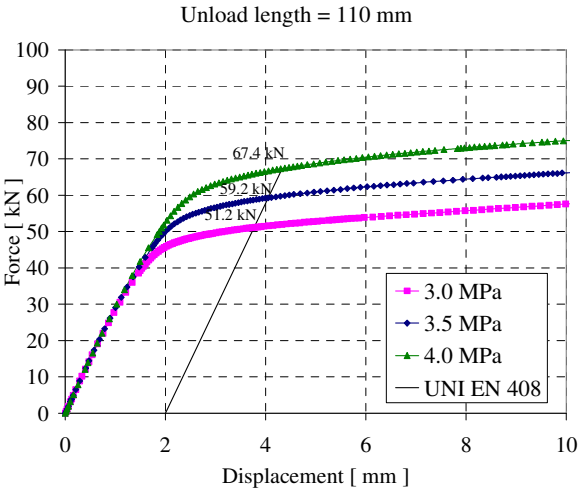
Unload length = 110 mm
Force [kN]
Displacement [mm]
67.4 kN
59.2 kN
51.2 kN
3.0 MPa
3.5 MPa
4.0 MPa
UNI EN 408

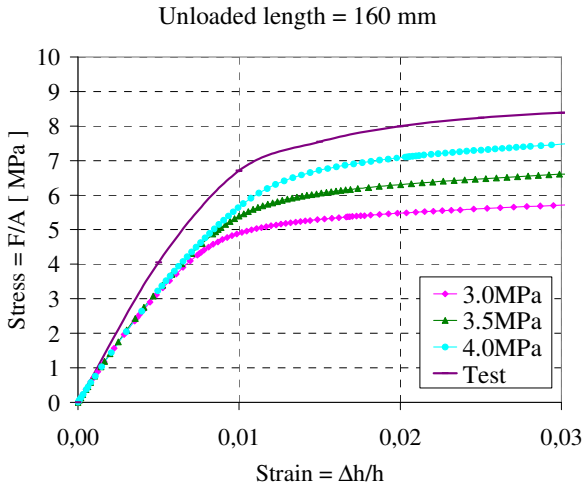

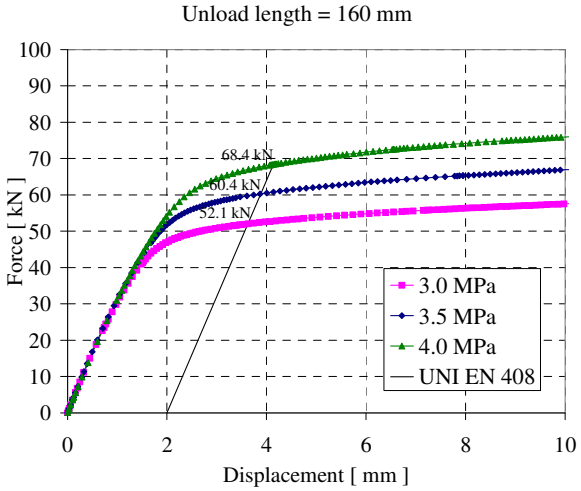

Differences both in strength and in stiffness, between the test curves and the model curves can be observed. It is noticeable that with an increase of unloaded length an increase of yield stress must be considered in the model in order to cover the test curves. This is probably due to the collaboration of the fibres that are not directly loaded but gives a beneficial contribution. This effect becomes stable and an increase of yield strength is not necessary when the unloaded length is more than 110 mm.

In the sequent table, see Table 6.10, the stress–strain relationships obtained by the FE-model for the cases where the yield stress is equal to 3.0, 3.5 and 4.0 MPa is displayed.

Table 6.10 Stress –Strain Curves for the FE-models with yield stress equal to 3.0, 3.5 and 4.0 MPa

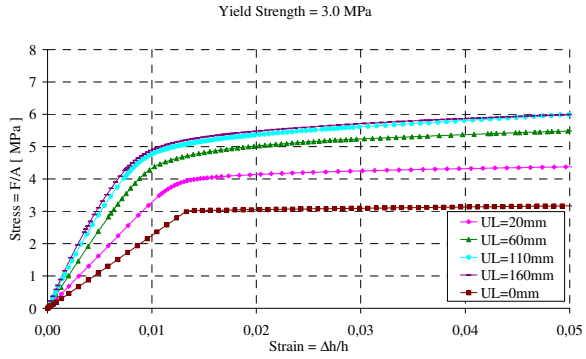

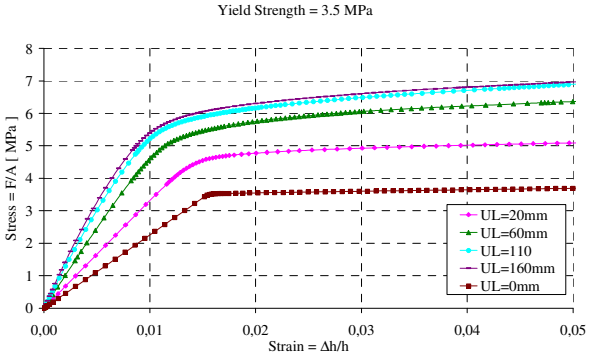

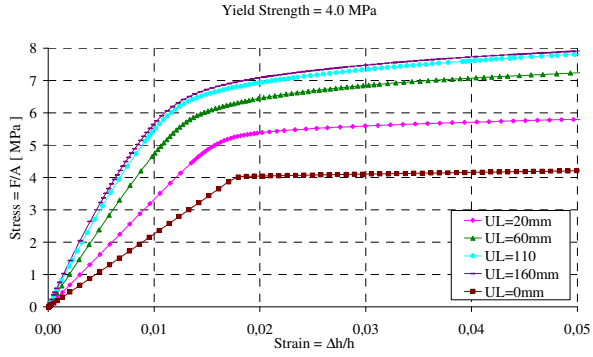

It is possible to notice that in each single relationship the increment of unload length produces an increment of the stiffness of the timber in elastic range and also an increase in strength. Also when the timber enters the plastic field, the transmission zone between elastic and plastic

becomes softer. By increasing the yield strength also the capacity increases proportionally as expected.

6.4.9 Comparison and conclusion

- Comparison of FE-models to German code DIN 1052:2004

The German code treats the unloaded length effect by considering two influences separately. First by considering the projection of member end by increasing the contact length of the applied load, as shown in the sequent equation, see Figure 6.40 and equation (6.7), [15]:

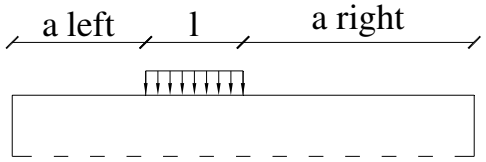

Figure 6.40 Geometrical parameter

$$A_{ef} = \left(l + \min\left\{a_{left}\ ; l\ ; 30\ mm\right\} + \min\left\{a_{right}\ ; l\ ; 30\ mm\right\}\right) \cdot b \qquad (6.7)$$

Secondly by considering the influences of load distribution with the assumption of a distribution line with inclination of 45˚, [15], see Figure 6.41. For the configuration of the FE-models performed it is shown the derivation of the factor ξ that take into account this effect, equations (6.8-6.11):

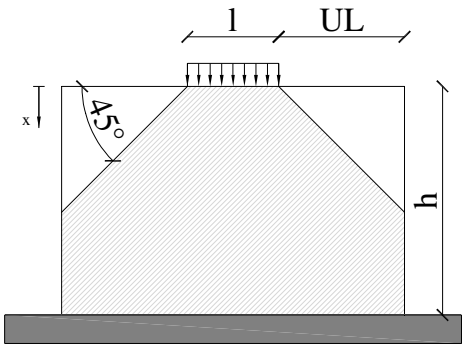

Figure 6.41 Assumed load distribution on a timber element supported on its whole length

$$\sigma(x) = \frac{F}{l \cdot b + 2 \cdot x \cdot b} \qquad \text{for } 0 < x < UL \qquad (6.8)$$

$$\sigma = \frac{F}{l \cdot b + 2 \cdot UL \cdot b} \qquad \text{for } UL < x < h \qquad (6.9)$$

The total deformation Δh is calculated as following integral equation:

$$\Delta h = \int_0^{UL} \frac{\sigma(x)}{E_{90}} dx + \int_{UL}^{h} \frac{\sigma}{E_{90}} dx = \Delta h_{UL=0} \cdot \xi \qquad (6.10)$$

So by inverting the formula it is possible to calculate the factor $\xi = funct\ (\ UL\ )$:

$$\xi = \frac{l}{2 \cdot h} \cdot \ln\left(2 \cdot \frac{UL}{l} + 1\right) + \frac{(1 - UL/h)}{(1 + 2 \cdot UL/b)} \tag{6.11}$$

If the unloaded length *UL* is more or equal to the depth *h* of the element the equation is simplified as seen below, see equation (6.12):

$$\xi = \frac{l}{2 \cdot h} \cdot \ln\left(2 \cdot \frac{h}{l} + 1\right) \tag{6.12}$$

In the sequent table factor ξ is calculated for the different configurations of the models proposed (l = 80 mm; h = 200 mm; b = 120 mm):

Table 6.11 Value of the factor ξ for different unloaded length

UL	[mm]	0	20	60	110	160
ξ	[-]	1	0,98	0,88	0,71	0,52

This assumption is applied to the results from the performed models. In the sequent diagrams, see Figure 6.42 the unmodified results are shown together with the modified results taking into account both the projecting member ends by the increase of contact length A_{ef} and stress distribution by ξ.

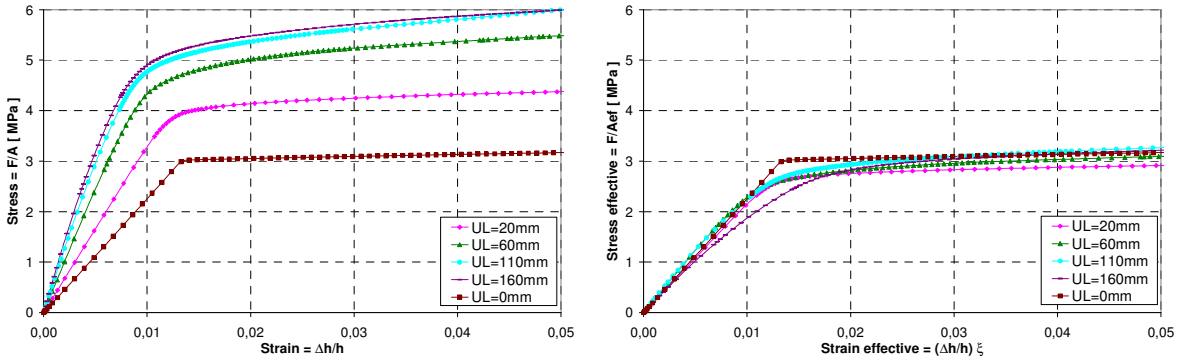

Figure 6.42 Stress-strain-relationships for models with stress yield = 3.0 MPa

In the transformation A_{ef} only influences the final capacity of the models whereas the factor ξ affects the stiffness of the models. In Figure 6.42 (right), the two assumptions proposed by the German code are well verified by the FE-models since the agreement is good. This behaviour is independent on the yield stress of the models.

- Comparison of FE-models to different codes regarding the characteristic capacity

In order to compare the results from the FE-models the relationship of the characteristic strength perpendicular to the grain $F_{c,90,k}$, calculated as a function of the unloaded length, is shown below, see Figure 6.43. The relationship regards the different yield stress equal to 3.0, 3.5, 4.0 MPa and the value is calculated according to UNI EN 408. The yield stress used in the evaluation of the codes is set to 2.7 MPa. Furthermore, the test performed by Reichegger, [11] is represented as dots in the sequent relationship.

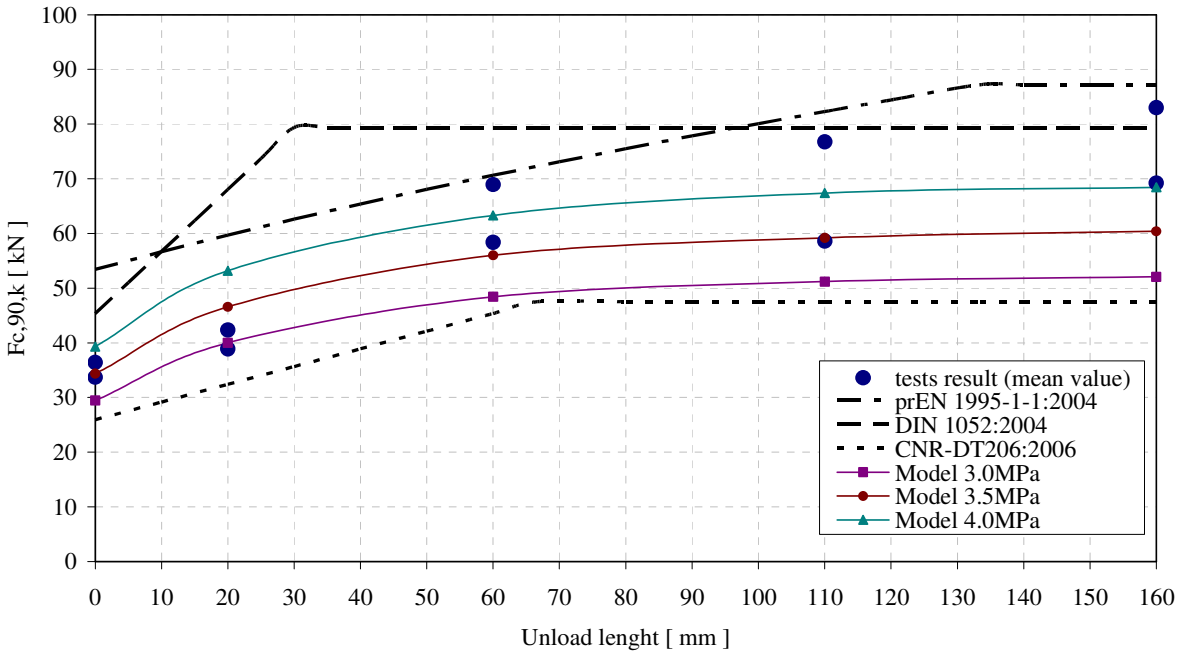

Figure 6.43 Comparison of $F_{c,90,k}$ between the FE-models and the different codes

In Figure 6.43 it can be noticed that the Italian code treats the effect of the unloaded length most conservatively. The evaluated codes and the FE-models all show an increase of capacity when the unloaded length is increased. When increasing the yield stress the $F_{c,90,k}$ - Unloaded length curves are simply parallel shifted in height without changing the shape.

Table 6.12 Capacities according to different codes and models with varying unloaded length

Specimen **class**	Load **surface**	Strength	Unloaded **length**	prEN 1995-1-1			DIN 1052:2004			CNR-DT 206:2006		Model 3MPa	Model 3.5MPa	Model 4MPa
		$f_{c,90,k}$	**a**	l_{ef}	$K_{c,90}$	$F_{c,90,k}$	l_{ef}	$K_{c,90}$	$F_{c,90,k}$	l_{ef}	$F_{c,90,k}$	$F_{c,90,k}$	$F_{c,90,k}$	$F_{c,90,k}$
GL24	[mm]	[MPa]	[mm]	[mm]	[-]	[kN]	[mm]	[-]	[kN]	[mm]	[kN]	KN	KN	KN
80x120x100	80x120	2,7	0	80	2.06	53.40	80	1.75	45.4	80.	25.9	29.4	34.4	39.3
120x120x200	80x120	2.7	20	100	2.30	59.70	120	1.75	68	120	38.9	40.0	46.6	53.2
200x120x200	80x120	2.7	60	140	2.73	70.64	140	1.75	79.4	146.7	47.5	48.4	56.0	63.3
300x120x200	80x120	2.7	110	190	3.17	82.29	140	1.75	79.4	146.7	47.5	51.2	59.2	67.4
400x120x200	80x120	2.7	160	213.3	3.36	87.19	140	1.75	79.4	146.7	47.5	52.1	60.4	68.4

7 Final remarks

7.1 Conclusions

The anchor improvement subjected to a compressive load of 230 kN result in the following conclusions:

- The reinforcement of compression perpendicular to the grain with the use of self-tapping screws increases the capacity of the anchor by 50 to 85% for screw diameter 10 mm and 12 mm, respectively.

- The reinforcement with the screws reduces the loss of pre-stressing force over time. This is due to, as expected, the distribution of the load deeper into the timber and therefore reducing the compressive load beneath the plate.

- The configuration with steel plate 200x200x15 and reinforced with four SPAX 300ϕ10/12 mm self-tapping screws fails to meet the requirements set by the serviceability limit state due to flexural yielding of the plate.

- The configuration with steel plate 200x200x20 mm and reinforcement with four SPAX 12x300 mm self-tapping screws considerably improve the overall performance compared to the current configuration (hardwood plate 200x200x45 mm).

The laboratory tests result in the following conclusions:

- The influence of knots is of such kind that they can change the failure mode from pushing failure to buckling failure of the screws.

- A brittle failure occurs when the screw is fractured due to excessive flexural yielding.

- It was observed that if the thickness of the plate allows bending due to yielding, the head of the screws follows the bended plate which induces bending of the screw (bended column) and reduces the critical buckling load. As an effect of this the failure mode could be changed from pushing in to buckling due to an imperfection of the screw shape.

The FE-models of the anchor result in the following conclusions:

- The configuration without reinforcement is a good predictor of the behaviour as the test has shown.

- The reinforced configurations present an improvement of the capacity compared to the un-reinforced configuration due to the load transfer effect of the screw.

- The effect of the screws in terms of displacement and stress fields enhances the understanding of the load transfer and the general structural behaviour of the specimens investigated.

Regarding the FE - models performed on the unloaded length effect:

- The unloaded length effect is taken into account
- The increase of the yield stress should be considered when increasing the unloaded length in the FE-model.
- No contribution of capacity when using an unloaded length more than 110 mm was shown.
- The FE-models performed have a good agreement with the assumptions made in the German code (DIN 1052:2004).

Regarding compression perpendicular to the grain according to different codes:

- The Swedish code (BKR:2003) uses a characteristic value of compression perpendicular to the grain, $f_{c,90,k}$, that is too high and should be reduced so that the effect of the unloaded length, $k_{c,90}$, could be considered which is a more realistic approach.
- The Eurocode 5 (prEN 1995-1-1:2004) allows use of a value of $k_{c,90}$ less than 1 and in the case of the whole length being loaded, a value that can be different from 1.
- The bending of the steel plate has to be prevented when using the model of Karlsruhe.
- The German code (DIN 1052:2004) used with the model of Karlsruhe is a good predictor of the capacity of the reinforced anchor if bending of the plate is prevented. The Italian code (CNR-DT206:2006) presents values that are conservative.
- Since the withdrawal capacity of the other codes evaluated is similar to the German code (DIN 1052:2004) and the buckling capacity is independent of the codes it is safe to say that the other codes are theoretically applicable with the model of Karlsruhe.
- The Swedish code (BKR:2003) and Eurocode 5 (prEN 1995-1-1:2004) generates a value of the capacity that is higher then the other codes investigated and should therefore be used with great care.

7.2 Limitations

Limitations that has been found during the process of investigation or been considered inevitable in order to proceed with the study are point wise displayed here.

Regarding the FE-model of reinforced anchor:

- Buckling of the screws is not modelled or considered in the FE-analysis
- The interaction between screws and timber is modelled with linear springs neglecting the effect of bond slip.
- The interaction between plate and timber is modelled with a simplified approach when the plate is yielding since it includes complex non-linear behaviour of the contact area.
- The presence and effect of the knots are non predictable in the FE-analysis

Regarding the analytical approach:

- The model of Karlsruhe does not consider the influence of plate bending and the change of load distribution due to this effect. This limitation is due to the assumption in the model that considers a uniform load distribution from a stiff plate.

Regarding the laboratory tests:

- The number of tests is a limiting factor since it does not result in statistically correct values.
- Non-symmetric loading

7.3 Future research

Topics that require further research and topics that could not be treated in this thesis due to their complexity or time consumption are discussed here.

- Non-linear buckling of the screws should be included in the FE-model in order to improve the model of Karlsruhe.
- In order to gain better knowledge of the interaction between the screws and timber pushing in tests of the screws are recommended so that the difference between withdrawal behaviour and pushing in behaviour can be investigated.
- All the different unloaded length configurations displayed in the codes should be studied using FE-models in order to improve the definition of $k_{c,90}$.
- Investigate how the buckling phenomenon behaves during the bond slip of the interaction between timber and the screw.
- The long-term behaviour needs to be investigated in a stress-laminated bridge deck with the reinforced anchor subjected to the actual change of climate for a long time period.

8 References

[1] Edlund, B. (1995), Tension and compression, Lecture B2 Timber Engineering, Step 1, STEP/Eurofortech, Centrum Hout, The Netherlands

[2] Blass, H. J.; Bejtka, I. (2004): Reinforcements perpendicular to the grain using self-tapping screws, Proceedings of the 8th World Conference on Timber Engineering, Volume I, Lahti, Finland 2004.

[3] Nilsson, K (2002): Skruvarmering som förstärkning i trä vid belastning vinkelrätt fiberriktningen – en försöksstudie, Examensarbete, Avdelningen för Konstruktionsteknik, Lunds Tekniska Högskola, Rapport TVBK- 5112, Lund 2002

[4] Piazza M., Tomasi R., Modena R. (2005): Strutture in legno – Materiale, calcolo e progetto secondo le nuove normative europee, HOEPLI, Milano, Italy

[5] Blass, H.J.; Ehlbeck, J.; Kreuzinger, H.; Steck, G. (2004): Entwurf, Berechnung und Bemessung von Holzbauwerken, Allgemeine Bemessungsregeln und Bemessungsregeln für den Hochbau, Version vom 20.07.2004, Gefördet durch die DGfH Innovations- und Service GmbH aus Mitteln der Holzabsatzfonds.

[6] BKR:2003 (2003), Design regulations BKR. Boverket, BFS 1998:39

[7] prEN-1-1:2004, Eurocode 5: Design of timber structures. Part 1-1: General- Common rules and rules of buildings, CEN, European Committee for Standardisation

[8] Bejtka, I. (2005):Verstärkung von Bauteilen aus Holz mit Vollgewindeschrauben, Ph.D. Thesis. Fakultät für Bauingenieur-, Geo- und Umweltwissenschaften, der Universität Fridericiana zu Karlsruhe (TH), Karlsruhe, Germany, 2005.

[9] CNR-DT 206 (2006), Istruzioni per il Progetto, l´Esecuzione e il Collaudo delle Strutture di legno, Consiglio Nazionale delle Ricerche, Roma, Italy

[10] Persson, K. (2000): Micromechanical modelling of wood and fibre properties. Ph.D. Thesis. Department of Mechanics and Materials, Structural Mechanics, Lund University, ISRN LUTVDG/TVSM—00/1013—SE (1-223), Lund Sweden

[11] Reichegger, M. (2004): Compressione ortogonale alle fibre negli elementi strutturali lignei secondo le nuove proposte di normative. Analisi e sperimentazione su differenti sistemi di rinforzo. Tesi di laurea discussa presso l´Universitá degli Studi di Trento, Trento Italy

[12] Michael A. Ritter; Paula D. Hilbrich Lee (1996): Recommended Construction Practices for Stress-Laminated Wood Bridge Decks, International Wood Engineering Conference ´96, USA.

[13] Bygg, Handbok för hus-, väg- och vattenbyggnad, Allmänna grunder Huvuddel 1A (1971), AB Byggmästarens förlag, Stockholm 1971, Sverige

[14] Ritter. M.A. (1990): Timber bridges: design, construction, inspection and maintenance, USDA Forest Service, Washington DC, 1990, USA

[15] Blass, H. J.; Goerlacher, R. (2004): Compression perpendicular to the grain, Proceedings of the 8th World Conference on Timber Engineering, Volume II, Lahti, Finland 2004.

Electronic sources:

[16] http://www.mackblackwell.org/OLD/research/finals/arc1057/framereport1057.html

APPENDIX A: Verification of a beam support in compression perpendicular to the grain - comparison with different codes

In this example the verification at the ultimate limit state of a simple supported beam in compression perpendicular to the grain at support is shown. The calculations are made according to different codes. The chosen class of glue-laminated timber is the GL32 according to UNI EN 1194:2000 and L40 according to BKR:2003, the service class chosen is 2 and regarding the load the short term duration is considered (less than a week).

- **Geometric characteristics of the support**

Length of the beam $l = 24\,m$

Depth of the beam $h = 1807\,mm$

Width of the beam $b = 220\,mm$

Length of support $l_{sup} = 300\,mm$

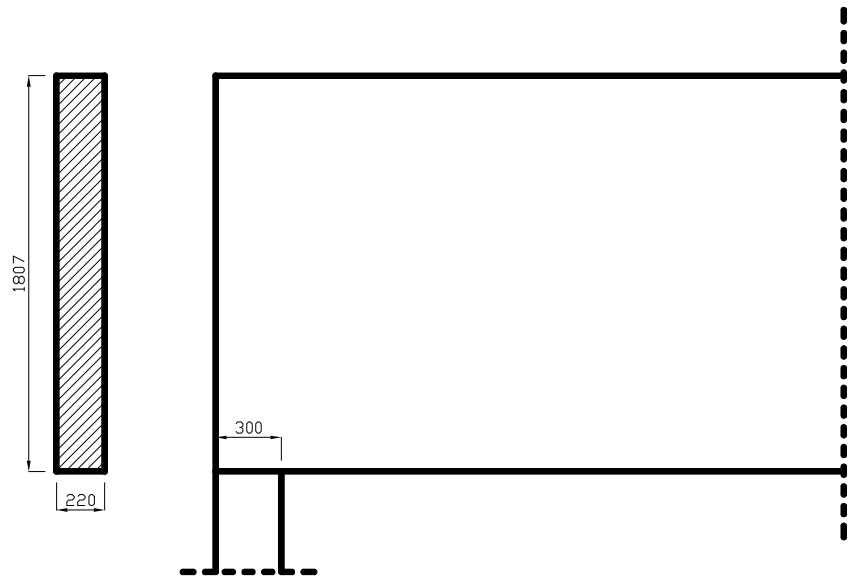

Figure A.1 Geometry of the beam support

- **Design value of strength in compression perpendicular to the grain**

According to Eurocode 5 prEN 1995-1-1:2004, German code DIN 1052:2004, Italian code CNR-DT 206:2006 the design value for $f_{c,90,d}$ of compressive strength perpendicular to the grain is calculated as:

$$f_{c,90,d} = \frac{k_{\mathrm{mod}}\, f_{c,90,k}}{\gamma_M}$$

where:

$f_{c,90,k}$ is the characteristic value of strength in compression perpendicular to the grain

γ_M is the partial factor for the material property

k_{mod} is the modification factor taking into account the effect of the duration of load and moisture content

According to Swedish code BKR:2003 the design value for $f_{c,90,d}$ of compressive strength perpendicular to the grain is calculated as:

$$f_{c,90,d} = \frac{k_r\, f_{c,90,k}}{\gamma_m\, \gamma_n}$$

where:

γ_m is the partial factor which takes account of the uncertainty in determining resistance, for timber equal to 1.15

γ_n is the partial factor which takes into account the safety class in ultimate limit state, in this example assumed safety class 3

k_r is the equivalent of the modification factor k_{mod} of Eurocode 5.

In the sequent table, see Table A.1, follows the calculation of design strength values in compression perpendicular to the grain according to different codes:

Table A.1 Calculation of design strength in compression perpendicular to the grain according to different codes

	prEN 1995-1-1:2004 GL32	DIN 1052:2004 GL32	CNR-DT 206:2006 GL32		BKR:2003 L40
$f_{c,90,k}$	3.3 MPa	3.3 MPa	3.3 MPa	$f_{c,90,k}$	8.0 MPa
γ_M	1.25	1.3	1.25	γ_m γ_n	1.25 – 1.2
k_{mod}	0.90	0.90	0.90	k_r	0.85
$f_{c,90,d}$	2.38 MPa	2.28 MPa	2.38 MPa	$f_{c,90,d}$	4.53 MPa

- **Design value of reaction force**

The ultimate limit state is considered:

Distributed design load $q_d = 27\,kN/m$

Design reaction force $R_d = \frac{q_d \cdot l}{2} = \frac{27 \times 24}{2} = 324.0\,kN$

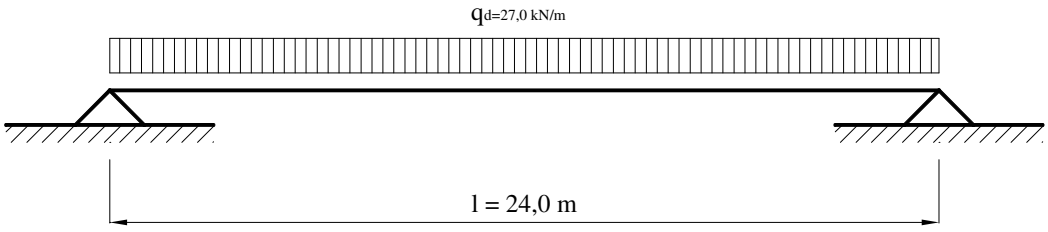

Figure A.2 Simply supported beam

- **Verification at beam support according to Eurocode 5 (prEN 1995-1-1:2004)**

The contact area is equal to:

$$A = b \cdot l_{\sup} = 220 \times 300 = 66000 mm^2$$

The value of the design compressive stress in the contact area perpendicular to the grain is equal to:

$$\sigma_{c,90,d} = \frac{R_d}{A} = \frac{324000}{220 \times 300} \cong 4.91 MPa$$

The factor $k_{c,90}$ taking into account the unload length effect is equal to:

$$k_{c,90} = \left(2.38 - \frac{l_{\sup}}{250}\right)\left(1 + \frac{h}{12 l_{\sup}}\right) = \left(2.38 - \frac{300}{250}\right)\left(1 + \frac{1807}{12 \times 300}\right) \cong 1.77$$

Resulting in the following verification formula:

$$\sigma_{c,90,d} \cong 4.91 MPa \leq k_{c,90} \cdot f_{c,90,d} \cong 1.77 \times 2{,}38 \cong 4.21 MPa$$ Not satisfied

- **Verification at beam support according to German code (DIN 1052:2004)**

The effective area is equal to:

$$A_{ef} = b\, l_{ef} = 220 \times 330 = 72600 mm^2,$$

Where

$$l_{ef} = l_{\sup} + 30\, mm = 330\, mm$$

The value of the design compressive stress in the contact area perpendicular to the grain is equal to:

$$\sigma_{c,90,d} = \frac{F_{c,90,d}}{A_{ef}} = \frac{324000}{220 \times 330} \cong 4.46\, MPa$$

The factor $k_{c,90}$ taking into account the unload length effect is equal to:

$$k_{c,90} = 1.75$$

In fact l =300 mm < 400 mm.

Resulting in the following verification formula:

$$\frac{\sigma_{c,90,d}}{k_{c,90} \cdot f_{c,90,d}} = \frac{4.46}{1.75 \times 2.28} \cong 1.13 > 1 \quad \text{Not satisfied}$$

- **Verification at beam support according to Italian code (CNR-DT 206:2006)**

The effective length is equal to:

$$l_{ef} = \min\left\{l_{\sup} + h/3\,;\, 2\,l_{\sup}\right\} = \min\left\{300 + 1807/3\,;\, 2 \times 300\right\} = \min\left\{902.3\, mm;\, 600\, mm\right\} = 600\, mm$$

The value of the design compressive stress in the contact area perpendicular to the grain is equal to:

$$\sigma_{C,90,d} = \frac{F_{90,d}}{b \cdot l_{ef}} = \frac{324000}{220 \times 600} \cong 2.45\, MPa$$

Resulting in the following verification formula:

$\sigma_{C,90,d} \cong 2.45\ MPa \leq f_{C,90,d} = 2.38\ MPa$ Not satisfied

- **Verification at beam support according to Swedish code (BKR:2003)**

The verification procedure is the same for EC5, only the design value of compressive strength change and the factor $k_{c,90}$ is taken equal to 1, so follow the verification formula.

$\sigma_{c,90,d} \cong 4.91 MPa \leq k_{c,90} \cdot f_{c,90,d} \cong 1 \times 4.53 \cong 4.53 MPa$ Not satisfied

It is possible to see that verifications are not satisfied in any case. If it is not possible to increase the length of the support l_s, it is necessary to reinforce the support for example by using self-tapping full-treaded screws. In the following paragraph a calculation is proposed.

APPENDIX B: Verification of reinforcement perpendicular to the grain using self-tapping screw

In order to increase the strength of a beam support in compression perpendicular to the grain it is possible to reinforce the support by using self-tapping screw drilled into the timber perpendicular to the grain. In this example such a procedure is proposed in order to verify the reinforcement chosen according to model of Karlsruhe and the German code DIN 1052:2004. This example refers to the case treated before.

- Reinforcement characteristic

Four self-tapping full-treaded screws ϕ 10 mm, length l_s = 400 mm, and characteristic yield strength of the steel equal to $f_{y,k}$ = 1000 MPa.

- Verification of the geometry

- Longitudinal direction:

Distances between two screws and between screw and border, see Figure B.1:

$$a_1 = a_{1c} = 100\ mm > (5 \cdot \phi) = 60\ mm$$

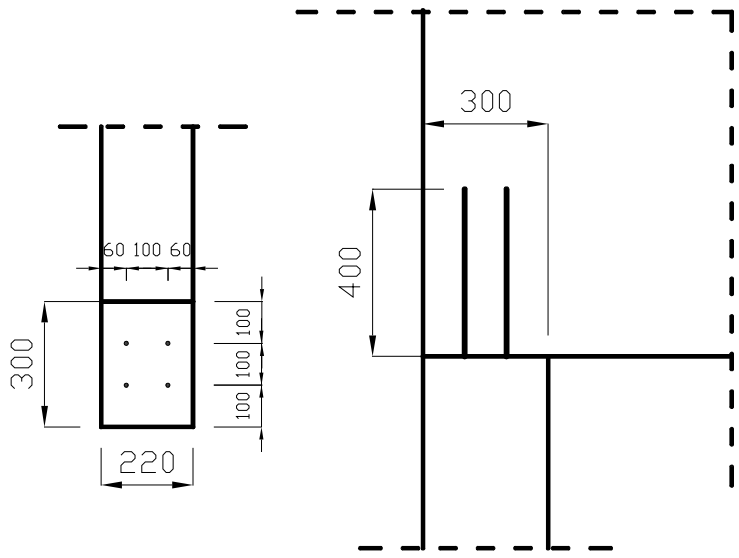

Figure B.1 Geometry of the reinforcement with self-tapping screws

- Transversal direction

Distances between two screws:

$a_2 = 100\ mm > (5 \cdot \phi) = 60\ mm$

Dimension from border:

$a_2 = 60\ mm > (4 \cdot \phi) = 48\ mm$

- Verification of the load carrying capacity of the reinforced support

The following equations must be satisfied:

$$F_{c,90,d} \le \min\begin{Bmatrix} n \cdot R_d + k_{c,90} \cdot A_{ef,1} \cdot f_{c,90,d} \\ k_{c,90} \cdot A_{ef,2} \cdot f_{c,90,d} \end{Bmatrix}$$

Where:

$F_{c,90,d} = 324\ kN$

$n = 4$

$k_{c,90} = 1.75$

$l_{ef,1} = l_{\sup} + 30\ mm = 300 + 30 = 330\ mm$

$l_{ef,2} = l_{ef,1} + l_s = 330 + 400 = 730\ mm$

The capacity of the screw is equal to:

$$R_d = \min\left(R_{ax,d}; R_{c,d}\right)$$

where $R_{ax,d}$ and $R_{c,d}$ represent the pushing in and the buckling capacity of the screw.

The pushing in capacity of the screw is equal to:

$$R_{ax,d} = f_{1,d} \cdot d \cdot l_s = 10.24 \times 12 \times 400 \cong 49.15\ kN$$

Where, $f_{1,d} = 80 \cdot 10^{-6} \cdot \rho_k^2 \cdot k_{\mathrm{mod}} / \gamma_m = 10.24\ MPa$ according to DIN 1052:2004.

The buckling capacity of the screw is equal to:

$$R_{c,d} = k_c \cdot N_{pl,d} = 0.65 \times 50.38 \cong 32.54\ kN$$

Where

$$N_{pl,d} = \frac{(0.7 \cdot d)^2}{4} \cdot \pi \cdot \frac{1000}{1.1} \cong 50.38\ kN$$

$$k_c = \frac{1}{k + \sqrt{k^2 - \overline{\lambda}_k^2}} = \frac{1}{0.99 + \sqrt{0.99^2 - 0.83^2}} \cong 0.65$$

Where λ_k is the relative slenderness of the screw in the timber for the case in compression perpendicular to the grain that can be calculated as follows:

$$\overline{\lambda}_k = \sqrt{\frac{N_{pl,k}}{N_{crit,G/E,k}}} = \sqrt{\frac{55.42}{83.23}} \cong 0.82$$

Where the critical buckling load is calculated with the following approximated formula:

$$N_{crit,G/E,k} = \sqrt{0.32 \cdot \rho_k \cdot E \cdot J} = \sqrt{0.32 \times 430 \times 206000 \times 244.39} \cong 83.23\ kN$$

While the value of k can be calculate as follow:

$$k = 0{,}5 \cdot \left[1 + 0.49 \cdot \left(\overline{\lambda}_k - 0.2\right) + \overline{\lambda}_k^2\right] = 0.5 \times \left[1 + 0.49\left(0.82 - 0.2\right) + 0.82^2\right] \cong 0.99$$

Resulting in a capacity of the screw equal to $R_d = \min\left(R_{ax,d}; R_{c,d}\right) = 32.54\ kN$ and the verification can be applied as follow:

$$F_{c,90,d} = 324.00\ kN \le \min\left\{\begin{array}{c} 4 \times 32.54 + 1.75 \times \left(220 \times 330\right) \times 2.28 \times 10^{-3} \cong 419.83\ kN \\ 1.75 \times \left(220 \times 730\right) \times 2.28 \times 10^{-3} \cong 640.79\ kN \end{array}\right\} = 419.83\ kN$$

Both the verifications are satisfied.

APPENDIX C: Calculation of the buckling load for a beam on a elastically embedded support

In this example the buckling load for a screw in inside the timber is calculated. Different approximations are considered in order to compare the behaviour. The elastic solution is considered. The geometry and material property of the screw and timber are as follows:

Length of the screw = 300mm

Diameter of the screw = 10 (also the case d = 12 mm, the result is reported in the end)

Density of the timber = 450 kg/m^3

Coefficient of stiffness of the elastic foundation:

$$C = c_h = \frac{(0.22 + 0.014 \cdot d) \cdot \rho}{1.17 \cdot \sin^2 \alpha + \cos^2 \alpha} = \frac{(0.22 + 0.014 \times 10) \cdot 450}{1.17 \times \sin^2 (90) + \cos^2 (90)} = 138.5 \; N/mm^2$$

Moment of inertia of the inner core of the screw

$$J = \frac{\pi}{64} \cdot (0.7 \cdot d)^4 = \frac{\pi}{64} \times (0.7 \times 10)^4 = 117.9 \; mm^2$$

Modulus of elasticity of the screw

$$E = 210000 \; N/mm^2$$

- Buckling load of a beams supported on 7 springs according to BYGG Huvuddel 1A, Allmänna grunder, 1971, [13]

To calculate the buckling load the case shown in figure where the number of spring is equal to 7 is considered. In this case there is no support in the end of the beam so μ is taken equal to 1.

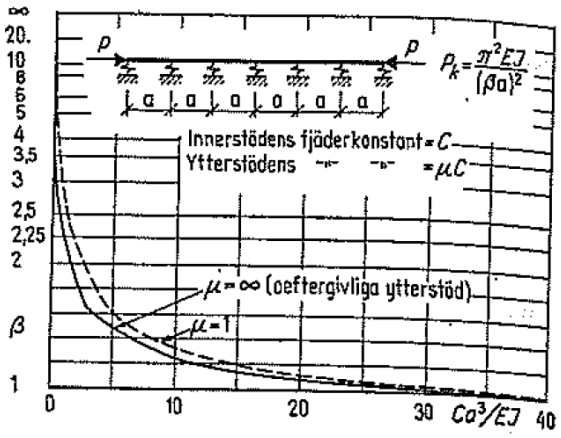

Figure C.1 Relationship regarding the buckling load calculation of a beam supported on 7 springs, [13]

The sequent non-dimensional coefficient is calculated in order to get the coefficient β from the relationship:

$$\frac{C \cdot a^3}{E \cdot J} = \frac{138.5 \times 50^3}{210000 \times 117.9} = 6.995 \xrightarrow{graph} \beta = 1.5$$

Where the buckling load is calculated as:

$$P_k = \frac{\pi^2 \cdot E \cdot J}{(\beta \cdot a)^2} = \frac{\pi^2 \times 210000 \times 117{,}9}{(1.5 \times 50)^2} = 43.4\ kN$$

For the case with d=12 mm the buckling load is equal to 62.5 kN

- Buckling load for elasticity bedded beams without support

To calculate the buckling load the case of elastically bedded beam without support is considered in the following calculation:

$$N_{ki} = \sqrt{c_h \cdot E \cdot J} = \sqrt{138.5 \times 210000 \times 117.9} = 58.6\ kN$$

For the case with d=12 mm the buckling load is equal to 87.5 kN.

APPENDIX D: Calculation of the spring stiffness in different directions and syntax for ABAQUS

The spring stiffness is calculated according to the formulation given by Bejtka, [8]

Where the vertical spring stiffness is equal to:

$$c_V \cdot \Delta l_S = 234 \cdot \frac{(\rho \cdot d)^{0,2}}{l_s} \cdot \Delta l_S \cdot 1000 \quad in \quad \frac{N}{m}$$

and the horizontal spring stiffness is equal to:

$$c_H \cdot d = \frac{(0.22 + 0.014 \cdot d) \cdot \rho}{1.17 \cdot \sin^2 \alpha + \cos^2 \alpha} \cdot d \cdot 1000 \quad in \quad \frac{N}{m}$$

$\rho = 450\ kg/m^3$ is the density of the timber

$d = 10\ mm, 12\ mm$ is the diameter of the screw

$l_S = 300\ mm$ is the length of the screw

$\Delta l_S = 30\ mm$ is the gap between the springs

α is the angle between the force and the direction of the grain

Since there are two horizontal directions, two different α values are used:

$\alpha = 0°$ represents the case when the force is parallel to the grain

$\alpha = 90°$ represents the case when the force is perpendicular to the grain

In the vertical direction (3-direction in the FE model) the spring stiffness is then:

$$c_V \cdot \Delta l_S = 234 \cdot \frac{(450 \cdot 10)^{0,2}}{300} \cdot 30 \cdot 1000 = 1.232 \cdot 10^6 \quad \frac{N}{m} \qquad \text{for } d = 10\ mm$$

$$c_V \cdot \Delta l_S = 234 \cdot \frac{(450 \cdot 12)^{0,2}}{300} \cdot 30 \cdot 1000 = 1.278 \cdot 10^6 \quad \frac{N}{m} \qquad \text{for } d = 12\ mm$$

In the parallel direction to the grain (1-direction in the FE model) the spring stiffness is then:

$$c_H \cdot d = \frac{(0.22 + 0.014 \cdot 10) \cdot 450}{1} \cdot 10 \cdot 1000 = 1.62 \cdot 10^6 \quad \frac{N}{m} \qquad \text{for } d = 10\ mm$$

$$c_H \cdot d = \frac{(0.22 + 0.014 \cdot 12) \cdot 450}{1} \cdot 12 \cdot 1000 = 1.944 \cdot 10^6 \quad \frac{N}{m} \qquad \text{for } d = 12\ mm$$

In the perpendicular direction to the grain (2-direction in the FE model) the spring stiffness is then:

$$c_H \cdot d = \frac{(0.22 + 0.014 \cdot 10) \cdot 450}{1.17} \cdot 10 \cdot 1000 = 1.385 \cdot 10^6 \quad \frac{N}{m} \qquad \text{for } d = 10\ mm$$

$$c_H \cdot d = \frac{(0.22 + 0.014 \cdot 12) \cdot 450}{1.17} \cdot 12 \cdot 1000 = 1.791 \cdot 10^6 \quad \frac{N}{m} \qquad \text{for } d = 12\ mm$$

- Syntax when defining springs and spring stiffness in ABAQUS input file, in this example vertical springs for one screw with d = 10 mm were used:

*Element, type=Spring2, elset=Springs-1-spring

5, Screw300-d10-1.1, Timber-1.10

6, Screw300-d10-1.2, Timber-1.296

7, Screw300-d10-1.3, Timber-1.582

8, Screw300-d10-1.4, Timber-1.868

9, Screw300-d10-1.5, Timber-1.1154

10, Screw300-d10-1.6, Timber-1.1440

11, Screw300-d10-1.7, Timber-1.1726

12, Screw300-d10-1.8, Timber-1.2012

13, Screw300-d10-1.9, Timber-1.2298

14, Screw300-d10-1.10, Timber-1.2584

15, Screw300-d10-1.11, Timber-1.2870

*Spring, elset=Springs-1-spring

3, 3

1.232e6

APPENDIX E: Design calculations of the test specimens

In this appendix some calculations regarding the design of the members needed in the tests are presented.

Design load and material parameters

$F_{,\max}$ = 300 kN is the maximum load applied

$f_{yd,bar}$ = 900 MPa is the design yield strength of the Dywidag bar

$f_{yd,plate}$ = 287.9 MPa is the design yield strength of the steel in the plate and washer

Minimum diameter of the Dywidag bar:

$$d_b = \sqrt{4 \cdot \frac{F_{,\max}}{\pi \cdot f_{yd,bar}}} = \sqrt{4 \cdot \frac{300 \cdot 10^3 \ N}{900 \ N/mm^2}} = 21 \ mm$$

Area of the hole in the timber:

d = 30 mm is the diameter of the hole in the timber

$$A_{hole} = d^2 \cdot \frac{\pi}{4} = (30 \ mm)^2 \cdot \frac{\pi}{4} = 7.069 \cdot 10^{-4} \ m^2$$

Steel washer (circular):

Assumed that the nut is not applying the load, the load is applied as a point load at the centre.

d_W = 100 mm is the diameter of the washer

$A_W = {d_W}^2 \cdot \frac{\pi}{4} = (100 \ mm)^2 \cdot \frac{\pi}{4} = 7.854 \cdot 10^{-3} \ m^2$ is the area of the washer without hole

d_h = 28 mm

$A_{hole,Washer} = {d_h}^2 \cdot \frac{\pi}{4} = (28 \ mm)^2 \cdot \frac{\pi}{4} = 5.983 \cdot 10^{-4} \ m^2$ is the area of the hole in the washer

Net area of the washer:

$$A_{net} = A_W - A_{hole,Washer} = 7.854 \cdot 10^{-3} \ m^2 - 5.983 \cdot 10^{-4} \ m^2 = 7.256 \cdot 10^{-3} \ m^2$$

Thickness of the washer:

$\sigma_W = \frac{F_{\max}}{A_{net}} = \frac{300 \cdot 10^3 \ N}{7.256 \cdot 10^{-3} \ m^2} = 4.35 \ MPa$ is the compressive stress on the washer

$$x = \frac{d_W - d}{2} = \frac{100\ mm - 30\ mm}{2} = 35\ mm$$ is the distance to the edge

Minimum thickness of the washer in order not to yield:

$$t_W = \sqrt{6 \cdot \sigma_W \cdot \frac{x^2}{2 \cdot f_{yd,plate}}} = \sqrt{6 \cdot 4.35\ MPa \cdot \frac{(35\ mm)^2}{2 \cdot 287.9\ MPa}} = 23\ mm$$

Steel plate (rectangular):

$b_S = 200$ mm is the width of the plate

$l_S = 200$ mm is the length of the plate

$$A_{hole,Plate} = A_{hole,Washer} = 5.983 \cdot 10^{-4}\ m^2$$

$$A_{net} = b_S \cdot l_S - A_{hole,Plate} = 0.2 \cdot 0.2\ m^2 - 5.983 \cdot 10^{-4}\ m^2 = 0.039\ m^2$$

$$\sigma_P = \frac{F_{\max}}{A_{net}} = \frac{300 \cdot 10^3\ N}{0.039\ m^2} = 7.614\ MPa$$ is the compressive stress on the plate

Edge distances:

$$x_p = \frac{b_S - d_W}{2} = \frac{200\ mm - 100\ mm}{2} = 50\ mm$$

$$y_P = \frac{l_S - d_W}{2} = \frac{200\ mm - 100\ mm}{2} = 50\ mm$$

Plate thickness:

$$t_X = \sqrt{6 \cdot \sigma_P \cdot \frac{x_p^{\ 2}}{2 \cdot f_{yd,plate}}} = \sqrt{6 \cdot 7.614\ MPa \cdot \frac{(50\ mm)^2}{2 \cdot 287.9\ MPa}} = 14\ mm$$

$$t_Y = \sqrt{6 \cdot \sigma_P \cdot \frac{y_p^{\ 2}}{2 \cdot f_{yd,plate}}} = \sqrt{6 \cdot 7.614\ MPa \cdot \frac{(50\ mm)^2}{2 \cdot 287.9\ MPa}} = 14\ mm$$

The washer needs to be at least 23 mm thick and the plates needs to be at least 14 mm in order to not bend when loading at 300 kN.

APPENDIX F: Design buckling load for screw according to model of Karlsruhe

In the sequent tables are shown the value of coefficient needed to valuate the buckling load capacity of the screw for different length, nominal diameter and bending stiffness at the top of the screw (K = 0 or K = ∞), according to model proposed by University of Karlsruhe.

$$N_{pl,k} = \pi \cdot \frac{(0.7 \cdot d)^2}{4} \cdot f_{y,k} \text{ for the screws } f_{y,k} = 640\,N/mm^2$$

	ρk = 310 kg/m³					ρk = 380 kg/m³					ρk = 410 kg/m³					ρk = 450 kg/m³				
	Diameters in [mm]					Diameters in [mm]					Diameters in [mm]					Diameters in [mm]				
$N_{pl,k}$ [kN]	**4**	**6**	**8**	**10**	**12**	**4**	**6**	**8**	**10**	**12**	**4**	**6**	**8**	**10**	**12**	**4**	**6**	**8**	**10**	**12**
K = 0	3,94	8,87	15,76	24,63	35,47	3,94	8,87	15,76	24,63	35,47	3,94	8,87	15,76	24,63	35,47	3,94	8,87	15,76	24,63	35,47

K = ∞

$$\overline{\lambda_k} = \sqrt{\frac{N_{pl,k}}{N_{ki,k}}}$$

$\overline{\lambda_k}$ (K = 0)		ρk = 310 kg/m³					ρk = 380 kg/m³					ρk = 410 kg/m³					ρk = 450 kg/m³				
		Diameters in [mm]					Diameters in [mm]					Diameters in [mm]					Diameters in [mm]				
		4	**6**	**8**	**10**	**12**	**4**	**6**	**8**	**10**	**12**	**4**	**6**	**8**	**10**	**12**	**4**	**6**	**8**	**10**	**12**
Screwslength lS in [mm]	**20**	0,99	1,40	1,78	2,14	2,47	0,90	1,27	1,61	1,93	2,24	0,87	1,22	1,55	1,86	2,15	0,83	1,17	1,48	1,78	2,05
	40	0,72	0,84	1,04	1,24	1,43	0,69	0,77	0,95	1,12	1,30	0,67	0,74	0,91	1,08	1,25	0,66	0,72	0,87	1,03	1,19
	60	0,73	0,74	0,81	0,93	1,07	0,69	0,69	0,74	0,85	0,96	0,68	0,68	0,72	0,82	0,93	0,66	0,66	0,69	0,78	0,89
	80	0,73	0,73	0,74	0,79	0,88	0,69	0,69	0,70	0,73	0,81	0,68	0,68	0,68	0,71	0,78	0,66	0,66	0,67	0,69	0,75
	100	0,74	0,73	0,74	0,75	0,79	0,70	0,69	0,70	0,70	0,73	0,69	0,68	0,68	0,69	0,71	0,67	0,66	0,66	0,67	0,69
	120	0,74	0,73	0,73	0,74	0,75	0,70	0,69	0,69	0,70	0,71	0,69	0,68	0,68	0,68	0,69	0,67	0,66	0,66	0,66	0,67
	140	0,74	0,73	0,73	0,73	0,74	0,70	0,69	0,69	0,69	0,70	0,69	0,68	0,67	0,68	0,68	0,67	0,66	0,66	0,66	0,67
	160	0,74	0,73	0,73	0,73	0,74	0,70	0,69	0,69	0,69	0,69	0,69	0,68	0,67	0,67	0,68	0,67	0,66	0,66	0,66	0,66
	180	0,74	0,73	0,73	0,73	0,73	0,70	0,69	0,69	0,69	0,69	0,69	0,68	0,67	0,67	0,67	0,67	0,66	0,66	0,65	0,65
	200	0,74	0,73	0,73	0,72	0,73	0,70	0,69	0,69	0,68	0,68	0,69	0,68	0,67	0,67	0,67	0,67	0,66	0,66	0,65	0,65
	220	0,74	0,73	0,73	0,72	0,72	0,70	0,69	0,69	0,68	0,68	0,69	0,68	0,67	0,67	0,67	0,67	0,66	0,66	0,65	0,65
	>240	0,74	0,73	0,73	0,72	0,72	0,70	0,69	0,69	0,68	0,68	0,69	0,68	0,67	0,67	0,67	0,67	0,66	0,66	0,65	0,65

$\overline{\lambda_k}$ (K = ∞)		ρk = 310 kg/m³					ρk = 380 kg/m³					ρk = 410 kg/m³					ρk = 450 kg/m³				
		Diameters in [mm]					Diameters in [mm]					Diameters in [mm]					Diameters in [mm]				
		4	6	8	10	12	4	6	8	10	12	4	6	8	10	12	4	6	8	10	12
Screwslength lS in [mm]	20	0,54	0,72	0,92	1,11	1,28	0,52	0,65	0,84	1,00	1,16	0,51	0,63	0,80	0,96	1,11	0,50	0,60	0,77	0,92	1,06
	40	0,49	0,60	0,66	0,79	0,92	0,45	0,56	0,60	0,72	0,83	0,44	0,55	0,57	0,69	0,80	0,43	0,53	0,56	0,66	0,76
	60	0,48	0,53	0,62	0,66	0,75	0,45	0,48	0,57	0,62	0,68	0,44	0,47	0,55	0,60	0,65	0,43	0,45	0,53	0,58	0,62
	80	0,48	0,49	0,55	0,63	0,68	0,45	0,46	0,51	0,58	0,63	0,45	0,45	0,49	0,56	0,61	0,44	0,44	0,47	0,54	0,59
	100	0,50	0,49	0,51	0,58	0,64	0,48	0,46	0,48	0,53	0,59	0,47	0,45	0,47	0,51	0,57	0,46	0,44	0,45	0,49	0,55
	120	0,50	0,50	0,50	0,53	0,60	0,48	0,47	0,47	0,49	0,54	0,47	0,46	0,46	0,48	0,52	0,46	0,45	0,45	0,46	0,50
	140	0,50	0,50	0,50	0,52	0,56	0,48	0,47	0,47	0,48	0,51	0,47	0,46	0,46	0,47	0,49	0,46	0,45	0,44	0,46	0,48
	160	0,50	0,50	0,49	0,51	0,53	0,48	0,47	0,46	0,48	0,49	0,47	0,46	0,45	0,46	0,48	0,46	0,45	0,44	0,45	0,47
	180	0,50	0,50	0,49	0,50	0,52	0,48	0,47	0,46	0,47	0,49	0,47	0,46	0,45	0,46	0,48	0,46	0,45	0,44	0,45	0,46
	200	0,50	0,50	0,49	0,50	0,51	0,48	0,47	0,46	0,47	0,48	0,47	0,46	0,45	0,46	0,47	0,46	0,45	0,44	0,45	0,45
	220	0,50	0,50	0,49	0,50	0,51	0,48	0,47	0,46	0,47	0,48	0,47	0,46	0,45	0,46	0,46	0,46	0,45	0,44	0,45	0,45
	>240	0,50	0,50	0,49	0,50	0,50	0,48	0,47	0,46	0,47	0,47	0,47	0,46	0,45	0,46	0,46	0,46	0,45	0,44	0,45	0,45

$$k = 0.5 \cdot \left[1 + 0.49 \cdot \left(\overline{\lambda_k} - 0.2\right) + \overline{\lambda^2{}_k}\right]$$

κ (K = 0)		ρk = 310 kg/m³					ρk = 380 kg/m³					ρk = 410 kg/m³					ρk = 450 kg/m³				
		Diameters in [mm]					Diameters in [mm]					Diameters in [mm]					Diameters in [mm]				
		4	6	8	10	12	4	6	8	10	12	4	6	8	10	12	4	6	8	10	12
Screwslength l_S in [mm]	20	1,19	1,78	2,48	3,27	4,12	1,08	1,56	2,15	2,80	3,50	1,04	1,50	2,04	2,64	3,29	1,00	1,42	1,91	2,47	3,07
	40	0,89	1,01	1,25	1,53	1,83	0,85	0,94	1,13	1,36	1,61	0,84	0,91	1,09	1,30	1,53	0,83	0,88	1,05	1,24	1,45
	60	0,89	0,90	0,97	1,11	1,28	0,86	0,86	0,91	1,02	1,15	0,84	0,85	0,89	0,99	1,11	0,83	0,83	0,86	0,95	1,06
	80	0,90	0,90	0,91	0,96	1,06	0,86	0,86	0,87	0,90	0,97	0,85	0,85	0,85	0,88	0,94	0,83	0,83	0,84	0,86	0,91
	100	0,90	0,90	0,90	0,92	0,96	0,87	0,86	0,86	0,87	0,90	0,85	0,85	0,85	0,86	0,88	0,84	0,83	0,83	0,84	0,85
	120	0,90	0,89	0,90	0,91	0,92	0,87	0,86	0,86	0,87	0,87	0,85	0,85	0,85	0,85	0,86	0,84	0,83	0,83	0,83	0,84
	140	0,90	0,89	0,89	0,90	0,91	0,87	0,86	0,86	0,86	0,87	0,85	0,85	0,84	0,85	0,85	0,84	0,83	0,83	0,83	0,84
	160	0,90	0,89	0,89	0,89	0,90	0,87	0,86	0,86	0,86	0,86	0,85	0,85	0,84	0,84	0,85	0,84	0,83	0,83	0,83	0,83
	180	0,90	0,89	0,89	0,89	0,90	0,87	0,86	0,86	0,85	0,86	0,85	0,85	0,84	0,84	0,84	0,84	0,83	0,83	0,83	0,83
	200	0,90	0,89	0,89	0,89	0,89	0,87	0,86	0,86	0,85	0,85	0,85	0,85	0,84	0,84	0,84	0,84	0,83	0,83	0,82	0,82
	220	0,90	0,89	0,89	0,89	0,89	0,87	0,86	0,86	0,85	0,85	0,85	0,85	0,84	0,84	0,84	0,84	0,83	0,83	0,82	0,82
	>240	0,90	0,89	0,89	0,89	0,89	0,87	0,86	0,86	0,85	0,85	0,85	0,85	0,84	0,84	0,84	0,84	0,83	0,83	0,82	0,82

κ (K = ∞)		ρk = 310 kg/m³					ρk = 380 kg/m³					ρk = 410 kg/m³					ρk = 450 kg/m³				
		Diameters in [mm]					Diameters in [mm]					Diameters in [mm]					Diameters in [mm]				
		4	6	8	10	12	4	6	8	10	12	4	6	8	10	12	4	6	8	10	12
Screwslength l_S in [mm]	20	0,73	0,89	1,10	1,34	1,59	0,71	0,83	1,00	1,20	1,40	0,71	0,80	0,97	1,15	1,34	0,70	0,78	0,93	1,10	1,28
	40	0,69	0,78	0,83	0,96	1,10	0,67	0,75	0,78	0,88	1,00	0,66	0,73	0,76	0,86	0,96	0,65	0,72	0,74	0,83	0,93
	60	0,68	0,72	0,79	0,83	0,92	0,66	0,69	0,75	0,79	0,85	0,66	0,68	0,74	0,78	0,83	0,65	0,66	0,72	0,76	0,80
	80	0,68	0,69	0,74	0,81	0,85	0,67	0,67	0,70	0,76	0,80	0,66	0,67	0,69	0,75	0,79	0,65	0,66	0,68	0,73	0,77
	100	0,70	0,69	0,71	0,76	0,82	0,68	0,67	0,68	0,72	0,77	0,68	0,66	0,67	0,70	0,75	0,67	0,65	0,66	0,69	0,73
	120	0,70	0,70	0,70	0,72	0,77	0,68	0,68	0,68	0,69	0,73	0,68	0,67	0,67	0,68	0,72	0,67	0,66	0,66	0,67	0,70
	140	0,70	0,70	0,70	0,71	0,74	0,68	0,68	0,67	0,69	0,71	0,68	0,67	0,67	0,68	0,69	0,67	0,66	0,66	0,67	0,68
	160	0,70	0,70	0,69	0,71	0,72	0,68	0,68	0,67	0,68	0,69	0,68	0,67	0,67	0,67	0,68	0,67	0,66	0,66	0,66	0,67
	180	0,70	0,70	0,69	0,70	0,72	0,68	0,68	0,67	0,68	0,69	0,68	0,67	0,67	0,67	0,68	0,67	0,66	0,66	0,66	0,67
	200	0,70	0,70	0,69	0,70	0,71	0,68	0,68	0,67	0,68	0,68	0,68	0,67	0,67	0,67	0,68	0,67	0,66	0,66	0,66	0,67
	220	0,70	0,70	0,69	0,70	0,71	0,68	0,68	0,67	0,68	0,68	0,68	0,67	0,67	0,67	0,67	0,67	0,66	0,66	0,66	0,66
	>240	0,70	0,70	0,69	0,70	0,70	0,68	0,68	0,67	0,68	0,68	0,68	0,67	0,67	0,67	0,67	0,67	0,66	0,66	0,66	0,66

$$\kappa_c = 1 \quad for \quad \overline{\lambda_k} \le 0.2 \quad or \quad \kappa_c = \frac{1}{k + \sqrt{k^2 - \overline{\lambda^2}_k}} \quad for \quad \overline{\lambda_k} > 0.2$$

k_c (K = 0)		ρk = 310 kg/m³					ρk = 380 kg/m³					ρk = 410 kg/m³					ρk = 450 kg/m³				
		Diameters in [mm]					Diameters in [mm]					Diameters in [mm]					Diameters in [mm]				
		4	6	8	10	12	4	6	8	10	12	4	6	8	10	12	4	6	8	10	12
Screwslength lS in [mm]	20	0,54	0,35	0,24	0,17	0,13	0,60	0,40	0,28	0,21	0,16	0,62	0,42	0,30	0,22	0,17	0,64	0,45	0,32	0,24	0,19
	40	0,71	0,64	0,52	0,41	0,34	0,73	0,68	0,57	0,47	0,39	0,74	0,70	0,59	0,49	0,41	0,75	0,71	0,62	0,52	0,44
	60	0,71	0,70	0,66	0,58	0,50	0,73	0,73	0,70	0,63	0,56	0,74	0,74	0,71	0,65	0,58	0,75	0,75	0,73	0,67	0,61
	80	0,71	0,70	0,70	0,67	0,61	0,73	0,73	0,72	0,70	0,66	0,74	0,74	0,73	0,72	0,68	0,75	0,75	0,74	0,73	0,70
	100	0,70	0,71	0,70	0,69	0,67	0,73	0,73	0,73	0,72	0,71	0,73	0,74	0,74	0,73	0,72	0,74	0,75	0,75	0,74	0,73
	120	0,70	0,71	0,70	0,70	0,69	0,73	0,73	0,73	0,73	0,72	0,73	0,74	0,74	0,74	0,73	0,74	0,75	0,75	0,75	0,74
	140	0,70	0,71	0,71	0,70	0,70	0,73	0,73	0,73	0,73	0,73	0,73	0,74	0,74	0,74	0,73	0,74	0,75	0,75	0,75	0,75
	160	0,70	0,71	0,71	0,71	0,70	0,73	0,73	0,73	0,73	0,73	0,73	0,74	0,74	0,74	0,74	0,74	0,75	0,75	0,75	0,75
	180	0,70	0,71	0,71	0,71	0,71	0,73	0,73	0,73	0,73	0,73	0,73	0,74	0,74	0,74	0,74	0,74	0,75	0,75	0,75	0,75
	200	0,70	0,71	0,71	0,71	0,71	0,73	0,73	0,73	0,73	0,73	0,73	0,74	0,74	0,74	0,74	0,74	0,75	0,75	0,75	0,75
	220	0,70	0,71	0,71	0,71	0,71	0,73	0,73	0,73	0,73	0,74	0,73	0,74	0,74	0,74	0,74	0,74	0,75	0,75	0,75	0,76
	>240	0,70	0,71	0,71	0,71	0,71	0,73	0,73	0,73	0,73	0,74	0,73	0,74	0,74	0,74	0,74	0,74	0,75	0,75	0,75	0,76

k_c (K = ∞)		ρk = 310 kg/m³					ρk = 380 kg/m³					ρk = 410 kg/m³					ρk = 450 kg/m³				
		Diameters in [mm]					Diameters in [mm]					Diameters in [mm]					Diameters in [mm]				
		4	6	8	10	12	4	6	8	10	12	4	6	8	10	12	4	6	8	10	12
Screwslength lS in [mm]	20	0,82	0,71	0,59	0,48	0,40	0,83	0,75	0,64	0,54	0,45	0,84	0,77	0,66	0,56	0,48	0,84	0,79	0,68	0,59	0,50
	40	0,85	0,78	0,75	0,67	0,59	0,87	0,81	0,79	0,71	0,64	0,88	0,82	0,80	0,73	0,66	0,88	0,83	0,81	0,75	0,69
	60	0,85	0,83	0,77	0,75	0,69	0,87	0,85	0,80	0,77	0,74	0,87	0,86	0,81	0,78	0,75	0,88	0,87	0,82	0,80	0,77
	80	0,85	0,85	0,81	0,77	0,74	0,87	0,86	0,84	0,80	0,77	0,87	0,87	0,85	0,81	0,78	0,88	0,87	0,86	0,82	0,79
	100	0,84	0,85	0,84	0,80	0,76	0,86	0,86	0,86	0,83	0,79	0,86	0,87	0,86	0,84	0,80	0,87	0,88	0,87	0,85	0,82
	120	0,84	0,85	0,84	0,82	0,79	0,86	0,86	0,86	0,85	0,82	0,86	0,86	0,86	0,86	0,83	0,87	0,87	0,87	0,86	0,84
	140	0,84	0,85	0,84	0,83	0,81	0,86	0,86	0,86	0,85	0,84	0,86	0,86	0,87	0,86	0,85	0,87	0,87	0,87	0,87	0,86
	160	0,84	0,85	0,85	0,84	0,83	0,86	0,86	0,86	0,86	0,85	0,86	0,86	0,87	0,86	0,85	0,87	0,87	0,87	0,87	0,86
	180	0,84	0,85	0,85	0,84	0,83	0,86	0,86	0,86	0,86	0,85	0,86	0,86	0,87	0,86	0,86	0,87	0,87	0,87	0,87	0,86
	200	0,84	0,85	0,85	0,84	0,83	0,86	0,86	0,86	0,86	0,85	0,86	0,86	0,87	0,87	0,86	0,87	0,87	0,87	0,87	0,87
	220	0,84	0,85	0,85	0,84	0,84	0,86	0,86	0,86	0,86	0,86	0,86	0,86	0,87	0,87	0,86	0,87	0,87	0,87	0,87	0,87
	>240	0,84	0,85	0,85	0,84	0,84	0,86	0,86	0,86	0,86	0,86	0,86	0,86	0,87	0,87	0,86	0,87	0,87	0,87	0,87	0,87

$$R_{c,d} = \kappa_c \cdot \frac{N_{pl,k}}{\gamma_M} \qquad with \quad \gamma_M = 1.1$$

R_c (K = 0)		ρk = 310 kg/m³					ρk = 380 kg/m³					ρk = 410 kg/m³					ρk = 450 kg/m³				
		Diameters in [mm]					Diameters in [mm]					Diameters in [mm]					Diameters in [mm]				
		4	6	8	10	12	4	6	8	10	12	4	6	8	10	12	4	6	8	10	12
Screwslength l_S in [mm]	20	2,14	3,09	3,75	4,29	4,78	2,36	3,57	4,42	5,11	5,73	2,44	3,76	4,70	5,45	6,13	2,53	4,00	5,05	5,89	6,64
	40	2,79	5,64	8,13	10,17	11,98	2,89	6,03	9,01	11,62	13,84	2,92	6,18	9,35	12,15	14,61	2,96	6,34	9,72	12,81	15,54
	60	2,79	6,23	10,37	14,28	17,82	2,88	6,46	11,02	15,58	19,88	2,92	6,54	11,24	16,03	20,62	2,96	6,63	11,48	16,56	21,50
	80	2,78	6,24	10,99	16,39	21,63	2,88	6,47	11,43	17,35	23,37	2,91	6,54	11,57	17,68	23,98	2,95	6,63	11,74	18,04	24,68
	100	2,76	6,26	11,06	17,10	23,72	2,86	6,48	11,46	17,79	25,06	2,89	6,55	11,61	18,04	25,51	2,93	6,64	11,78	18,32	26,01
	120	2,76	6,27	11,11	17,23	24,51	2,86	6,48	11,51	17,88	25,56	2,89	6,55	11,65	18,12	25,92	2,93	6,64	11,81	18,39	26,34
	140	2,76	6,27	11,14	17,33	24,75	2,86	6,48	11,53	17,97	25,72	2,89	6,55	11,67	18,19	26,06	2,93	6,64	11,83	18,47	26,47
	160	2,76	6,27	11,16	17,41	24,90	2,86	6,48	11,54	18,04	25,86	2,89	6,55	11,68	18,25	26,20	2,93	6,64	11,84	18,51	26,59
	180	2,76	6,27	11,16	17,46	25,03	2,86	6,48	11,54	18,07	25,97	2,89	6,55	11,68	18,29	26,30	2,93	6,64	11,84	18,55	26,69
	200	2,76	6,27	11,16	17,50	25,14	2,86	6,48	11,54	18,10	26,05	2,89	6,55	11,68	18,32	26,38	2,93	6,64	11,84	18,56	26,75
	220	2,76	6,27	11,16	17,50	25,23	2,86	6,48	11,54	18,10	26,11	2,89	6,55	11,68	18,32	26,42	2,93	6,64	11,84	18,56	26,80
	>240	2,76	6,27	11,16	17,50	25,28	2,86	6,48	11,54	18,10	26,16	2,89	6,55	11,68	18,32	26,42	2,93	6,64	11,84	18,56	26,83

R_c (K = ∞)		ρk = 310 kg/m³					ρk = 380 kg/m³					ρk = 410 kg/m³					ρk = 450 kg/m³				
		Diameters in [mm]					Diameters in [mm]					Diameters in [mm]					Diameters in [mm]				
		4	6	8	10	12	4	6	8	10	12	4	6	8	10	12	4	6	8	10	12
Screwslength l_S in [mm]	20	3,22	6,29	9,23	11,80	14,07	3,27	6,67	10,09	13,29	16,13	3,29	6,81	10,40	13,82	16,92	3,32	6,96	10,77	14,47	17,86
	40	3,34	6,96	11,80	16,41	20,91	3,42	7,17	12,41	17,59	22,86	3,45	7,25	12,61	18,00	23,55	3,48	7,34	12,78	18,48	24,35
	60	3,37	7,34	12,20	18,44	24,55	3,43	7,56	12,65	19,07	26,16	3,45	7,63	12,81	19,30	26,70	3,47	7,72	13,00	19,58	27,34
	80	3,37	7,51	12,80	18,88	26,12	3,42	7,65	13,23	19,64	27,20	3,44	7,70	13,37	19,90	27,59	3,46	7,76	13,55	20,22	28,07
	100	3,32	7,52	13,20	19,67	26,93	3,37	7,67	13,50	20,40	28,07	3,39	7,71	13,59	20,64	28,53	3,41	7,77	13,70	20,91	28,98
	120	3,32	7,50	13,25	20,31	27,94	3,37	7,62	13,53	20,88	29,02	3,39	7,66	13,62	21,07	29,41	3,41	7,72	13,74	21,27	29,83
	140	3,32	7,50	13,31	20,53	28,78	3,37	7,62	13,58	20,98	29,72	3,39	7,66	13,67	21,16	30,04	3,41	7,72	13,77	21,32	30,38
	160	3,32	7,50	13,35	20,62	29,29	3,37	7,62	13,60	21,07	30,01	3,39	7,66	13,68	21,24	30,26	3,41	7,72	13,78	21,43	30,56
	180	3,32	7,50	13,35	20,72	29,45	3,37	7,62	13,60	21,16	30,14	3,39	7,66	13,68	21,30	30,38	3,41	7,72	13,78	21,47	30,67
	200	3,32	7,50	13,35	20,78	29,61	3,37	7,62	13,60	21,19	30,29	3,39	7,66	13,68	21,32	30,53	3,41	7,72	13,78	21,50	30,80
	220	3,32	7,50	13,35	20,78	29,72	3,37	7,62	13,60	21,19	30,38	3,39	7,66	13,68	21,32	30,61	3,41	7,72	13,78	21,50	30,87
	>240	3,32	7,50	13,35	20,78	29,83	3,37	7,62	13,60	21,19	30,44	3,39	7,66	13,68	21,32	30,67	3,41	7,72	13,78	21,50	30,92

APPENDIX G: U33 field of unloaded length FE-models

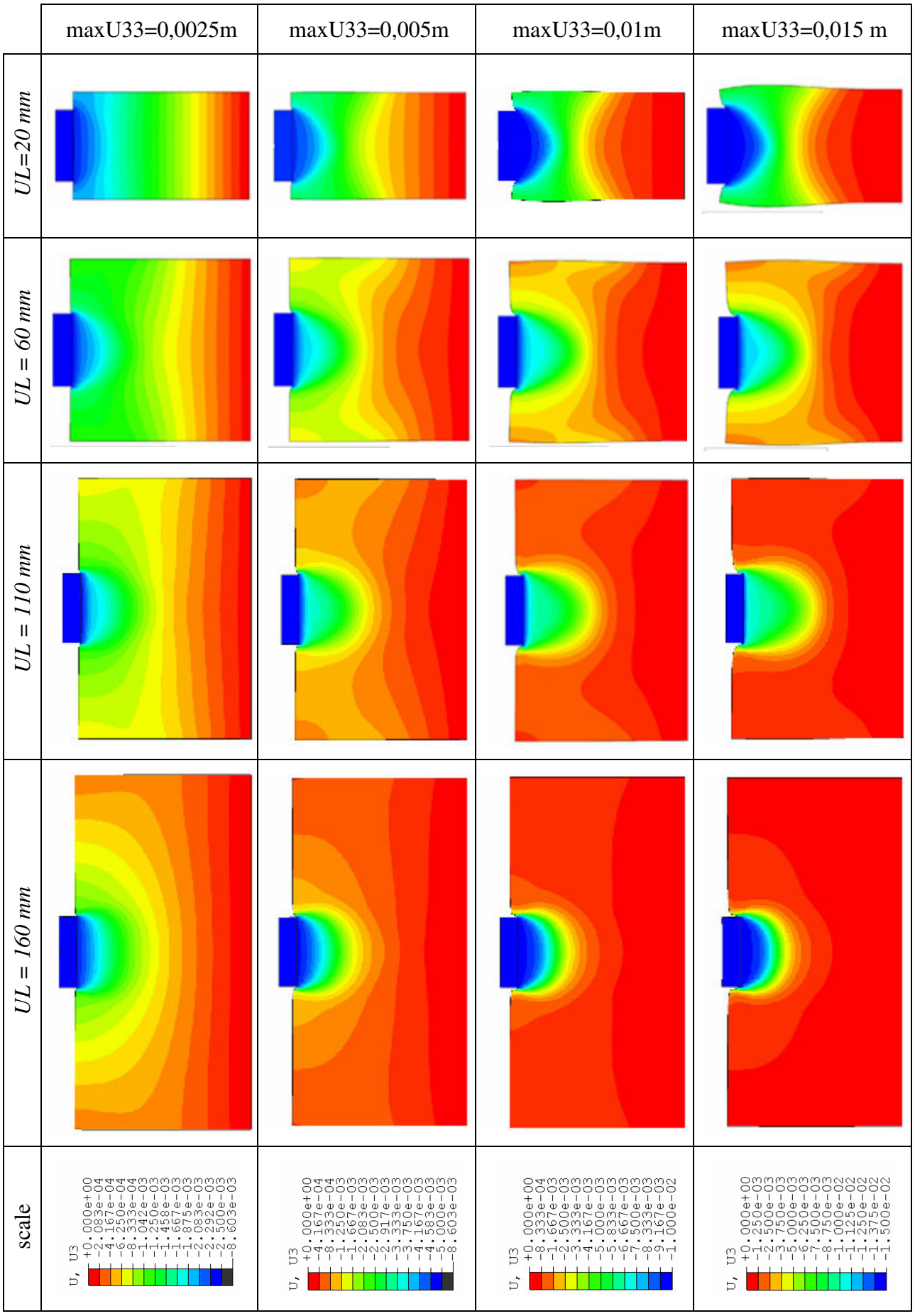

APPENDIX H: Explanation of $k_{c,90}$ and an evaluation of maximum capacity, $F_{c,90}$, according to Eurocode 5 (prEN 1995-1-1)

According to Eurocode 5 (prEN 1995-1-1) the design capacity in compression perpendicular to the grain is formulated as follows:

$$F_{c,90,d} = \frac{k_{\text{mod}} \cdot f_{c,90,k}}{\gamma_M} \cdot k_{c,90} \cdot A_{\text{sup}}$$

where:

$f_{c,90,k}$ is the characteristic strength in compression perpendicular to the grain

γ_M is the partial factor for the material property

k_{mod} is the modification factor

$k_{c,90}$ is the amplificatory factor

A_{sup} is the contact area

If only the geometry is considered as the variable, the formula is only dependent on the parameters $k_{c,90}$ and A_{sup} and can be treated as:

$$F_{c,90,d} = C \cdot k_{c,90}\, funct(h;l) \cdot A_{\text{sup}}\, funct(l;b) = C \cdot k_{c,90}\, funct(h;l) \cdot (b \cdot l)$$

where:

b is the contact width

l is the contact length

h is the member depth

$C = \frac{k_{\text{mod}} \cdot f_{c,90,k}}{\gamma_M} = f_{c.90.d}$ is independent on the geometry

As it is possible to notice the design capacity in compression perpendicular to the grain has a linear relation with the width b, instead of the relation in term of height h and length l is non linear and varies with the formulation proposed by the Eurocode 5 (prEN 1995-1-1:2005).

In the sequent it is investigated the case of internal, end supports and continuous, discontinuous supports.

- Internal Support

As described in Chapter 3.3.1 the equation of $k_{c,90}$,(3.3), is represented in the following relationship, Figure H.1, with the height h of the member and the contact length l of the loading surface as y- and x-axes, respectively.

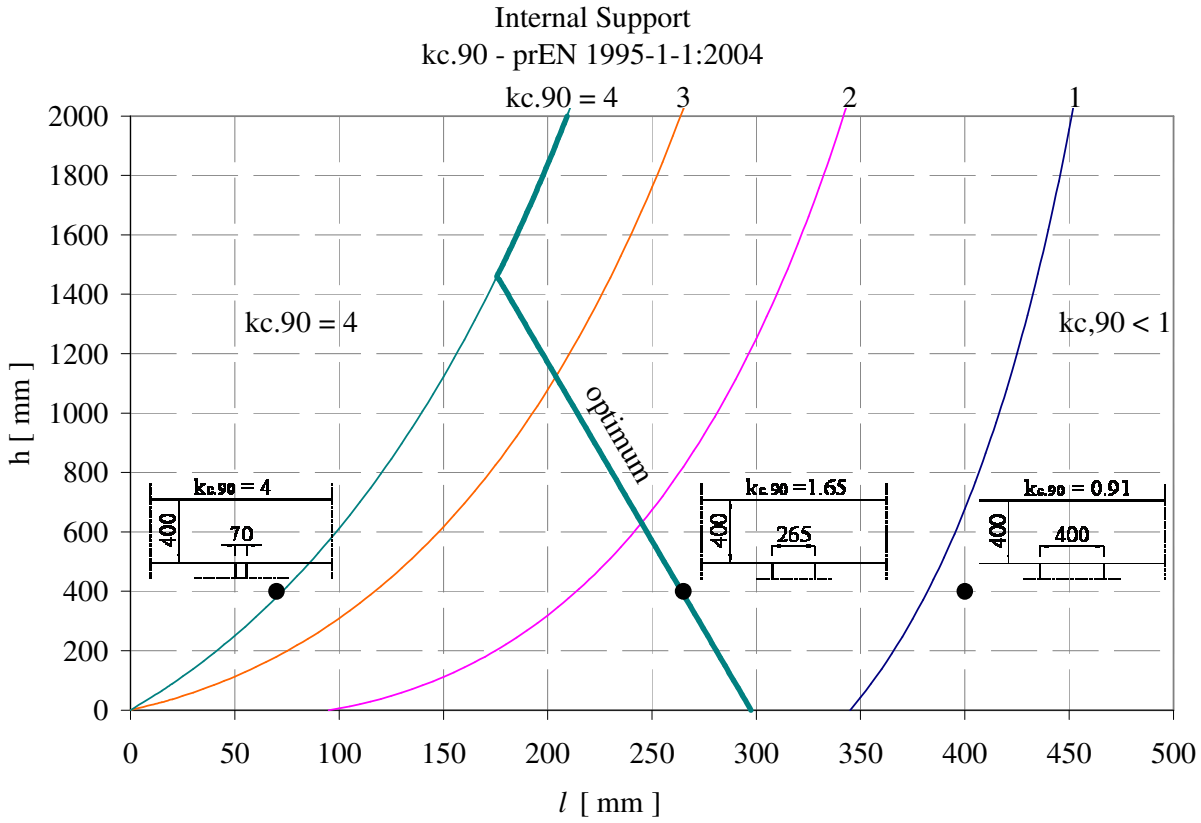

Figure H.1 The value of $k_{c,90}$ for internal support according to Eurocode 5

The relationship displays different lines for each values of $k_{c,90}$ equal to 1,2,3 and the border of the zone where $k_{c,90}$ reach the maximum of 4. Three characteristic examples are used in order to display the practical meaning of the $k_{c,90}$ formulation. The example on the left illustrates the extreme case which suggests that with a very short contact length l, $k_{c,90}$ reaches its maximum. The example on the right shows that by increasing the loading length $k_{c,90}$ can reach a value less than one. The example in the middle shows the optimized relationship, since multiplying the length with the value of $k_{c,90}$ results in a product higher compared to the product obtained by the other two examples. The optimized relationship between contact length l and member height h is illustrated by a separate line. This relationship is described in the following paragraph:

- For a given member height h the contact length l, which gives the highest capacity when using the criteria stated by Eurocode 5 is derived into the following expression:

$$\max F_{c.90}(l;h)\left\{\begin{array}{ll}\dfrac{\partial(k_{c.90}\cdot l)}{\partial l}=0 & for\ h<1461\ mm\\ k_{c.90}=4 & for\ h>1461\ mm\end{array}\right\}$$

$$l_{optimum} = \begin{cases} 297.5 - \dfrac{h}{12} & for\ h < 1461\ mm \\ \dfrac{1}{2} \cdot \left(\sqrt{36 \cdot h^2 - 16860 \cdot h + 354025} - 6 \cdot h + 595 \right) & for\ h > 1461\ mm \end{cases}$$

By use of the equation above the maximum capacity is therefore not dependent on the width of the loaded are, *b*, but merely just a function of the height of the beam and the length of the loaded area. This is schematically illustrated in the following 3D-relationship, see Figure H.2, displaying the contact length of the loaded area, *l*, the member height, *h*, and the product of $k_{c,90}$ on its xyz-axes.

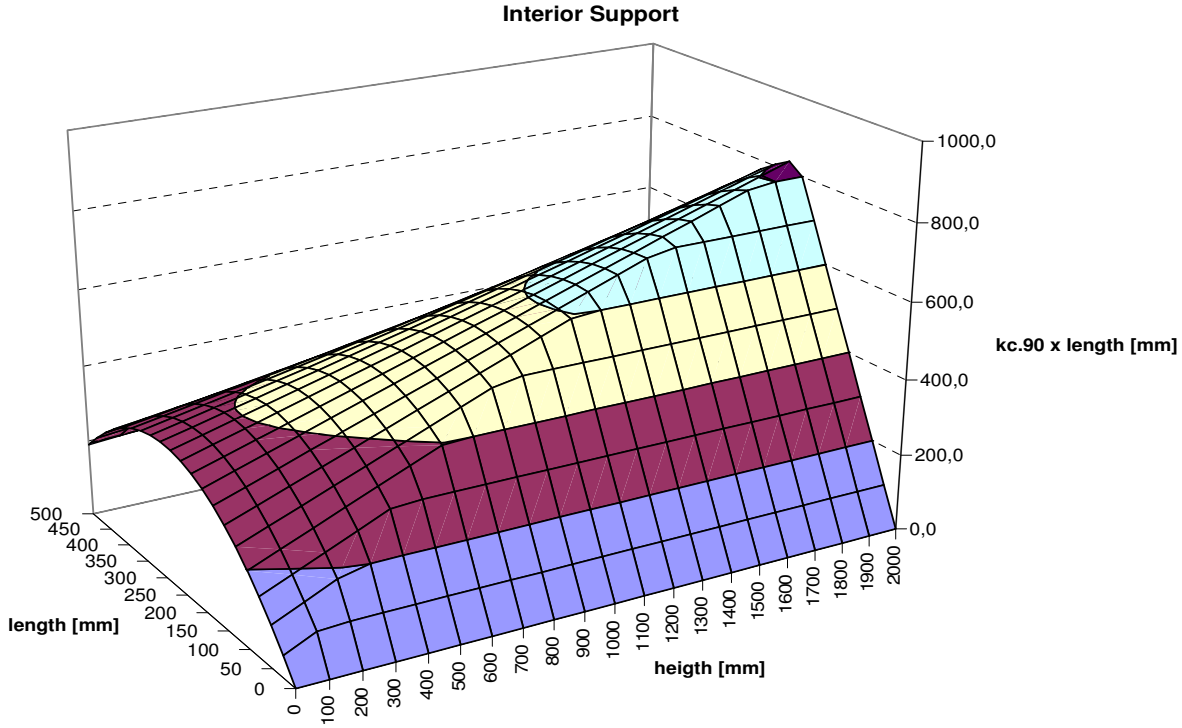

Figure H.2 Relationship between length, height and $k_{c,90}$

- End Support $a \leq h/3$

The equation that governs the appropriate value of $k_{c,90}$ suggested by Eurocode 5 is presented in Chapter 3.3.1 (3.2). The following figure, see Figure H.3, displays $k_{c,90}$ represented as lines and examples of different extreme cases, analogy to presented above.

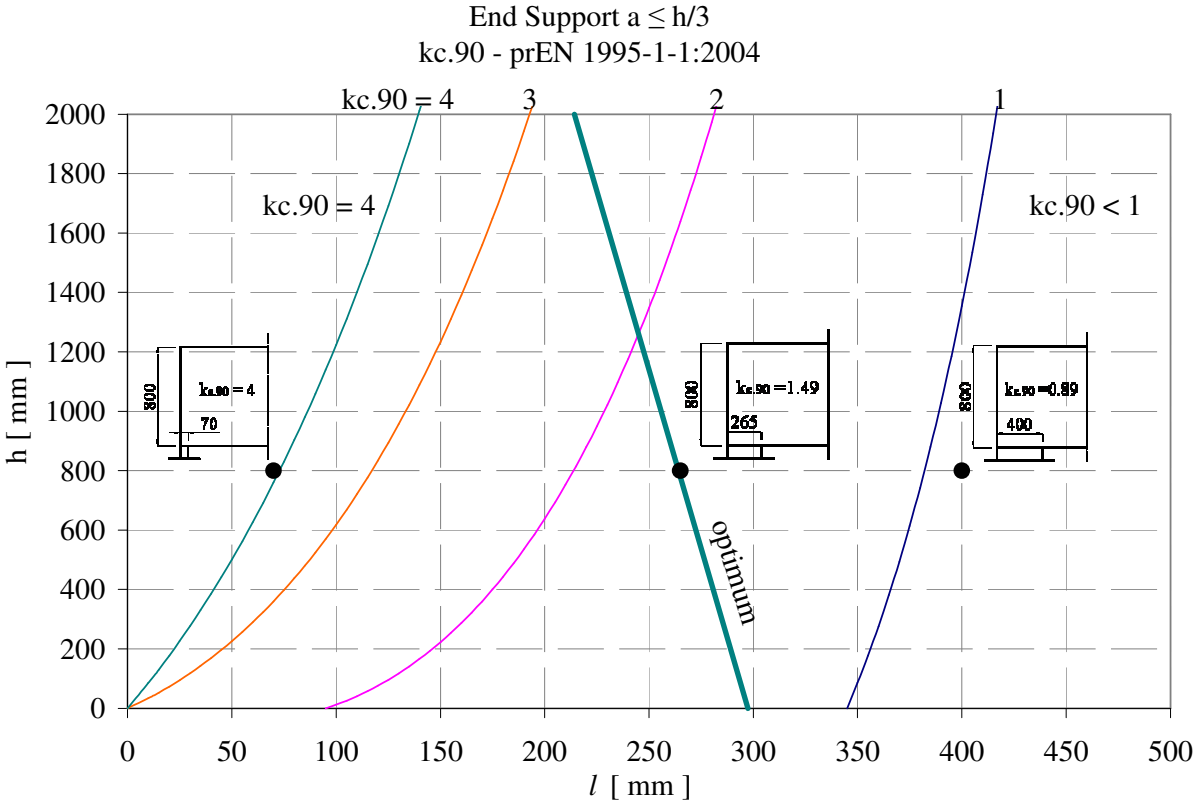

Figure H.3 The value of $k_{c,90}$ for an end support according to Eurocode 5

The main difference when compared to the case with internal support is that the line which represents the optimum case does not intersect the line where $k_{c,90} = 4$ which means that for any given height, $h \in [0,2000]$, the most favourable situation does not include $k_{c,90}$ being at its maximum. The line of optimum relationship between height and length is derived similarly as to above and is expressed as follows:

$$\max F_{c.90} = \left(\frac{\partial (k_{c.90} \cdot l)}{\partial l} = 0 \right) \quad for\ a \leq \frac{h}{3}\ mm$$

$$l_{optimum} = 297.5 - \frac{h}{24} \quad for\ a \leq \frac{h}{3}\ mm$$

In Figure H.3, three examples are also represented with the same purpose as discussed in the case of internal support.

- Continuous and Discontinuous Support

The equation that governs the appropriate value of $k_{c,90}$ suggested by Eurocode 5 is presented in Chapter 3.3.1 (3.4). In this case, see Figure H.4, the line $l = l_{ef}$, represents the lower border of the domain of $k_{c,90}$ which corresponds to cubic compression and therefore l_{ef} can never be physically less than l.

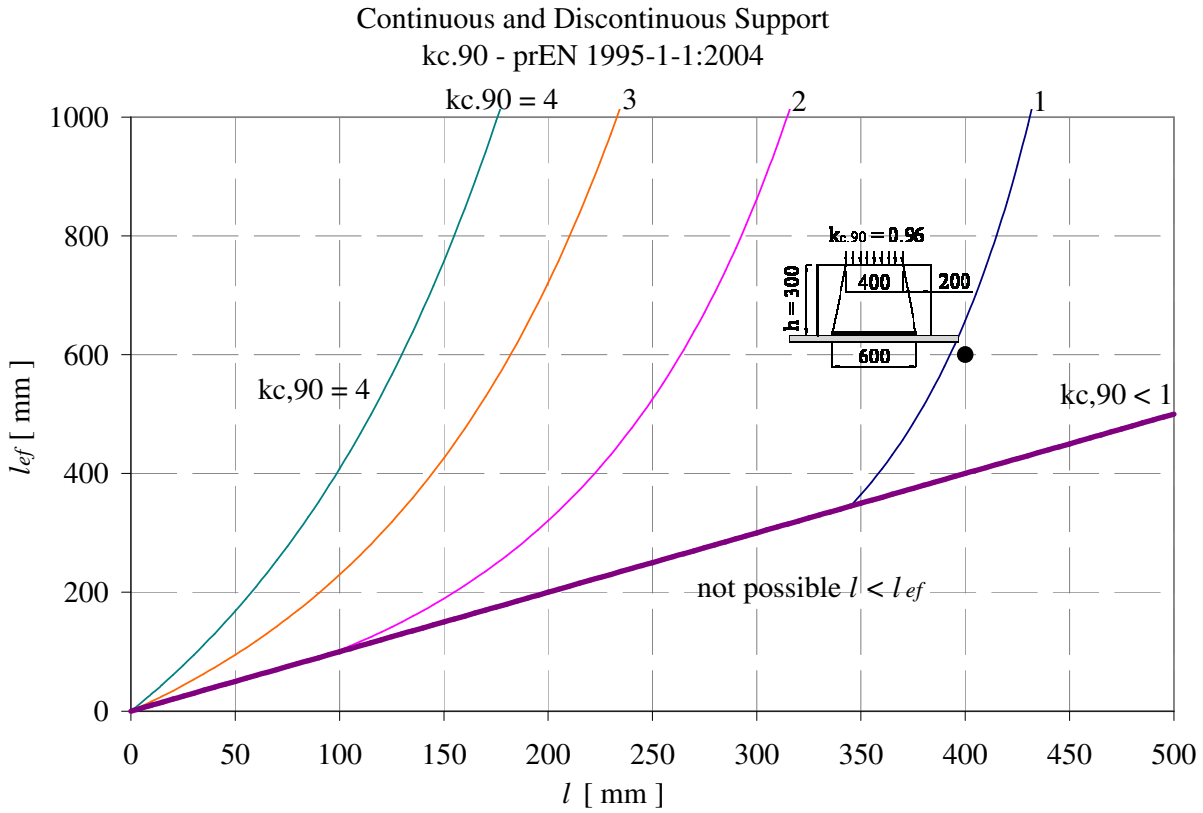

Figure H.4 The value of $k_{c,90}$ for continuous and discontinuous supports according to Eurocode 5

The optimized relationship between height of the beam and length of the loaded area is simply the line where $k_{c,90}$ is equal to 4. It is worth to notice that even if cubic compression is investigated $k_{c,90}$ can be different than 1. In Figure H.4 an example is also represented in order to give a physical meaning to the problem considered.

APPENDIX I: Characteristic capacity perpendicular to the grain of test configuration

The following tables display the capacities using the model of Karlsruhe by applying characteristic values from different codes. The thickness of the plate is not considered in the model of Karlsruhe.

Table I.1 regards the un-reinforced specimens and their characteristic capacities, Table I.2 considers reinforcement using screws with d = 10 mm and Table I.3 displays the reinforced specimens using d = 12 mm screws.

Table I.1 Characteristic capacities of the un-reinforced specimen

200x200mm 4 screws *d*=10mm *l*=300mm					
Glulam					
	BKR:2003	DIN 1052:2004	EN 1995-1-1:2004	CNR-DT 206:2006	
Class	L40	GL32	GL32	GL32	
$f_{m,k}$	33	32	32	32	N/mm^2
$f_{c,90,k}$	8	3.3	3.3	3.3	N/mm^2
rk	470	430	430	430	kg/m^3
l	200	200	200	200	mm
l_{ef}	-	260	-	350	mm
b	200	200	200	200	mm
A hole	615.7	615.7	615.7	615.7	mm2
A	39384	51384	39384	69384	mm2
$E_{0.mean}$	13000	13700	13700	13700	N/mm^2
$k_{c,90,k}$	1.0	1.75	2.5	-	-
$k_{c,90,k} * f_{c,90,k}$	8.0	5.8	8.3	-	N/mm^2
R timber,k	315.07	296.74	324.92	228.97	kN

Table I.2 Characteristic capacities of the reinforced specimen with screw diameter, d = 10

Reinforcement with screws, d = 10 mm		
n	4	
d	10	mm
l_s	300	mm
$f_{y,k}$	640	N/mm^2
class	3	-
$f_{1,k}$	14.79	N/mm^2
$R_{ax,k}$	44.38	kN
$R_{c,k}$	18.44	kN
R_k	18.44	kN

Capacity when reinforced					
	BKR:2003	DIN 1052:2004	EN 1995-1-1:2004	CNR-DT 206:2006	
$R_{90,k}$	388.83	370.50	398.68	302.73	kN

Table I.3 Characteristic capacities of the reinforced specimen with screw diameter, d = 12

Reinforcement with screws, d = 12 mm		
n	4	
d	12	mm
ls	300	mm
fy,k	640	N/mm^2
class	3	-
f 1,k	14.79	N/mm^2
R ax,k	53.25	kN
R c,k	26.75	kN
R k	26.75	kN

Capacity when reinforced					
	BKR:2003	DIN 1052:2004	EN 1995-1-1:2004	CNR-DT 206:2006	
R 90,k	422.07	403.74	431.92	335.97	kN

Appendix J: Pictures of the failure modes of the test specimen

- S10pl15

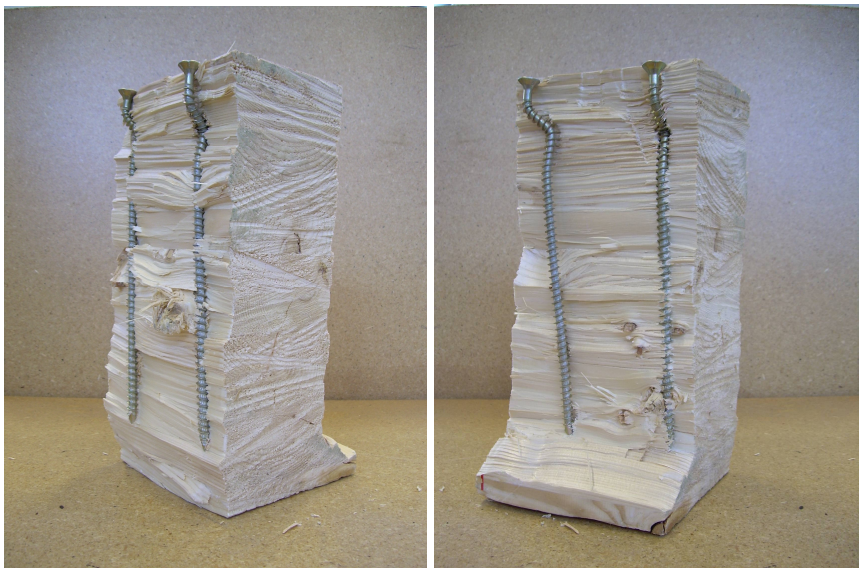

- S12pl15

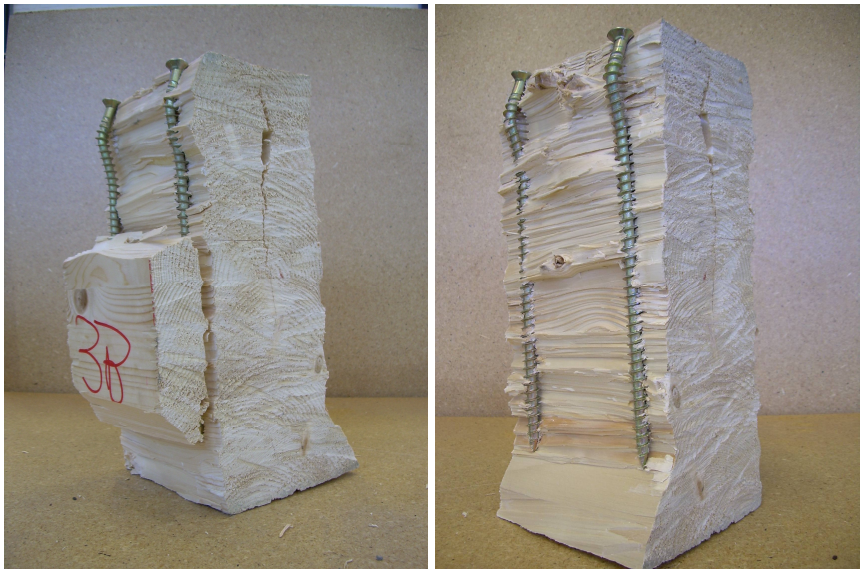

- S10pl20 (8)



- S12pl20

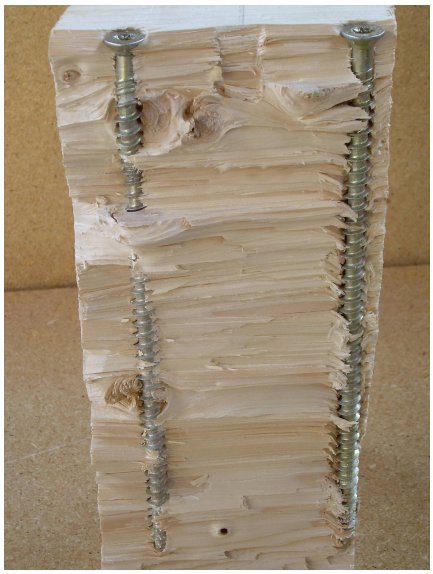


Appendix K: Calibration of the hydraulic jack and equipment required for the tests

Calibration of the hydraulic jack

The hydraulic jack had to be calibrated in order to know how much pre-stressing force that is applied compared to the hydraulic pressure. This was done by placing the jack in the ALPHA Universal testing machine and measuring the weight it lifts when the hydraulic pressure increases, see Figure K.1. The weight is then converted into kilo Newton's which corresponds to the tension force that is applied onto the pre-stressing bars.

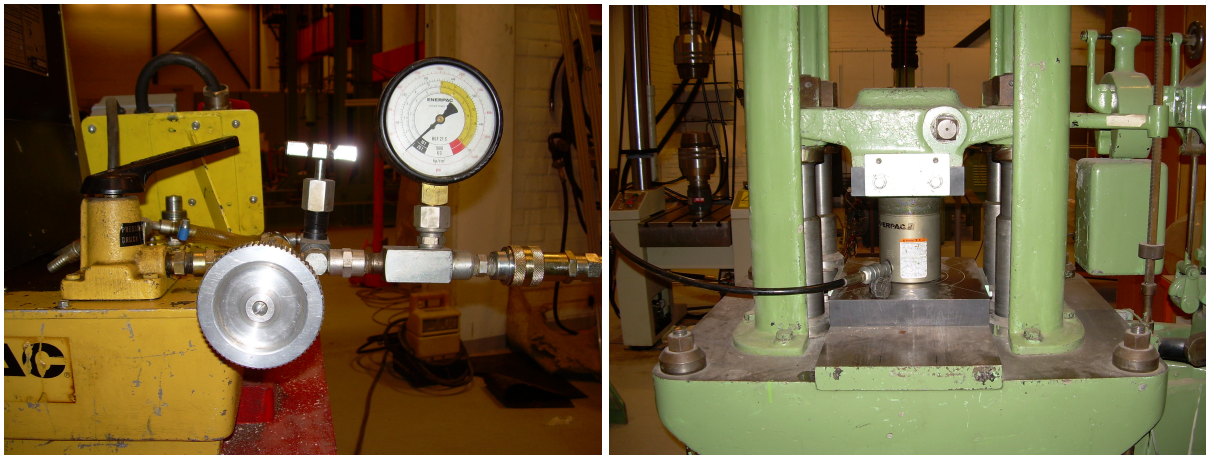

Figure K.1 Calibration configuration

Calibrating the hydraulic jack requires a compressor that produces steady flow of pressure. At high pressure the machine proved to be a little unstable, thus the difficulties acquiring good measurement. The calibration curve can be seen in Figure K.2.

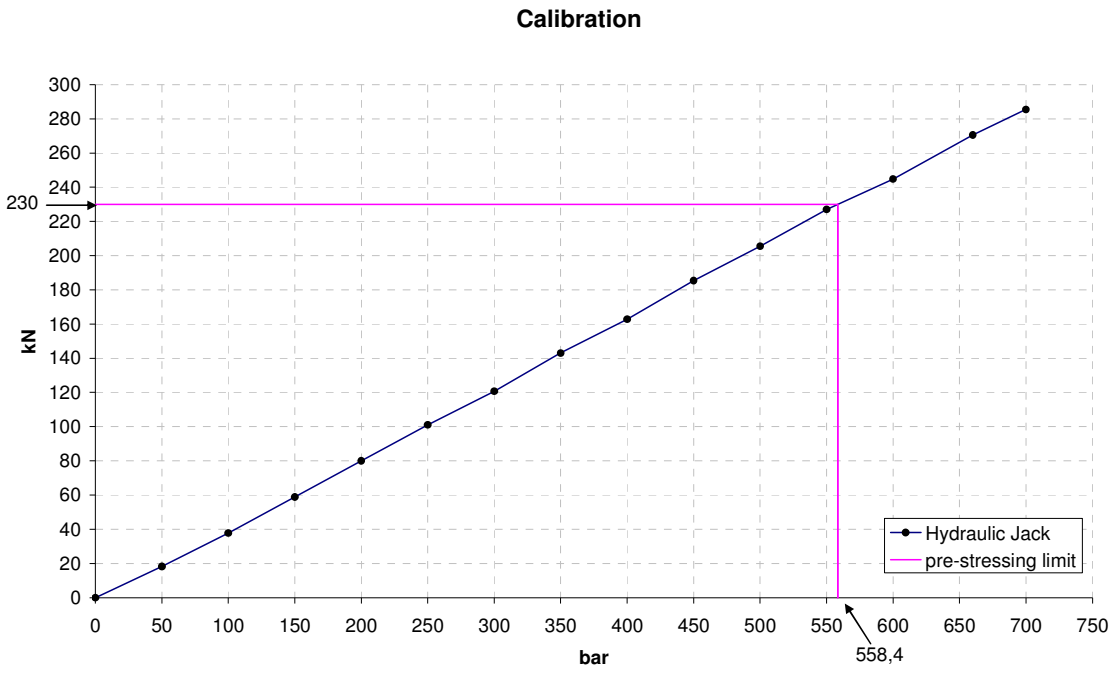

Figure 1.2 Relationship showing the load-pressure curve of the calibration of the hydraulic jack

Equipment required for the tests of ultimate load carrying capacity

Some equipment was needed in order to conduct the tests and monitor the load and displacement. Here follows a short description of the different machines and instruments:

- ALPHA Universal testing machine

Tests both in compression and tension, displacement controlled, max capacity 75 tons

- Loading Cell (Load indicator 500 kN)

Measures the applied load and connected to the amplifier, max capacity 500 kN, see Figure K.3.

- LVDT HBM W20TS ± 20 mm

Measures the displacement and connected to the XY-Recorder, applied on top and centre of the steel plate, max displacement ± 20 mm.

- Amplifier HBM MGC

Amplifies the signal from the loading cell, connected to the loading cell and the XY-Recorder, see Figure K.4.

- XY- Recorder GRAPHTECH WX3000

Draws a relationship of the load-displacement curve, see Figure K.5.

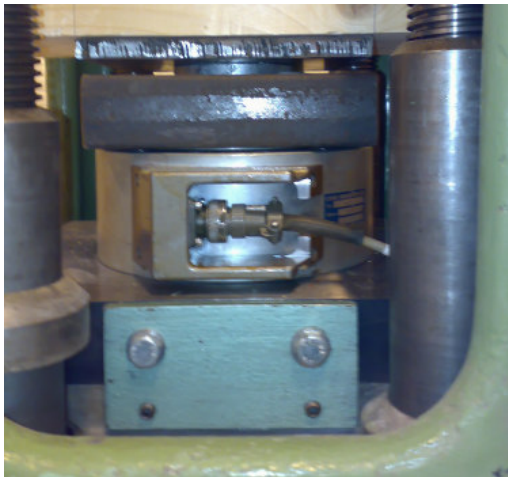

Figure K.3 Load indicator

Figure K.4 Amplifier

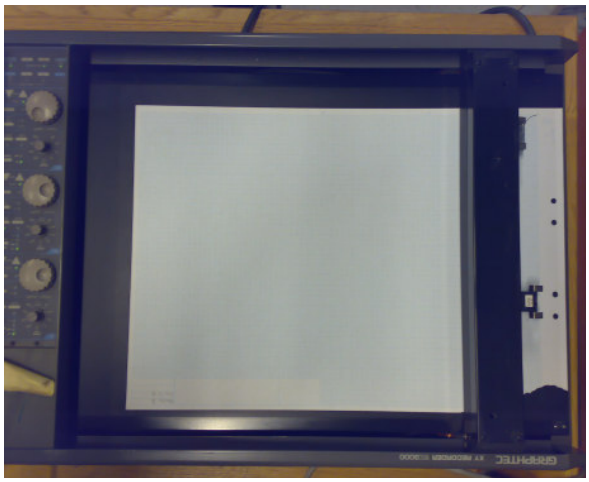

Figure K.5 XY- Recorder

Equipment required for the long-term test

The equipment that was required to perform the tests was:

- Enerpac Hydraulic Jack 300 kN
- Compressor

Adds hydraulic pressure to the jack

- Strain Gauges HBM

Measures the strain in the Dywidag bar

- Data Logging machine

Records the strain from the bars